The Role of Gibberellin in Wheat Grain Development

Aakriti Wanchoo-Kohli, MSc.

Thesis submitted to the University of Nottingham

for the degree of Doctor of Philosophy

December 2016

Abstract

The plant hormone gibberellin (GA) is known to influence grain size and flour quality, flowering, development and germination in wheat. GA also induces the production of α-amylase by the aleurone layer and premature production of this enzyme during development results in degraded starch in the mature grain. While GA is proposed to have a negative effect on flour quality, it is essential for early grain development and these effects are separated both temporarily and spatially in the grain. It was the aim of this project to further understand the role GA plays in wheat grain development and in order to achieve this constructs were designed to alter GA metabolism or signalling in the seed-coat, endosperm, embryo or aleurone of developing wheat grains.

In plants where GA content was manipulated in the developing endosperm it was shown that GA produced by this tissue is involved in regulating grain size and morphology. This was demonstrated by the differences observed between the transgenics and their nulls in grain size, hardness index and moisture content. Additionally, in these lines no differences were observed in the α-amylase levels, implying that GA produced by the endosperm might not be influencing the production of this enzyme. However, GA insensitivity introduced in the embryo and aleurone layers did not display the hypothesised phenotypes and was inconclusive in determining the role of GA signalling in grain development.

During this project a reliable qPCR based method using TaqMan assays was also developed to determine zygosity of transgenic plants in the T1 generation. This method was successful in reducing the number of generations required to select homozygous material compared to more conventional methods.

Acknowledgements

I would like to begin by thanking my supervisors for all the help and guidance that they have provided me over the last four years. Thank you specially to Simon Vaughan and Peter Hedden for giving me the opportunity to do this PhD, and the considerable amount of support they have given me since, including editing my thesis over the Christmas holidays. This PhD could not have been completed without them. Thank you also to Andy Phillips and Alison Huttly for their vast amount of knowledge about plants and for sharing it with me. Thank you to Mike Holdsworth and Alexander Goldshmidt for all their advice during the course of this project.

I would also like to thank the various members the GA lab, both past and present for their help and friendship during my time here. Thank you to Rob for being a great friend and support both in the lab and outside. A special thank you to David for being a sounding board in my moments of crisis. They were both greatly missed over the past year. Thank you to Archana for all the fun we've had gossiping in Hindi while nobody could understand us. Thank you to Steve for all his advice and help even though I wasn't one of his students. Also, thank you to Matt, George, Beth and Megan for all the fun in the lab. I would also like to thank others at Rothamsted who have been great friends over the years including Till, Imogen, Mark, Marc and Elena.

A very big thank you to Helen, Ian, Imogen, Clare and Lucy for the amazing support they have provided in the lab over the years and for always being so cheerful and lovely. Thank you to Steve Powers for all his help with the stats and his infinite patience while explaining it all to me. Thank you also to Fiona, Anthony and Mark for all their help with my plants in the glasshouse.

I'd like to thank my family for being amazingly supportive over the years and I couldn't have done this without them. Thank you to Arjun for being there through the good and the bad and for believing that I could do this. Lastly, thank you to my amazing parents who have supported me through everything and always believed I could achieve anything, even when I didn't.

Table of Contents

List of Tables and Figures x

Abbreviations xiv

Chapter 1. Introduction 1

1.1 Wheat **1**

1.1.1 Food Security and Wheat 2

1.1.2 Genetically modified (GM) plants and food security 8

1.2 Wheat Grain **12**

1.2.1 Morphology and Composition 15

1.2.1.1 Starch 16

1.2.1.2 Protein 18

1.2.1.3 Lipids 20

1.2.1.4 Minor components 20

1.2.2 Wheat Grain Development 20

1.2.2.1 Classification of Grain Development 25

1.2.3 Source-sink Relationship in Grains 32

1.2.4 Seed Dormancy and Germination 34

1.2.4.1 Pre-harvest sprouting (PHS) and Premature α-amylase (PMA) 40

1.3 Gibberellins (GAs) **44**

1.3.1 GA Biosynthesis 45

1.3.1.1 GGDP to *ent*-kaurene 46

1.3.1.2 *ent*-kaurene to GA_{12} 47

1.3.1.3 GA_{12}/GA_{53} to bioactive GAs 49

1.3.2 GA Inactivation 52

1.3.3 GA Signalling 54

1.3.4 GA Regulation 58

1.3.5 GA Transport 62

1.4 Tissue Specific Promoters **65**

1.5 Aims of the project **69**

Chapter 2. Materials and Methods **70**

2.1 Plant Material and Growth Conditions..... 70
2.1.1 Yield and Development Experiments.....71
2.2 Molecular Methods..... 72
2.2.1 Genomic DNA (gDNA) Extractions 72
2.2.2 Polymerase Chain Reaction (PCR).....73
2.2.3 TaqMan Assay 73
2.2.4 RNA extraction with 1st DNase treatment 74
2.2.5 Second DNase treatment.....76
2.2.6 cDNA synthesis.....76
2.2.7 Real Time Quantitative PCR (qRT-PCR).....77
2.2.8 Southern Hybridisation 78
2.2.8.1 Restriction endonuclease digestion and electrophoresis of gDNA restriction fragments 78
2.2.8.2 Transfer of digested gDNA to nylon membranes.....79
2.2.8.3 Synthesis of Digoxigenin-II-dUTP (DIG) labelled probe.....79
2.2.8.4 Hybridisation of membranes.....80
2.2.8.5 Detection of DIG labelled probes 81
2.3 Yield Measurements 82
2.4 Quality Analysis 83
2.4.1 Single Kernel Characterisation System (SKCS) 83
2.4.2 Alpha amylase assay 83
2.4.3 Grain Nitrogen Measurements 85
2.5 Analysis of GA content 86
2.6 Data Analysis 87
2.7 Bioimaging..... 88
2.8 Controlled cross pollination of transgenic wheat lines 89
2.8.1 Emasculation.....89
2.8.2 Pollination 89
Chapter 3. Identifying Homozygous Plants using TaqMan Assays 90
3.1 Introduction..... 90
3.2 Results and Discussion 94

3.2.1 Zygosity and copy number analysis of plants transformed with *TaTri::PcGA2ox1* 97
3.2.1.1 PCR analysis to confirm presence of transgene 97
3.2.1.2 TaqMan assay to select homozygous material 98
3.2.1.3 PCR analysis to confirm zygosity of T2 plants 100
3.2.1.4 Copy number analysis of *TaTri::PcGA2ox1* transgenic lines 102
3.2.2 Zygosity analysis of plants transformed with the other constructs .104
3.3 Conclusions 106
Chapter 4. Effects of GA insensitivity in developing embryo and aleurone layer of wheat grains 107
4.1 Introduction 107
4.2 Results and discussion 112
4.2.1 Production of homozygous material 112
4.2.2 Experimental design....112
4.2.3 Analysis of transgenic lines expressing the *Atgai* gene under control of the aleurone-specific *HvChi26* promoter 113
4.2.3.1 GFP visualisation of *HvChi26* activity....113
4.2.3.2 *HvChi26::Atgai* transgene expression 115
4.2.3.3 *HvChi26::Atgai* effects on yield 117
4.2.3.4 *HvChi26::Atgai* effects on quality....119
4.2.3.5 *HvChi26::Atgai* effects on endogenous gene expression....122
4.2.4 Analysis of transgenic lines expressing the *Atgai* gene under control of the embryo- and aleurone-specific *HvBeg1* promoter 125
4.2.4.1 GFP visualisation of *HvBeg1* activity 125
4.2.4.2 *HvBeg1::Atgai* transgene expression 127
4.2.4.3 Analysis of *HvBeg1::Atgai* effect on yield 129
4.2.4.4 Analysis of *HvBeg1::Atgai* effect on quality 131
4.2.4.5 *HvBeg1::Atgai* effect on endogenous gene expression 133
4.3 Conclusions 136
Chapter 5. Effects of manipulating GA in the pericarp and seed coat layers of developing wheat grain 138
5.1 Introduction 138
5.2 Results and Discussion 143
5.2.1 Production of homozygous material 143
5.2.2 Experimental design....143

5.2.3 Analysis of transgenic lines expressing the *AtGA20ox1* gene under control of the pericarp-specific *HvGerF* promoter.....144

5.2.3.1 GFP visualisation of *HvGerF* activity.....144
5.2.3.2 *HvGerF::AtGA20ox1* transgene expression.....146
5.2.3.3 Analysis of *HvGerF::AtGA20ox1* effects on yield.....147
5.2.3.4 Analysis of *HvGerF::AtGA20ox1* effects on quality.....150

5.2.4 Analysis of transgenic lines expression the *AtGA20ox1* gene under control of the inner integument-specific *TaDFR-D* promoter.....152

5.2.4.1 GFP visualisation of *TaDFR-D* activity.....152
5.2.4.2 *TaDFR-D::AtGA20ox1* transgene expression.....154
5.2.4.3 Analysis of the effect *TaDFR-D::AtGA20ox1* on yield.....155
5.2.4.4 Analysis of *TaDFR-D::AtGA20ox1* effects on grain quality.....158

5.2.5 Analysis of *HvGerF::AtGA20ox1* and *TaDFR-D::AtGA20ox1* effects on grain development.....160

5.2.5.1 Average weight per grain.....161
5.2.5.2 Average area per grain.....169

5.3 Conclusions..... 175

Chapter 6. The effect of manipulating GA in the endosperm of developing wheat grain 177

6.1 Introduction..... 177

6.2 Results and discussion..... 182

6.2.1 Production of homozygous material.....182

6.2.2 Experimental design.....183

6.2.2.1 *TaTri::PcGA2ox1*.....183
6.2.2.2 *TaEND1::AtGA20ox1* and *TaEND1::Atgai*.....183

6.2.3 GFP visualisation of promoter activity.....184

6.2.3.1 *TaTri* activity.....184
6.2.3.2 *TaEND1* activity.....185

6.2.4 Analysis of transgenic lines expressing the *PcGA2ox1* gene under control of the endosperm-specific *TaTri* promoter.....187

6.2.4.1 *TaTri::PcGA2ox1* transgene expression.....187
6.2.4.2 Analysis of *TaTri::PcGA2ox1* effects on yield.....188
6.2.4.3 Analysis of *TaTri::PcGA2ox1* effects on quality.....192
6.2.4.4 *TaTri::PcGA2ox1* effect on endogenous gene expression.....193

6.2.5 Analysis of transgenic lines expressing the *AtGA20ox1* gene under control of the ETC-specific *TaEND1* promoter 197

6.2.5.1 *TaEND1::AtGA20ox1* transgene expression 197
6.2.5.2 Analysis of *TaEND1::AtGA20ox1* effects on yield.....198
6.2.5.3 Analysis of *TaEND1::AtGA20ox1* effects on quality 202
6.2.5.4 Analysis of *TaEND1::AtGA20ox1* effects on GA levels 204
6.2.5.5 Analysis of *TaEND1::AtGA20ox1* effects on endogenous gene expression 207

6.2.6 Analysis of transgenic lines expressing the *Atgai* gene under control of the ETC-specific *TaEND1* promoter 208

6.2.6.1 *TaEND1::Atgai* transgene expression.....208
6.2.6.2 Analysis of *TaEND1::Atgai* effects on yield 210
6.2.6.3 Analysis of *TaEND1::Atgai* effects on quality.....212
6.2.6.4 Analysis of *TaEND1::Atgai* effects on GA levels 214
6.2.6.5 Analysis of *TaEND1::Atgai* effects on endogenous gene expression 216

6.3 Conclusions..... 218

Chapter 7. Effects of manipulating gibberellin metabolism in both the endosperm and scutellum of developing grains 222

7.1 Introduction..... 222

7.2 Results and discussion..... 226

7.2.1 Production of hybrid plants 226

7.2.2 Production of homozygous material 227

7.2.2.1 Identifying segregating genotypes 227
7.2.2.2 TaqMan Assays to identify homozygous material 229
7.2.2.3 PCR analysis to confirm zygosity of F3 plants 235

7.2.3 Experimental design of grain yield and quality studies in *TaHMW-GS::AtGA20ox1* X *ZmGlb1::PcGA2ox1* hybrid lines.....237

7.2.4 Transgene expression of *AtGA20ox1* and *PcGA2ox1* 238

7.2.5 Analysis of *TaHMW-GS::AtGA20ox1* X *ZmGlb1::PcGA2ox1* effects on yield 240

7.2.5 Analysis of *TaHMW-GS::AtGA20ox1* X *ZmGlb1::PcGA2ox1* effects on quality.....245

7.2.5.1 Grain hardness and moisture content 245
7.2.5.2 α-amylase and nitrogen content.....247

7.3 Conclusions..... 250

Chapter 8. General Discussion **252**

Chapter 9. References **265**

Appendices **306**

Appendix 1: Primer sequences **306**

Appendix 2: TaqMan assay results for various constructs **308**

Appendix 3: GA internal standards **320**

List of Tables and Figures

Figure 1.1: Structure of a wheat plant 2

Figure 1.2: Annual global wheat production, area harvested and yield 5

Figure 1.3: Semi- and extreme dwarf varieties of wheat 6

Figure 1.4: Anatomy of a wheat grain 13

Figure 1.5: Cell layers in a developing wheat grain 13

Figure 1.6: Mature wheat spikelet and ears 14

Figure 1.7: Zadoks growth scale for wheat 26

Figure 1.8: Zadoks growth scale detailing grain development 26

Figure 1.9: Embryogenesis in a monocot grain 28

Figure 1.10: Developmental stages of a wheat grain 29

Figure 1.11: Development of different tissues of a wheat grain 31

Figure 1.12: Early stages of GA biosynthesis. 47

Figure 1.13: Late stages of GA biosynthesis and GA inactivation 50

Figure 1.14: GA signalling in plants 55

Figure 1.15: Basic schematic of promoter::GFP expression cassettes 69

Figure 3.1: Schematic of TaqMan assays 93

Table 3.1: List of available promoter: effector combinations 95

Table 3.2: T1 zygosity PCR results for *TaTri::PcGA2ox1* transgenic lines 98

Figure 3.2: TaqMan assay results for *TaTri::PcGA2ox1* transgenic lines 99

Table 3.3: Confirmation PCR results for T2 *TaTri::PcGA2ox1* transgenic lines 101

Figure 3.3: Southern hybridisation of *TaTri::PcGA2ox1* transgenic lines 103

Table 3.4: Success rate of TaqMan assays of transgenic lines harbouring various constructs 104

Figure 4.1: Basic structure of *HvChi26::Atgai* and *HvBeg1::Atgai* 108

Figure 4.2: Activity of aleurone specific promoter in wheat grain 114

Figure 4.3: Activity of embryo specific promoter in germinating grains 115

Figure 4.4: NRQs of *Atgai* and *GFP* in *HvChi26::Atgai* transgenic lines 116

Figure 4.5: Analysis of yield componenets on *HvChi26::Atgai* transgenic lines 118

Figure 4.6: Analysis of quality components on *HvChi26::Atgai* transgenic lines 121

Figure 4.7: NRQs of *TaAmy1* and *TaAmy2* on *HvChi26::Atgai* transgenic lines 123

Figure 4.8: Activity of embryo and aleurone specific promoter in wheat grain 126

Figure 4.9: Activity of embryo and aleurone specific promoter in germinating grain 127
Figure 4.10: NRQs of *Atgai* and *GFP* in *HvBeg1:Atgai* transgenic lines 128
Figure 4.11: Analysis of yield components of *HvBeg1::Atgai* transgenic lines 130
Figure 4.12: Analysis of quality components of *HvBeg1::Atgai* transgenic lines 132
Figure 4.13: NRQs of *TaAmy1* and *TaAmy2* in *HvBeg1::Atgai* transgenic lines 134
Figure 5.1: Basic structure of *HvGerF::AtGA20ox1* and *TaDFRd::AtGA20ox1* 140
Figure 5.2: Activity of inner integument and pericarp-specific promoter in wheat grain 145
Figure 5.3: NRQs of *AtGA20ox1* in *HvGerF::AtGA20ox1* transgenic lines 147
Figure 5.4: Analysis of yield components in *HvGerF::AtGA20ox1* transgenic lines ... 149
Figure 5.5: Analysis of quality components on *HvGerF::AtGA20ox1* transgenic lines 151
Figure 5.6: Activity of inner integument-specific promoter in wheat grain 153
Figure 5.7: NRQs of *AtGA20ox1* in *TaDFR-D::AtGA20ox1* transgenic lines 155
Figure 5.8: Analysis of yield components in *TaDFR-D::AtGA20ox1* transgenic lines. 157
Figure 5.9: Analysis of quality components on *TaDFR-D::AtGA20ox1* transgenic lines 159
Figure 5.10: Formula to fit nonlinear model 161
Table 5.1: Estimates of parameters of average weight per grain in *HvGerF::AtGA20ox1* and *TaDFR-D::AtGA20ox1* transgenic lines 163
Table 5.2: Estimates of time to maximal weight per grain in *HvGerF::AtGA20ox1* and *TaDFR-D::AtGA20ox1* transgenic lines 165
Figure 5.11: Fitted curves for average weight per grain of *HvGerF::AtGA20ox1* transgenic lines 167
Figure 5.12: Fitted curves for average weight per grain of *TaDFR-D::AtGA20ox1* transgenic lines 168
Table 5.3: Estimates of parameters of average area per grain in *HvGerF::AtGA20ox1* and *TaDFR-D::AtGA20ox1* transgenic lines 170
Table 5.4: Estimates of time to maximal size per grain in *HvGerF::AtGA20ox1* and *TaDFR-D::AtGA20ox1* transgenic lines 172
Figure 5.13: Fitted curves for average area per grain of *HvGerF::AtGA20ox1* transgenic lines 173

Figure 5.14: Fitted curves for average area per grain of *TaDFR-D::AtGA20ox1* transgenic lines 174
Figure 6.1: Basic structure of *TaTri::PcGA2ox1, TaEND1::AtGA20ox1* and *TaEND1::Atgai* 181
Figure 6.2: Activity of endosperm specific promoter in wheat grain 185
Figure 6.3: Activity of endosperm transfer layer specific promoter in wheat grain . 186
Figure 6.4: NRQs of *PcGA2ox1* gene in *TaTri::PcGA2ox1* transgenic lines 188
Figure 6.5: Analysis of yield components in *TaTri::PcGA2ox1* transgenic lines..... 190
Figure 6.6: Analysis of quality components in *TaTri::PcGA2ox1* transgenic lines 193
Figure 6.7: NRQs of *TaAmy1*, *TaAmy2* and *TaGA20ox3* genes in *TaTri::PcGA2ox1* transgenic lines 195
Figure 6.8: NRQs of *AtGA20ox1* in *TaEND1::AtGA20ox1* transgenic lines 198
Figure 6.9: Analysis of yield components in *TaEND1::AtGA20ox1* transgenic lines.. 200
Figure 6.10: Analysis of quality components on *TaEND1::AtGA20ox1* transgenic lines 203
Table 6.1: GA concentrations in grain from *TaEND1::AtGA20ox1* transgenic lines .. 205
Figure 6.11: NRQs of *TaGA20ox3* in *TaEND1::AtGA20ox1* transgenic lines 207
Figure 6.12: NRQs of *Atgai* in *TaEND1::Atgai* transgenic lines..... 209
Figure 6.13: Analysis of yield components on *TaEND1::Atgai* transgenic lines 211
Figure 6.14: Analysis of quality components on *TaEND1::Atgai* transgenic lines..... 213
Table 6.2: GA concentrations in grains of *TaEND1::Atgai* transgenic lines..... 215
Figure 6.15: NRQs of *TaGA20ox3* in *TaEND1::Atgai* transgenic lines..... 217
Figure 7.1: Basic schematic of *TaHMW-GS::AtGA20ox1* and *ZmGlb1::PcGA2ox1* 222
Table 7.1: Crossing plan for hybrid wheat lines..... 226
Table 7.2: Genotypes identified for yield and quality study..... 227
Table 7.3: Mendelian segregation ratio in the F2 generation 228
Table 7.4: PCR analysis of segregating F2 progeny..... 229
Figure 7.2: TaqMan assay for F2 progeny resulting from cross A 231
Figure 7.3: TaqMan assay for F2 progeny resulting from cross B 232
Figure 7.4: TaqMan assay for F2 progeny resulting from cross C 233
Figure 7.5: TaqMan assay for F2 progeny resulting from cross D 234
Table 7.5: Zygosity analysis and genotype confirmation in F3 transgenic lines..... 236
Figure 7.6: NRQs of *AtGA20ox1* and *PcGA2ox1* expression in *TaHMW-GS::AtGA20ox1* X *ZmGlb1::PcGA2ox1* transgenic lines. 239

Figure 7.7: Analysis of yield components on *TaHMW-GS::AtGA20ox1* X *ZmGlb1::PcGA2ox1* hybrid lines....242
Figure 7.8: Analysis of grain hardness and moisture content on *TaHMW-GS::AtGA20ox1 X ZmGlb1::PcGA2ox1* hybrid lines....246
Figure 7.9: Analysis of α-amylase and nitrogen of *TaHMW-GS::AtGA20ox1* X *ZmGlb1::PcGA2ox1* hybrid lines....248
Table A.1: Sequences of genotyping primers....306
Table A.2: Sequences of TaqMan assay primers and probes....306
Table A.3: Sequences of qRT-PCR primers....307
Figure A.1: TaqMan assay results for *TaEND1::AtGA20ox1*....308
Table A.4: Confirmation PCR results for T2 *TaEND1::AtGA20ox1* transgenic lines....309
Figure A.2: TaqMan assay results for *HvGerF::AtGA20ox1*....310
Table A.5: Confirmation PCR results for T2 *HvGerF::AtGA20ox1* transgenic lines....311
Figure A.3: TaqMan assay results for *TaDFR-D::AtGA20ox1*....312
Table A.6: Confirmation PCR results for T2 *TaDFR-D::AtGA20ox1* transgenic lines....313
Figure A.4: TaqMan assay results for *HvChi26::Atgai*....314
Table A.7: Confirmation PCR results for T2 *HvChi26::Atgai* transgenic lines....315
Figure A.5: TaqMan assay results for *HvBeg1::Atgai*....316
Table A.8: Confirmation PCR results for T2 *HvBeg1::Atgai* transgenic lines....317
Figure A.6: TaqMan assay results for *TaEND1::Atgai*....318
Table A.9: Confirmation PCR results for T2 *TaEND1::Atgai* transgenic lines....319
Table A.10: Amounts of 2H2-GA standards....320

Abbreviations

GA	Gibberellin
FAO	Food and Agricultural Organisation of the United Nations
Rht	Reduced Height
LI	Light intercepted
RUE	Radiation use efficiency
HI	Harvest index
GM	Genetically modified
PSI	Particle size index
AX	Arabinoxylans
WEAX	Water-extractable AX
WUAX	Water-unextractable AX
GPC	Grain protein content
dpa	Days post anthesis
GS	Growth stage
ABA	Abscisic acid
NO	Nitric oxide
TFs	Transcription factor
BRs	Brassinosteroids
SA	Salicylic acid
CK	Cytokinin
JA	Jasmonic acid
SL	Strigolactones
ROS	Reactive oxygen species
PHS	Pre-harvest sprouting
PMA	Premature α-amylase
GGDP	Geranylgeranyl diphosphate
P450s	cytochrome P450 mono-oxygenases
2-ODDs	2-oxoglutarate-dependant dioxygenases
CPP	ent-copalyl diphosphate
MEP	2-C-methyl-D-erythritol-4-phosphate
CPS	CPP synthase
KS	ent-kaurene synthase
MVA	Mevalonic acid
Ent-CDP	ent-copalyl diphosphate
KO	ent-kaurene oxidase
KAO	ent-kaurenoic acid oxidase
GFP	green fluorescent protein

CaMV35S	Cauliflower mosaic virus
ml	Millilitre
mm	Millimetre
mM	Millimolar
ng	Nanogram
µg	Microgram
µl	Microlitre
µm	Micrometre
RCBD	Randomised complete block design
DNA	Deoxyribonucleic acid
RNA	Ribonucleic acid
gDNA	Genomic DNA
rpm	revolutions per minute
PCR	Polymerase chain reaction
Sec	Seconds
Min	Minutes
qRT-PCR	real-time quantitative PCR
SDS	sodium dodecyl sulphate
RQ	Relative quantification
Ct	threshold cycle
NRQ	Normalised relative quantification
BSA	Bovine serum albumen
TGW	thousand grain weight
SKCS	Single Kernel Characterisation System
ANOVA	analysis of variance
LSD	Least significant difference
REML	Residual Maximum Likelihood
Kb	kilo bases
bp	base pairs
ΔCt	comparative Ct
HFN	Hagberg falling number
CDS	coding sequence
SEM	standard errors of the mean
WT	wild-type
SED	standard error of the difference
df	degrees of freedom
CU	ceralpha units
ETC	Endosperm transfer cells
FRET	Fluorescence resonance energy transfer

Chapter 1. Introduction

1.1 Wheat

Wheat (Figure 1.1), a monocotyledonous plant along with other cereals belongs to the grass family Poaceae, which with about 10,000 species is one of the largest families of flowering plants (Peterson, 1965, Kellogg, 2001). Being one of the main food grains consumed throughout the world, wheat has the broadest geographic range of cultivation of all cereal crops (Briggle and Curtis, 1987) and is grown on more land area than any other crop, on every continent except Antarctica and grows from 67^{o} N in Scandinavia and Russia to 45^{o} S in Argentina. It also grows at a range of elevations from 260 m below sea level in the Jordan valley to 4,000 m on the Tibetan plateau (Feldman, 1995, FAOSTAT, 2016). The earliest cultivated forms of wheat were the diploid Einkorn (genome AA) and the tetraploid Emmer (genome AABB), known to be in cultivation about 10,000 years ago in south eastern Turkey (Heun *et al.*, 1997, Nesbitt, 1998, Dubcovsky and Dvorak, 2007). Modern-day hexaploid, bread wheat (*Triticum aestivum*) (genome AABBDD) arose through hybridisation of Emmer and a wild grass *Triticum tauschii* (genome DD) (Shewry, 2009) and spread to the east around 9,000 years ago. As hexaploid wheat arose relatively recently little divergence is observed between the D genomes of the hexaploid and ancestral diploid species *Triticum tauschii* (Feldman, 2001). Of all the wheat grown worldwide 95% is hexaploid bread wheat and the other 5% is tetraploid (*Triticum durum*) wheat grown mainly for making pasta (Shewry, 2009). Currently there are approximately 5,000 varieties of bread wheat in cultivation around the world and throughout history there have been about 35,000 varieties – more than any other cereal crop – most of which are no longer commercially grown (Kew, 2016).

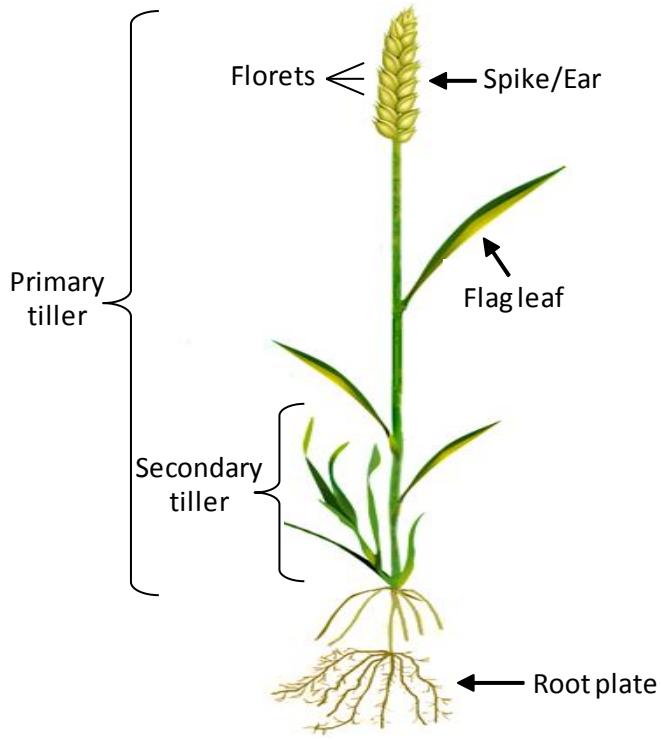


Figure 1.1: Structure of a wheat plant

1.1.1 Food Security and Wheat

Food security is achieved when every person, at all times has physical and economic access to sufficient, safe and nutritious food. According to the Food and Agricultural Organisation of the United Nations (FAO), globally around 795 million people are undernourished, which is a reduction from around 1 billion in 1990-1992. However, this reduction has slowed down in recent years due to a gap in the socio-economic growth and political instability in many developing regions (FAO, 2015). Of the world's chronically poor and hungry, 75% live in rural areas and 50% of all undernourished people in the world are small-scale farmers in developing countries (World Bank, 2007). Apart from this about two billion people in parts of southern Asia and sub-Saharan Africa also suffer from "hidden hunger", a form of malnutrition due to the lack of or inadequate consumption of micronutrients (Grebmer *et al.*, 2014, FAO, 2015). Micronutrient deficiency can occur even where food supply is adequate to meet energy requirements, but the diet lacks variety. Fruits, vegetable and

animal-sourced foods contain large amounts of micronutrients and are unaffordable in large parts of the developing world. Along with that a minimum amount of fat is required in the diet for the absorption of vitamins A, D, E and K (Kennedy *et al.*, 2002). This malnutrition limits the growth, development, health and working capacity of the sufferers, who are mainly women and children as they have a greater requirement of micronutrients (Grebmer *et al.*, 2014). Micronutrient deficiency can also cut the gross domestic product of developing countries by 0.7-2% pushing countries into a cycle of poor nutrition and lost productivity leading to further poverty (UNICEF and Micronutrient Initiative, 2004).

To increase further the already immense pressures on food security exerted by the current mal- and undernourished people, median estimates predict that the world population will increase to nine billion by 2050, with the majority of the increase in low income countries (Department of Economic and Social Affairs, 2015, Foresight, 2011). It is also predicted that global temperatures will increase and the climate will continually change at a rapid rate in this century, mainly due to greenhouse gas emissions including CO_2. This will result in altered rainfall and increased drought having a direct impact on crop production, posing a further threat to food security (McKersie, 2015). Rising mean temperatures will also result in the shortening of the time to maturity for crops and reduced grain set (Moriondo *et al.*, 2011). Though the relationship between weather and yields is specific for each crop and region and depends on the baseline climate, soil management systems, duration and timing of the exposure of the crop to different conditions, it has been shown that yields of wheat begin to decline with every 1^{o}C to 2^{o}C increase in local temperature in the tropics (Porter *et al.*, 2014). However, adaptation of wheat to 2-3^{o}C rise in local temperature could help avoid this yield loss in tropical regions (Challinor *et al.*, 2014)

It is critical that the global production of wheat is increased to match future demands. However, agriculture already has major environmental impacts

where land clearing to increase crop production threatens biodiversity, a quarter of global greenhouse gas emissions are a result of land clearing, crop production and fertilisation and in addition the use of fertilisers can also be harmful to marine and terrestrial ecosystems (Dirzo and Raven, 2003, Burney *et al.*, 2010, Tilman *et al.*, 2011). Thus, it is crucial that any increase in yield is adaptable to climate change, and is generated without an increase in the amount of land used or additional inputs into agricultural systems, and does not come at the expense of nutritional quality.

Wheat provides a high amount of vegetable protein compared to other major cereals like maize and rice (USDA, 2016), and provides about 20% of humanity's protein and 21% of the food calories consumed globally. In 2014 the production of wheat was at its highest with almost 729 million tonnes produced globally with an increase from 711.4 million tonnes in 2013 (FAOSTAT, 2016). Figure 1.2 also shows that the yield per hectare has greatly increased over the last 50 years while the area harvested has remained almost the same. This increase in yield has largely been due to higher yielding varieties, increased use of fertilisers and modernisation of agricultural practices (Evans, 1998).

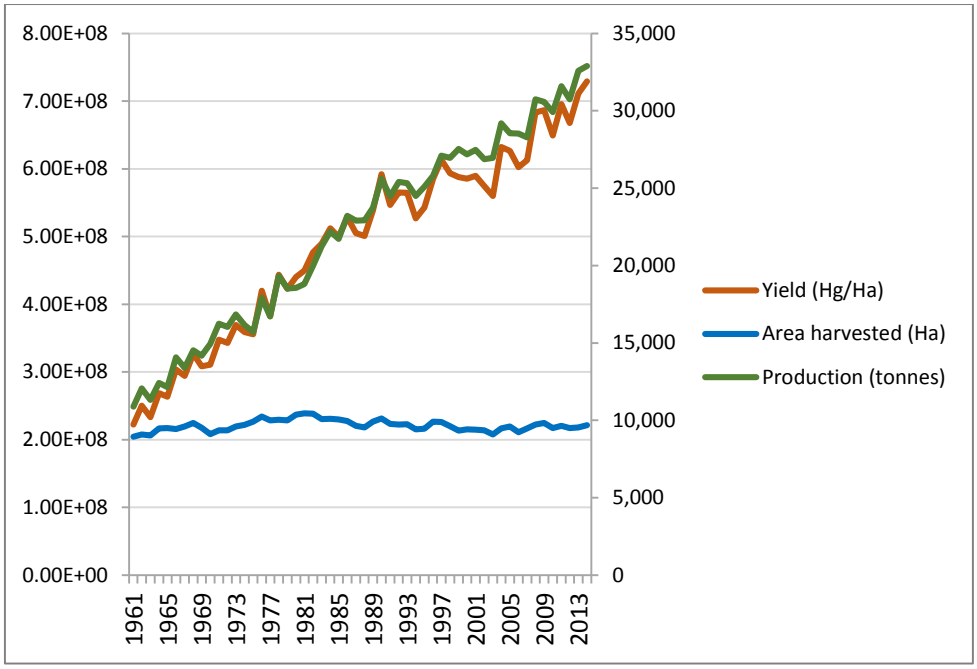


Figure 1.2: Annual global wheat production, area harvested and yield
Ha: hectare, Hg/Ha: Hectogram per hectare (FAOSTAT, 2016)

The "Green Revolution" of the 1960s was responsible for greatly increasing wheat and rice yields due to use of high yielding varieties along with the application of fertilisers and pesticides (Evenson and Gollin, 2003). The introduction of dwarfing genes in cereal crops played a significant role in this improvement (Hedden, 2003), producing plants with a shorter stem (Figure 1.3) which were more resistant to lodging and where resources were diverted to grain production rather than stem elongation (Flintham *et al.*, 1997). This resulted in the doubling of wheat yields between the years of 1965 and 1970 preventing large scale famines in Asia and Latin America (Evans, 1998).

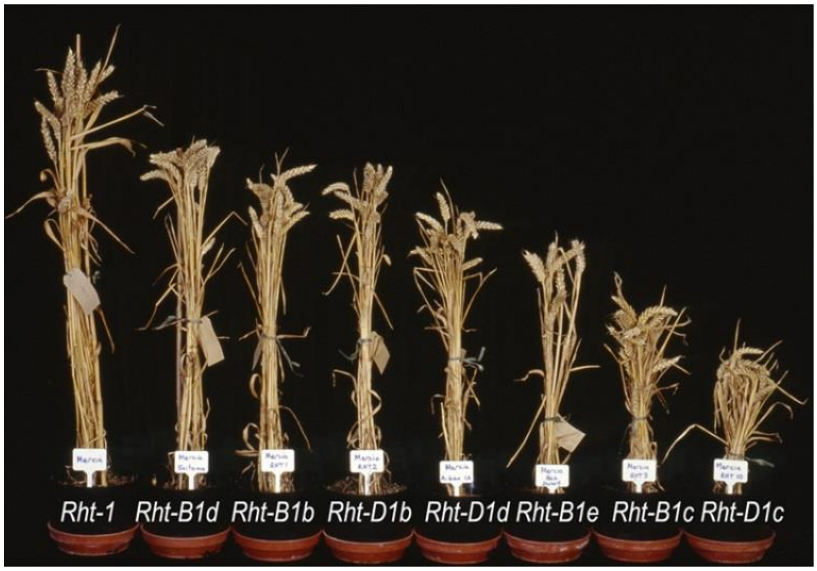


Figure 1.3: Semi- and extreme dwarf varieties of wheat

The *Reduced Height* (*Rht1*) genes governing the dwarf phenotypes of wheat were identified and shown to interfere with the signalling pathway of the growth hormone gibberellin (GA) (Peng *et al.*, 1999). There are multiple forms of GAs which are diterpenoid compounds forming a large family of compounds endogenous to higher plants as well as some lower plants, fungi and bacteria. GAs are involved in multiple growth and development processes, including: stem and root elongation, flower and fruit development, seed germination and development, and leaf expansion (Hedden and Kamiya, 1997). GA is also known to play an important role in seed development affecting germination, grain size and flour quality (Vaughan, unpublished data) (Jacobsen and Chandler, 1987, Swain *et al.*, 1997). GA is central to the approaches adopted in this thesis and is discussed in more detail in section 1.3.

Despite advances made through the green revolution and modern agronomic practice, the demand for wheat is predicted to increase at a faster rate than the genetic gains currently being realised (Rosegrant and Cline, 2003, Fischer, 2007). Wheat yield is a complex trait controlled by multiple genes contributing to a yield potential which, in turn, is affected by multiple biotic and abiotic stresses. In simplest terms, yield potential is the amount of yield achievable in the absence of water, nutrient, disease and weed limitation (Evans and Fischer,

1999). It is expressed as a function of the light intercepted (LI) and radiation use efficiency (RUE), the product of which gives biomass. Harvest index (HI) is the partitioning of biomass to the grains. The efficiency of plants to harvest photosynthetic energy by mature leaves and then its use by non-photosynthetic organs also effects yield potential (Reynolds *et al.*, 2009, Curtis and Halford, 2014).

However, the steady increase in yields since the green revolution has also been due to improved agronomic practices, genetic improvements in yield potential, improved disease resistance and better adaptation to various abiotic stresses (Evenson and Gollin, 2003). In the UK the yield increase from the 1970s to 1980s was due to an increase in HI coinciding with the introduction of semi-dwarfing genes, whereas the increase from the 1980s to 1990s was a result of the introduction of alien chromatin, such as the 1BL.1RS translocation in the Great Plains and the 7DL.7Ag wheat-*Agropyron elongatum* translocation in Mexico which resulted in an increase in biomass (Foulkes *et al.*, 2007). Light interception, which is related to establishment, and delayed senescence is not believed to be a bottle neck for improving yield potential. Theoretically there is a limit of 62% to HI, but it has not increased since the mid-1980s from approximately 50%. RUE which is the utilisation of solar radiation per unit of dry matter production has not changed much recently, although it is believed that the theoretical limit of RUE has not been reached (Sayre *et al.*, 1997, Donmez *et al.*, 2001, Evenson and Gollin, 2003, Reynolds and Borlaug, 2006, Reynolds *et al.*, 2009).

It is believed that RUE can be further increased by increasing the sink-strength in wheat (Reynolds *et al.*, 2005). There is a negative relationship between average grain weight and number of grains, indicating that an increase in grain number results in a reduction in grain weight (Miralles and Slafer, 1995). This reduction in grain weight may not be due to limitation in source availability, but due to an increased proportion of grains in the distal positions of the spikelets (Acreche and Slafer, 2006). According to Borras *et al*. (2004), sucrose

limitation is not a factor in grain growth and yield potential needs to be improved by increasing the sink strength during grain filling (Miralles and Slafer, 2007). It is believed that sink strength is a critical yield limiting factor in wheat and improving the balance between source and sink is important for increasing RUE, biomass and yield (Calderini *et al.*, 1997, Reynolds *et al.*, 2005). The source-sink relationship is also affected by water deficiency as it results in in a modification of growth priorities by reducing photosynthetic rate and grain size and number (Roitsch, 1999, Jamieson *et al.*, 1995). In addition the availability of nitrogen also improves yields by increasing the relative growth rate, leaf area, net assimilation rate and the rate and duration of grain filling (Warraich *et al.*, 2002). To achieve grain yields it is important to understand the genetic and molecular mechanisms that control the partitioning of assimilates during grain development and those that determine grain size and use this information to improve grain yield.

1.1.2 Genetically modified (GM) plants and food security

Biotechnology offers a capability to accelerate crop improvement for traits that might be not be possible through conventional breeding methods. Traits that improve resistance to biotic and abiotic stresses, nitrogen and water use efficiency and improved yield and quality can also reduce the dependence on agricultural inputs (Huesing *et al.*, 2016). According to Qaim and Kouser (2013) GM crops could impact food security in three ways: first they could increase food production and improve availability of food, second they could improve food safety and quality and third they could influence the economic and social situation of small scale farmers.

Agricultural biotechnology emerged in the 1980s and GM crops were commercially first introduced in 1996 in the USA (Kok and Kuiper, 2003). Since then their use by farmers has increased by a significant rate and within the first decade of their introduction the area under GM crops went up by more than

50-fold (Bhalla, 2006). In 2010 the direct global farm income benefit from GM crops was estimated at 14 billion US dollars, adding an extra 4.3% to the global production of four crops – soybean, maize, oilseed rape and cotton. From 1996 till 2010 the cumulative increase in farm income from GM technologies has reached approximately 78.4 billion US dollars and in 2014, 18 million farmers in 28 countries were growing GM crops on a total of 181.5 million hectares (Yongjun and Lin, 2013, Huesing *et al.*, 2016). The first generation of GM crops introduced insect-resistance and herbicide tolerance in four crops and these plants account for 99% of commercialised GM crops grown around the world. No GM crops with complex traits such as abiotic stress tolerance, nutritional use efficiency or yield potential have been commercialised (Yongjun and Lin, 2013).

Genetically Modified crops have been one of the fastest adopted agricultural technologies in history, though this has been geographically very uneven. While countries in North and South America and some parts of Asia have accepted the use of GM crops, this has not occurred in Europe and Africa (Qaim, 2016a). Despite the potential benefits of GM crops they have faced significant opposition from the public. One of the concerns with glyphosate resistant GM crops is that they increase the presence of herbicide-resistant 'superweeds' due to the liberal use of glyphosate. Since the introduction of herbicide tolerant plants, weeds resistant to glyphosate have been identified, but resistance to other herbicides has also been seen (Gilbert, 2013). Another concern with GM crops is that they are responsible for the high number of farmer suicides in developing countries due to the high cost of seeds and the misinformation on how to use them leading to financial losses. Gruere and Sengupta (2011) conducted a comprehensive study of available data on the use of *Bt* cotton and farmer suicides in India and concluded that the number of farmer suicides from 1997 to 2007 remained around 20,000 per year, whereas farmer profits have risen. Even though *Bt* cotton wasn't very successful in the beginning it has resulted in increased yields due to reduced losses from insect pests. Between 2002 and 2008 farmer profits rose by over 50% mainly due to

these yield gains and now 90% of the cotton grown in India is genetically modified (Kathage and Qaim, 2012).

One of the earliest environmental concerns with GM crops was the possibility of their out-crossing with other indigenous crops. Opponents of the technology also consider the use of genes across species boundaries as unethical and unnatural (Qaim, 2016a). In field trials in Europe it was shown that the pollen mediated gene flow between GM and non-GM rice plants was between <0.2% for neighbouring plants and <0.0125% for those at 10 m. Other studies have also shown similar results with gene flow always being less than 1%, even when GM and non-GM plants are grown together in the same plot (Messeguer *et al.*, 2004, Rong *et al.*, 2007, Jia *et al.*, 2007). Several solutions have been proposed to avoid any cross pollination between GM and non-GM plants such as using different crop species as natural barriers, maintaining a minimum distance between crops, and planting to ensure differences in flowering time (Devos *et al.*, 2009, Serrat *et al.*, 2013). Several molecular strategies are also used, such as maternal inheritance of the transgene, male sterility of the GM crops and seed sterility (Daniell, 2002).

There are also believed to be health risks associated with GM crops due to the introduction of foreign genes that might produce substances toxic to humans and other organisms. Several long-term studies have been carried out to confirm the safety record of GM crops (Snell *et al.*, 2012, Qaim, 2016b). Another concern regarding health risks is the use of antibiotic resistant genes, which are used as selection markers in the production of GM plants. It is believed that they could through horizontal gene transfer be transferred to the bacteria in gastrointestinal tract of humans, making antibiotic treatments less effective. Even under highly artificial conditions it was shown that the likelihood of horizontal transfer of antibiotic resistance genes is less than one in one-trillion. Though Netherwood *et al.* (2004) did show gene flow from transgenic plants to the small bowel of people with ileostomies. They also propose that the gene transfer events are unlikely to alter gastrointestinal

function or endanger human health. However, to ensure that this does not pose as a risk to human health new GM technologies have been developed which either use different selection markers or antibiotic resistance that has no use in human medicine, or are completely marker-free (Qiu *et al.*, 2010, Qaim, 2016b).

There are many risks that might be associated with the use of GM crops and they need to be addressed on a case by case basis before they are commercialised for human use. There are also many potential advantages that GM crops provide and the development of 'Golden Rice' (Ye *et al.*, 2000) is an example of this. Vitamin A deficiency effects 250 million preschool children and more than seven million pregnant women in more than half the countries of the world, particularly in Africa and south-east Asia. It is estimated that 250,000 to 500,000 of these children will become blind every year, half of them dying within 12 months of losing their sight (World Health Organisation, 2016). Golden Rice produces provitamin A (β-carotene) in the endosperm of the grain, something that doesn't happen naturally. In developing countries where rice is a staple food this biofortification of rice offers a solution towards dealing with this form of malnutrition (The Golden Rice Project, 2016).

1.2 Wheat Grain

The wheat grain, a single seeded fruit is surrounded by a closely connected pericarp derived maternally from the ovary wall and is botanically known as a caryopsis. The different tissues of the grain are described in terms of their structure and embryonic origin and there are six main components; the embryo, starchy endosperm, aleurone layer, nucellar epidermis, testa and pericarp (Figure 1.4). The seed coat and other pericarp tissues which are made up of the outer pericarp, inner pericarp (comprising cross cell and tube cells), seed coat (testa), nucellar epidermis (hyaline layer) and the aleurone layer (Figure 1.5) enclose the starchy endosperm and the embryo, which consists of the scutellum and embryonic axis (Figure 1.4). The scutellum forms the back of the embryo and is present as a shield shaped structure and is considered the first leaf (cotyledon) of the embryo (Bradbury *et al.*, 1956, Peterson, 1965, Bennett *et al.*, 1975, Evers and Millar, 2002). During germination, the scutellum acts not only as a source of food for the embryo, but also digests and absorbs the reserves stored in the endosperm to support development. The endosperm consists of a mass of thin walled cells, the starchy endosperm which is surrounded by a single layer of thick walled aleurone cells (Peterson, 1965). The seed coat and other pericarp tissues, making up the bran, amount to 2-13% of the grain, the embryo makes up 2.8-3.5% and the aleurone layer 6.5%. The major part of a mature grain is comprised of the endosperm (56-74%) comprising the sub-aleurone layer and the starchy endosperm which is primarily made up of carbohydrates and gluten proteins. The protein content in the grain has an average range of 8-11% while lipids (2-4%) and minerals (1-3%) form a minor constituent. Moisture content of a grain at the time of harvest is between 11 and 14%. (Briggle and Curtis, 1987, Barron *et al.*, 2007, Koehler and Wieser, 2013). In a mature grain, each of the outer layers are of different thickness and are closely associated with each other. The thickest is the aleurone layer (up to 65 µm), followed by the outer pericarp (15-30 µm) and the seed coat being the thinnest (5-8 µm) (Barron *et al.*, 2007).

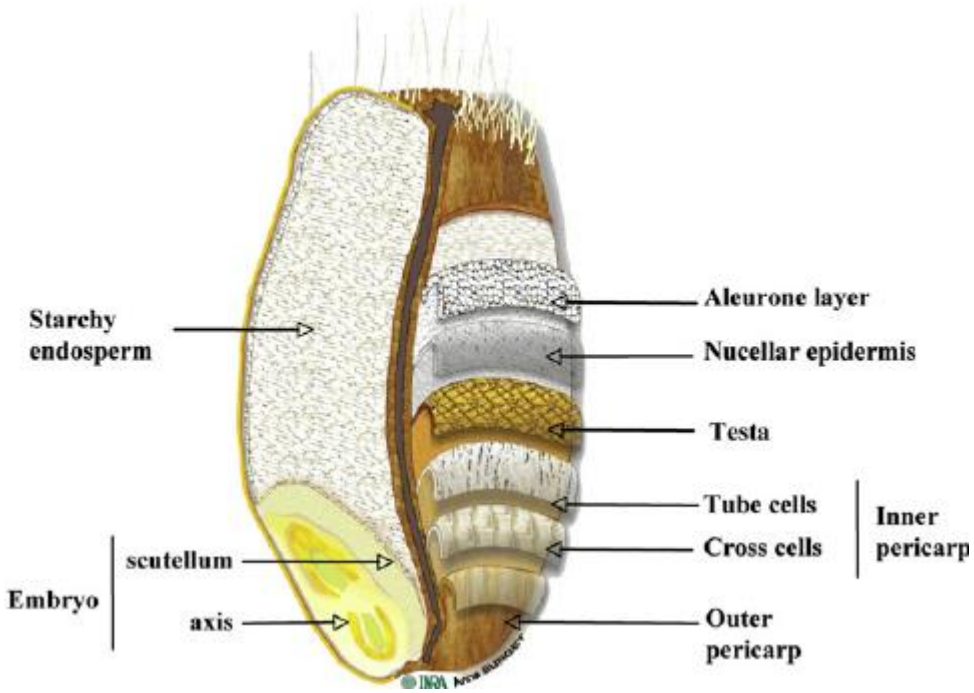


Figure 1.4: Anatomy of a wheat grain
(Saulnier *et al.*, 2012)

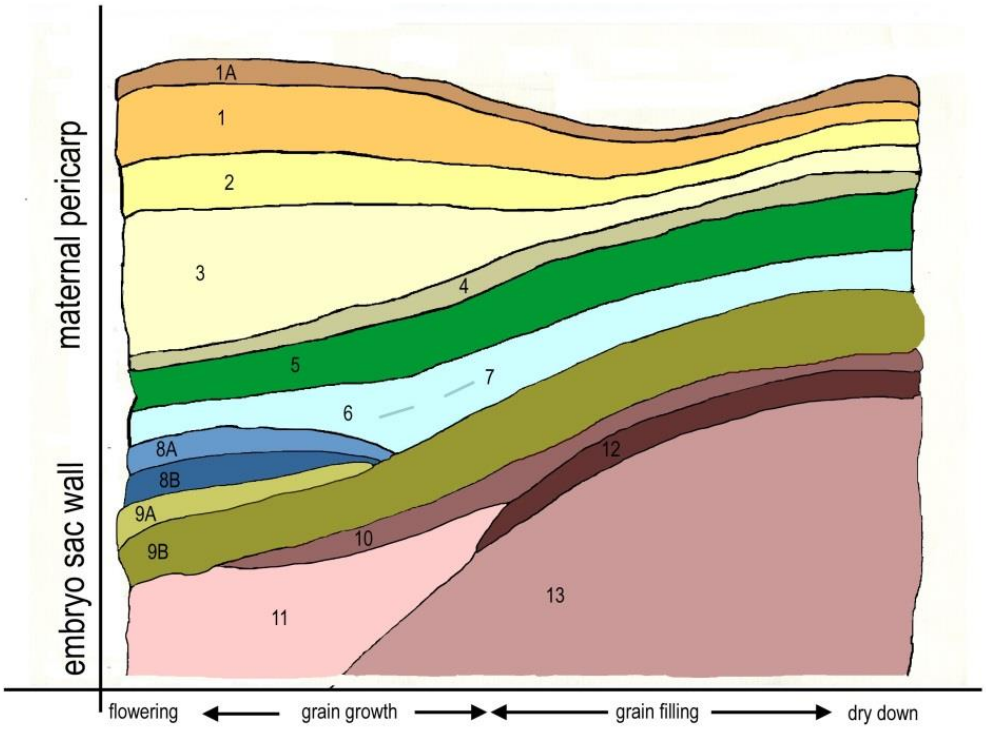


Figure 1.5: Cell layers in a developing wheat grain
Theoretical changes in the constituent layers of the grain from flowering until dry down. 1A: Cuticle of outer epidermis, 1: outer epidermis, 2: Hypodermis, 3: Parenchyma, 4: Intermediate cells, 5: Cross cells, 6 & 7: Inner epidermis/tube cells, 8A & 8B: outer integument, 9A & 9B: inner integument, 10: nucellar epidermis, 11: nucellus, 12: aleurone, 13: starchy endosperm (WheatBP, 2016).

Wheat grains are borne on an ear (Figure 1.1) where the major axis is known as the rachis and bears two rows of spikelets in alternating order (Figure 1.6). The axis of the spikelet is also branched alternately and bears a pair of empty or nonflowering glumes at the base and up to six florets in the spikelet. Each floret consists of a pair of flowering glumes comprising the outer lemma and an inner palea which enclose the ovary and later the grain (Bonnett, 1966). The growth of a grain is determined by many different factors such as the availability of resources and environmental conditions along with the plants genotype which determines its capacity to accumulate dry matter (growth potential) and the resistance of the phloem to the movement of resources. The growth potential of a grain is believed to exert the most pressure on grain weight and size. Individual grain size is also dependant on its position in the inflorescence and within the floret with grains in the central spikelets, being larger than those in the upper and lower spikelets, and grains in floret one and two bigger than those in the middle; this is due to both the rate and duration of grain filling (Bremner and Rawson, 1978).

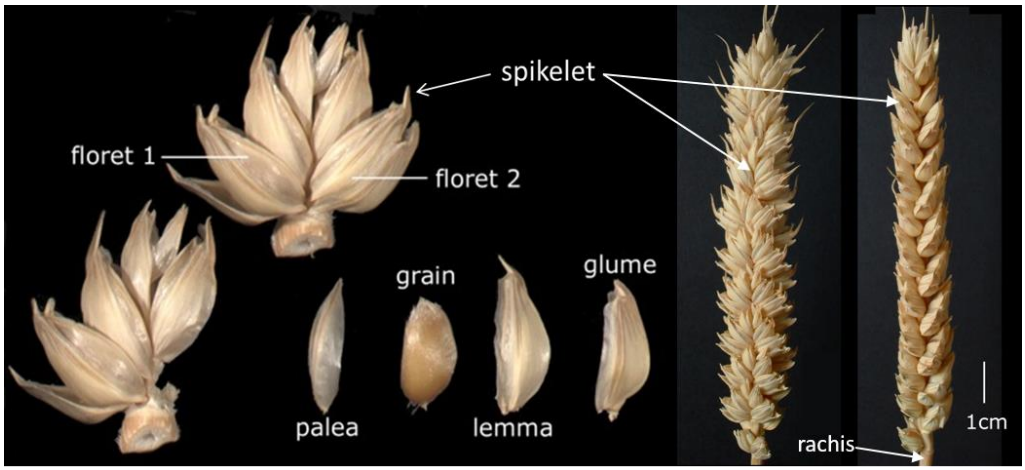


Figure 1.6: Mature wheat spikelet and ears
[modified from (WheatBP, 2016)]

1.2.1 Morphology and Composition

The members of the Triticeae family are distinguished from other cereals by the presence of a crease on the ventral side, extending along the grain's length and being deepest in the middle. It is most prominent in wheat and causes difficulty in separating the starchy endosperm from other tissues during milling to produce white flour (Evers and Millar, 2002). On the other side of the grain the outline of the embryo can be seen at the base of the grain (Peterson, 1965).

Bread wheat can be classified based on various characteristics: hard or soft, based on protein content, winter or spring depending on when its sown and red or white, based on the colour of the grain (Percival, 1921). For milling purposes a well-filled kernel is preferred as this ensures maximum endosperm to bran ratio (Morris and Rose, 1996). For processing, uniformity in grain shape and size is important, as more uniform samples have a more predictable milling performance (Edney, 1996).

The texture of the endosperm and kernel mass determines grain hardness, a trait that affects the baking, milling and end-use quality of flour. Different wheats are classified as hard or soft depending on their particle size index (PSI). Soft wheat kernels fracture more easily and release more intact starch granules and produce finer flour upon grinding with reduced starch damage (Giroux and Morris, 1997, Morris and Rose, 1996). During milling hard wheat produces large well-defined particles which form coarse textured flours with a higher level of starch damage (Maghirang and Dowell, 2003).

Wheat is classified as red or white according to the presence or absence of red pigment in the seed coat layer, accumulating in the inner integument during development (Peterson, 1965). Pigmentation in the aleurone layer can also give them a blue, red or a black appearance (Evers and Millar, 2002).

1.2.1.1 Starch

Starch is an important part of human diet and it is the major storage carbohydrate in cereals, present in the endosperm in granular form. The two forms of starch in cereal grain are amylose (25-28%) and amylopectin (72-75%) with amylose/amylopectin ratios affecting the quality of flour (Hung *et al.*, 2006). Amylopectin is responsible for the granular nature of starch due to its higher molecular weight than amylose (Buleon *et al.*, 1998). In the endosperm of wheat, rye and barley grains, two sizes of starch granules are present which is in contrast to most other plant species. They contain large ellipsoid A-granules with diameters around 20 µm and small spherical B-granules with an average size of 5 µm (Karlsson *et al.*, 1983). Within a cell the size of the starch granules is relatively uniform but this gradually declines in cells from the centre to the periphery (Evers and Millar, 2002).

Grains also contain other minor constituents such as arabinoxylans (AX) (1.5-8%), β-glucan (0.5-7%), sugars (~2.5%) and glucofructans (~1%) (Koehler and Wieser, 2013). Due to its high starch content, the major monosaccharide present in the endosperm as a component of starch is glucose (96% of the neutral sugars). Polysaccharides other than starch are the main constituents of cell walls and are much more abundant in the outer than the inner layers of the grain. These non-starch polysaccharides provide dietary fibre which has many positive health benefits (Blackwood *et al.*, 2000, Garcia *et al.*, 2007, Babio *et al.*, 2010). The major cell wall polysaccharide in the endosperm, AX gives rise to arabinose and xylose which account for 2% of the neutral sugars. Small amounts of arabinogalactan can contribute as much as 20% of the total arabinose present (Loosveld *et al.*, 1998). Based on their solubility AX can be subdivided into water-extractable (WEAX) and a water-unextractable (WUAX) fraction. In wheat WEAX accounts for 12-30% of total AX and has considerable functionality in bread making (Izydorczyk and Biliaderis, 1995, Koehler and Wieser, 2013).

AX is able to absorb 15-20 times its weight in water, forming a highly viscous solution which may be able to increase the gas holding capacity of wheat doughs by stabilising the gas bubbles. WEAX binds up to 25% of the water added to doughs (Gan *et al.*, 1995). WUAX fractions do not dissolve water and even though they have a high water holding capacity and assist in water binding during dough mixing they are considered to have a negative impact on bread making. This is because they form physical barriers against the gluten network, destabilising the gas bubbles (Koehler and Wieser, 2013). WEAX consists of two populations of alternating open and highly branched regions that are distinguished by their characteristic arabinose/xylose ratio, which is different for each layer if the grain (Dervilly *et al.*, 2000).

In the embryo, the amounts and composition of the neutral sugars is different from those in the endosperm. The scutellum and the embryonic axis contain 12% and 25% of carbohydrate, respectively (Barron *et al.*, 2007). In these tissues, arabinose and xylose make up 65% of the total neutral carbohydrates with a high arabinose/xylose ratio, similar to that in the seed coat (Antoine *et al.*, 2004). The nucellar epidermis is made up of neutral carbohydrates comprised of xylose, arabinose and glucose and account for 72% of this layer. This tissue is mainly cell wall polysaccharides composed of 93.7% AX and has a much lower arabinose/xylose ratio than the starchy endosperm (Izydorczyk and Biliaderis, 1993, Dervilly *et al.*, 2000). It is not possible to isolate pure seed coat from a mature grain and thus it is only possible to deduce the composition of carbohydrates in this layer. It appears to be poor in neutral carbohydrates with arabinose and xylose as the main components and a low arabinose/xylose ratio (Barron *et al.*, 2007). Cellulose is an abundant cell wall polysaccharide in the outer pericarp (25%) and intermediate layer (12.2%) whereas the aleurone is the main source of β-glucans (23%) (Pomeranz, 1988, Antoine *et al.*, 2004, Parker *et al.*, 2005). In wheat, β-glucans account for only 2% of the grain and possess a higher water solubility than AX (Koehler and Wieser, 2013).

1.2.1.2 Protein

The protein content in a wheat grain can vary from 6-20% dependent on the genotype, growing conditions and the amount of nitrogen (N) supplied. The majority of the protein, up to 30%, is present in the embryo and aleurone layers whereas the bran layers (~7%) and starchy endosperm (~13%) contain much lower levels (Belitz *et al.*, 2009). Grain Protein Content (GPC) is an important quality trait in bread wheat for which there is a positive relationship between protein content and loaf volume, while in Durum wheat high GPC and strong gluten are important for good quality flour (Finney and Barmore, 1948, Degidio *et al.*, 1990). The amino acid composition of all flours is typical in the fact that glutamine forms the major part of grain protein (15-31%). In wheat, this is followed by proline (12-14%), leucine (7-14%) and alanine (4-11%). Tryptophan (0.2–1.0%), methionine (1.3–2.9%), histidine (1.8–2.2%) and lysine (1.4–3.3%) which are nutritionally important are present only at very low levels (Koehler and Wieser, 2013).

Seed storage proteins are classified into different groups based on their extraction and their solubility in water (albumins), dilute saline (globulins), alcohol/water mixtures (prolamins) and dilute acid or alkali (glutelins), (Osborne, 1924). Albumins and globulins are metabolic proteins, mainly enzymes and enzyme inhibitors. These proteins are concentrated in the aleurone layer, bran and embryo, with very low concentrations in the endosperm (Koehler and Wieser, 2013). The main storage proteins in cereal grains are prolamins and glutelins and are located only in white flour. Their only biological function is to provide a developing seedling with nitrogen and amino acids during germination (Shewry and Tatham, 1990). Prolamins (gluten proteins) comprise of monomeric gliadins and polymeric glutenins which include both low (LMW-GS) and high (HMW-GS) molecular-weight glutenin subunits (Shewry and Tatham, 1990).

The ability of wheat flour to form a cohesive, viscoelastic dough when mixed with water makes it unique among cereals. It is the ability of wheat dough to

retain the gas produced during fermentation that results in a leavened loaf of bread after baking. It is known that gluten proteins account for the physical properties of wheat dough and both fractions of the protein are important contributors to this. Gliadins contribute mainly to the viscosity and elasticity of the dough whereas glutenins are responsible for dough strength and elasticity (Wrigley *et al.*, 2006). Even though high protein content has been a target for breeders there has been a decline in protein content in modern cultivars compared to historical ones. This is probably because any increase in protein content has been outstripped by increases in yield (Shewry *et al.*, 2016).

Metabolic proteins have better nutritional amino acid composition than storage proteins mainly due to their higher lysine content. The enzymes that hydrolyse carbohydrates and proteins to provide the developing seedling with nutrients during germination are of significant importance (Koehler and Wieser, 2013). The main carbohydrate hydrolysing enzymes are α-amylase, β-amylases, debranching enzymes, cellulases, β-glucanases and glucosidases. Amylases can be classified as endohydrolases as they hydrolyse polysaccharides in starch granules by attacking their glucosidic bonds at or near the end of the chains (Corder and Henry, 1989). α-amylase is the most important enzyme of the endohydrolase type and it hydrolyses the α-1,4-glucosidic bonds of amylose and amylopectin to produce a mixture of dextrins along with smaller amounts of maltose and oligosaccharides (Koehler and Wieser, 2013). Proteinases, proteases and peptidases are proteolytic enzymes that hydrolyse proteins and their biological function is to provide nutrients to a germinating embryo and thus their activity is highest during germination (Wang and Grant, 1969). Another class of metabolic proteins are lipases that attack triacylglycerides resulting in mono- and diacylglycerides and free fatty acids which are more susceptible to oxidative rancidity than fatty acids bound in triacylglycerides. Whereas, phytases hydrolyse phytic acid to inositol and free phosphoric acid, which is nutritionally beneficial because a complexation of cations such as zinc, calcium and magnesium ions by phytic acid is reduced (Singer and Hofstee, 1948, Lim and Tate, 1973).

1.2.1.3 Lipids

The embryo is the main source of lipids in grains with a small amount being present in the aleurone layer and much smaller amount in the endosperm. Lipids in most cereal species have similar fatty acid composition where linoleic acid content is the highest (39-69%) and the rest is made up by oleic acid (11-36%) and palmitic acid (18-28%). Even though lipids only form a small portion of wheat flour they greatly impact its baking performance (Delcour and Hoseney, 2010). Polar lipids have a positive effect on bread making with glycolipids contributing to the high baking performance of wheat flour and phospholipids being less important (Morrison *et al.*, 1975). Polar lipids affect the dough properties by improving their gas holding capacity, which is increased during proofing and enables a prolonged oven spring, increased loaf volume and better crumb resilience (Daftary *et al.*, 1968, Macritchie, 1981).

1.2.1.4 Minor components

The major proportion of minerals are present in the bran, the aleurone layer and the embryo of the grain. Compared to other foods, cereals have an intermediate concentration of minerals such as magnesium, zinc, and copper. Cereals are a good source of the B-group vitamins, thiamine, riboflavin, niacin, pantothenic acid, pyridoxine, biotin and folates and these are present in the same layers as the minerals. They also provide vitamin E and carotenoids (Oakenfull and Topping, 1987, Stevenson *et al.*, 2012).

1.2.2 Wheat Grain Development

The ovule comprising the embryo sac is embedded in the nucellus tissue and is delineated by the nucellar epidermis. Two integument layers surround the nucellus, one of which forms the micropyle. Preferential growth of the dorsal

side of the ovule causes it to bend from its initial upward position and this process completes before fertilisation, causing the position of the micropyle to move by about 180^{o} (Aziz, 1972). The embryo sac contains an egg nucleus and two polar nuclei at the micropylar end and several antipodal nuclei at the other end. In the final anatropous position of the ovule the antipodal cells are at the ventral side of the embryo sac close to the carpel wall and the extended chalaza (Bechtel *et al.*, 2009).

At the time of fertilisation pollen grains fall on a receptive stigma, a pollen tube develops and two male nuclei in the grain migrate down the style through the micropyle into the embryo sac (Evers and Millar, 2002). The first event post anthesis is the double fertilisation where one pollen reproductive nucleus fuses with two female polar nuclei within the embryo sac and give rise to the triploid endosperm nucleus, and the second pollen nucleus fuses with the egg nucleus to form the diploid zygote (Shewry *et al.*, 2012). The endosperm nuclei undergo several rounds of mitosis in the absence of cytokinesis for one to two days before cellularisation begins resulting in a single multinucleate cell with a peripheral zone of cytoplasm (syncytium) and a large central vacuole (Drea *et al.*, 2005, Shewry *et al.*, 2012). At this stage these tissues are surrounded by several layers of maternally originated cells – nucellus, nucellar epidermis, inner integument, outer integument, tube cells, cross cells and maternal pericarp (Figure 1.5) (Shewry *et al.*, 2012). Cellularisation begins nearest to the nucellus which is on the outside and then proceeds inwards (Evers, 1970, Mares *et al.*, 1975, Morrison and Obrien, 1976). Anticlinal cell walls separate the nuclei in the endosperm syncytium and form 'open cylinders' or alveoli and first appear in the crease region and then spread laterally along the endosperm lobes to the dorsal side. Periclinal walls also first appear on the innermost cells in the crease region, with walls of several adjacent cells occurring simultaneously (Fineran *et al.*, 1982).

After fertilisation, along with the embryo sac, the nucellus, integuments and carpel wall all undergo new development. The fertilised egg cell divides to form

a club-shaped embryo which begins differentiation after about seven days post anthesis (dpa) resulting in the embryonic axis comprising the plumule surrounded by the coleoptile, the mesocotyl and the radicle, and the scutellum (cotyledon) (Shewry *et al.*, 2012). When the embryo contains 10-15 cells, a single continuous layer of endosperm cells line the central vacuole (Evers and Millar, 2002). Several layers are then formed due to periclinal and anticlinal cell wall formation between the dividing nuclei and this process is completed by about four dpa when the walls growing from the ventral and dorsal sides of the grain meet (Shewry *et al.*, 2012). In the most rapid stage of embryo sac extension in early development the distal parts of the enclosing cell layers elongate by cell growth, and later less rapid elongation is accompanied by the development of all the coverings of the grain by the meristematic zones in their basal halves. The cells of the carpel wall at all stages are larger than those of the integuments, and carpel growth is more by cell elongation than cell division (Bhatnagar and Chandra, 1975). The ovule is a solid block of placento-chalazal tissue connecting its ventral side to the pericarp between the emerging points of the endosperm resulting in a fused zone that extends along the ventral side of the grain which leads to the formation of the crease of the wheat grain (Aziz, 1972, Bechtel *et al.*, 2009).

During early stages of development, the pericarp is made up of about 25 layers of parenchymatous cells attached to the outside by an outer epidermis and hypodermis and on the inside by a layer of chloroplast-containing cells and an inner epidermis. All pericarp cells have a large central vacuole and little cytoplasm (Evers and Millar, 2002, Bechtel *et al.*, 2009). The pericarp is important during development as it performs various useful functions: the cuticle on the outer epidermis limits water movement, the turgid parenchymatous cells are a fleshy tissue layer that provide protection and support for the growing grain and the chloroplast-containing cells may conduct photosynthesis along with storing starch (Evers and Millar, 2002). In the chalazal region, the pericarp and the nucellus are in direct contact with each other, whereas in other parts the nucellar surface is surrounded by two

integument layers, each composed of two layers of cells. As the grain develops the outer layers undergo progressive differentiation and degradation. By about 27 dpa the pericarp has reduced to a layer four or five cells thick, and is devoid of starch, while the inner integument changes and compresses to form a coloured layer. Together with the cuticle, they form the seed coat and in a mature grain all that remains of a nucellus, except in the crease region, are the epidermis and its cuticle (Bradbury *et al.*, 1956, Campbell *et al.*, 1981).

The endosperm starts differentiating at the beginning of the cellularisation stage with the cells derived from the first periclinal division of the alveolar nuclei becoming the aleurone layer and the inner layer of cells becoming highly vacuolated thin-walled cells which will form the starchy endosperm (Olsen, 2001). The aleurone cells behave like a cambium and divide periclinally till about 19 dpa. This results in the formation of a sub-aleurone layer due to the division and re-differentiation of aleurone cells. This layer is distinct from both the aleurone and the starchy endosperm cells (Jennings and Morton, 1963). In the inner part of the grain constituting the starchy endosperm the cell divisions are orientated randomly resulting in the loss of a pattern in the cell file (Sandstedt, 1946). The basic structure of the endosperm is established by 10 dpa and the synthesis and deposition of starch and storage proteins begins. Starch granules are first deposited in the peripheral cytoplasm, adjacent to the cell walls and as development proceeds these become enlarged and new granules are initiated. Deposition of protein bodies begins in the subaleurone layer and, as development proceeds, the number and size of these remains larger than those present in the central cheek cells of the endosperm. The synthesis of starch and proteins is most active between 14 and 28 dpa and continues till about 35-40 dpa followed by maturation and desiccation (Campbell *et al.*, 1981, Shewry *et al.*, 2012).

The endosperm cells located adjacent to the nucellar projection are morphologically distinct from the rest of the endosperm cells and are known as the modified aleurone (Morrison *et al.*, 1978), which develops transfer cell

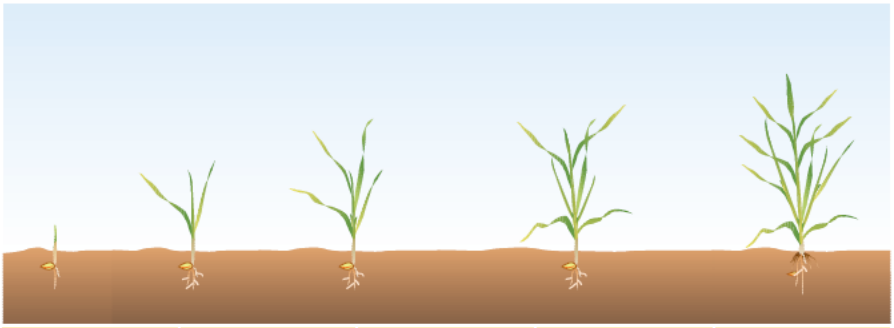
morphology characteristic of cells active in apoplastic/symplastic solute transport (Thompson *et al.*, 2001, Offler *et al.*, 2003). The nucellar cells adjacent to the aleurone transfer cells also show transfer-cell morphology (Wang *et al.*, 1994a). A symplastic transport system connecting the phloem to the endosperm is formed by the nucellar and aleurone transfer cells which facilitates the transport of sucrose from the vascular system to the endosperm, where it is converted to starch (Wang *et al.*, 1994b, Wang *et al.*, 1995a, Wang *et al.*, 1995b). The pericarp layer also contains simple vascular bundles during development and those in the chalazal region deliver nutrients to the endosperm and other vascular tissues. These cell layers are isolated from maternal tissues and have no plasmodesmatal connections (Evers and Millar, 2002). As the grain is developing, symplasmic continuity exists between the vascular tissue and the nucellus only through the chalazal zone and as the grain matures this layer becomes the pigment strand. The pigmentation in this layer is due to the accumulation of adcrusting substances that become coloured in red wheats (Zee and Obrien, 1970). Before differentiation of the aleurone layer is completed nutrients enter the grain via the nucellar epidermis and after that they are restricted to passage through the nucellar projection (Evers and Millar, 2002).

As the grain develops, the embryo and endosperm increase in mass and volume and the parenchymatous pericarp tissue next to the chlorophyll-containing cells starts to degenerate and this continues progressively outward. The degeneration of the pericarp is at a faster rate than the enlargement of the endosperm and this results in a space between the remaining outer and inner pericarp. During rapid accumulation of starch, the endosperm stretches and crushes the surrounding tissues. In the crease region, the tissue is not crushed and the nucellar cells remain as a pillar of tissue running along the inner margin of the crease. The vascular tissues and the associated parenchyma in the crease region do not degenerate as they do in other parts of the grain. During development, a cylindrical shaft of these cells between the vascular tissue and nucellar projection accumulate hydrophobic compounds of a corky and waxy

nature. The margins of the nucellar and integumental cuticle insert into this pigment strand and complete a water resistant barrier around the endosperm and embryo (Bechtel *et al.*, 2009).

1.2.2.1 Classification of Grain Development

The development of a wheat grain is most commonly classified by the Zadoks decimal code of growth stages of cereals based on the six stages of endosperm development – watery, milky, soft dough, hard dough, ripe and dead ripe (Zadoks *et al.*, 1974). This scale has 10 main stages of plant development which are sub divided further into each individual growth stage (GS). It starts at GS0 with germination and ends at GS9 with grain ripening (Figure 1.7). Anthesis begins at GS6.0 with the emergence of the anthers just above the middle of the ear, reaches half way when the anthers have emerged half way up the ear (GS6.5) and completes at GS6.9. At GS7.0 milk development of the grain begins and the caryopsis is water ripe at GS7.1 (Figure 1.8). From stage GS7.3 (early milk) to GS7.7 (late milk) there is an increase in the solids of the liquid endosperm which is notable when the grain is crushed between fingers and milky solution appears. Dough development begins at GS8.0 and at GS8.3 the grain is a soft dough and when squeezed the finger nail does not make an impression and liquid no longer appears. By GS8.7 the grain is a hard dough and when squeezed the finger nail leaves an impression and the ear is starting to lose chlorophyll. Grain ripening begins at GS9.0 and at GS9.1 the grain is hard and difficult to divide by thumb nail. At GS9.2 the grain is ripe and is no longer dented by thumbnail and at GS9.3 the kernel starts loosening at daytime. The grain is over-ripe and the straw is dead and starts collapsing by GS9.4. at GS9.5 the seed is in a dormant state and only reaches 50% viability at GS9.6. At GS9.7 the seeds are no longer dormant but secondary dormancy sets in at GS9.8 which is then lost at GS9.9 (Zadoks *et al.*, 1974).



Zadoks Growth Stage	GS 00 - 09	GS10 - 19	GS20 - 29	GS30 - 39	GS40 - 49
Development phase	Germination	Seedling growth	Tillering	Stem elongation	Booting



Zadoks Growth Stage	GS 50 - 59	GS60 - 69	GS70 - 79	GS80 - 89	GS90 - 99
Development phase	Ear emergence	Flowering	Milk Development (grain fill period)	Dough Development (grain fill period)	Ripening

Figure 1.7: Zadoks growth scale for wheat
(Poole, 2005)

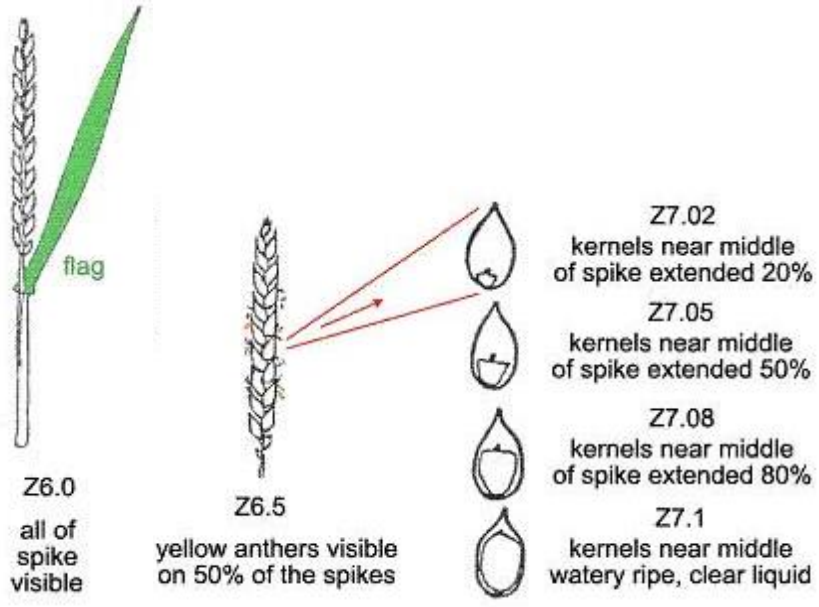


Figure 1.8: Zadoks growth scale detailing grain development
[Modified from (Stapper and Murray, 1986)]

An alternative method of classification based on the development of both the endosperm and the embryo and the appearance of the seeds was proposed by Noda *et al*. (1994). Based on their classification at stage 1, from fertilisation to five dpa, the embryo is globular and has not yet differentiated and the endosperm is growing rapidly (Figure 1.9). From five to 10 dpa, stage 2, the embryo has differentiated into the embryonic axis and the scutellum and the endosperm continues to expand rapidly. Starch and proteins start to accumulate at an early stage in endosperm development with starch granules observed at five dpa and protein bodies seen at six to seven dpa (Hoshikawa, 1961, Bechtel *et al.*, 1982). Just before anthesis the ovary is about 2 mm in length and white in colour but by five dpa the seeds are 4 mm in length and about 6 mm at 10 dpa and their colour is white-green (Figure 1.10). The green colour is due to the presence of chlorophyll in the inner pericarp cells and is partly obscured by small starch granules that are present in the parenchymatous cells between the inner and outer epidermis (Evers and Millar, 2002).

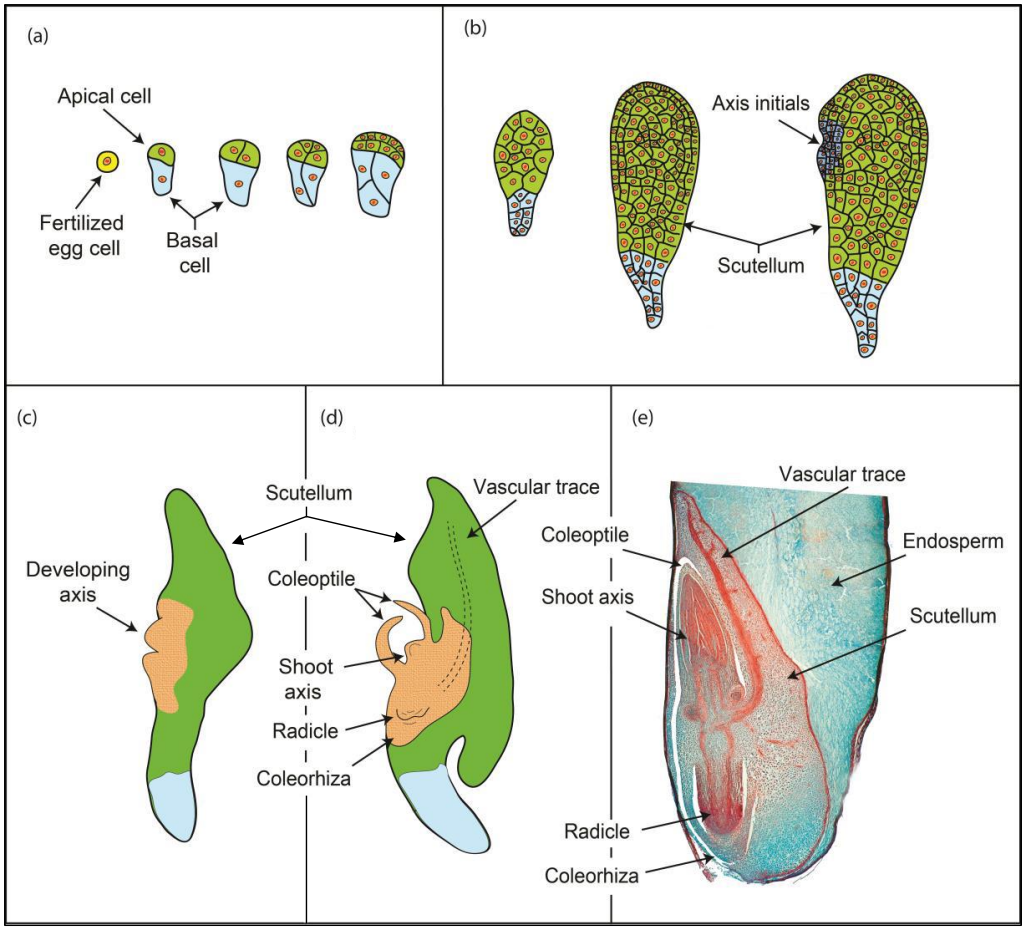


Figure 1.9: Embryogenesis in a monocot grain

Schematic of embryogenesis in corn (*Zea mays*) as a representative of a monocot grain. a: proembryo stage, b: globular stage, c: scutellar stage, d: coleoptile stage and e: a mature seed. [Modified from (College of Agriculture Food and Environment, 2016)].

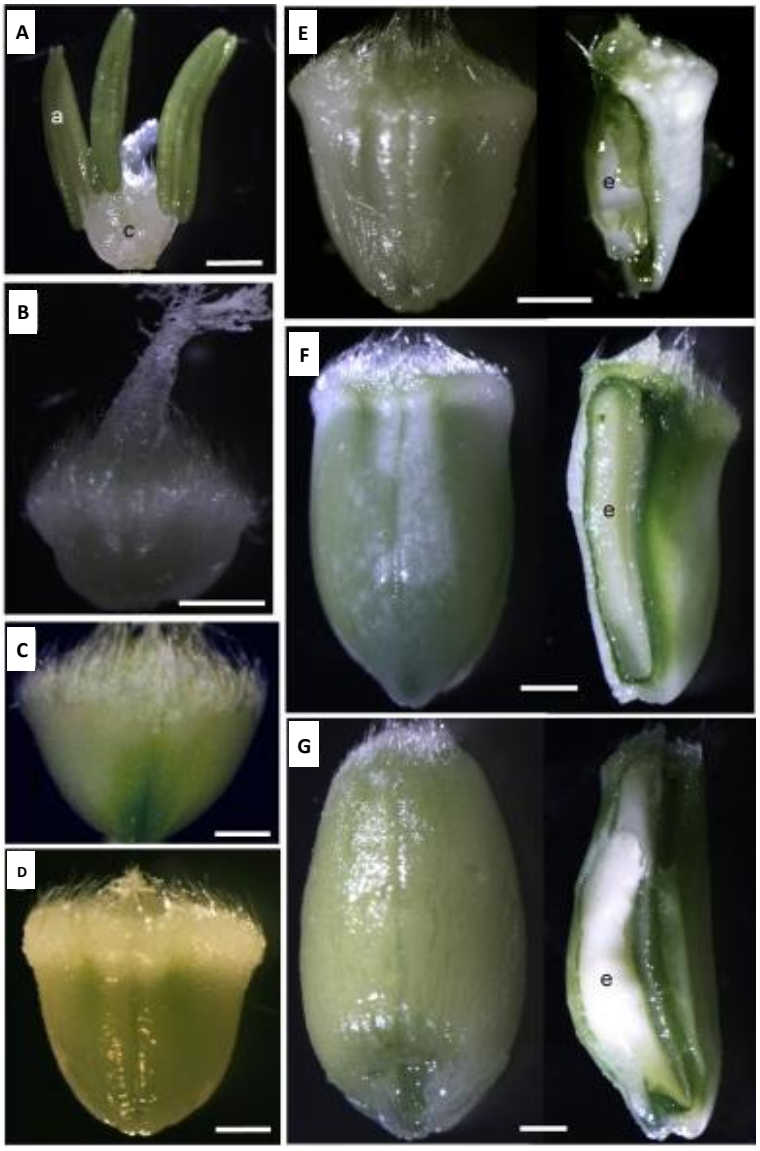


Figure 1.10: Developmental stages of a wheat grain
A: carpel 1 day before anthesis, B: 1 dpa, C: 2 dpa, D: 4 dpa, E: 7 dpa, F: 14 dpa, G: 21 dpa. a – anther; c – carpel; e – endosperm. Scale bars = 1 mm. [Modified from (Song *et al.*, 2012)]

At stage 3, 10 to 15 dpa, the scutellum elongates and the dry weight of the seed increases rapidly and the endosperm becomes milky. The outermost endosperm cell layer differentiates into the aleurone layer by 12 dpa whereas the cells on the inside develop into starch and protein storing cells and continue to differentiate till about 15 dpa when the seed reaches its maximum length (Evers, 1970, Huber and Grabe, 1987, Drea *et al.*, 2005) (Figure 1.11). From 15

to 20 dpa, stage 4, the primary leaf, radicle and coleoptile differentiate in the embryonic axis and the size of the endosperm and the seed reaches its maximum and it is fresh green in colour. The epithelium and vascular system also develop in the scutellum and the embryo now appears as a bump at the end of the seed.

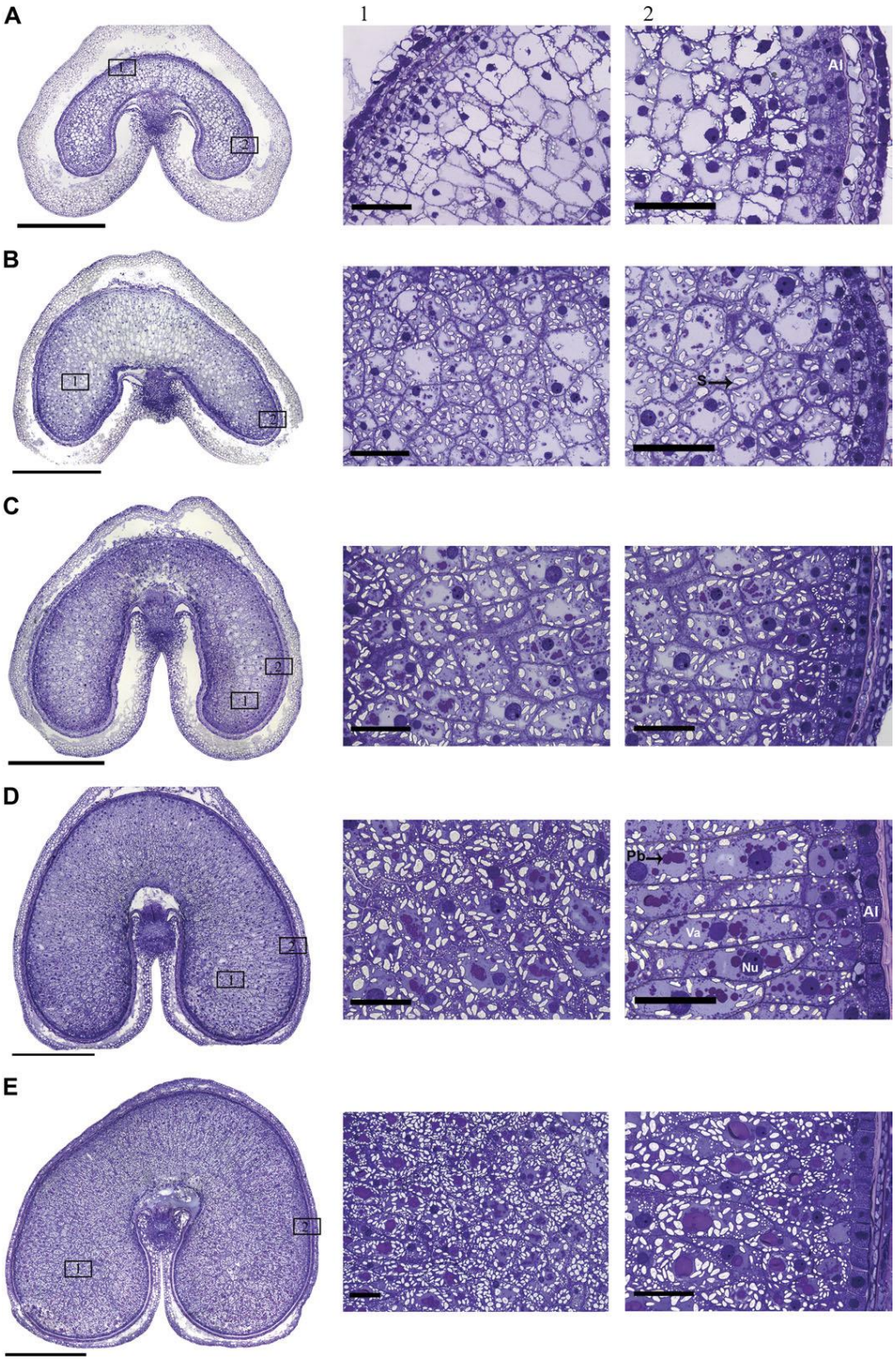


Figure 1.11: Development of different tissues of a wheat grain

Toluidine blue-stained cross-sections and enlargements of specific areas of the wheat grain at A: 8, B: 12, C: 16, D: 20, and E: 22 dpa. Bars in cross-sections correspond to 1 mm; bars in enlargements correspond to 100 µm. Al, aleurone layer; Pb, protein bodies; S, starch granules; Nu, nucleus. (Tosi *et al.*, 2009).

At stage 5, from 20 to 30 dpa, the embryo differentiates further and the endosperm reserve accumulation shows a second peak with both fresh and dry weight reaching their maximum. By 30 dpa the embryo differentiation is complete (Rogers and Quatrano, 1983). At this stage the endosperm is a soft dough and the seeds are starting to yellow and have reached physiological maturity (Hanft and Wych, 1982). At the last stage of development, stage 6, from 30 to 50 dpa, the seeds desiccate and turn brown. After 30 dpa the endosperm becomes harder and the fresh weight of the seed decreases. At this stage, there is no further differentiation of the embryo or accumulation of reserves but some authors have observed an increase in fresh weight till as late as 50 dpa (Hanft and Wych, 1982, Rogers and Quatrano, 1983, Lingle and Chevalier, 1985). This stage includes hard dough, ripe and dead ripe stages of development (Noda *et al.*, 1994).

1.2.3 Source-sink Relationship in Grains

The genetically programmed process of senescence of vegetative organs results in the remobilisation of degradation products, mainly sucrose to the reproductive organs supporting the development of cereal grains. The concentration gradient of assimilates between source and sink is the primary determinant of the rate of transport and pattern of partitioning (Brenner and Cheikh, 1995). It is believed that the grain filling rate in cereals is closely associated with the sink strength and that grains do not behave as a passive transient storage place, but develop a temporary sink activity (Venkateswarlu and Visperas, 1987, Kong *et al.*, 2015). Sink strength is described as the product of sink size, which is a physical restraint that includes cell number and cell size and sink activity, which is the physiological constraint upon a sink organ's assimilate import (Ho, 1988).

The central feature of a source-sink relationship that determines grain yield is the path of sucrose transfer from its source to its utilisation in sink organs

(Bihmidine *et al.*, 2013). In developing seeds sucrose import differs from that in other parts of the plant: in seeds phloem transport terminates in the maternal tissue and photo-assimilates must move apoplastically to the developing embryo where they are utilised (Brenner and Cheikh, 1995). In wheat, unloading from phloem for development occurs in the pericarp of the grain. Along with sugars, nitrogen uptake, transport and recycling also impact on source-sink relationships and general plant growth (Masclaux-Daubresse *et al.*, 2010). In wheat, the nitrogen stored in vegetative organs prior to anthesis is remobilised to the grain and contributes 60-95% of the grain nitrogen, with only a minor portion being derived from nitrogen uptake post flowering (Kichey *et al.*, 2007).

An integrated signalling network of hormones, sugars and environmental cues coordinate the balance of source production and sink utilisation of carbon to regulate plant development and stress-adaptive processes (Ruan, 2014). The direction of nutrient flow and metabolic pathways is determined by these signalling pathways (Yu *et al.*, 2015). It is known that hormones are involved in the development of seeds which have a higher concentration of hormones than all other plant parts and are important in determining sink strength (Brenner and Cheikh, 1995). Hormones might function to increase the sink strength by increasing cell number or by modifying the duration or rate of dry matter accumulation of developing grains (Davies, 1995). Immediately post anthesis the levels of cytokinin (CKs) are at their maximum followed by peaks in GA and auxin during the linear phase of grain development, and then ethylene and ABA as the grain matures (Kong *et al.*, 2015).

In pea during rapid pod elongation gibberellin-like material (analysis of hormones based on bioassay rather than on physico-chemical determinations) is highest in the liquid endosperm, whereas in whole pea seeds GAs occur maximally during rapid seed growth and very low quantities during early seed development or maturation (Eeuwens and Schwabe, 1975, Sponsel, 1983). In barley the increase in levels of GA-like material corresponds to dry weight

increase of the grain, with the highest levels in the endosperm (Mounla, 1978). In peas, it was observed that GA biosynthesis inhibitors have no effect on seed growth indicating that GA may not be acting within the seed for growth and thus not involved with sucrose uptake by seeds (Baldev *et al.*, 1965, Brenner and Cheikh, 1995). Yang *et al.*, (2003b) observed that during early grain filling in rice the levels of GA are high reaching a maximum at 8-10 dpa which is associated with enlargement of the embryo. They also observed that GA levels were not correlated with cell division rate, suggesting that in rice GAs may not regulate endosperm cell division during grain filling but play an important role in embryogenesis.

1.2.4 Seed Dormancy and Germination

All seeds are believed to be dispersed from the parent in a dormant state and it is during late embryo maturation, with the accumulation of nutrients and desiccation tolerance (Galau *et al.*, 1991, Hilhorst, 1995), that dormancy is established. Dormancy allows the seed time for dispersal and prevents germination out of season. Seed dormancy is believed to be a condition with many contributing causes and not a single phenomenon and can be described as either primary or secondary. Primary dormancy is present in freshly harvested mature seeds and is induced by abscisic acid (ABA) accumulation during seed maturation, while secondary dormancy is induced in seeds after dispersal when favourable conditions required for germination are not present (Finch-Savage and Leubner-Metzger, 2006). Both temporal and spatial distribution of seed germination is essential for the survival of seed plants. The seed and fruit morphology which enhances the dispersal of seeds from its maternal habitat determines the spatial distribution of germination. The temporal distribution is controlled by a variation in the physiological status of each seed within a population. This variation exists to allow each seed to

germinate at a different time to avoid competition with its siblings or extinction of all individuals due to unfavourable conditions (Nonogaki, 2014).

A common method of releasing dormancy is after-ripening where a freshly harvested mature seed is stored in dry conditions at room temperature for several months (Bewley, 1997). After-ripening increases the temperature range for germination, decreasing the ABA concentration and sensitivity and increases GA sensitivity of the seeds. It can also remove the requirement for light for germination in seeds that do not germinate normally in the dark. After-ripening also increases the germination velocity and removes the requirement for nitrates to germinate (Finch-Savage and Leubner-Metzger, 2006). The moisture and oil content, seed coat, ABA and temperature all contribute to the after-ripening of a seed (Koornneef *et al.*, 2002). In very dry seeds after-ripening is prevented as it requires moisture above a threshold value. This value is species-specific and is lower in oilseeds compared to starchy cereal seeds (Leubner-Metzger, 2005). Dormancy can also be broken by cold stratification which involves imbibing seeds in the cold, or by exposure to light (Bewley, 1997).

Germination starts with imbibition and ends with the emergence of the embryonic root from the seed, and is followed by seedling growth and establishment. This start of germination depends on the balance between the weakening of the micropylar endosperm (CAP) surrounding the radicle and an increase in the embryo growth potential required for the elongation of the lower hypocotyl radicle axis (RAD) [(Urbanova and Leubner-Metzger, 2016), and references therein]. The influence of the endosperm on testa rupture is not clear and could involve either the release of hydrolytic enzymes to weaken the testa or a physical rupture of this layer caused by the expansion of the endosperm in imbibed seeds (Holdsworth *et al.*, 2008a). The progress of germination can be split into three phases of water uptake: in phase I the seed rapidly takes up water and reinitiates metabolic processes, in phase II it enters a lag phase of water uptake and finally in phase III further water uptake results

in the emergence of the radicle (Bewley, 1997). Phase II is an important developmental stage where a prolonged non-germinating dormant state must be relieved before radicle emergence can occur (Holdsworth *et al.*, 2008b). A completely non-dormant seed is able to germinate over the widest range to normal environmental conditions possible for that species (Bewley and Black, 1994, Baskin and Baskin, 2003). On taking up water a dry seed rapidly resumes metabolic activity and the enzymes required for this process are believed to be present in the dry seed having survived the desiccation phase (Bewley, 1997). Along with the requirement for water, oxygen and optimal temperature for germination, a seed may also need appropriate light conditions and nitrates for germination with nitric oxide (NO) shown to increase the germination potential of seeds (Finch-Savage and Leubner-Metzger, 2006, Holdsworth *et al.*, 2008a).

The ratio of ABA/GA present influences germination and this balance must be strictly regulated. There are two aspects of this balance: the balance of ABA to GA signalling and the balance of the hormone levels (Finch-Savage and Leubner-Metzger, 2006, Shu *et al.*, 2016). ABA supresses GA biosynthesis and GA negatively regulates ABA biosynthesis during germination. These two hormones interact and both act as a cause and effect to maintain the ABA/GA ratio during germination (Seo *et al.*, 2006, Shu *et al.*, 2013). AP2 domain containing transcription factors (TFs) are believed to play an important role in the dual regulation of the ABA/GA signalling pathways and hormone levels. These genes positively regulate endogenous ABA and decrease GA levels and a DNA motif present in these TFs may be involved in regulating the ABA/GA signalling levels (Shu *et al.*, 2016). A protein phosphatase 2C (PP2C) protein called HONSU acts as a negative regulator of seed dormancy by inhibiting ABA and activating GA signalling pathways, indicating that this protein might be another key component in the ABA and GA crosstalk during seed dormancy (Kim *et al.*, 2013).

The temporal- and tissue-specific regulation of hormone content and regulation is also believed to play an important role during germination. In

Arabidopsis, bioactive GAs accumulate prior to radicle emergence and GA biosynthesis is known to occur in two locations in the embryo. The early biosynthetic steps in the pathway occur in the provasculature whereas the late biosynthetic steps take place in the cortex and endodermis. The expression of genes encoding for the AtKO (*ent*-kaurene oxidase) enzyme is higher in the RAD compared to other compartments in the grain, indicating this to be the main site of GA_{12} production during germination (Yamaguchi *et al.*, 2001, Ogawa *et al.*, 2003, Kucera *et al.*, 2005). GA is known to play two roles during germination, first by cell expansion it increases the growth potential of the embryo to enable radicle emergence. This is aided by the weakening of the tissues surrounding the radicle by hydrolytic enzymes, which also requires GA and is necessary to overcome the physical restraints applied by the layers covering the embryo (Penfield *et al.*, 2006, Yamaguchi *et al.*, 2007, Linkies and Leubner-Metzger, 2012).

The crucial role of ABA in dormancy was identified by studying GA- and ABA-deficient mutants in *Arabidopsis* and tomato (Hilhorst, 1995, Debeaujon and Koornneef, 2000). ABA-deficient mutants have an absence of primary dormancy in the mature seeds and those with increased levels of ABA have enhanced seed dormancy (Finkelstein, 2004). The exogenous application of ABA inhibits seed germination, but is unable to induce seed dormancy. It is only the ABA synthesised by the seeds that can establish dormancy (Kucera *et al.*, 2005). Sensitivity to both GA and light increases as after ripening progresses in Arabidopsis and light is known to promote GA biosynthesis (Kamiya and Garcia-Martinez, 1999). In Arabidopsis, hyperaccumulating mutants show decreased dormancy and GA biosynthesis mutants are non-germinating and this can be rescued by the external application of GA showing that GA is required to break dormancy and initiate germination (Helliwell *et al.*, 1998, Yamauchi *et al.*, 2007). DELLA proteins, the negative regulators of the GA signalling pathway, maintain the embryo in a quiescent state by restricting cell-cycle progression by repressing the activity of TCP14 (TEOSINTE BRANCHED1/CYCLOIDEA/PROLIFERATING CELL FACTOR) and TCP15 (Resentini

et al., 2015). In Arabidopsis, the *RGL2* DELLA gene is a negative regulator of germination and mutations in this gene are able to rescue the non-germinating phenotype of GA biosynthetic mutants (Lee *et al.*, 2002). The enzyme GA3ox has been identified as having a major role in germination completion with *AtGA3ox1* and *AtGA3ox2* being expressed in the embryo during imbibition before germination (Mitchum *et al.*, 2006). GAs may also stimulate germination by initiating the transition from embryonic to vegetative development mediated by the chromatin remodelling factor PICKLE (PKL) (Henderson *et al.*, 2004).

Apart from the central role played by ABA and GA in seed dormancy and germination other compounds are also involved in this process. Brassinosteroids (BRs) that are involved in stem elongation and leaf unfurling also promote germination by enhancing the embryo growth potential in a GA-independent manner (Leubner-Metzger, 2001). Ethylene promotes dormancy breaking by antagonism of the ABA signalling pathway (Shu *et al.*, 2016). Auxins may play a role in regulating dormancy and germination as it has been shown that they supress germination under stress conditions (Park *et al.*, 2011). It is believed that auxins regulate seed dormancy alongside ABA (Liu *et al.*, 2013). Salicylic acid (SA) under normal conditions suppresses germination by inhibiting the expression of α-amylase genes, whereas under high salt conditions it reduces oxidative damage and promotes germination (Xie *et al.*, 2007, Lee *et al.*, 2010). CKs promote germination by antagonising ABA signalling by inducing the degradation of the ABI5 protein (Guan *et al.*, 2014). Jasmonic acid (JA) has also been shown to delay seed germination and is known to repress ABA biosynthetic gene expression (Nambara *et al.*, 2010, Jacobsen *et al.*, 2013). Strigolactones (SL) stimulate germination in parasitic weeds and other species by reducing the ABA/GA ratio and the *SMAX1* (*SUPPRESSOR OF MORE AXILLARY GROWTH 1*) gene in the SL pathway controls seed germination (Toh *et al.*, 2012, Stanga *et al.*, 2013). Nitrogen containing compounds such as NO gas, nitrite, nitrate, nitrogen dioxide, ammonium, azide and cyanide promote germination in different species (Bethke *et al.*, 2007). This may be due

to their effects on metabolism, oxidation state or signalling. They induce the expression of genes that encode enzymes in the pentose phosphate pathway which may provide nutrients during germination (Finch-Savage *et al.*, 2007). Germination is also known to be enhanced by smoke in about 1200 species that grow globally. The active compounds in smoke that stimulate germination are a family of butenolide molecules known as karrikins which require light and GA biosynthesis for their action (Dixon *et al.*, 2009, Nelson *et al.*, 2009). Most dormant seeds are considered "orthodox" where ABA induces desiccation tolerance during grain maturation which allows the grain to survive long periods in a dry state. Seeds that do not have desiccation tolerance are "recalcitrant" and produce reactive oxygen species (ROS) during desiccation, germination and ageing which results in oxidative stress and cellular damage causing seed deterioration. Seeds that possess desiccation tolerance have detoxifying enzymes and antioxidant compounds that are able to scavenge ROS and enable seed survival (Bailly, 2004, Berjak, 2006).

In higher plants dormancy and germination are controlled by many genes and different environmental factors. A dormant seed is equipped to survive long periods under unfavourable conditions and this is an adaptive trait that allows optimal germination time in a population of seeds (Bentsink and Koornneef, 2008). During grain maturation the embryo remains in a quiescent state where the stored nutrients are not mobilised and there is no cell division or elongation. In this state germination-promoted genes are not actively expressed. It is known that chromatin structure determines gene expression and genes associated with chromatin remodelling are known to regulate seed dormancy and germination (Liu *et al.*, 2007, Cho *et al.*, 2012). It has been shown that ABA is also involved in chromatin remodelling and epigenetic regulators are up-regulated during the induction of seed dormancy. This indicates that these genes play important roles during seed maturation and affect the dormancy establishment process (Liu *et al.*, 2007, Chinnusamy *et al.*, 2008). At the release of dormancy and the start of germination the chromatin structure is modified making the germination-promoted genes available for

transcription. This results in cell division and elongation and the rupture of the seed coat and endosperm ending with the emergence of the radicle (Shu *et al.*, 2016). The *DELAY OF GERMINATION 1* (*DOG1*) gene expressed during seed maturation is known to play a key role in the induction and maintenance of dormancy and it is not regulated through changes in hormone levels. The levels of DOG1 protein in seeds acts as a timer for seed dormancy release and works independently of ABA (Bentsink *et al.*, 2006, Nakabayashi *et al.*, 2012). DOG1 also provides dormancy adaptation to distinct environments. It mediates a conserved coat-dormancy and inhibits the expression of GA-regulated genes encoding cell-wall remodelling proteins in a temperature dependant manner. It causes the alterations in the expression of GA-biosynthetic genes also in a temperature dependant manner. This results in a highly adaptable temperature sensing mechanism to control the timing of germination through the expression of *DOG1* and its control of GA levels (Graeber *et al.*, 2014). DOG1 is believed to be epigenetically regulated and chromatin remodelling of *DOG1* is involved in dormancy cycling (Footitt *et al.*, 2015, Shu *et al.*, 2016).

1.2.4.1 Pre-harvest sprouting (PHS) and Premature α-amylase (PMA)

In agricultural crops, there is often a requirement for rapid cycling of generations. However, a degree of dormancy can be advantageous, particularly in preventing the phenomenon of PHS where the grain germinates while still on the parent plant, the endosperm is hydrolysed and the subsequent flour quality significantly impaired (Bewley, 1997, Koornneef *et al.*, 2002). PHS is one of the most important factors that affect the yield and quality of wheat especially in cool, wet conditions and it is determined by both environmental and genetic factors. Temperature and moisture, especially during late stages of development, are mainly responsible for PHS in wheat (Gao *et al.*, 2013). Wheat varieties that have enhanced dormancy are more resistant to PHS and have increased sensitivity to applied ABA (Walker-Simmons, 1987). In wheat, there is also a relationship between grain colour and PHS where white varieties

are more susceptible to PHS compared to red varieties (Torada and Amano, 2002). This is since red grain varieties show a higher dormancy which indicates that genes that control dormancy may also regulate grain colour (Shu *et al.*, 2015). Another factor that affects the quality of wheat flour is PMA which is a genetic defect that causes accumulation of unacceptably high levels of α-amylase in the grain. This can occur due to adverse weather conditions during the middle stages of grain ripening and in lodged crops (Mrva *et al.*, 2006, Gooding *et al.*, 2012). The production of PMA was believed not to be associated with the stimulation of the aleurone by embryo-derived GA as is the case for germinating α-amylase (Mrva and Mares, 1996). However, recent work has shown the involvement of GA in the production of PMA (Kondhare *et al.*, 2013). In addition, work in our laboratory has also shown that reduction in GA production in the embryo and scutellum during development does lead to a decrease in α-amylase levels in mature grains (Vaughan, S. unpublished data). A difference between germination α-amylase and PMA is its distribution in the grain. α-Amylase is distributed evenly throughout the length of the grain under PMA and not concentrated in the tissues next to the embryo as seen during germination (Mares and Gale, 1990). In developing wheat grains two main families of α-amylase isozymes are produced, α-amy-1 and α-amy-2 and these can both persist till maturity. The α-amy-1 or malt or high pI amylase is the primary product of germination and PHS, and is encoded by the *TaAmy1* genes located on the long arms of chromosome 6A, 6B and 6D. The production and subsequent deposition of this isozyme into the endosperm without sprouting damage is one of the main contributors to PMA. The α-amy-2 or green or low pI amylase occurs in high concentration in the pericarp of immature grains and its concentration decreases as the grain matures. This enzyme also occurs during germination, but at a later stage than α-amy-1 and is encoded by the *TaAmy2* genes on the long arms of group 7 chromosomes. If α-amy-2 activity is present in later stages of grain development it results in an increase in α-amylase levels in mature grains (Gale *et al.*, 1983, Lunn *et al.*, 2001a, Lunn *et al.*, 2001b). A third group of α-amylase genes - *TaAmy3* – present on the group

5 chromosomes have also been described. These genes are expressed only in developing grains in the outer layer of the pericarp (Baulcombe *et al.*, 1987).

The promoters of these α-amylase genes have been shown to possess a 21 base pair (bp) GA responsive element (GARE) which contains a conserved sequence, TAACAA/GA also found in the promoters of all known GA-responsive genes (Skriver *et al.*, 1991). This GARE has been shown to play an important role in mediating the GA and ABA regulation of these genes and mutations in this sequence results in these promoters no longer being responsive to GA (Gubler and Jacobsen, 1992). A *trans*-acting factor that binds with these GARE sequences of the α-amylase genes was identified from the aleurone cells of barley. This GA-regulated *Myb* transcription factor called *HvGAMYB* binds specifically to the TAACAA/GA sequence of the GARE and acts as a transcriptional activator of α-amylase genes. The overexpression of this gene in aleurone cells is enough to trigger α-amylase promoter activity indicating that it can replace the requirement for GA (Gubler *et al.*, 1995, Woodger *et al.*, 2003). It has also been shown that GA induces a rapid increase in the expression of this gene prior to the expression of α-amylase genes in barley aleurone layers and its expression remains high for up to 12 hrs (Gubler *et al.*, 2002). *GAMYB* homoeologues have also been isolated from other plant species such as rice and wheat which contain a single copy of this gene, and *Arabidopsis* which has three copies (Gubler *et al.*, 1997, Chen *et al.*, 2001, Stracke *et al.*, 2001). The nucleotide sequence of the functional MYB domain is almost completely conserved between barley and the three wheat genomes, with only a few amino acid differences (Haseneyer *et al.*, 2008). The *TaGAMYB* gene has been shown to colocalise with a QTL influencing PHS and grain colour indicating that it may regulate this trait (Groos *et al.*, 2002).

The mechanism through which GA regulates the expression of these genes is not entirely clear. It has been demonstrated in barley and rice that it may be controlled via the signalling pathway by the action of the DELLA proteins, which negatively regulate their expression. In the aleurone layer these DELLA proteins

are rapidly degraded upon GA application and the *HvGAMYB* gene is expressed an hour after this degradation, indicating that this gene acts downstream of DELLAs and is not directly targeted by them. It has been suggested that DELLAs act on GAMYBs through an intermediary such as cGMP (Gomez-Cadenas *et al.*, 2001, Gubler *et al.*, 2002). However, it has also been shown that GA signalling causes changes in the sub-cellular localisation of GAMYB (Hong *et al.*, 2012). The aleurone layer of *Sln1d* DELLA gain-of-function mutant requires 100-fold more GA than the wild type to induce expression of both *HvGAMYB* and α-amylase genes showing their involvement in the regulation of these genes (Chandler *et al.*, 2002). In the aleurone layer ABA induces PKABA1 (ABA-inducible protein kinase) which inhibits the expression of GAMYB and is known to act downstream of DELLAs as well (Gomez-Cadenas *et al.*, 2001). GAMYBs have also been shown to be involved in GA-mediated processes in other tissues apart from the aleurone layer. Work with mutants in rice and barley has illustrated their role in anther and seed development (Diaz *et al.*, 2002, Aya *et al.*, 2009). In addition in anthers GAMYBs have been shown to be negatively regulated by miRNA159, but no such regulation was seen in the aleurone layer indicating that the regulation of the expression and function of GAMYBs is different in the aleurone and anthers (Tsuji *et al.*, 2006).

1.3 Gibberellins (GAs)

GAs are diterpenoid compounds forming a large family of compounds endogenous to higher plants as well as some lower plants, fungi and bacteria. They comprise a group of 136 structurally related compounds only a few of which are biologically active. Many of the other GAs are either biosynthetic precursors, inactivation products of bioactive GAs or have no known function and could be classified as secondary metabolites. They are involved in multiple growth and development processes, including: stem and root elongation, flower and fruit development, seed germination and development, and leaf expansion (Hedden and Kamiya, 1997, Hedden and Phillips, 2000). GAs are also involved in the response to various environmental stimuli, such as light and temperature, which have an effect on both GA biosynthesis and sensitivity that subsequently produces changes (Phillips, 1998). The main function of GA in plants is to promote growth by stimulating cell elongation and in some cases cell division. They also promote other developmental processes such as the transition from dormancy to germination, and from vegetative to reproductive development, although in some species they may have the opposite effect (Hedden and Thomas, 2012).

GA was first described in 1935 as a substance produced by the fungus *Gibberella fujikuroi* that caused the bakanae disease in rice seedlings and produced an overgrowth phenotype. GAs are named GA_1 to GA_{136} in order of their discovery, the first GA to be structurally classified being GA_3 (plant-hormones.info, 2016). The substance produced by the fungus *Gibberella fujikuroi* was shown to be a mixture of different GAs, of which the major component was GA_3 (Hedden and Proebsting, 1999). Most GA structures have been identified from immature seeds as these contain very high concentrations of GAs and a broad range of different GA structural forms (Hedden and Thomas, 2012). GA_1 has been identified as the main bioactive hormone in many different species, though GA_4 is also ubiquitous and is the major bioactive GA present in

some plant species, including *Arabidopsis* and the Cucurbitaceae (MacMillan, 2002). The role of GA_1 compared to GA_4 and other bioactive forms is still not clear (Yamaguchi, 2008).

In 1917 it was discovered that the stem length character of pea seedlings observed by Gregor Mendal in 1866 was due to the presence or absence of a factor for tallness (Orland, 1917). This factor was later identified as GA when the application of GA_3 on dwarf pea plants caused them to elongate to normal length (Brian and Hemming, 1955). Subsequent application of purified extracts from tall pea seedlings also caused the elongation of dwarf peas and confirmed that GA was endogenous in higher plants (Radley, 1956). Genetic mutations have played a major role in understanding the role of GAs in plant growth and other developmental processes (Ross *et al.*, 1997). The complex GA metabolism pathway was first explained in *G. fujikuroi* and then in higher plants (Hedden and Phillips, 2000). In monocots, rice and barley have been used to characterise GA pathway genes (Spielmeyer *et al.*, 2004, Chandler *et al.*, 2002, Ueguchi-Tanaka *et al.*, 2005).

1.3.1 GA Biosynthesis

GA biosynthesis occurs from geranylgeranyl diphosphate (GGDP), which is a C_{20} precursor for all diterpenoids, and involves initially membrane localised cytochrome P450 mono-oxygenases (P450s) and then soluble 2-oxoglutarate-dependant dioxygenases (2-ODDs) (Yamaguchi, 2008). The early steps in the pathway from GGDP to GA_{12}-aldehyde are common in all systems studied (Hedden and Phillips, 2000). The biosynthesis pathway can be divided into three parts:

1.2.1.1 GGDP converted to *ent*-kaurene via *ent*-copalyl diphosphate (CPP)
1.2.1.2 *ent*-kaurene converted to GA_{12}
1.2.1.3 Conversion of GA_{12} to bioactive GAs

1.3.1.1 GGDP to *ent*-kaurene

In plants, GGDP, formed mainly via the 2-C-methyl-D-erythritol-4-phosphate (MEP) pathway is converted in plastids to *ent*-kaurene by two diterpene cyclases, CPP synthase (CPS) and *ent*-kaurene synthase (KS). However, in fungi both activities are catalysed by a single enzyme (Duncan and West, 1981, Tudzynski *et al.*, 1998). When the MEP pathway is limited plants utilise the mevalonic acid (MVA) pathway for the production of *ent*-kaurene. In green tissues the MEP pathway is the major source of precursors for *ent*-kaurene biosynthesis (Kasahara *et al.*, 2002) whereas in non-photosynthetic leucoplasts where *ent*-kaurene is synthesised in the endosperm the precursors may be obtained through the MVA pathway [(Hedden, 2016) and references therein].

GGDP in the first step is converted to *ent*-copalyl diphosphate (*ent*-CDP) by CPS, while in the second step CPD is converted by KS to *ent*-kaurene (Figure 1.12) (Hedden and Phillips, 2000). Both CPS and KS contain N-terminal sequences that target them to the plastids (Sun and Kamiya, 1994, Yamaguchi *et al.*, 1996). Evidence to support the function of the two enzymes is provided by the *Arabidopsis* loss of function *ga1* and *ga2* mutants which are GA responsive male sterile dwarfs that fail to germinate. They contain deletions in the single genes which encode the CPS and KS enzymes, respectively, producing only very low levels of GA (Sun and Kamiya, 1994, Koornneef and Vanderveen, 1980). Multiple *CPS*- and *KS*-like genes have been cloned from rice and wheat though only a few of these are involved in *ent*-kaurene synthesis (Hedden, 2016).

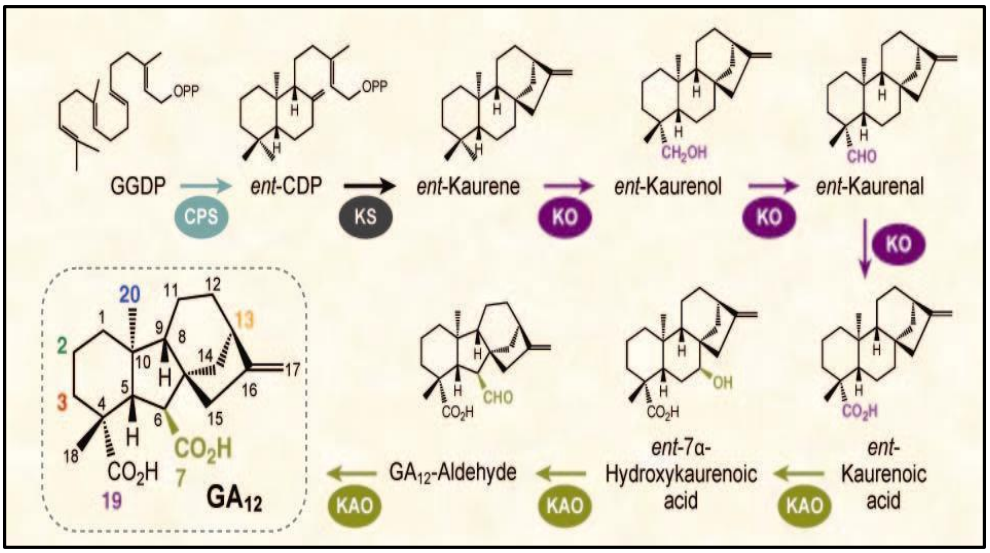


Figure 1.12: Early stages of GA biosynthesis.
GGDP is converted to ent-kaurene by CPS and KS, with ent-CDP produced as an intermediate. ent-Kaurene is then oxidised to produce GA_{12} via reactions catalysed by KO and KAO (Yamaguchi, 2008).

1.3.1.2 *ent*-kaurene to GA_{12}

This conversion occurs by the action of two P450s on the membranes outside the plastid which need *ent*-kaurene to move from the organelle. This process occurs by an unknown mechanism (Hedden and Phillips, 2000). The oxidation on C-19 by *ent*-kaurene oxidase (KO) which belongs to the CYP701A family produces *ent*-kaurenoic acid in three steps via the alcohol and aldehyde. This is then converted to GA_{12} by *ent*-kaurenoic acid oxidase (KAO; CYP88A) also in three steps via 7β-hydroxy-*ent*-kaurenoic acid and GA_{12}-aldehyde (Figure 1.12) (Yamaguchi, 2008, Helliwell *et al.*, 2001a). After the production of GA_{12} the pathway is divided into two parallel parts due to the 13-hydroxylation of GA_{12} to give GA_{53}. These are the substrates for the final stages of GA biosynthesis (Hedden and Phillips, 2000).

The intermediates in the steps oxidised by KO and KAO do not normally accumulate except in tissues where GA biosynthesis levels are very high (Graebe *et al.*, 1972, Morrone *et al.*, 2010). Using a fusion with green fluorescent protein (GFP) it was shown that KO is present in the outer plastid

membrane and KAO in the endoplasmic reticulum (ER). The location of both these enzymes may facilitate the movement of the plastid-produced *ent*-kaurene to the endomembrane system (Helliwell *et al.*, 2001b). It has also been shown that *ent*-kaurene is able to exchange with the external environment through the membrane system or via a protein carrier. It is also possible that *ent*-kaurene synthesis and metabolism may be located in different tissues (Otsuka *et al.*, 2004, Yamaguchi *et al.*, 2001). In pumpkin and cucumber there is present a 2-ODD, GA7ox which converts GA_{12}-aldehyde to GA_{12} (Lange, 1997, Lange *et al.*, 2013) and the over expression of this gene in Arabidopsis results in increased growth implying that KAO may be growth limiting in this species (Radi *et al.*, 2006). The only other species where this 2-ODD has been detected is potato (Fixen *et al.*, 2012).

The role of the enzyme KO is demonstrated by the *Arabidopsis ga3* mutant which is a non-germinating GA-responsive dwarf and is known to be deficient in KO. Point mutations in the single *GA3* gene in Arabidopsis which encodes the KO enzyme results in plants that do not respond to *ent*-kaurene but application of *ent*-kaurenoic acid restores growth (Koornneef and Vanderveen, 1980, Helliwell *et al.*, 1998). In rice, there are five *KO*-like genes but only one of them is involved in GA biosynthesis. Mutations in this *OsKO2* gene were responsible for the d35 semi-dwarf phenotype of modern rice varieties (Itoh *et al.*, 2004, Sakamoto *et al.*, 2004). Cereals contain only one KAO gene, mutations in which results in dwarf phenotypes, whereas Arabidopsis has two fully redundant genes (Helliwell *et al.*, 2001a, Sakamoto *et al.*, 2004). GA13ox catalyses the 13-hydroxylation of GA_{12} to GA_{53} which is controlled by two genes, *TaGA13ox1* and *TaGA13ox2* which in wheat are expressed in all tissues except mature spikes with *TaGA13ox1* expression being higher. These genes have the highest levels of expression in the most mature developmental stage that was sampled (Pearce *et al.*, 2015). In rice, two cytochrome P450s are known to encode GA 13-oxidase, and their overexpression in Arabidopsis results in semidwarfism. In addition the exogenous application of bioactive GA upregulates their expression indicating they may regulate plant growth by reducing GA

bioactivity and may also be involved in GA feedback regulation (Magome *et al.*, 2013).

1.3.1.3 GA_{12}/GA_{53} to bioactive GAs

The two parallel 13-hydroxylation and non-13-hydroxylation pathways produce bioactive GAs that differ only in the presence or absence of a 13-OH group (Figure 1.13). In the 13-hydroxylation pathway GA_{53} is converted through several steps to GA_1 and in the non-13-hydroxylation pathway GA_{12} is converted through the same steps to GA_4. In most species of plants both pathways occur in the vegetative tissues and the strength of the 13-hydroxylase activity decides the predominance of one over the other (Hedden and Phillips, 2000). The final stages of the biosynthesis pathway are catalysed by two soluble 2-ODDs present in the cytosol (Helliwell *et al.*, 2001b), GA 20-oxidase (GA20ox) which removes C-20 to form a C-4-C-10 lactone, and GA 3-oxidase (GA3ox) which inserts a 3β-hydroxyl group (Figure 1.13). GA20ox catalyses the sequential oxidation of C-20 from a methyl to the alcohol and then to the aldehyde, which is then removed with the formation of C_{19} γ-lactone GAs. The last step of the biosynthesis pathway involves the conversion of GA_9 and GA_{20} to bioactive GA_4 and GA_1 respectively by 3 β-hydroxylation by GA3ox ODDs [(Hedden, 2016), and references therein].

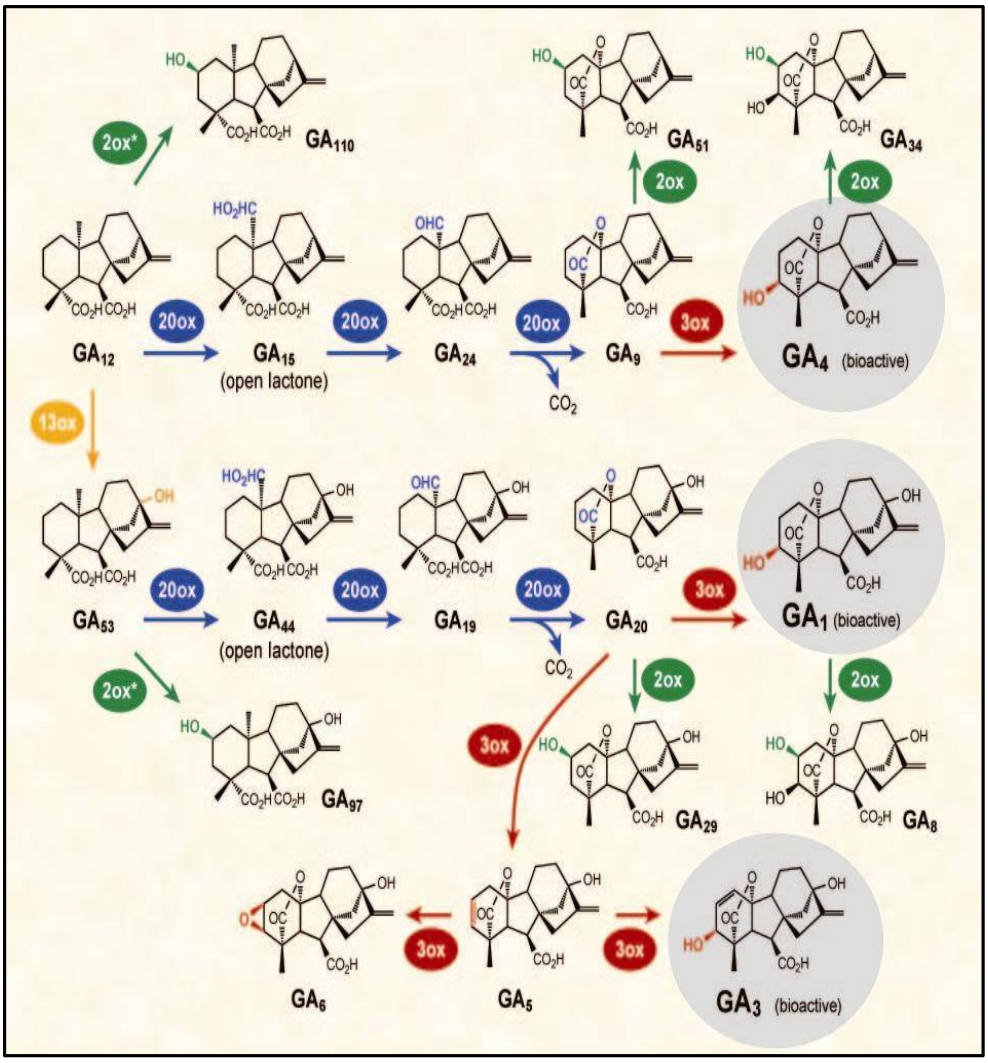


Figure 1.13: Late stages of GA biosynthesis and GA inactivation

GA_{12} is converted to GA_{53} by GA13ox and these two intermediates act as substrates for two parallel pathways. GA_{12}/GA_{53} is then oxidised by GA20ox (blue) to GA_9/GA_{20}, respectively. The final GA activation step involves 3β-hydroxylation by GA3ox (red) that converts GA_9/GA_{20} to the bioactive products GA_4/GA_1, respectively. The inactivation of bioactive forms involves GA2ox (green) that hydroxylates the C-2 of GA_4 and GA_1 or their precursors, GA_9 and GA_{20}, respectively. GA2ox also acts on the C_{20}-GAs (GA_{12} and GA_{53}) forming inactive GA_{110} and GA_{97}, respectively (Yamaguchi, 2008).

The 2-ODDs are encoded by multigene families in most plant species unlike the early stages of the pathway where the enzymes are generally encoded by single genes. The 2-ODD genes have distinct expression patterns in different organs and display a level of functional redundancy (Hedden and Phillips, 2000). It is

due to this functional redundancy that mutation in a single gene does not cause a complete GA deficient dwarf phenotype. In rice four *GA20ox* genes have been characterised and are expressed in different organs of the plant with *OsGA20ox2* being the main gene involved in stem elongation. *OsGA20ox1* and *OsGA20ox4* expressed in vegetative organs and *OsGA20ox3* expressed in the developing seed (Sakamoto *et al.*, 2004). In Arabidopsis there are five *GA20ox* genes though *AtGA20ox5* is able to carry out only the first two steps in the pathway to the aldehyde intermediate (Rieu *et al.*, 2008b, Plackett *et al.*, 2012). In wheat there are four *GA20ox* genes and *TaGA20ox1* and *TaGA20ox2* are the most highly expressed *GA20ox* genes in vegetative tissues. *TaGA20ox1* is expressed in nodes and ears of elongating stems and is the highest expressed GA20ox in roots. *TaGA20ox2* shows a contrasting pattern to *TaGA20ox1* and is expressed late in plant developed being highest towards tissue maturity. The *TaGA20ox1* and *TaGA20ox3* genes are also expressed in developing and germinating embryos, where *TaGA20ox3* is very high and exclusively expressed. *TaGA20ox4* has been shown to be expressed in the inner pericarp of developing grain and is the highest in the spike at anthesis (Appleford *et al.*, 2006, Pearce *et al.*, 2015).

In contrast to *GA20ox* there are only two *GA3ox* genes in rice whereas in Arabidopsis four have been reported. The two rice genes have different expression patterns with *OsGA3ox2* being expressed in all vegetative organs of the plant and *OsGA3ox1* is only in the tapetum and scutellum epithelium, where both genes are expressed. This allows for high levels of GA biosynthesis for GA to be exported to other tissues (Kaneko *et al.*, 2003, Sakamoto *et al.*, 2004, Yamaguchi, 2008). In Arabidopsis the *AtGA3ox1* and *AtGA3ox2* are expressed in vegetative tissues whereas all four genes are present in reproductive organs (Mitchum *et al.*, 2006, Hu *et al.*, 2008). In wheat there is no true orthologue of the rice *OsGA3ox1* but it does possess likely orthologues of *OsGA3ox2* with three homoeologues located on the group 3 chromosomes. *TaGA3ox2* was shown to be expressed in the elongating stem with expression found in nodes, internodes and the ear and it also has high expression in the

germinating and developing embryo. The TaGA3ox2 protein also shows some 13-oxidase activity in vitro (Appleford *et al.*, 2006) suggesting that it might also be involved in GA inactivation. Recently, four further potential GA3ox genes all located on the long arms of group 2 chromosomes were identified: *TaGA3ox-A3*, *TaGA3ox-B3*, *TaGA3ox-D3* and *TaGA3ox-B4*, which was subsequently identified as a GA 1β-hydroxylase (GA 1-oxidase, GA1ox). This gene in wheat was renamed *TaGA1ox-B1* and shows some expression in roots. *TaGA1ox-B1* and *TaGA3ox-B3* are both expressed at high levels mid-way through development of the grain, where *TaGA1ox-B1* converts GA_9 to GA_{61} and *TaGA3ox-B3* converts GA_{61} to GA_{54}. The *TaGA20ox1* and *TaGA3ox2* are considered important for stem architecture and grain development due to their high expression in stems and in germinating and developing seeds, making them important for grain yield and quality (Appleford *et al.*, 2006, Pearce *et al.*, 2015).

1.3.2 GA Inactivation

To balance bioactive GA levels in the plant there is a continual process of inactivation. This is important for the effective adjustment of hormone concentration, such as in response to environmental stimuli. GAs can be deactivated in different ways and the best characterised reaction is by another 2-ODD, GA 2-oxidase (GA2ox) which by introduction of a hydroxyl group at the 2β position of the C_{19} GAs, including bioactive GA_1 and GA_4 and their immediate precursors GA_{20} and GA_9, leads to inactivation (Figure 1.13). GA2ox was the first recognised inactivating enzyme and belong to either class I or II based on phylogenetic relationships. Another type of GA2ox acts on C_{20}-GAs and belongs to class III (Lee and Zeevaart, 2005). These are believed to act on precursors such as GA_{12} and GA_{53} which would otherwise be converted to bioactive forms (Schomburg *et al.*, 2003). This inactivation is believed to be the most common

in flowering plants due to the presence of orthologous *GA2ox* genes in various plant species (Martin *et al.*, 1999, Thomas *et al.*, 1999, Sakamoto *et al.*, 2001b)

In most species the GA2ox enzyme is encoded by multigene families leading to high levels of functional redundancy and not all the genes have been functionally characterised. Thus, mutations in single genes only give a subtle phenotype, whereas overexpression results in a dwarf phenotype (Hedden and Phillips, 2000, Schomburg *et al.*, 2003). The pea *slender* mutant is an exception where a mutation in the single *PsGA2ox1*/*SLENDER* (*SLN*) gene results in a GA overdose phenotype (Martin *et al.*, 1999). There are ten *GA2ox* genes in rice, encoding enzymes that act either on C_{19}- or C_{20}-GAs and they have different patterns of expression during development, with *OsGA2ox1* being expressed in roots, panicles and vegetative shoot apices. *OsGA2ox3* and *OsGA2ox4* are expressed in all organs whereas *OsGA2ox2* transcript was not detected in any organ (Sakamoto *et al.*, 2004). In wheat the orthologues of all of the rice *GA2ox* are found except *OsGA2ox5*. There is also present another group of GA2ox genes on the homoeologous group 4 chromosomes called *TaGA2ox-A11*, *TaGA2ox-B11* and *TaGA2ox-D11*. Another two potential paralogues are present only on chromosome 4BL, *TaGA2ox-B12* and *TaGA2ox-B13*. Many of these genes have very low or undetectable expression in most tissues. *TaGA2ox3*, *TaGA2ox4* and *TaGA2ox9* are overall the most highly expressed GA2ox genes in roots, leaves and stems. In developing grains *TaGA2ox7* is most highly expressed with low levels of expression of *TaGA2ox9* in the early stages. In developing spikes, it is *TaGA2ox9* which has the highest expression with low levels of expression of *TaGA2ox3*, *TaGA2ox6*, *TaGA2ox7* and *TaGA2ox8* at anthesis (Pearce *et al.*, 2015). In *Arabidopsis* there are five *GA2ox* genes which act on C_{19}-GAs, and another two genes, *AtGA2ox7* and *AtGA2ox8* which act on C_{20}-GAs (Thomas *et al.*, 1999, Rieu *et al.*, 2008a, Schomburg *et al.*, 2003).

In rice another mechanism of inactivation has been identified. Here the *ELONGATED UPPERMOST INTERNODE (EUI*) gene which encodes a P450 mono-oxygenase deactivates non-13-hydroxy C_{19}- and C_{20}-GAs by the epoxidation of

the C-16, 17 double bond. Over-expression of this gene gives dwarf plants and the recessive *eui* mutants accumulate large amounts of bioactive GAs in the uppermost internode (Zhu *et al.*, 2006). GA 16, 17-hydrodiols, formed by hydrolysis of the epoxide, have been found in many different species indicating that this inactivation mechanism is present in a number of different plants (Magome and Kamiya, 2016). A third inactivation method, which was found in *Arabidopsis* is thought to be more specific to developing and germinating seeds. It involves the methylation of GA by two members of the SABATH methyl-transferases family GAMT1 and GAMT2, causing the irreversible inactivation of GAs. Both these enzymes act on a range of GAs including both precursors and bioactive forms. The *gamt1 gamt2* double mutant has increased levels of bioactive GAs in siliques and is resistant to GA inhibitors during germination (Varbanova *et al.*, 2007, Xing *et al.*, 2007).

1.3.3 GA Signalling

The main components of the GA signalling pathway are the DELLA proteins, members of the GRAS (GAI, RGA and SCARECROW) family of proteins and are known to be negative regulators of growth. They are believed to be nuclear localised and contain an N-terminal DELLA regulatory domain and a C-terminal functional GRAS domain. They interact with TFs to control GA responsive genes and repress growth (Dill *et al.*, 2001). GA signalling begins with the interaction of bioactive GAs with the soluble nuclear localised GIBBERELLIN INSENSITIVE DWARF 1 (GID1) receptor which was first identified in rice (Ueguchi-Tanaka *et al.*, 2005). In *Arabidopsis* three paralogues of the GID1 receptor are present, *GID1a*, *GID1b* and *GID1c*. This results in high level of functional redundancy where single mutants only show small differences in vegetative growth compared to the wild type, whereas the triple mutant has a more severe dwarf phenotype than the biosynthesis mutants (Griffiths *et al.*, 2006). The rice *gid1* and barley *gse1* loss of function mutants both also show severely dwarfed

phenotypes suggesting that GID1 is the main GA receptor (Ueguchi-Tanaka *et al.*, 2005, Chandler *et al.*, 2008).

The GID1 protein upon binding with GA undergoes a conformational change providing a binding domain for DELLA proteins on the outer surface of its N-terminal binding domain. The GA-GID1 binding activity is stronger in the presence of DELLA proteins (Griffiths *et al.*, 2006, Ueguchi-Tanaka *et al.*, 2007). This GA-GID1 complex interacts with the DELLA proteins and binds to the highly conserved DELLA and VHYNP and poly S/T/V domains (Figure 1.14) (Murase *et al.*, 2008, Hirano *et al.*, 2008). This interaction promotes the recognition of the DELLA proteins by the F-box protein SLEEPY1 (SLY1) in *Arabidopsis* and GID2 in rice, which then interacts with the 3' GRAS domain of the DELLA protein. SLY1/GID2 are the F-box components of the $SCF^{SLY1/GID2}$ (Skp1, Cullin, F-box) E3 ligase which polyubiquitinates DELLAs, targeting them for degradation via the 26S proteasome and this releases the DELLA repression on GA responsive genes, allowing growth (Silverstone *et al.*, 2001, Sun and Gubler, 2004, Thomas and Sun, 2004, Griffiths *et al.*, 2006).

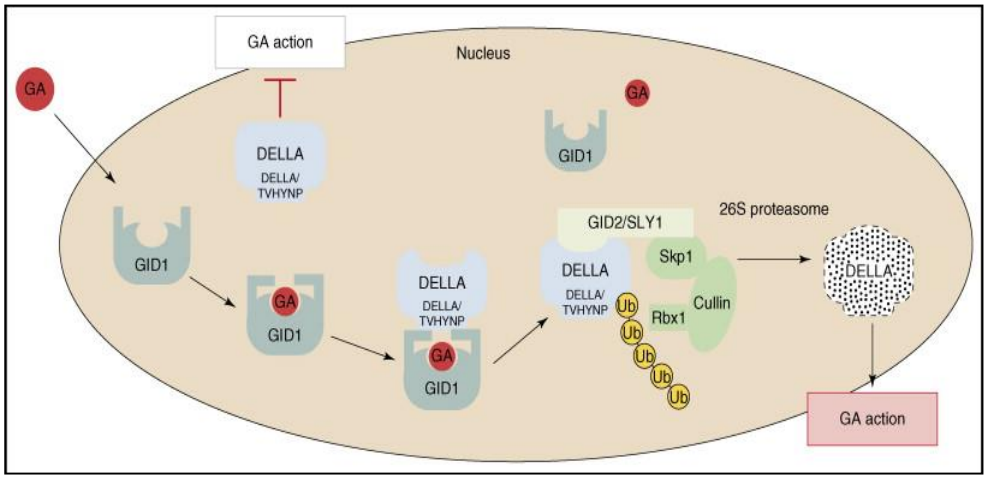


Figure 1.14: GA signalling in plants
GID1 receptor binds with GA and this complex interacts with the DELLA and TVHYNP motifs of the DELLA proteins causing their polyubiquitination by the $SCF^{GID2/SLY1}$complex. This leads to the degradation of the DELLA proteins by the 26S proteasome pathway, resulting in release of repression on growth (Hirano *et al.*, 2008).

In *Arabidopsis* there are five genes that encode DELLA proteins, *RGA* (*REPRESSOR OF GA*), *GAI* (*GA insensitive*), *RGL1* (*RGA-like*), *RGL2* and *RGL3* (Dill *et al.*, 2001). The main repressors of stem elongation in Arabidopsis are RGA and GAI with RGL1 playing a minor role. Seed germination is known to be repressed by RGL2 since the *ga1-3 rgl*-2 is the only *ga1-3 della* double mutant that can germinate without GA application in light but not in the dark (Cao *et al.*, 2005). Additional mutations in the RGA and GAI genes (*ga1-3 rgl2-1 gai-t6 rga-t2*) allows the seeds to germinate in the dark as well indicating the ability of these genes to supress germination. The *RGL3* gene is known to supress the rupture of the testa and endosperm during germination (Dill and Sun, 2001, King *et al.*, 2001, Lee *et al.*, 2002, Wen and Chang, 2002, Piskurewicz and Lopez-Molina, 2009). Across plant species the DELLA proteins are highly conserved, such as in wheat (Rht-1), rice (Slender Rice 1, SLR1), barley (Slender 1, SLN1) and brassica (BnRGA) (Fu *et al.*, 2002, Sun and Gubler, 2004, Gao *et al.*, 2008). As previously mentioned in section 1.1.1 the semi-dwarf varieties of wheat that, in part, underpinned the green revolution had mutations in *Rht* genes. Due to the reduction in stem height these plants are more resistant to lodging and are able to remobilize resources to grain filling rather than stem elongation, thus increasing yield (Hedden, 2003). Mutations in the DELLA domain results in the inability of the GA-GID1 complex to recognise the DELLA proteins and they can no longer be degraded. The *Arabidopsis gai* gain-of-function DELLA protein has a 17 amino acid deletion in the DELLA region and can no longer be degraded in response to bioactive GAs. This was the first DELLA mutant to be characterised. Plants containing this mutation are extremely dwarfed and this phenotype cannot be rescued by the external application of GA (Koornneef *et al.*, 1985, Peng *et al.*, 1997). Mutations in the GRAS functional domain of the DELLA proteins results in the loss of DELLA repression leading to a tall, 'slender' plant phenotype which has been observed in the barley *sln1* and rice *slr1* mutants (Ikeda *et al.*, 2001, Chandler *et al.*, 2002).

It has been suggested that DELLA proteins can function as TFs but the lack of a DNA binding domain within these proteins suggests they primarily function trough transactivation and interaction with other regulatory proteins (Daviere and Achard, 2013). Three modes of action for DELLA proteins to supress GA mediated growth have been suggested: 1) they block the ability of TFs to bind the promoters of GA-regulated transcriptional activators, 2) they act as coactivators of genes that negatively regulate GA signalling and 3) they recruit chromatin remodelling complexes to promoter elements (Nelson and Steber, 2016). DELLA proteins are known to interact with several different TFs and the first example of this was shown in the Arabidopsis hypocotyl where they repress growth by interacting with the bHLH TFs PHYTOCHROME INTERACTING FACTOR (PIFs), PIF3 and PIF4. It was shown that the binding of these TFs to the promoters of their target genes was inhibited upon their interaction with DELLA proteins. This ability of DELLAs to sequester TFs away from their target genes has been shown for several different developmental processes involving different TFs (Alabadi *et al.*, 2008, de Lucas *et al.*, 2008, Feng *et al.*, 2008, Thomas *et al.*, 2016). DELLAs have also been shown to associate with specific gene promoters (Zentella *et al.*, 2007). Marin-de la Rosa *et al*., (2015), through ChIP analysis and sequencing, demonstrated that RGA binds to the regulatory regions of 421 genes showing a preference for *cis* elements recognised by specific TF families involved in biotic and abiotic responses, response to red and far-red light and GA signalling. They found *cis* elements bound by the GARP-*ARABIDOPSIS* RESPONSE REGULATOR (ARR) family which are positive regulators in the CK signalling pathway and interact with both GAI and RGA. These two DELLAs enhance the ability of ARR1 to activate several target genes and control at least two responses known to be controlled antagonistically by GA and CK – root meristem size and de-etiolation. DELLAs have also been shown to interact with several other TFs to activate their expression (Lim *et al.*, 2013, Fukazawa *et al.*, 2014, Yamaguchi *et al.*, 2014). DELLAs are also known to interact with transcriptional regulators such as the JAZ proteins where they mediate the antagonistic role of GA and JA in controlling root growth in *Arabidopsis* (Hou *et al.*, 2010). A chromatin remodelling protein of the CHD3

type, PICKLE (PKL) has been shown to be physically associated with DELLAs which results in reducing its binding ability to target promoters of genes involved in cell elongation. This demonstrated the ability of DELLAs to directly regulate epigenetic mark deposition through their interaction with PKL. It has also been reported that RGL2 and RGL3 interact with the catalytic sub-unit SWI3C of the SWITCH/SUCROSE NONFERMENTING (SWI/SNF) chromatin remodeller suggesting another mechanism for epigenetic regulation by DELLAs (Sarnowska *et al.*, 2013, Zhang *et al.*, 2014)

1.3.4 GA Regulation

The concentration of bioactive GAs in a plant is maintained at an optimal level in response to environmental cues by a feedback mechanism. The expression of CPS is very low and it activity limits the influx of metabolites into the GA pathway and thus it was believed to be rate limiting. However, the over expression of this gene in Arabidopsis only caused an increase in the levels of C_{20}-GAs and not C_{19}-GAs indicating that the 2-ODD genes might be the regulatory step in GA production (Silverstone *et al.*, 1997, Fleet *et al.*, 2003). These genes have also been shown to underlie major growth QTLs (Abe *et al.*, 2012, Teng *et al.*, 2013). The spatial and temporal segregation of GA biosynthetic and inactivating genes is also believed to be an important regulator of GA production. It was shown that the pea *lele* (*psga3ox1*) dwarf mutant phenotype is rescued less successfully by the constitutive overexpression of *PsGA3ox1* compared to re-introduction of the native gene by crossing (Reinecke et al., 2013). It has been shown in several species that expression of the *GA2ox* genes is localised to the base of the meristem to protect it from an influx of GA (Sakamoto *et al.*, 2001b, King *et al.*, 2008). Several TFs are also known to regulate the pattern of GA biosynthetic gene expression. The expression of *GA20ox* genes is supressed in the shoot apical meristem by the homeodomain Class-I KNOX (KNOTTED-like homeobox) TFs to

maintain a pool of undifferentiated stem cells (Sakamoto *et al.*, 2001a, Hay *et al.*, 2002). In Arabidopsis during embryogenesis GA biosynthesis is controlled by two TFs LEC2 and FUS3 which down regulate *AtGA3ox2* expression to allow correct tissue specification (Curaba *et al.*, 2004). The expression of *AtGA2ox6* is up-regulated in developing embryos by the MADS domain transcription factor AGAMOUS-LIKE 15 also indicating the need to restrict GA production during embryogenesis (Wang *et al.*, 2004). Whereas in developing flowers to promote floral organ development the expression of *AtGA3ox1* is upregulated by another MADS box protein AGAMOUS (Gomez-Mena *et al.*, 2005).

In most species, including wheat, GA20ox activity is known to limit the production of bioactive GAs and the over-expression of this gene increases GA content and growth (Huang *et al.*, 1998, Coles *et al.*, 1999, Radi *et al.*, 2006). This was first indicated from work with the Norin-10 dwarf lines which contain gain-of-function mutations in the *Rht-1* gene and are insensitive to applied GA application and have elevated levels of this hormone (Radley, 1970). The maize *d1* dwarf mutant which is defective in the *GA3ox* gene has high levels of GA_{20} but reduced levels of its C_{20}-GA precursors, indicating that there may be a negative feedback regulation of the *GA20ox* genes (Hedden and Croker, 1992). The effects of this mechanism have been demonstrated by showing that the GA biosynthetic genes, *GA20ox* and *GA3ox* are down-regulated by bioactive GAs (Xu *et al.*, 1999, Phillips *et al.*, 1995) and *GA2ox* expression is up-regulated (Thomas *et al.*, 1999). It was also shown that the regulation of *GA20ox* transcription plays a significant role in maintaining the levels of endogenous GAs (Middleton *et al.*, 2012). The early and middle GA biosynthetic genes are not regulated by this feedback mechanism (Hedden and Phillips, 2000, Yamaguchi, 2008).

Transcript analysis has shown that this feedback mechanism involves regulation of the expression of specific 2-ODD genes. In Arabidopsis three of the five *GA20ox* and the *GA3ox1* genes are down regulated by GA treatment whereas genes earlier in the pathway and other ODD paralogues are not

influenced (Phillips *et al.*, 1995, Olszewski *et al.*, 2002, Mitchum *et al.*, 2006, Rieu *et al.*, 2008b). This feedback regulation also involves GA-induced up-regulation of some members of both C_{19} and C_{20} *GA2ox* genes which encode GA inactivating enzymes, and down-regulation of the GA-receptor *GID1* (Thomas *et al.*, 1999, Griffiths *et al.*, 2006). Based on these studies it is likely that transcriptional changes mediated by GA result in changes in the expression of 2-ODD genes which in turn alters the levels of the enzymes they encode. This leads to changes in the availability of GAs through the biosynthetic pathway which is essential in controlling the levels of bioactive GAs. The confirmation of this hypothesis has been difficult due to the low abundance and unstable nature of GA enzymes. Studies in photoperiod regulation of *GA20ox* in spinach did show an increase in *SoGA20ox1* protein levels upon application of GA inhibitors. No changes in transcript levels were observed indicating that GA homeostasis may also have potential post-transcriptional regulatory mechanisms (Lee and Zeevaart, 2007, Hedden and Thomas, 2012).

The levels of DELLA proteins and the GA signalling pathway control the transcriptional feedback and feedforward regulation of GA metabolism. In mutants deficient in GA signalling components including GID1 and GID2/SLY1 the expression levels of feedback regulated *GA20ox* genes are very high and are not down regulated upon GA application. The levels of bioactive GAs are also very high in these mutants. This has also been observed in loss- and gain-of-function DELLA mutants in various species including wheat (Fujioka *et al.*, 1988, Appleford and Lenton, 1991, Ueguchi-Tanaka *et al.*, 2005, Griffiths *et al.*, 2006, Willige *et al.*, 2007, Chandler *et al.*, 2008). The transcript levels of feedback regulated genes in loss-of function DELLA mutants are low whereas in gain-of-function mutants they are very high (Dill and Sun, 2001, Silverstone *et al.*, 2001). The role of DELLAs has also been shown in the feedforward regulation of *GA2ox* genes in pea loss-of-function mutant (*la cry-s*) where along with the reduction in biosynthetic genes there is also an increase in the expression of the two inactivating genes, *PsGA2ox1* and *PsGA2ox2* (Weston *et al.*, 2008). GA regulation is very rapid with DELLA degradation in GA deficient

tissues occurring within 5-10 min of GA treatment and the expression levels of *GA3ox1* and *GA20ox2* decreasing after 15 min (Gubler *et al.*, 2002). The feedback regulation of the *GA20ox* genes is also very important in determining the endogenous levels of DELLA proteins (Middleton *et al.*, 2012).

Several TFs have been identified that underlie GA feedback regulation through specific genes. In tobacco GA supresses the nuclear localisation of the bZIP transcription factor REPRESSION OF SHOOT GROWTH (RSG) which is an activator of *NtGA20ox1* expression (Fukazawa *et al.*, 2010). GA also enhances the expression of *OsYABBY1* (*OsYAB1*) which down-regulates *OsGA3ox2.* The expression of *OsYAB1* increases upon GA treatment and reduces with the application of GA inhibitors indicating the changes in this gene expression are brought about by GA signalling (Dai *et al.*, 2007). In Arabidopsis AGF1 (AT hook protein of GA feedback 1) is involved in down regulating *AtGA3ox1* (Matsushita *et al.*, 2007). Another GA signalling component, SCARECROW LIKE-3 (SCL3) has been recognised to play a role in GA feedback regulation. In SCL3 loss-of function mutant the expression of feedback regulated GA biosynthetic genes are up-regulated indicating that the expression of SCL3 represses the biosynthetic genes (Zhang *et al.*, 2011). It is believed that several mechanisms may exist for the feedback regulation of different genes which might also allow interaction with different environmental and developmental stimuli (Hedden, 2016). Recently it was shown that the DELLA protein GAI interacts with GAF1 (GAI-ASSOCIATED FACTOR1) to promote expression of *AtGA20ox2*, *AtGA3ox1* and *GID1B*. Whilst GAF1 in association with GAI promoted the expression of these genes, a WD-repeat protein TOPLESS-RELATED (TPR) suppressed expression by binding to GAF1, implying that expression of *AtGA20ox2* and possibly other feedback-regulated genes is regulated by a balance between DELLA and TPR (Fukazawa *et al.*, 2014).

1.3.5 GA Transport

The transport of GA from its site of production to other locations in the plants is not completely understood, although evidence of its importance is emerging. The highest levels of bioactive GAs are found in actively growing tissues which also show the highest levels of GA biosynthetic gene expression, indicating that GA is synthesised at its site of action (Kaneko *et al.*, 2003, Teale *et al.*, 2006, Kuromori *et al.*, 2014). However, early intermediaries of the GA biosynthetic pathway have been proposed to be transportable. In germinating *Arabidopsis* seeds *AtCPS1* is expressed in the provasculature whereas *AtKO1* and *AtGA3ox1* and *AtGA3ox2* are all expressed in the cortex and endodermis indicating the transport of intermediaries between these tissues (Yamaguchi *et al.*, 2001). In developing wheat grains while *TaCPS* and *TaKS* are expressed in all tissues, *TaKO* and *TaKAO* are expressed only in the endosperm and inner pericarp but not the outer pericarp. It was also shown that the late biosynthetic genes (*Ta20ox3* and *Ta3ox3*) and the novel *TaGA1ox* are all expressed highly in the endosperm but not the seed coat layer, where the signalling genes are expressed exclusively. This indicates that GA is not produced in the seed coat but moves into and is perceived in this tissue (Pearce *et al.*, 2015). The GA precursor *ent*-kaurene has been shown to be volatile and when produced by a plant is released into the atmosphere. This *ent*-kaurene released by overproducing lines was able rescue the dwarf phenotype of *ent*-kaurene synthesis mutants (ga1-3 and ga2-1) suggesting a mechanism for GA-mediated interaction between plants or between organs of the same plant (Otsuka *et al.*, 2004).

The physical properties of GA also make them likely to be transported as they are weak acids, similar to ABA and IAA making them subject to an ion-trapping mechanism that would concentrate them to the neutral cytoplasm. This indicates it would require an efflux carrier to transport the negatively charged GA molecule from the cytosol (Vieten *et al.*, 2007, Kuromori *et al.*, 2010). It is believed that cells would use specific carriers for GA transport as is the case

with ABA and IAA. It is also possible that since the hormones become uncharged due to protonation once in the acidic apoplast they could diffuse across membranes [(Vieten *et al.*, 2007, Dayan, 2016), and references therein]. However, Pauls *et al*., (1982) showed that GA only disturbs the phospholipid membranes of liposomes rather than penetrating into them restricting the diffusion of GA into cells. Therefore, it is believed that both influx and efflux carriers must exist for GA transport.

The first studies on GA transport involved grafting experiments which showed that GA signals are transportable between graft fusions (Katsumi *et al.*, 1983, Reid *et al.*, 1983, Proebsting *et al.*, 1992). More recent grafting experiments have shown that GA produced by the shoot is necessary for hypocotyl xylem expansion (Ragni *et al.*, 2011). Regnault *et al*., (2015) showed GA_{12} to be transportable in both an acro- and basipetal direction over long distances through the plant vasculature. Wild type root stocks were able to rescue the phenotypes of plants unable to produce precursors of GA_{12} but not of those deficient at later stages in the pathway. They also showed that this GA_{12} is able to initiate the rest of the GA biosynthetic mechanism and activate the signalling cascade in the grafted plants. In another experiment the same authors showed that endogenous bioactive GAs are not transmitted to the offspring and are unable to rescue the non-germinating phenotype of biosynthetic mutants (Regnault *et al.*, 2016).

A well-known example of GA transport in a plant comes from germinating cereal seeds where GA produced by the scutellum moves to the aleurone layer which does not produce its own GA or express GA-biosynthetic genes (section 1.2.5.1) (Kaneko *et al.*, 2003). GA produced by the scutellum is impermeable through the membranes of aleurone layer cells and a GA receptor different from the nuclear localised GID1 must exist on the plasma membrane but it hasn't yet been identified (Hooley *et al.*, 1991, Lovegrove and Hooley, 2000). However, Yano *et al*. (2015) demonstrated in rice that GA perception through the GID1 receptor was sufficient for all GA responses. These experiments

however used GA_3 as the source of GA leaving the possibility of an intermediary being perceived by the plasma membrane or the existence of a transporter able to move GA into the nucleus (Dayan, 2016). Recently several non-specific transporters have been shown to actively transport GA – AIT3 (ABA-IMPORTING TRANSPORTER), GTR1 (glucosinolate transporter) and NPF3 (nitrate transporter) (Kanno *et al.*, 2012, Saito *et al.*, 2015, Tal *et al.*, 2016) and one of these or a yet unidentified GA transporter could be involved in the transport of GA from the scutellum to the aleurone layer during germination.

1.4 Tissue Specific Promoters

A promoter is a specific genetic region located at the 5' end of the transcription start site and is involved in the binding of a RNA polymerase to initiate transcription. They are a set of transcriptional control modules clustered around the initiation site of RNA polymerase II and are involved both quantitatively and qualitatively in gene expression (Mitsuhara *et al.*, 1996, Russell, 1996, Zheng and Baum, 2008). In the nucleus of eukaryotic cells there are present three RNA polymerases, RNA polymerase I, II and III. Plant cells in addition also contain RNA polymerase IV and V. RNA polymerase I synthesises the precursors of rRNA, RNA polymerase II produces the precursors of mRNA and RNA polymerase III synthesises the precursors of tRNAs, 5S-rRNAs and other miRNAs. RNA polymerases IV and V are both involved in the synthesis of miRNAs involved in gene silencing (Lodish *et al.*, 2000, Haag and Pikaard, 2011).

Most cellular genes are transcribed by RNA polymerase II which binds with elements in the genomic DNA but it cannot initiate transcription on a DNA template. This requires nuclear proteins such as TFs called transcription factor for polymerase II (TFII) which assemble with RNA polymerase II at the promoter region and initiate transcription. RNA Polymerase II also requires activator, mediator and chromatin-modifying proteins to correctly transcribe DNA (Alberts *et al.*, 2002). The basal or core promoter is located about 25 to 40 nucleotides upstream of the transcription start site and the promoter can extend up to 200 base pairs upstream. The initiation of transcription depends on sequences found in this core promoter, and along with this region other DNA motifs occurring in the surrounding DNA are involved in the regulation of gene expression (Potenza *et al.*, 2004).

Highly conserved sequence motifs known as *cis*-elements are regions of non-coding DNA that regulate the transcription of nearby genes. These sequences bind with sequence targeted TFs within the promoter of a gene (Alberts *et al.*,

2002). Located about 25 base pairs upstream from the transcription start site in the promoter region of most genes exists a DNA sequence known as the TATA box which signals the start of transcription. This was the first element recognised in eukaryotes and is the only element with a relatively fixed location in relation to the transcription start site (Breathnach and Chambon, 1981). The sequence composed entirely of A and T is approximately 8 base pairs long, often surrounded by GC rich sequences and is highly conserved in both plants and animals (Yamamoto *et al.*, 2007, Porto *et al.*, 2014). The TFII recognises and binds to the TATA box which causes other TFs to assemble at the promoter leading to gene expression (Alberts *et al.*, 2002). In promoters that lack a TATA box a downstream promoter element located about 30 base pairs downstream of the transcription start site is recognised by the TFII which binds to it (Burke and Kadonaga, 1996).

Depending on their activity, promoters are classified as either constitutive, those that promote gene expression uniformly throughout the plant, or tissue specific, those that determine gene expression only in certain tissues or induced by certain physiological conditions, age and biotic and abiotic factors (Hochheimer and Tjian, 2003). Diverse, semi-conserved sequences of DNA present around the RNA polymerase binding site lead to variability in gene expression. Protein factors involved in controlling the level and pattern of gene expression bind to these DNA sequences. These sequences known as enhancers have the ability to spatially and temporally control the pattern of gene expression and are considered as part of the core promoter (Potenza *et al.*, 2004). Enhancers are usually discovered through promoter deletion studies, DNA foot-printing and site specific sequence mutation (Cal *et al.*, 2007). They can be located hundreds or thousands of base pairs away or either upstream or downstream of, within the coding region or in the intron or in regions adjacent to the promoter of the gene they control. They are also orientation independent. The proteins acting on enhancers are combined for expression to occur only at required sites and at specific times giving them temporal and spatial specificity. While most *cis*-elements are involved in

enhancing gene expression, some known as silencers repress this (Alberts *et al.*, 2002, Fessele *et al.*, 2002, Kolovos *et al.*, 2012). Gene expression or repression occurs when regulatory proteins bind to their specific enhancers. This results in the formation of DNA loops which allows the regulatory proteins to interact with TFs bound to promoter elements (Alberts *et al.*, 2002, Potenza *et al.*, 2004).

Constitutive promoters control genes that are active in almost all cells and throughout development, though their expression levels can be varied depending on the cell type. In plant biotechnology cauliflower mosaic virus promoter (CaMV35S) is the most commonly used constitutive promoter and most commercial varieties of genetically modified plants contain it (Odell *et al.*, 1985, Park *et al.*, 2010, Ranjan *et al.*, 2011). The domains present in this promoter have been characterised and can be manipulated to give this promoter spatial or temporal roles (Kay *et al.*, 1987, Benfey and Chua, 1990). Even though this promoter is widely used its expression is relatively low in reproductive tissues particularly in pollen. To overcome this problem several other constitutive promoters have been identified in various species (Park *et al.*, 2012, Porto *et al.*, 2014).

To understand the molecular mechanisms that are involved in gene expression and tissue differentiation it is important to understand the functions of promoters that act in different organs. This helps in developing constructs that allow for the expression of target genes in specific tissues where these promoters are active (Ortiz, 1998). There is also a higher chance of silencing in constitutive promoters than in tissue-specific ones. Transgene silencing in the T_1 and T_2 generations has been shown in wheat when using a number of different constitutive promoters (Demeke *et al.*, 1999, Anand *et al.*, 2003), whereas seed specific promoters have been shown to be stable up to the T_5 generation in barley (Horvath *et al.*, 2001). Choi *et al.*, (2003) showed that the expression of GUS and GFP was stable in 93% of barley lines when driven by an endosperm specific promoter compared to the *bar* gene driven by *ZmUbi I*

constitutive promoter being stable in only 60% of the lines. Using constitutive promoters also results in unnecessary gene expression in non-target tissues that may interfere with normal plant development. Pino *et al.*, (2007) compared the activity of a constitutive and a stress inducible promoter to drive the expression of freezing tolerance genes in potato. They showed that constitutive expression resulted in the same level of freezing tolerance as the stress induced promoter but was associated with negative phenotypes such as smaller leaves, stunted plants, delayed flowering and reduced tuber formation. Similar results have also been shown in other plant species (Li *et al.*, 2013, Estrada-Melo *et al.*, 2015). The constitutive over-expression of GA-inactivating genes resulting in reduced levels of GA also causes extreme dwarf and semi-dwarf phenotypes in many plant species including wheat (Hedden and Phillips, 2000). Using tissue-specific promoters allows for the control of gene expression when and where needed and eliminates the problems posed by using constitutive promoters.

1.5 Aims of the project

- Determine whether insensitivity to GA in the embryo and aleurone layers can be used to reduce α-amylase levels in the mature grain and improve flour quality. Insensitivity to GA in the embryo will also potentially promote understanding of the role of GA in dormancy, germination and PHS.
- Determine if the seed coat restricts grain size and if increasing the levels of GA in these tissues will allow production of larger grain, without adverse effects on flour quality.
- Determine whether GA signalling in the endosperm transfer layer has a role in grain development by attempting to introduce GA insensitivity and increase GA biosynthesis in this tissue.
- Decrease the amount of GA in the endosperm late in grain development to determine if this has the potential to improve grain quality without impacting grain size.
- Study the effects of crossing lines previously generated in our laboratory to combine their phenotypes of increased grain size and improved flour quality.

For this purpose a range of transgenic lines were generated where GA biosynthesis, inactivation or signalling was modified and each line was co-transformed with nuclear-targeted green fluorescent protein (H2B::GFP) (Figure 1.15) expressed from the same promoter to monitor promoter activity.

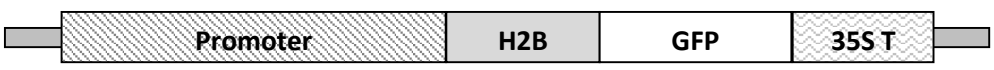


Figure 1.15: Basic schematic of promoter::GFP expression cassettes

Chapter 2. Materials and Methods

2.1 Plant Material and Growth Conditions

Wheat plants (cv. Cadenza) were previously co-transformed by particle bombardment (Pastori *et al.*, 2001, Sparks and Jones, 2014) with the constructs listed in Table 3.1. The pBRACT vector containing the selectable marker for BASTA under control of a Maize ubiquitin promoter (ZmUbi::BAR::NosT) was used as the donor vector for creating these constructs. The vector was modified to contain an additional expression cassette containing each promoter linked to the H2B nuclear targeting signal (Kanda *et al.*, 1998): green fluorescent protein and a CaMv35S terminator (Figure 1.13).

Segregating T1 transgenic wheat lines harbouring constructs one to seven (Table 3.1) were available at the start of the project, along with homozygous seed (T4) for constructs eight and nine. T1 transgenic seeds were sown in standard seed trays of 24 cells in Rothamsted standard compost with one grain sown per cell. Plants were grown in the GM glasshouse under controlled conditions of 16-hour photoperiod with day/night temperatures of 23/18^{o}C under 400 W sodium lamps (Philips SON-T Agro 400). Leaf material was harvested for genotyping from 2-week-old seedlings and during this time the plants were moved to a cold room. After genotyping (sections 2.2.1, 2.2.2 and 2.2.3 and Chapter 3) PCR-positive transgenic plants were potted on to 15 cm pots with one plant per pot. Plants were allowed to self-pollinate and in order to avoid any cross pollination each ear was covered with a crossing bag once it reached the booting stage.

2.1.1 Yield and Development Experiments

Homozygous plants were used for either yield and/ or development experiments depending on the constructs involved. These experiments were all set up in randomised complete block designs (RCBD) in consultation with a statistician with either three or four replicates in each experiment set-up as separate blocks. Experiments varied in that plots consisted of either one plant per pot in 15 cm pots or two plants in 20 cm pots. All plants were cut down to five tillers and automated flood bench irrigation was used to ensure uniformity of treatment across each experiment. During the experiment the timing of anthesis was scored and each ear considered to have anthesed when floret one and two (Figure 1.6) on every spikelet on the ear had anthesed. Grains were harvested for transcript analysis at given time points post-anthesis by collecting the grains from floret one and two of every spikelet along the ear, except the top and bottom most spikelets. These grains were then counted, weighed, flash frozen and stored at -80^{o}C to be analysed at a later date. Grain development was also studied at different time points by microscopy, using four grains per time point, two grains harvested from the middle of the ear, one from towards the top and one towards the bottom. Two of the grains were examined in a transverse section and two in a longitudinal section. Mature grains were harvested to determine yield and grain quality for each line.

2.2 Molecular Methods

2.2.1 Genomic DNA (gDNA) Extractions

One 8-cm long leaf from each individual plant was harvested and collected in 2-ml 96 deep-well plates (Thermo Scientific, UK) containing two 2-mm ball-bearings (Atlas laboratories, UK) per well. The samples were then lyophilised and ground to a fine powder using a tissue lyser (Qiagen, UK).

For the extraction process 600 µl buffer [Tris base (100 mM), KCl (1 M), EDTA (10 mM), pH 9.5 with 0.75% PVP-40 and 0.36% sodium bisulphite added on day of use] was added to the lyophilised leaf powder and incubated at 65°C for 60 minutes (min). At the same time 330 µl of 100% isopropanol was dispensed into each well of a fresh 96-well plate and stored at -20^{o}C. After the 60-min incubation, 200 µl of 5 M potassium acetate (pH 5.8) was added to the extraction buffer and the mixture shaken to form a homogenous suspension.

Samples were then centrifuged at 2500 revolutions per minute (rpm) for ten min and 300 µl of the supernatant transferred to the cold isopropanol blocks. This was incubated at room temperature (RT) for ten min and then centrifuged at 2500 rpm for ten min. The supernatant was carefully poured off making sure none of the pellet was lost. To this pellet 800 µl of 70% ethanol (v/v) was added and the blocks centrifuged at 2500 rpm for five min, after which the supernatant was poured off carefully. The DNA pellets were dried at 50 °C for 60 min making sure all the liquid had evaporated. The pellet was then re-suspended in 200 µl of TER [TE Buffer - Tris-HCl (10 mM) and EDTA (1 mM), pH7.5 with 0.05 mg/ml Pancreatic RNase]. This was incubated at 50°C for 60 min and then at 4°C overnight. The gDNA was stored at -20 °C for future use.

2.2.2 Polymerase Chain Reaction (PCR)

Standard 25 µl PCR reactions were carried out to amplify wheat gDNA extracted in section 2.2.1 using GoTaq Flexi DNA polymerase (Promega Corporation, USA). In the PCR, 10 ng of DNA served as template in a reaction containing 1X GoTaq green flexi buffer, 1.5 mM $MgCl_2$, 0.2 mM each dNTPs (Invitrogen/Thermo Fisher Scientific, USA), 0.2 µM each of upstream and downstream primers (Appendix 1) and 1 unit of GoTaq DNA polymerase enzyme.

The reactions were placed in a thermal cycler with a preheated lid and the cycling started with an initial denaturation of two min at 95^{o}C. The samples were then cycled for 25-30 times through standard PCR conditions of denaturation at 95^{o}C for 30 seconds (sec), annealing for 30 sec at temperatures ranging from 56^{o}C to 68^{o}C (depending on the melting temperature of the primers) and extension for a time of one min/kb (depending on the anticipated size of the PCR product) at 72^{o}C. The reaction had a final extension of seven min at 72^{o}C and was then stored at 4^{o}C.

To visualise the PCR product, 20 µl of each reaction was run on a 1X TBE-buffered (45 mM Tris-borate, 1 mM EDTA pH 8.3) 1% agarose gel containing 0.5 µg/ml ethidium bromide. Alongside the PCR products 0.5 µg of a 1-KB DNA ladder (Thermo Fisher Scientific, USA) was run as a size standard. The products were run for 90 min at 100 V and visualised on a UV transilluminator (Syngene, UK).

2.2.3 TaqMan Assay

The TaqMan assay is a real-time quantitative PCR (QRT-PCR)-based assay which was used to determine the zygosity status of transgenic plants in order to identify homozygous lines. Reactions containing 50 ng of gDNA were set up in white semi-skirted 96-well PCR plates (Starlab International GmbH, Germany)

to simultaneously amplify the transgene and an endogenous gene. The reaction mixture contained 1X Absolute qPCR low Rox mix (Thermo Fisher Scientific, USA), 0.5 µM of each forward and reverse primers and hybridisation probe to amplify the transgene and 0.75 µM of forward and reverse primers and hybridisation probe (Appendix 1) to amplify the endogenous reference gene - *TaHd1*.

Primers and probes were designed using the Primer3Plus software (Untergasser *et al.*, 2007) to amplify products of 50-200 base pairs (bp) in length. Each primer measured between 15-30 bp in length with a Tm of 58-60^{o}C. The Tm of the probes was 10^{o}C higher than the primers and measured 20-30 bp in length and each contained a fluorescent dye at the 5' end and a quenching dye at the 3' end.

The assay was performed in the 7500 Real Time PCR System (Applied Biosystems/Thermo Fisher Scientific, USA) with an initial step to activate the enzyme at 95^{o}C for 15 min. The reaction was then continued for 40 cycles with denaturation at 95^{o}C for 30 sec and annealing/extension at 60^{o}C for one min. The data was collected at the 60^{o}C step.

2.2.4 RNA extraction with 1st DNase treatment

RNA extractions were performed using a modified version of the sodium dodecyl sulphate (SDS)/TRIzol method (Wang *et al.*, 2012) on wheat grain samples which had been ground using a liquid nitrogen mill (SpexSample Prep, UK). To 150-170 mg of ground tissue 500 µl of extraction buffer [Tris-HCl (100mM), pH 9.0 with 2% β-mercaptoethanol added on day of use] was added and mixed by vortex to homogenise the mixture and then incubated at RT for 15 min. To this was added 25 µl of 20% SDS, the sample mixed by inverting four to five times and the solution incubated at RT for a further five min. Samples were then centrifuged at 4^{o}C at 5000 rpm for ten min. The

supernatant was removed to a fresh 2 ml tube and 800 µl of Trizol (Ambion/Thermo Fisher Scientific, USA) was added and the solution mixed by vortex and incubated at RT for ten min. To this solution was added 240 µl of chloroform (Arcos organics/Thermo Fisher Scientific, USA), after which the sample was centrifuged at 4^{o}C at 5000 rpm for ten min. Approximately 700 µl of the aqueous phase was removed to a fresh 2 ml tube and 700 µl of isopropanol was added and mixed by inverting four to five times. The samples were then incubated for 20 min at -20^{o}C and centrifuged at 4^{o}C at 5000 rpm for ten min. The supernatant was then discarded and the pellet re-suspended in 130 µl of DEPC-treated water (0.1% diethylpolycarbonate).

For the DNase treatment, 15 µl of RNase-free DNase 10X Reaction buffer (RQ1, Promega Corporation, USA) and 5 µl of RNase-free DNase were added and samples incubated at 37^{o}C for 30 min. To this was added 250 µl of DEPC-treated water and samples mixed by inverting four to five times. To this solution 400 µl phenol:chloroform (1:1, low pH) was added and the sample mixed by inverting four to five times and then centrifuged at 4^{o}C at 5000 rpm for ten min. Approximately 400 µl for the aqueous phase was removed to a fresh 2 ml tube and to this was added 400 µl of chloroform, the sample mixed by inverting and centrifuged at 4^{o}C at 5000 rpm for ten min. The aqueous phase was removed to a fresh 1.5 ml tube, to which 40 µl of sodium acetate (3 M, pH 4.8) and 800 µl chilled 100% ethanol were added and the sample mixed by inverting. The samples were then incubated at -80^{o}C for 30 min or -20^{o}C for two hrs and then centrifuged at 4^{o}C at 5000 rpm for 20 min.

The supernatant was discarded using a pipette, the pellet re-suspended in 500 µl of chilled 70% ethanol (v/v) and then centrifuged at 4^{o}C at 5000 rpm for five min. The supernatant was discarded and pellet dried in a vacuum concentrator for ten min to ensure all liquid had evaporated and then re-suspended in 30-50 µl DEPC-treated water. The RNA was stored at -80^{o}C for future use.

2.2.5 Second DNase treatment

The RNA extracted as described in section 2.2.4 was subjected to a 2nd DNase treatment to ensure complete removal of any remaining gDNA. The RNA was quantified using a Nanodrop™ ND-1000 spectrophotometer (LabTech International Ltd, UK) and prior to the DNase treatment a 500-ng aliquot of the RNA sample was run on a 1X TBE buffered gel to confirm the presence of the expected ribosomal RNA bands and validate the RNA quantification. For the DNase treatment, a 2.5 µg aliquot of RNA was made up to 10 µl with DEPC-treated water. To this were added 1.25 µl RNase-free DNase 10X Reaction buffer (RQ1, Promega Corporation, USA) and 1.25 µl (0.5 unit/µg of RNA) RNase-free DNase enzyme and the reaction incubated at 37°C for 30 min. To terminate the reaction 1.25 µl of DNase stop solution was added to the samples and incubated at 65°C for ten min. The DNase treated RNA was stored at -80°C for future use.

2.2.6 cDNA synthesis

Superscript III reverse transcriptase (Thermo Fisher Scientific, USA) was used to generate cDNA from DNase-treated RNA. For each sample of RNA along with a positive RT reaction a non-RT – no enzyme – negative control was also prepared. Each RT reaction consisted of 10 µl RNA (2.0 µg), 0.5 µl oligo dTV (100 µM), 1 µl dNTP's (10 mM) and 1.5 µl DEPC-treated water. For the NRT reactions, 0.5 µg of RNA was treated the same as for the RT reaction. These samples were heated to 65°C for five min in a thermo cycler and then immediately moved to ice. To each of the RT samples was added 4 µl of 5X 1st strand buffer, 1 µl DTT (0.1 M), 1 µl Superscript enzyme and 1 µl water. In the NRT reactions the Superscript enzyme was replaced by water. These samples were then heated to 25°C for five min, 50°C for 60 min and 70°C for 15 min and then held at 4°C. The cDNA samples were stored at -20°C for future use.

2.2.7 Real Time Quantitative PCR (qRT-PCR)

For the purpose of qRT-PCR a 1/20 dilution was made of the cDNA samples generated in section 2.2.6. This was done by diluting an aliquot of 10 µl of cDNA in 190 µl of DEPC-treated water and then stored in strips of eight PCR tubes. Primer mix containing 2.4 µl (100 µm) of each forward and reverse primers (Appendix 1), 240 µl $MgCl_2$ (25 mM), 2 µl reference dye (100X Rox) and 253.2 µl DEPC-treated water was prepared for each of the primers used in the qRT-PCR. This mix was dispensed equally into strips of eight PCR tubes (62.5 µl/tube).

The qRT-PCR was set-up in white 96-well semi-skirted plates (Starlab International GmbH, Germany) containing 10 µl SYBR (SYBR Green JumpStart Taq ReadyMix without $MgCl_2$ in buffer, Sigma-Aldrich Co., USA), 5 µl primer mix and 5 µl of the 1/20 diluted cDNA. Each plate was set-up using Biomek NX S8 laboratory automation workstation (Beckman Coulter Ltd., UK). For each RT sample its corresponding NRT sample was tested for at least one reference gene and the transgene being studied. The reactions were run on a 7500 Real Time PCR System (Applied Biosystems/Thermo Fisher Scientific, USA) with an initial denaturation step at 95^{o}C for ten min. Each primer pair was optimised to run on standard cycling conditions of 95^{o}C for 15 sec and then 60^{o}C for one min, and this was continued for 40-45 cycles. This was followed by a default dissociation stage as a quality control measure to check for the presence of only one product for each primer pair used. The data were collected at the 60^{o}C stage.

The relative quantification (RQ) of each individual reaction was calculated based on their threshold cycle (Ct) values and the efficiency of the reaction which was obtained using the LinRegPCR software v12.3 [HFRC, Netherlands (Ramakers *et al.*, 2003)]. For each sample two technical replicates were averaged to provide the RQ for that sample and if these were more than one Ct apart they were discarded.

Normalised relative quantification (NRQ) was calculated (Rieu *et al.*, 2008b) for the genes of interest using the geometric mean of three endogenous genes – *Ta2526*, *TaGapDH* and *TaSDH* – that were chosen based on their consistent levels of expression throughout grain development. The qRT-PCR was performed on *Ta2526* using forward primer qTa2526-Fext and reverse primer qTa2526-Rext, on *TaGapDH* using forward primer qGAPDH-ex3F and reverse primer qGAPDH-ex4R and on *TaSDH* using forward primer qSDH-01F and reverse primer qSDH-01R (Appendix 1).

2.2.8 Southern Hybridisation

Southern blot hybridisation was performed for wheat using the DIG detection system.

2.2.8.1 Restriction endonuclease digestion and electrophoresis of gDNA restriction fragments

Genomic DNA (15 µg) was digested overnight in 440 µl reactions containing three units of restriction enzyme per µg of DNA (1.5 unit enzyme/µg gDNA added in the evening and the rest added the next morning). To this reaction was also added 0.3 mg/ml Bovine Serum Albumen (BSA) and 4 mM spermidine. The digests were incubated at 37^{o}C for a minimum of 16 hrs.

After the digestion 20µl of 3M sodium acetate (pH 5.2) and 450µl 100% ethanol were added to the reaction and incubated at -20^{o}C for one hr. The reaction was centrifuged at 13,000 rpm at 4^{o}C for 30 min and the supernatant removed. To the pellet was added 70% (v/v) ethanol and centrifuged at 13,000 rpm for 15 min at RT. The supernatant was discarded and the pellet air dried for one hr. The pellet was re-suspended in 30 µl TE buffer and stored at -20^{o}C. Control plasmid digests representing 1 copy and 10 copies, estimated based on probe and plasmid size were also digested using the same restriction enzyme.

Before electrophoresis the reactions were incubated at 65^{o}C for ten min and then transferred to ice and 5 µl of loading dye (15% w/v ficoll, 0.25% w/v bromophenol blue and 0.25% w/v xylene cyanol FF in sterile distilled water) added. The samples were loaded on to a 1X TBE buffered 0.7% agarose gel containing 0.5 µg/ml ethidium bromide and allowed to settle in the wells for 10 min before starting electrophoresis. The gels were run slowly at ~1 V/cm until digested DNA had reached the bottom of the gels. The digested DNA was visualised and photographed under UV illumination against a ruler (to measure relative position of 1-KB ladder markers) and the dimensions of the gels recorded before transfer.

2.2.8.2 Transfer of digested gDNA to nylon membranes

After the completion of electrophoresis the gels were soaked in depurination solution (0.25 M HCl) for ten min and then rinsed in distilled water. The gels were then transferred to denaturation solution (1.5 M NaCl and 0.5 M NaOH) for 2 X 15 min washes and then to neutralisation solution (0.5 M Tris HCl, pH 7.5 and 3 M NaCl) for 2 X 15 min washes. The final neutralisation step was performed for a longer duration in order to achieve a pH of 7 – 7.5. The gels were then washed three times in distilled water. All steps were performed on a shaker. After this the digested gDNA was transferred from the neutralised gels to positively charged nylon membranes (Roche Molecular Biochemicals, USA) as described by Sambrook *et al*. (1989). The transfer of DNA was continued for 36 hrs, after which the membranes were fixed in a UV Stratalinker (Stratgene, USA) at 12,000 J (auto settings) and stored at 4^{o}C between two sheets of Whatman 3M filter paper prior to hybridisation.

2.2.8.3 Synthesis of Digoxigenin-II-dUTP (DIG) labelled probe

Plasmid DNA was used as a template and DIG label incorporated into double stranded DNA probes in a PCR reaction. This was done according to the protocol for PCR DIG probe synthesis (Roche Molecular Biochemicals, USA).

The PCR products were visualised on a 1X TBE buffered 1% agarose gel to confirm the incorporation of the DIG label against control reactions (higher mass DIG-UTP being incorporated instead of dTTP).

2.2.8.4 Hybridisation of membranes

The membranes were hybridised in rolling tubes in a hybridising oven (Hybaid/Thermo Fisher Scientific, USA) according to the DIG system User's Guide for Filter Hybridisation (Roche Molecular Biochemicals, USA). The membranes were first prehybridised in filter sterile DIG Easy Hyb buffer which was added at 20 ml/100 m^2 of membrane. The buffer was made up by adding 64 ml distilled water to DIG easy hyb granules and incubated at 42^oC to dissolve. Pre-hybridisation was carried out at 42^oC for two hrs, after which the pre-hybridisation solution was replaced with 15 ml of the DIG Easy-Hyb containing DIG-labelled probe and hybridisation carried out overnight. The probe was previously denatured by boiling at 65^oC for ten min and added to the DIG Easy Hyb at 1 µl/ml. After the completion of hybridisation, the probe solution was recovered and the membranes washed twice for five min in wash solution 1 [2X SSC (300 mM sodium chloride, 30 mM sodium citrate, pH 7.0), 0.1% SDS] at RT. After this the membranes were washed twice in wash solution 2 [0.5X SSC (75 mM sodium chloride, 30 mM sodium citrate, pH 7.0), 0.1% SDS] for 15 min, and then in wash solution 3 [0.1X SSC (15 mM sodium chloride, 1.5 mM sodium citrate, pH 7.0), 0.1% SDS] also twice for 15 min. The washes in solution 2 and 3 were carried out at 68^oC in a heated water bath.

After completing the washes, the membranes were rinsed in washing buffer [0.3% tween 20 in maleic acid buffer (MAB – 100 mM maleic acid, 150 mM NaCl, pH 7.5)] for one min and incubated in blocking solution (1X blocking in MAB) for 30 min. The blocking solution was replaced by the antibody solution and the membranes incubated in this for a further 30 min. The antibody solution was prepared by adding Anti-DIG AP (1:10,000) in blocking solution (5

µl in 50 ml). This step was performed in a sealed plastic bag. The membranes were then rinsed in washing buffer twice for 15 min each.

2.2.8.5 Detection of DIG labelled probes

The detection of the DIG labelled probe was performed as described in the DIG system users guide for filter hybridisation (Roche Molecular Biochemicals, USA) using CSPD [Disodium 3-(4-methoxyspiro {1,2-dioxetane-3,2'-(5'-chloro) tricyclo [3.3.1.1^{3,7}] decan} -4-yl) phenyl phosphate]. Before the addition of the chemiluminescent substrate the membranes were equilibrated by washing in detection buffer (100 mM Tris-HCl, pH 9.5, 100 mN NaCl) for two min. To 15 ml of detection buffer was added 15 µl of CSPD and this was spread on the membranes by the single filter method. The membranes were placed between two sheets of acetate and the chemiluminescent substrate scattered over the surface (DNA side). The acetate sheet was then lowered and the substrate gently and evenly distributed by rubbing the acetate with a tissue. The acetate was then sealed ensuring there were no air bubbles inside.

The sealed membranes were placed in an autoradiograph cassette (GRI) and exposed to X ray film (GRI). The cassette was initially incubated at 37^{o}C for 15 min and then incubated at RT. Multiple exposures were obtained from the membranes at different lengths of time.

2.3 Yield Measurements

Yield was measured in terms of grain number, weight, size and shape characteristics using a MARVIN digital seed counter (GTA Sensorik GmbH, Germany). The machine takes a 2D image of the grains and uses this to count the number of grains and measures the length, width and area of each individual grain.

The seed counter was set up to measure everything that falls within a specified range – 2-6.5 mm for width, 5-10 mm for length and 10-55 mm^2 for area. These parameters were set-up to ensure that the machine only counts and measures wheat grains and not soil particles or pollen grains that might be present in the samples. To collect the data the seeds were placed in the MARVIN chamber ensuring that no two grains were touching each other. An image was then taken of the sample which was used to measure the various yield parameters. These grains were then weighed to calculate their thousand grain weight (TGW).

2.4 Quality Analysis

2.4.1 Single Kernel Characterisation System (SKCS)

Grain hardness and moisture were measured on samples of 100 randomly selected mature grains using the SKCS-4100 (Perten instruments, Sweden). The SKCS (Martin *et al.*, 1993) is the most widely used method of measuring grain hardness and moisture and is one of the standards for measuring wheat kernel texture (Pearson *et al.*, 2007). The SKCS-4100 automatically separates grains and determines individual weights, diameters, moisture and crushing profiles. The crushed samples were collected to be used for further analyses. The hardness index is calculated for each individual grain from these measurements using a hardness algorithm developed by the United States Department of Agriculture, Agricultural Research Service (USDA/ARS) US grains marketing research laboratory (USDA, 2016).

2.4.2 Alpha amylase assay

The α-amylase content of wheat flour was measured by a modified version of the Amylazyme protocol (Megazyme International Ireland Ltd., Ireland). The level of α-amylase in grains tends to be stochastic with some grains being unusually high compared to others. In order to avoid variation due to the presence of a few high expressing grains a large pool of grains was used for the measurement. For each sample 100 crushed grains that had been used for grain hardness measurements, as described in section 2.4.1, were milled using a liquid nitrogen mill (SpexSample Prep, UK) and from this 25 mg of flour used for the assay. Wheat flour was weighed into a 2-ml tube and to this was added 500 µl buffer A (100 mM Sodium maleate, pH 6.0, 5 mM $CaCl_2$ and 0.02% NaN_3) and a magnetic micro stir bar. The tube was transferred to a 60^{o}C water bath with a submersible magnetic stirrer set at ~850 rpm and the extraction continued for exactly five min. With the sample still stirring, 100 µl of

amylazyme solution (one amylazyme tablet dissolved in 1 ml buffer A – solution kept constantly vortexed to ensure it is uniformly mixed) was added using a cut tip and the reaction continued for a further five min. The sample was then removed from the water bath and 1.2 ml of stop solution (2% w/v tris base, pH 9.5) added followed by thorough vortexing to stop the reaction. The samples were then kept at RT for a minimum of five min and then centrifuged at 3500 rpm for five min and the supernatant removed to a fresh 1.5 ml tube. A flat bottom assay plate was used to measure absorbance of 150 µl of the supernatant at 590 nm.

A standard curve was generated using α-amylase from barley malt (1.8 units/mg) (Sigma-Aldrich Co., USA) and was used to calculate the amylase content of the samples using their ODs. A solution containing 2 units of amylase was made using the barley malt and from it aliquots of 1, 0.5 and 0.25 units were taken and the α-amylase assay performed on them. From each of these serial dilutions were generated and their ODs measured and used to create standard curves. The values obtained from the standard curves for each sample were converted to Ceralpha units using the following formula:

Units/g = milliUnits/0.025 g (i.e. per assay) x 40 x 1/1000

where:
milliUnits (per assay) is obtained from the standard curves.
40 = conversion from 0.025 g (as assayed) to 1 g of flour

1/1000 = conversion from milliUnits to Units

2.4.3 Grain Nitrogen Measurements

The percentage of nitrogen in wheat grains was measured on flour samples from the pool of grains used in section 2.4.2. Prior to analysis the samples were heated at 80^{o}C for a minimum of four hours and then cooled for half an hour in a desiccator. For the analysis 150 mg (+/- 0.2 mg) was weighed out into foil parcels. The nitrogen measurements were performed by the Rothamsted Analytical Chemistry Unit using Leco CN628 (Leco corporation, USA).

2.5 Analysis of GA content

Developing grains harvested at 28 dpa were lyophilised and milled to fine powder using a ball mill in order to measure GA concentrations. GA content was measured on approximately 500 mg of this material as described in Griffiths *et al*. (2006) with the modification that the GC-MS equipment used in the current study was a Thermo Finnigan MAT95 GC-MS. In brief, samples were extracted overnight at 4°C in 80% methanol-water (approximately 100 ml) after addition of approximately 1 kBq ^{3}H-GA_1 and –GA_4, and $^{2}H_2$-labelled GA internal standards (Appendix 3). An acidic fraction containing GAs was obtained by chromatography on QAE Sephadex anion-exchange columns and C_{18} HyperSep cartridges. Samples were then methylated in ethereal diazomethane and partitioned between ethyl acetate and water, the organic phase passed through a HyperSep NH2 cartridge and reduced to dryness. The samples were separated by reverse-phase HPLC. Grouped fractions (based on the retention times of the ^{3}H-GA standards) were trimethylsilylated (by heating with MSTFA) and analysed by GC-MS with selected ion monitoring. Concentrations of endogenous GAs were determined by comparison to established calibration curves for unlabelled and deuterated analytes (where peak area ratios were plotted against a range of molar ratios of the two compounds).

2.6 Data Analysis

Statistical analysis was performed using the GenStat statistical software package (2014, Seventeenth Edition, © VSN International Ltd., UK). The experiments with a balanced design were analysed with analysis of variance (ANOVA) to assess differences between various genotypes. The analysis was initially performed at the population level between the wild-type, average of all transgenics and average of all azygous lines (nulls) in any experiment. This analysis was then performed to study the differences between each transgenic line and its corresponding null. Least significant difference (LSD) with a significance threshold of 5% was used to assess differences between the three populations or the transgenics and their nulls. The method of Residual Maximum Likelihood (REML) (Patterson and Thompson, 1971) was used to fit linear mixed models in certain experiments in order to account for either their unbalanced nature or their complex design.

2.7 Bioimaging

To examine GFP expression in developing grains, a Leica M205 FA stereo microscope (Leica Microsystems Ltd., UK) fitted with a 1.6X optic was used under bright field and through the GFP2 filter set (Excitation 460-500nm, Emission 510 long path). Grains from different constructs were examined at different stages of development depending on the timing of promoter activity. This was performed to confirm the tissue specificity of the promoter in question and its timing of activity during grain development. To visualise the grains on a flat surface, with minimal background, agar media supplemented with 5 g/l of activated charcoal in petri dishes was used to support the cut grains. Grains were cut in half using a double edged blade (TAAB Laboratories Equipment Ltd., UK) in either transverse or longitudinal sections and pushed onto the agar medium and examined under the microscope.

2.8 Controlled cross pollination of transgenic wheat lines

Transgenic lines were crossed under controlled conditions to bring together different traits.

2.8.1 Emasculation

Before emasculation, the florets were checked by prying open the glumes and visually inspecting the anthers to ensure that anthesis had not yet occurred. The bottom pair and top three spikelets (Figure 1.6) were removed from each ear using forceps. For each remaining spikelet all florets except floret one and two were also removed. The anthers were then carefully removed from each floret making sure not to damage the stigma. The top of the glume was cut off to ensure that the applied pollen accessed the stigma. The emasculated ear was then covered with a crossing bag prior to pollination after the stigma had matured for a further two to four days.

2.8.2 Pollination

Individual ears from the desired male parent were selected at a stage where anthers were mature, but had not yet dehisced. The peduncle was then cut and the pollen donor ear inverted and placed in the crossing bag containing the emasculated ear. The donor ear was and moved around the emasculated ear twice a day for 2-3 days to ensure release of the pollen as the anthers dehisce and uniform pollination of the female parent.

Chapter 3. Identifying Homozygous Plants using TaqMan Assays

3.1 Introduction

In order to answer several specific questions as to the role of GA in particular tissue types I employed a suite of promoters (Table 3.1) that allowed for the precise manipulation of GA levels or signalling in the different tissues of the wheat grain at different stages of development. A mutant version of a GA signalling gene from *Arabidopsis* (*Atgai*) was expressed to introduce GA insensitivity using the embryo- and aleurone layer-specific *Barley embryo globulin 1* (*HvBeg1*) (Kriz, 1999) and aleurone layer specific barley chitinase (*HvChi26*) promoters (Leah *et al.*, 1994), both these promoters being active from 26 dpa onwards. Additionally, to determine if the seed coat restricts grain size and if increasing the levels of GA in these tissues will allow production of larger grain, without adverse effects on flour quality a GA biosynthesis gene from *Arabidopsis* (*AtGA20ox1*) was expressed in the pericarp and the pigment strand using promoters that are switched on in the early stages of grain development. The two promoters selected for this study were from the inner integument- and pericarp-specific barley germin gene (*HVGerF*) (Wu *et al.*, 2000) and the inner integument-specific wheat dihydroflavanol-4-reductase gene (*TaDFR-D*) (Himi and Noda, 2004). In the grain the endosperm transfer layer is important as water and nutrients are transferred through this layer to the developing grain. In this layer the effects of both GA increase and insensitivity were investigated by expressing *Atgai* and *AtGA20ox1* using the endosperm transfer layer-specific wheat *Endosperm 1* (*TaEND1*) promoter (Doan *et al.*, 1996), which is active from seven to 40 dpa. Moreover, using a promoter which is switched on late in grain development to decrease the amount of GA in the endosperm by expressing a GA inactivating gene from bean (*PcGA2ox1*) has the potential to improve grain quality without impacting

grain size. For this purpose, the wheat *Tritin* (*TaTri*) (Habuka *et al.*, 1993) promoter, which is active from 25-53 dpa, was used. Lastly, lines previously generated in our laboratory where *AtGA20ox1* was expressed in the endosperm using the wheat high molecular weight glutenin subunit promoter (*TaHMW-GS*) (Lamacchia *et al.*, 2001) and the *PcGA2ox1* was expressed in the embryo and scutellum using the maize *globulin 1* promoter (*ZmGlb1*) (Belanger and Kriz, 1989) were crossed to each other to combine the two genotypes.

For each of the constructs studied in this project homozygous transgenic lines and azygous lines needed to be generated and identified prior to experimental analysis to ensure that all grain contributing to phenotypic and genotypic analysis of each independent line were of the same, and known, genotype. A selfed T1 generation of transgenic material is expected to have within its population plants which are homozygous, hemizygous or azygous (null) for the transgene. For the purpose of this thesis the azygous lines will hereafter be referred to as nulls. The process of identifying homozygous plants was carried out by PCR analysis and qPCR-based TaqMan assays of the various lines.

The conventional method of selecting homozygous material in wheat comprises a process involving multiple generations where positive plants in each generation are identified and their progenies subsequently tested for their zygosity status. This method usually provides homozygous material by the T3 or T4 generation and involves growing a large number of plants. Apart from being an expensive process due to the large number of plants that are needed and the multiple rounds of PCR analysis, it can also take up to two years to identify homozygous material. Using TaqMan assays allows for the identification of homozygous material as early as the T1 generation cutting down on both the costs and time that conventional PCRs require.

TaqMan assays involve the amplification of a target sequence in the presence of oligonucleotide probes designed to hybridise within this target sequence (Figure 3.1). These probes have a fluorescent label known as a reporter at the 5’ end which does not fluoresce in free solution due to the presence of a

quencher at the 3’ end. The quencher is also a fluorescent dye but emits at a much lower wavelength than reporter dyes (Bubner and Baldwin, 2004) and is not detected by real-time PCR machines. During PCR amplification, the 5’ – 3’ exonuclease activity of the *Taq* polymerase degrades the probe annealed to its specific target sequence into smaller fragments releasing the reporter from the quencher. This results in a cumulative increase in fluorescence with each amplification cycle with the signal increasing in proportion to the amount of PCR product present in each reaction cycle. During the assay the first significant increase in the amount of PCR product during the exponential phase correlates to the initial amount of target DNA. The higher the amount of initial target DNA present, the sooner a significant increase in fluorescence is observed. Multiplex assays can be performed using probes with different reporters allowing for the amplification of a target and an endogenous control sequence in the same reaction (Holland *et al.*, 1991, Lee *et al.*, 1993, Livak *et al.*, 1995, Hui *et al.*, 2008).

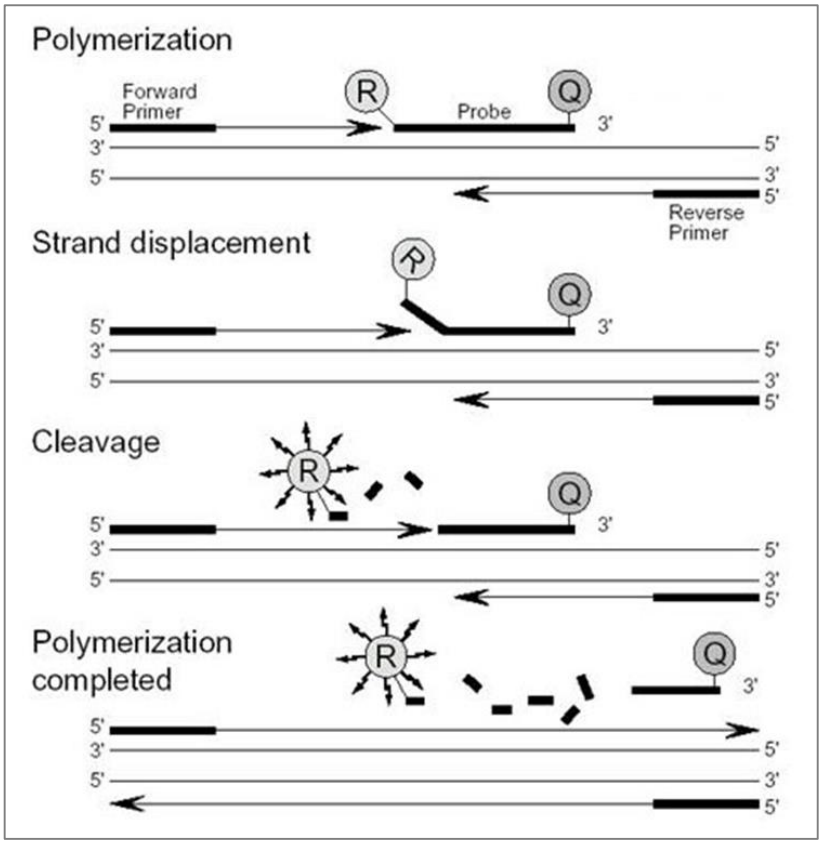


Figure 3.1: Schematic of TaqMan assays

A target specific probe labelled with reporter (R) and quencher (Q) is added to a qPCR reaction. During the PCR process, bound probe is degraded by *Taq* releasing the fluorescent marker from the quencher resulting in increased fluorescence in the reaction [modified from (e-oligos, 2016)].

The results of a TaqMan assay are presented as a Ct value (threshold cycle) which is the cycle number at which the fluorescence reaches a threshold t. This threshold is above the background fluorescence value before exponential growth begins. A low Ct value indicates a high initial target template and high value the opposite. In a reaction with 100% efficiency there is doubling of PCR product with each cycle thus a sample with double the amount of initial DNA will have a Ct value one cycle lower than those with half the initial amount. Since a homozygous plant will contain double the amount of transgenic DNA compared to its hemizygous sister plants this method can be used to determine zygosity (Bubner and Baldwin, 2004, Dorak, 2012).

3.2 Results and Discussion

The material available at the start of this project was the T1 generations of constructs one to seven and homozygous T4 generations of constructs eight and nine (Table 3.1). The zygosity analysis of constructs one to seven will be discussed here while the production and subsequent analysis of construct 10 will be discussed in chapter 7. PCR analysis (section 2.2.2) was performed on 24 T1 plants of each construct using primers in appendix 1 to confirm the presence or absence of the various transgenes. For each construct a large fragment [1-1.5 kilo bases (kb)] of DNA, spanning the junction of the promoter and effector sequences, was amplified in order to ensure the presence of an intact insertion. As expected, the T1 progeny segregated for lines that were either positive or negative for the presence of the transgene. The expected Mendelian segregation ratio of positive to negative plants is 3:1 but in the majority of cases ratios deviated from this value indicating that the transgene may be present in more than one copy and not integrated at a single locus. There were also occasional putative transformants for which no positive plants could be identified in the T1 generation and these were discarded. It is most likely these lines were 'escapes' in the selection process after transformation which were then falsely identified as PCR positive in the T0 generation.

Table 3.1: List of available promoter: effector combinations

No.	Promoter	Effector gene	Target Tissue	Available generations
1	*Tritin* (*TaTri*)	*PcGA2ox1*	Endosperm	T1
2	*Endosperm1* (*TaEND1*)	*AtGA20ox1*	Endosperm transfer layer	T1
3	*TaEND1*	*Atgai*	Endosperm transfer layer	T1
4	*Germin F* (*HvGerF*)	*AtGA20ox1*	Pericarp and inner integument	T1
5	*Dihydroflavanol-4-reductase* (*TaDFR-D*)	*AtGA20ox1*	Inner integument	T1
6	*Chitinase* (*HvChi26*)	*Atgai*	Aleurone	T1
7	*Barley Embryo Globulin* (*HvBeg1*)	*Atgai*	Embryo and Aleurone	T1
8	*High Molecular Weight Glutenin* (*TaHMWGlu*)	*AtGA20ox1*	Endosperm	T4
9	*Maize globulin* (*ZmGlb*)	*PcGA2ox1*	Embryo/ Scutellum	T4
10	*TaHMWGlu::AtGA20ox1* **X** *ZmGlb:: PcGA2ox1*		Endosperm **+** Embryo/ Scutellum	Plants generated during this project

Transgene-positive progeny were then subject to further analysis by TaqMan assay (section 2.2.3) to distinguish homozygous from hemizygous plants using primers and probes (Appendix 1) designed to anneal to the transgene and an endogenous reference gene. The reference gene chosen for this analysis was *TaHd1* which is an orthologue of the *CONSTANS-like* (*CO2*) gene from barley. This gene is known to be stably expressed throughout development and is present as a single copy. The comparative Ct method (ΔCt) for relative quantitation of transgene expression was used to analyse the data. This method compares the relative amount of the target sequence to the endogenous reference and requires the two reactions to have similar efficiencies. ΔCt is the difference between the Ct of the transgene and that of the endogenous control and is calculated for each sample and is used to determine zygosity. The ΔΔCt value is the difference between the ΔCt of a reaction with a single copy of the transgene, calculated using a standard curve, and the ΔCt of each reaction. This value can then be converted to absolute values using the formula $2^{-\Delta\Delta Ct}$ to give the copy number of the transgene (Livak and Schmittgen, 2001, Dorak, 2012).

For each construct the analysis was performed to compare the sister plants within each independent line. Mean ΔCt values were calculated for each positive progeny and those plants displaying a value approximately one ΔCt unit below that of the majority of the siblings were deemed to be homozygous as this is indicative of double the amount of initial DNA in these individuals compared to their hemizygous siblings. Along with the ΔCt values, normalised relative quantification (NRQ) of each reaction was also calculated based on Ct values that were normalised using the efficiency of each reaction. These values were log2 transformed to normally distribute the data. In certain lines the ΔCt and NRQ values did not correspond with each other. This may be due to the fact that the primers and probes used for this analysis perform at their threshold and any change in conditions does not result in accurate efficiency values. Therefore, the ΔCt values were judged to be more reliable and were used to select homozygous plants, which were grown to maturity. Null

segregants do not give a value in this assay due to the absence of the transgene and are thus not represented in the resultant graphs. However, for each line a null progeny was also grown on to maturity to provide seeds to use as a control for each line in subsequent experiments. The zygosity of the selected plants was determined by PCR in the T2 generation and those confirmed as being homozygous used for future experiments.

3.2.1 Zygosity and copy number analysis of plants transformed with *TaTri::PcGA2ox1*

3.2.1.1 PCR analysis to confirm presence of transgene

In order to select homozygous material, 24 T1 seeds were sown and the resultant seedlings that germinated were analysed and plants from each of the six transformants harbouring construct *TaTri::PcGA2ox1* were grown as described in section 2.1. These plants, generated as described in section 2.1, were analysed by PCR (section 2.2.2) using forward primer Tri-F and reverse primer 2ox-R (Appendix 1). This revealed that all progeny of line 6.4 were null, indicating that this was a false positive line and therefore this line was discarded from all further analysis. The other five lines contained a mix of positive and negative progeny. However, as previously mentioned a simple 3:1 segregation ratio was never observed, indicating the presence of multiple copies of the transgene (Table 3.2).

Table 3.2: T1 zygosity PCR results for *TaTri::PcGA2ox1* transgenic lines

Results of PCR on T1 plants to check for the presence of the transgene in six lines harbouring *TaTri::PcGA2ox1* construct.

Line	No. of +ve plants	No. of -ve plants	+ : - ratio
6.2	20	2	10:1
6.4	0	21	na
6.6	16	4	4:1
6.7	9	6	3:2
6.8	15	9	5:3
6.9	14	2	7:1

3.2.1.2 TaqMan assay to select homozygous material

The progenies of the five positive transformants were further analysed by TaqMan assay (Figure 3.2) using forward primer Q_ Pc2ox-F, reverse primer Q_Pc2ox-R and hybridization probe Q_Pc2ox-probe to amplify the transgene and primers HvCon2-F and HvCon2-R and probe HvCon2-probe (Appendix 1) to amplify the endogenous reference gene as described in section 2.2.3. For each of the five lines analysed the ΔCt and NRQ values correlated with each other and the three plants which displayed both low ΔCt and high NRQ (log2 transformed) values were selected as potential homozygous material and grown to maturity. In this instance both sets of parameters (ΔCt and NRQ) were considered as there were plants available that displayed approximately one ΔCt unit below that of the majority of the siblings whilst also having the similar results for their NRQs. For other constructs when the two values did not correlate only the ΔCt values were considered while selecting potential homozygotes to take through to the next generation for further testing. For lines 6.2, 6.6, 6.8 and 6.9 the three plants with the low ΔCt values (Figure 3.2, A), which also displayed high NRQ (Figure 3.2, B). were chosen as potential homozygotes. In line 6.7 only 15 of the 24 seeds sown germinated and it contained a smaller proportion of positive plants compared to the rest of the

lines with a 3:2 segregation ratio. The ΔCt values for this line did not display a wide enough distribution to enable the clear separation of plants into the two classes of homozygous and hemizygous and due to this potential homozygotes were selected based only on their NRQs.

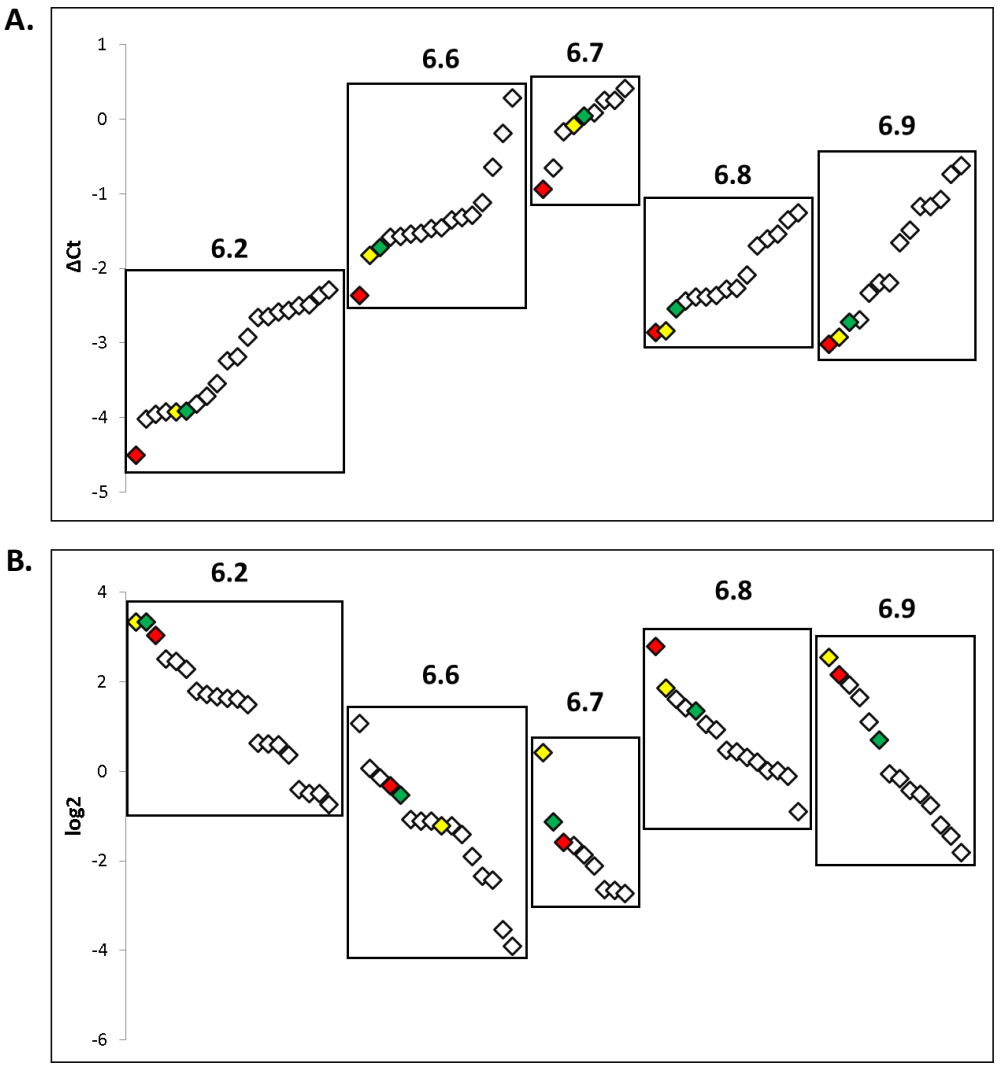


Figure 3.2: TaqMan assay results for *TaTri::PcGA2ox1* transgenic lines
ΔCt (A) and log2 transformed NRQ (B) values for five different lines. Each box contains values for positive progeny within an independent transgenic line. Coloured plots represent those plants selected as potential homozygotes for further analysis, with the three matching colours representing the same plants in both graphs.

3.2.1.3 PCR analysis to confirm zygosity of T2 plants

For each of the five lines, 24 T2 progenies of the three potential homozygous plants were grown as previously described in section 3.2.1.1. These plants were examined by PCR analysis (section 2.2.2) using primers Tri-F and 2ox-R (Appendix 1) as described above for the plants from the T1 generation (section 3.2.1.1). This analysis was performed to confirm the zygosity results from the TaqMan assays (Figure 3.2). As table 3.3 shows not all of the plants that were selected through the TaqMan assay were confirmed as homozygous but for four of the five lines at least one homozygous progeny was identified. In lines 6.2 and 6.9 all three progenies selected were confirmed to be homozygous, lines 6.6 and 6.8 contained two homozygous progenies each but in line 6.7 all progeny were found to be hemizygous. Whilst in the T1 generation this line displayed a low germination percentage, all T2 plants germinated. However, the segregation ratio in these lines in the T2 generation was 1:1 or 1:2, still not displaying normal segregation indicating towards other factors in this line leading to the failure of the TaqMan assay to identify any homozygous material.

Table 3.3: Confirmation PCR results for T2 *TaTri::PcGA2ox1* transgenic lines

Results of PCR on T2 generation plants of *TaTri::PcGA2ox1* to confirm TaqMan assay results. Rows in bold show homozygous lines.

Line	No. of +ve plants	No. of -ve plants	Zygosity
6.2.14	**24**	**0**	**Homozygous**
6.2.1	**24**	**0**	**Homozygous**
6.2.3	**24**	**0**	**Homozygous**
6.6.15	**23**	**0**	**Homozygous**
6.6.2	**24**	**0**	**Homozygous**
6.6.16	16	8	Hemizygous
6.7.11	11	13	Hemizygous
6.7.6	12	12	Hemizygous
6.7.14	8	16	Hemizygous
6.8.9	**21**	**0**	**Homozygous**
6.8.15	18	6	Hemizygous
6.8.1	**24**	**0**	**Homozygous**
6.9.17	**24**	**0**	**Homozygous**
6.9.10	**24**	**0**	**Homozygous**
6.9.11	**24**	**0**	**Homozygous**

3.2.1.4 Copy number analysis of *TaTri::PcGA2ox1* transgenic lines

Southern hybridisation was performed (section 2.2.8) on three positive T1 plants for each of the five lines of this construct as it was believed that two lines – 6.8 and 6.9 – might be clonal as they originated from the same explant. The enzyme *Xmn*1 (NEB, USA) which cuts once just before where the probe anneals in the *PcGA2ox1* gene was used for the restriction digests giving a minimum fragment size of 1200 bp for an intact cassette. Whilst there is some indication of segregation of some loci between sister progeny in lines 6.8 and 6.9 in general these lines display a highly similar digest pattern (Figure 3.3) indicating that these lines are clonal with an estimated 10 to 20 copies of the transgene present. Line 6.2 contains between eight to 18 estimated copies whereas 6.6 and 6.7 both had lower numbers with estimates of four and two copies, respectively. All copies are preseumed intact as they were above the minimum expected resitrction fragment size of 1200bp. Copy number of transgenic lines can also be obtained from TaqMan assay results using the ΔΔCt method. If accurate, this method could provide a useful alternative to southern hybridisations. Unfortunately, due to time constraints the ΔΔCt analysis could not be completed on these lines and at present no comment can be made about its validity in comparison to southern hybridisations.

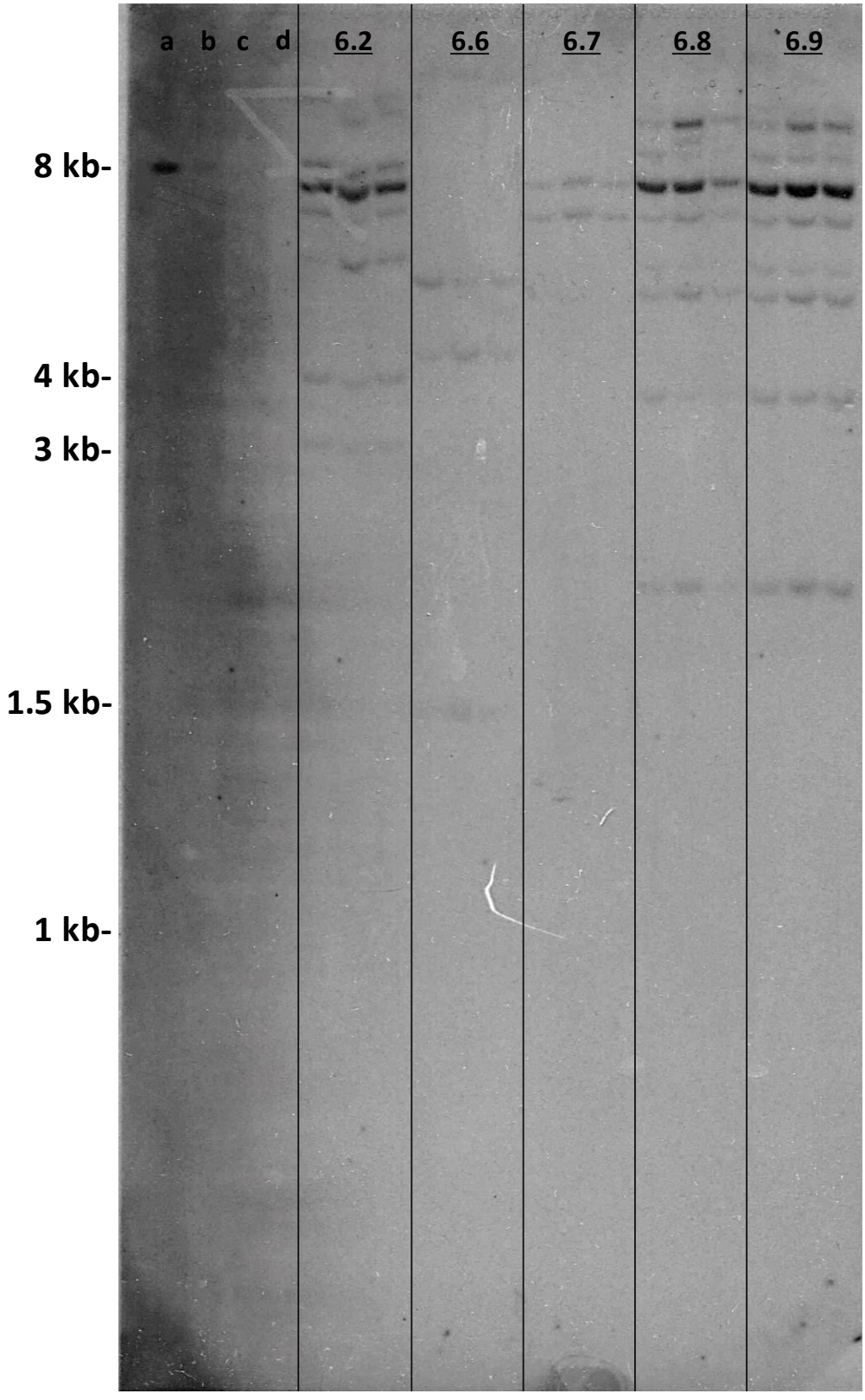


Figure 3.3: Southern hybridisation of *TaTri::PcGA2ox1* transgenic lines
Copy number analysis of three biological replicates of each independent line. a: 81.35pg plasmid ≅ 10 copies , b: 8.135pg plasmid ≅ 1 copy, c: WT CAD control and d: null control.

3.2.2 Zygosity analysis of plants transformed with the other constructs

Due to the success of the TaqMan assays in identifying the homozygous progeny in T1 lines harbouring *TaTri::PcGA2ox1* construct, this method was used for plants transformed with the remaining six constructs (Table 3.1). For each of these constructs the analyses described in sections 3.2.1.1, 3.2.1.2 and 3.2.1.3 were performed using primers and probes in appendix 1. The detailed zygosity analysis of each of these constructs will be discussed in their respective results chapters. In the T1 generation none of the plants tested for any of the constructs displayed a 3:1 segregation ratio (data not shown) indicating that all contain multiple copies of their respective transgenes. The TaqMan assay results and subsequent PCR analysis of the T2 generation plants from the selected putative homozygous lines for each construct are represented in appendix 2. The TaqMan assays were between 75-100% successful in identifying a homozygous progeny for each line (Table 3.4). At least one homozygous progeny was identified in 39 of the 43 lines tested by the T2 generation, representing a significant improvement over the traditional pot-luck approach.

Table 3.4: Success rate of TaqMan assays of transgenic lines harbouring various constructs

Results of TaqMan assays on plants transformed with different constructs. For each line in a construct, T2 progenies of three plants were tested for zygosity.

Construct	No. of lines tested	No. in which homozygous progeny identified	Success rate (%)
TaTri::PcGA2ox1	5	4	80
TaEND1::AtGA20ox1	6	5	83.30
HvGer::2 AtGA20ox1	7	7	100
TaDFR-D:: AtGA20ox1	6	6	100
HvChi26:: Atgai	7	7	100
HvBeg1::Atgai	8	7	87.50
TaEND1:: Atgai	4	3	75

The four lines in the four separate constructs where no homozygous plants were identified all displayed atypical segregation ratios in either the T1 or T2 generations. Line 2.4 whilst having a normal 3:1 segregation in the T1 generation and displaying consistent results for TaqMan Assay did not result in producing any homozygous material. The three lines chosen as potential homozygotes displayed a 5:3 or 1:1 segregation. Whereas, line 11.7 displayed an atypical 1:3 segregation in the T1 generation, however the three plants chosen as potential homozygotes all had a 3:1 T2 segregation. Line 10.10 did not display a typical segregation in either the T1 (1:1) or T2 (1:2, 7:1 and 3:5) generations. As discussed in sections 3.2.1.2 and 3.2.1.3, line 6.7 displayed atypical segregation in both T1 and T2 generations. Taken together these results indicate that for the majority of lines homozygous material wasn't identified when the T1 generation had a smaller proportion of positive plants. However, in line 2.4 this was not the case implying that there might be other issues with this line that is likely to prevent the identification of homozygous material for several generations.

In the majority of lines where hemizygous sisters where present along with homozygous lines, the hemizygous plants had a segregation ration close to 3:1 or around 22:2 indicating that either the segregation was normal in the T2 generation or effectively homozygous material was selected, but one copy of the transgene might still be segregating independently.

3.3 Conclusions

A qPCR based method – TaqMan assays – was developed to determine zygosity of transgenic wheat plants from various constructs and homozygous material identified for each of the seven constructs studied in this thesis. The development of this method using TaqMan assays allowed the identification of homozygous material as early as the T1 generation cutting down on both the costs and time that conventional PCRs require. However, this method did not have a 100% success rate which could potentially be due to the presence of multiple copies of the transgenes and, as previously mentioned, which may not all be co-segregating. The presence of higher amounts of transgene DNA in some plants compared to their siblings within a line could be an indication of the presence of higher number of copies of the construct and not homozygosity. Hence those plants chosen as homozygous due to their low ΔCt values may be unevenly segregating hemizygous plants containing additional copies of the transgene compared to some of their sisters. In spite of this, of the 43 independent transgenic lines tested from the seven constructs, at least one homozygous T1 plant was identified in 39 of these giving an overall success rate of 90%. This is much higher than the 33% chance (assuming simple Mendilan segregation) of randomly selecting a T1 homozygous plant from the positive progenies available.

Chapter 4. Effects of GA insensitivity in developing embryo and aleurone layer of wheat grains

4.1 Introduction

During germination, the aleurone layer of the grain produces the hydrolytic enzyme α-amylase, which is secreted to the endosperm where it breaks down starch to simple sugars to support the growing embryo (section 1.2.5). When α-amylase is present in small quantities in refined flours it is beneficial in bread making. However, when present in higher amounts in flour it makes the dough unusable due to starch degradation (Edney, 1996). Hagberg Falling Number (HFN) is a quality measure of flour and is inversely related to α-amylase activity (Gooding *et al.*, 2012). Flour with a low HFN, due to excessive α-amylase, produces bread with a sticky crumb while a high HFN produces a dry crumb (Perten, 1964). Whilst the presence of GA in the aleurone layer is necessary to produce α-amylase, GA is not produced in this tissue and GA biosynthesis genes are not expressed here. However, GA signalling genes are expressed in the aleurone, indicating that GA can be perceived in this tissue (Kaneko *et al.*, 2003). It is believed that α-amylase is produced in response to GA produced by the grain as application of GA biosynthesis inhibitors to the developing grain reduces the production of α-amylase (Delrot and Bonnemain, 1985). Furthermore, it is known that during germination GA synthesised by the embryo moves to the aleurone layer where it induces the production of α-amylase (Fincher, 1989). The expression of the GA biosynthesis genes *OsGA20ox1* and *Os3ox2* in the scutellum of rice grains, and *TaGA20ox1* and *TaGA3ox2* in the germinating embryo of wheat further confirm that this organ is an important site of GA biosynthesis in the grain (Kaneko *et al.*, 2003, Appleford *et al.*, 2006).

This study aimed to determine whether insensitivity to GA in the developing wheat embryo and aleurone (the sites of GA and α-amylase production, respectively) can be used to reduce α-amylase levels in the mature grain and therefore improve flour quality, by expressing the mutant *Arabidopsis* GA signalling gene *Atgai*, which confers insensitivity to GA (section 1.3.3), in these organs. It was also hoped that conferring GA insensitivity in the embryo, which is a site of GA production in the developing grain, would inform further understanding of the role of GA in dormancy, germination and PHS. The promoters selected for this study were the aleurone-specific barley Chitinase 26 (*HvChi26*) promoter and the barley embryo globulin (*HvBeg1*) promoter which confers activity in the embryo and aleurone layer (Table 3.1) (Figure 4.1).

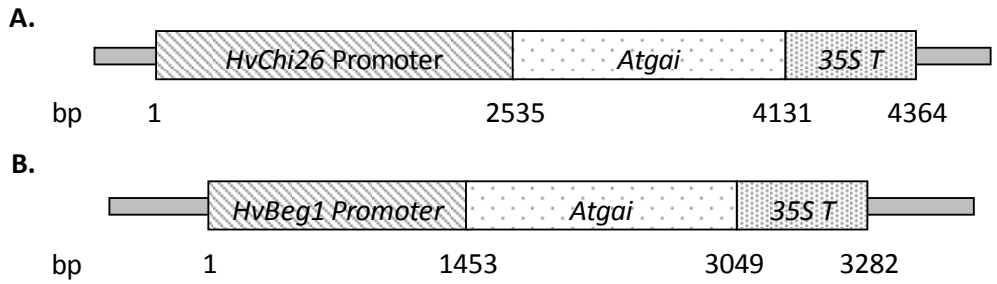


Figure 4.1: Basic structure of *HvChi26::Atgai* and *HvBeg1::Atgai*
Basic structure of constructs *HvChi26::Atgai* (A) and *HvBeg1::Atgai* (B). The position of junctions between elements is given in base pairs (bp). The cauliflower mosaic virus (CaMV)35S terminator is labelled 35S T.

Chitinases are known to play a role in defence against chitin-containing pathogens and are expressed in various plant tissues. They hydrolyse chitin which is a structural polysaccharide in fungal cell walls and thus act in plant resistance against fungal pathogens (Dahiya *et al.*, 2006). The aleurone layer specific Type II chitinase (*Chi26*) gene was first isolated from barley seeds and encodes a 26-kDa protein. This protein accumulates to high levels specifically in the aleurone layer during germination and late in grain development and is unaffected by GA (Leah *et al.*, 1991). The 5' upstream sequence (1514 bp) of

this gene was shown to drive the expression of the GUS reporter in 26-28 dpa and germinating aleurone tissues, and to a lesser degree in 16-18 dpa aleurone. No expression was observed in leaves, embryo, endosperm or developing pericarp tissues (Leah *et al.*, 1994). Hwang *et al*. (2001) further confirmed the aleurone-specific nature of the *Chi26* promoter through studies in rice. They used an 882-bp fragment from barley which showed a number of deletion/insertions compared to the sequence reported by Leah *et al*. (1994) and believe this could be due to the allelic difference between varieties. Further promoter deletion analysis carried out by Leah *et al*. (1994) indicated that the *cis*-acting elements controlling gene expression are situated between -200 and -140. These authors also showed that point mutations in two direct 6-bp repeats (GCCAAG and TTGATC) located between -179 and -147 resulted in reduced promoter activity. This 33 bp fragment was also shown to confer aleurone-specific expression, further indicating that this region contains tissue-specific regulatory elements (Leah *et al.*, 1994). For the present study the *HvChi26* promoter was isolated using genome walking as attempts to amplify it from barley using multiple primer pairs based on Genbank sequence L34210 were unsuccessful. Genome walking generated a single 3079 bp fragment from barley cv. Morex (Vaughan, S., unpublished data). This represented 545 bp of *HvChi26* coding sequence (CDS), which displayed 96.7% identity to the previously identified *HvChi26* CDS by Leah *et al*. (1994) (L34210), and 2534 bp of upstream promoter sequence. However, only the first 608 bp distal to the start codon displayed any significant homology (94.4% identity) to the previously reported 1697 bp promoter sequence described by Leah *et al*. (1994) with the remaining 1089 bp sequence only displaying 44.2% identity. Such a drastic change in the level of identity between the two sequences probably indicates a mistake *in-silico* and goes a long way to explain why attempts to amplify this fragment by PCR based on the published sequence failed. The extended and verified sequence, based on a single fragment and sequenced in both directions, was submitted to Genbank under the accession HM564396 and is the source of the *HvChi26* promoter used in this study. Promoter activity was studied during grain development in our laboratory using

seven independent lines expressing the *HvChi26* promoter directing nuclear-targeted GFP expression (Figure 1.15). This promoter was found to be highly active in the aleurone layer of the grain of all lines examined from 26 dpa onwards through to maturity. Expression was not observed in any other grain tissues. However, in two lines significant amounts of GFP were observed in the leaves although expression was not detected in any other non-target tissues (Vaughan, S., unpublished data).

The second promoter utilised in this chapter is associated with a cereal 7S Globulin gene. Globulins are salt-soluble seed storage proteins which primarily consist of 3S and 7S units present in different proportions in different species, with the 10-11S present as a minor component (Shewry *et al.*, 1995). The 3S and 7S globulins are orthologues of the vicilins of the Leguminoseae which are known to accumulate during seed development (Robert *et al.*, 1985). In cereal seeds the 7S globulins have highly regulated expression pattern and have been shown to accumulate in the embryo and aleurone layer (Yupsanis *et al.*, 1990) and are positively regulated by ABA (Heck *et al.*, 1993). Their distribution in the grain is in contrast with other storage proteins which accumulate in the starchy endosperm (Kriz, 1999). In maize and barley each globulin component is encoded by a single gene – *Glb1* and *Beg1*, respectively. However, in wheat three genes have been identified – *Glo-3A*, *Glo-3B* and *Glo-3C* (Loit *et al.*, 2009). The promoter used in this study was isolated from a vector supplied by Ralph Quatrano (Oregon State University, USA) under an MTA. This genomic clone previously reported to be a wheat 7S globulin (GenBank, M81719) has since been re-annotated as the barley *Beg1* gene (Kriz, 1999). To re-confirm the identity of the promoter sequence used in this study, the 1452 bp sequence used was BLAST searched against both the wheat and barley genomic databases. The sequence showed a 99.8% (1430 bp) identity to barley cv. Morex contig 136631 (Kersey *et al.*, 2016), whereas only small fragments aligned within the wheat genome confirming this to be the promoter of the *HvBeg1* gene. Promoter activity was further studied during grain development in our laboratory using 13 independent lines expressing nuclear-targeted GFP

under control of the *HvBeg1* promoter (Figure 1.15). GFP activity was observed in all lines in both the embryo and aleurone of the developing grains from 26 dpa through to maturity. Promoter activity was not observed in any of the non-target tissues except for low-level expression of GFP in the glumes of one line (Vaughan, S., unpublished data).

4.2 Results and discussion

4.2.1 Production of homozygous material

To select homozygous material for this study 24 T1 plants from six independent lines of *HvChi26::Atgai* and seven lines of *HvBeg1::Atgai* were genotyped as described in Chapter 3. TaqMan assays (section 2.2.3 and appendix 2) were performed on T1 plants of both constructs using forward primer Q_GAI-F, reverse primer Q_GAI-R and hybridization probe Q_GAI-probe (Appendix 1). For both constructs, three plants were chosen from each independent line as potential homozygotes. The T2 progenies of the plants harbouring construct *HvChi26::Atgai* were analysed by PCR (section 2.2.2) using forward primer Chi26-F and reverse primer Gai-R (Appendix 1). The same analysis was also performed on T2 *HvBeg1::Atgai* transgenic lines using forward primer 7Sg-F and reverse primer Gai-R (Appendix 1). Homozygous T2 plants were subsequently selected and an experiment performed with three biological replicates for each line.

4.2.2 Experimental design

Grain yield and quality studies were performed to examine the effects of ectopic expression of the *Atgai* gene in the embryo and aleurone layers of the grain using transgenic wheat lines harbouring the *HvChi26::Atgai* and *HvBeg1::Atgai* constructs generated as described in section 2.1. A single RCBD experiment was setup as described in section 2.1.1 with three replicates of each line. In this experiment for each line one plant was grown in a 15-cm pot, which was cut back to five tillers each. From ears one, three and four; grains were harvested at maturity to measure yield and analyse various quality parameters. Grains from ear two were harvested at 35 dpa to measure various transcript levels and grains from ear five were harvested at two time points (21

and 35 dpa – four grains each) to visualise GFP (section 2.7) to confirm promoter activity.

4.2.3 Analysis of transgenic lines expressing the *Atgai* gene under control of the aleurone-specific *HvChi26* promoter

4.2.3.1 GFP visualisation of *HvChi26* activity

GFP fluorescence was examined in grains at 21 and 35 dpa as described in section 2.7. These two time points were chosen to confirm the earlier studies in our laboratory which showed promoter activity beginning at 26 dpa. However, whilst restricted to the expected target tissues in the grain, in this experiment GFP expression was observed at 21 dpa (Figure 4.2). Due to this younger grains were also studied and GFP was observed as early as 16 dpa. Whilst growing conditions were consistent between experiments, the difference observed in the timing of promoter activity may be due to external environmental variables affecting the quality of growing conditions between experiments. It is also possible there may have been some differences in how the plants were staged by different researchers. However, due to time and resource constraints it wasn't possible to further characterise the temporal activity of this promoter across the multiple experiments. Promoter activity was also studied at germination and GFP was visible from 24 hours after imbibition (Figure 4.3) up to four days post germination. In these lines GFP was visible in the aleurone layer surrounding the germinating grain.

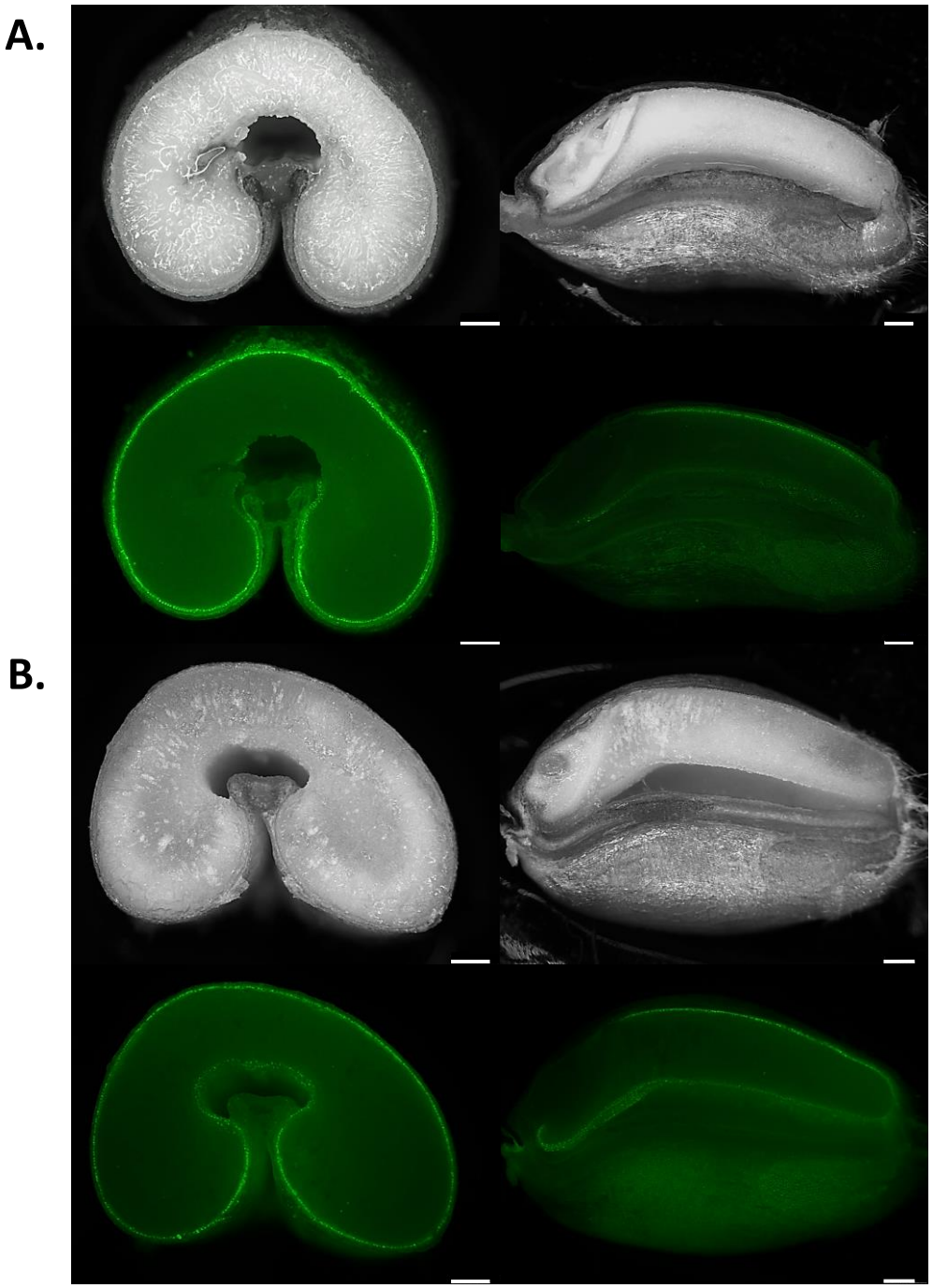


Figure 4.2: Activity of aleurone specific promoter in wheat grain

Transverse and longitudinal sections highlighting the aleurone layer are presented in bright field (top panel) and under a GFP filter set (excitation/ emission) (bottom panel) at 21 dpa (A) and 35 dpa (B) for typical transgenic lines harbouring GFP under control of the barley *HvChi26* promoter. Scale bars represent 500µm for each image.

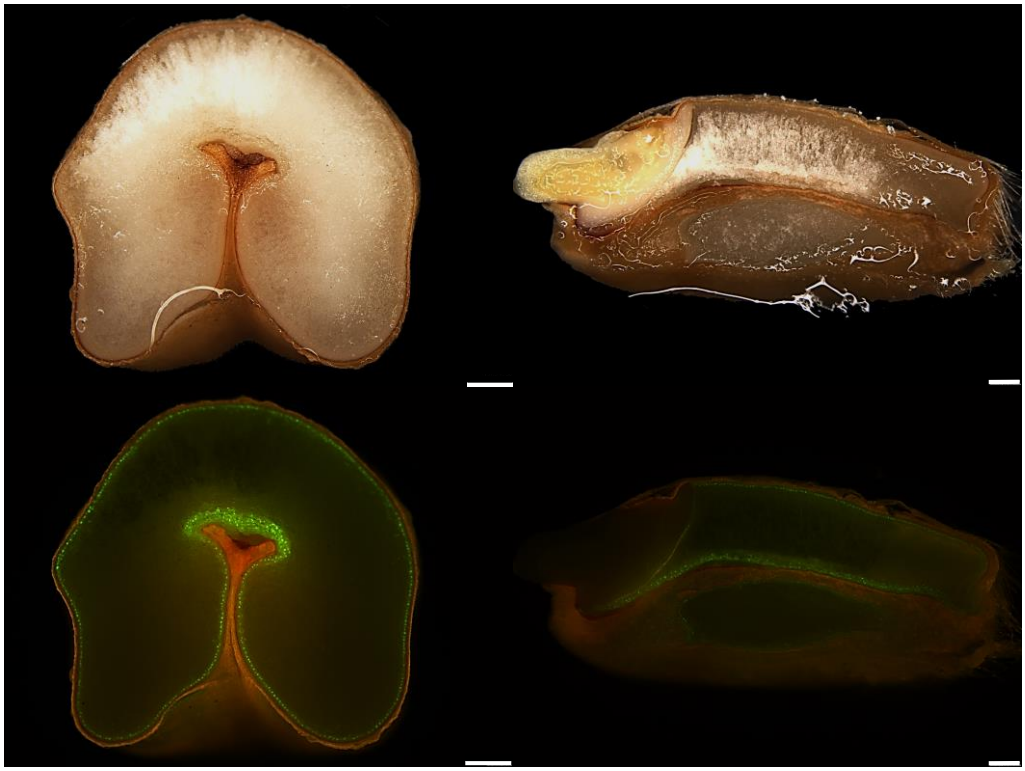


Figure 4.3: Activity of embryo specific promoter in germinating grains
Transverse and longitudinal sections highlighting the aleurone layer are presented in bright field (top panels) and under a GFP filter set (excitation/ emission) (bottom panels) at 24 hrs post imbibition for typical transgenic lines harbouring GFP under control of the barley *HvChi26* promoter. Scale bars represent 500µm for each image.

4.2.3.2 *HvChi26::Atgai* transgene expression

To confirm expression of the introduced transgene, transcript levels of the *Atgai* gene were measured in cDNA synthesised (section 2.2.6) from RNA extracted as described in sections 2.2.4 and 2.2.5 from 35 dpa grains. These grains were harvested from ear two of three biological replicates from each of the six independent lines in the experiment and their respective nulls and the wild-type control. qRT-PCR was performed on this material according to section 2.2.7 using forward primer gai_qPCR-F and reverse primer gai_qPCR-R (Appendix 1). The expression of the transgene (Figure 4.4, A) was normalised against the expression of two endogenous genes – *Ta2526* and *TaSDH* (section 2.2.7 and appendix 1). The data presented in Figure 4.4 is an average of the

normalised relative quantifications (NRQs) of three biological replicates, except for line 9.7 where cDNA synthesis of one replicate failed. The qRT-PCR was performed on all plants in the experiment, including the null and wild-type plants as controls. No expression of the transgene was observed in any of the control material (including the NRT controls) and as such these are excluded from the figures as presented.

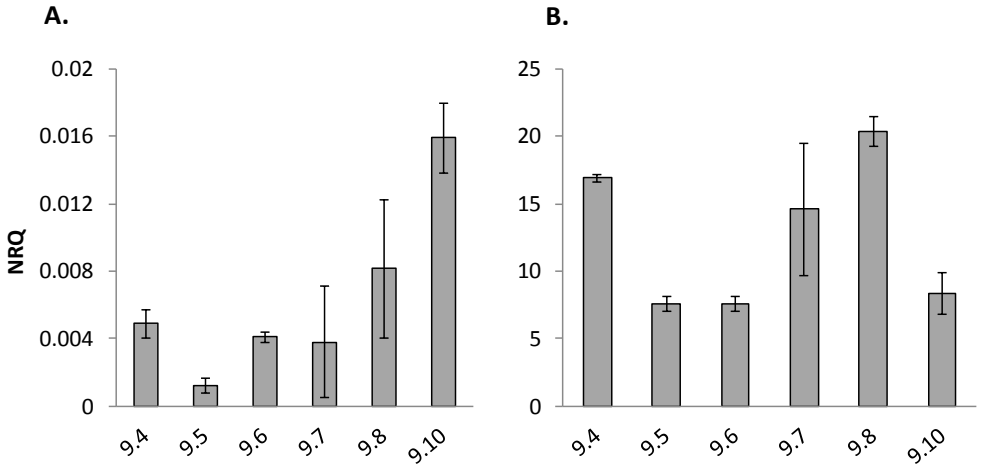


Figure 4.4: NRQs of *Atgai* and *GFP* in *HvChi26::Atgai* transgenic lines
Average of normalised expression levels of the *Atgai* (A) and *GFP* (B) genes in 35 dpa grains as measured in three biological replicates for each transgenic line. Vertical error bars denote standard errors of the mean (SEM).

It should be noted that, whilst detectable, *Atgai* NRQs ranged from 0.0012 to 0.015 (Fig. 4.4, A) which is very low compared with the other transgenes examined within this project. *GFP* transcript levels were also measured on the same material using forward primer GFP_qPCR_F and reverse primer GFP_qPCR_R (Appendix 1) and are presented in figure 4.4 B. *GFP* expression levels were between 500 to 6000 times higher than those observed for *Atgai* in these lines. This high expression of *GFP* is comparable to the expression of the *Pc2ox* transgene (chapter 6) though it is much higher than all other transgenes studied in this project. The high expression levels of *GFP* in these

lines indicates that the promoter used is functional, but suggests that potentially position effects, sequence conformation or *cis*-acting factors may be affecting expression of the *Atgai* gene. It should also be noted that it is possible that *Atgai* expression is so low in these lines as to be non-functional.

4.2.3.3 *HvChi26::Atgai* effects on yield

To study effects of expressing *HvChi26::Atgai* on grain yield, mature grains harvested from three ears (taken as a standardised proxy for total yield) of each plant in the experiment were assessed according to the methods described in sections 2.3 and 2.4.1. The MARVIN digital seed counter was used to count the number of grains and measure their surface area, length and width. These grains were then weighed to calculate thousand grain weights (TGW). The measurements for diameter were obtained from SKCS as described in section 2.4.1. The data presented in figure 4.5, A-E shows the average values for three biological replicates of each line. Whilst for the majority of lines the measurements for diameter (Figure 4.5, F) are also based on three biological replicates each, for the transgenic plants of lines 9.7 and 9.8 this is an average of two replicates only. In each of these lines one replicate did not produce enough grains to enable robust data analysis and thus was excluded. For all of the yield variables measured the difference between the transgenic, null and wild type was assessed at the population level using ANOVA. Using LSD at 5% no significant differences were observed between the three genotypes for any of the variables studied. This result agrees with the hypothesis that insensitivity to GA in the aleurone layer would not have any effect on grain yield.

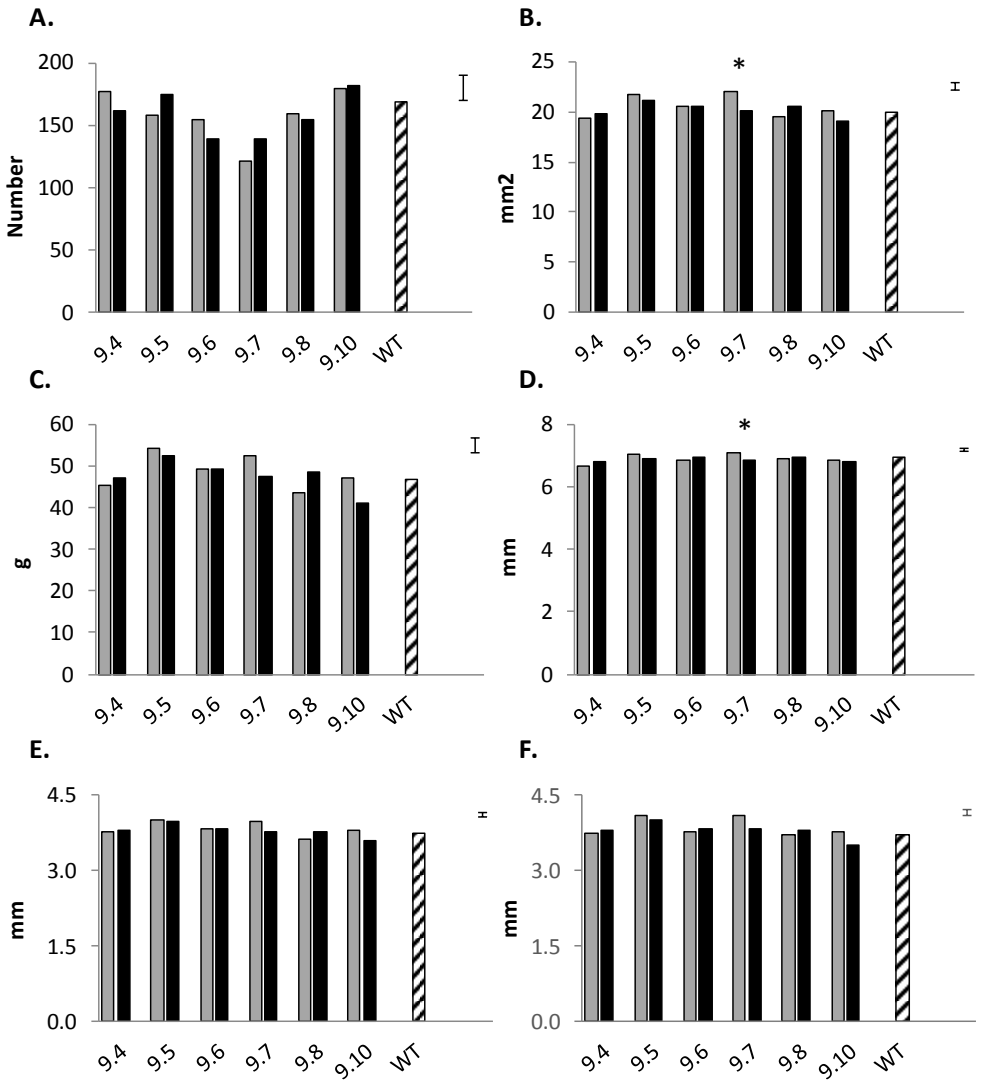


Figure 4.5: Analysis of yield componenets on *HvChi26::Atgai* transgenic lines
Averages are presented for several variables: grain number (A), grain surface area (B), TGW (C), grain length (D), grain width (E) and grain diameter (F) for measurements on mature grains. Grey bars – transgenic lines, black bars – null segregants and hatched bars – wild type (WT). * denotes significant difference between a transgenic and its null using LSD at 5%: p value at – *: ≤ 0.05. Vertical error bars denote standard error of the difference (SED) on 1, 24 degrees of freedom (df) in A-E and 1, 22 df in F.

The differences between the transgenic lines and their respective nulls were also analysed using ANOVA. Grain number, averaged from three ears, showed a broad range from a low of 121 (transgenic, line 9.7) to a high of 182 (null, line 9.10), but no significant differences between transgenics and nulls were

observed in any of the lines (Figure 4.5, A), indicating that, as expected, expression of this construct does not affect grain number. The average TGW also showed a wide range from a low of 41.1 g (null, line 9.10) to a high of 54.22 g (transgenic, line 9.5). However, again no significant differences were observed between the transgenics and nulls in any of the lines (Figure 4.5, C). For area and length measurements, whilst the majority of lines did not show a significant difference, in line 9.7 the transgenic grains had a significantly larger area ($p = 0.04$, F-test = 4.73) and length ($p = 0.037$, F-test = 4.86) than its null (Figure 4.5, B and D). Grain width in all lines showed no significant differences using LSD at 5% (Figure 4.5, E). However, using LSD at 10%, lines 9.7 and 9.10 both showed significant differences ($p = 0.081$, F-test = 3.31 in both lines) in width. In each line the transgenic grains were larger than their respective nulls. Likewise, grain diameter (Figure 4.5, F) also did not show any significant differences in any of the lines studied and ranged from 3.73 mm (transgenic, line 9.8) to 4.1 mm (transgenic, line 9.5). Taken as a whole there was no evidence that the *HvChi26::Atgai* construct affected grain yield or morphology.

4.2.3.4 *HvChi26::Atgai* effects on quality

To study the effect of expressing *HvChi26::Atgai* on grain quality, grain hardness, grain moisture content and the α-amylase content of flour were assessed. Grain hardness and moisture were measured using the SKCS system as described in section 2.4.1 and differences between the transgenic lines and their respective nulls analysed using ANOVA at 5% LSD. The data presented in Figure 4.6, A and B represents the average of three biological replicates for each line with the exception of transgenic lines 9.7 and 9.8 where only two replicates were available. Grain hardness did not show any significant differences in the majority of the lines except line 9.7 (Figure 4.6, A). In this line the transgenic plants had a significantly lower hardness index than the null plants ($p < 0.001$, F-test = 28.44). Whilst the moisture content of all lines in this experiment was in the normal range (11 -14%), only lines 9.4 and 9.7 displayed

significant differences between the transgenics and the nulls, with transgenic grains in line 9.4 having a higher moisture content than their null ($p = 0.005$, F-test = 9.86) and line 9.7 transgenics having a lower moisture content than their nulls ($p = 0.003$, F-test = 11.37).

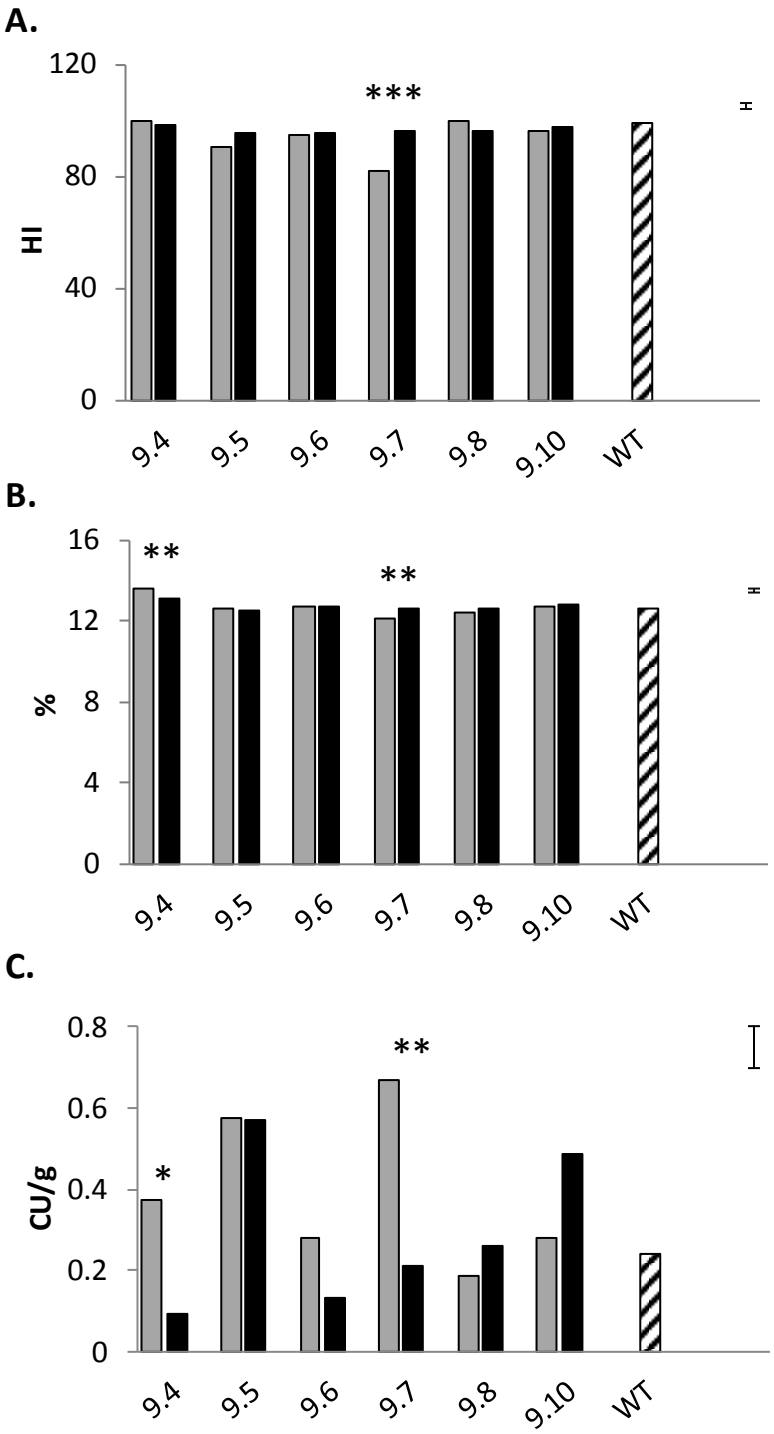


Figure 4.6: Analysis of quality components on *HvChi26::Atgai* transgenic lines

Averages are presented for several variables: grain hardness (A), moisture content (B) and α-amylase (C) for measurements on mature grains. Grey bars – transgenic lines, black bars – null segregants and hatched bars – WT. * denotes significant difference between a transgenic and its null using LSD at 5%: p value at – *: ≤ 0.05, **: ≤ 0.005 and ***: ≤ 0.001. Vertical error bars denote SED on 1, 22 df in A and B, and 1, 24 df in C.

Grains crushed during SKCS analysis were collected and milled to a fine flour and α-amylase measured on 25 mg of this material according to section 2.4.2. The data presented in figure 4.6, C shows ceralpha units (CU) for each line and is an average of three biological replicates. It should be noted that the level of α-amylase enzyme in the wild-type control was much lower (0.24 CU/g) in this experiment compared to the rest of the studies in this project. This could be due to the different times of year the experiments were conducted. Even though all plants were grown in a glasshouse under controlled environmental conditions external environmental variables affecting the quality of growing conditions has been observed between experiments. The α-amylase content in the rest of the lines showed a broad range with the highest value being 0.67 CU/g (transgenic, line 9.7) and the lowest 0.09 CU/g (null, line 9.4). We hypothesised that insensitivity to GA in the aleurone layer would result in a reduction in the α-amylase content and in order to test this the differences between the transgenics and their respective nulls were analysed using ANOVA. As shown in section 4.2.3.2 (Figure 4.4, A) line 9.10 has the highest expression of the *Atgai* transgene. However, this did not result in a corresponding, statistically significant reduction in the α-amylase content in this line compared to its null (Figure 4.6, C). Indeed, whilst there was large variation in the α-amylase content in the rest of the lines the only significant differences in the transgenics were observed in lines 9.4 ($p = 0.031$, F-test = 5.26) and 9.7 ($p = 0.001$, F-test = 13.98) where α-amylase levels were significantly higher. These results indicate that either GA insensitivity in the aleurone layer does not have an effect on α-amylase production or that the low levels of *Atgai* transgene expression are insufficient to confer the desired phenotype.

4.2.3.5 *HvChi26::Atgai* effects on endogenous gene expression

To further understand the variation observed in α-amylase levels in these lines the expression levels of two of the three endogenous α-amylase genes –

TaAmy1 and *TaAmy2* – were measured. As discussed in section 1.2.5.1, the third α-amylase gene, *TaAmy3* is expressed only in maternal tissues during the early stages of grain development and was thus not measured on this material. These measurements were performed according to section 2.2.7 and on the same cDNA from 35 dpa grain used in section 4.2.3.2. The expression of the two genes (Figure 4.7, A and B) was normalised against the expression of two endogenous genes – *Ta2526* and *TaSDH* (section 2.2.7 and appendix 1). The data presented in figure 4.7 (A and B) is an average of the NRQs of three biological replicates, expect for line 9.7 where cDNA synthesis of one replicate failed.

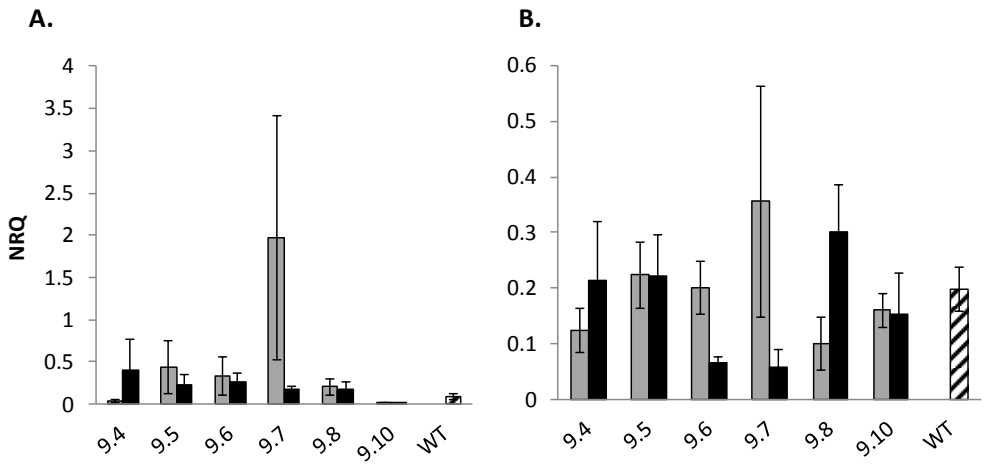


Figure 4.7: NRQs of *TaAmy1* and *TaAmy2* on *HvChi26::Atgai* transgenic lines

Endogenous levels of the *TaAmy1* (A) and *TaAmy2* (B) genes at 35 dpa. Grey bars – transgenic lines, black bars – null segregants and hatched bars – WT. Vertical error bars denote SEM.

The qRT-PCR for *TaAmy1* was performed using forward primer TaAmy1_F2 and reverse primer TaAmy_R2 (Appendix 1). The expression of this gene showed a large degree of variation within biological replicates and across and within lines. In the transgenics of line 9.7, whilst there was a high level of variation between replicated, *TaAmy1* was highly up-regulated (Figure 4.7, A) compared

to its null which could explain the extremely high levels of α-amylase in this line (Figure 4.6, C). Whilst there was an overall weak trend towards up-regulation of *TaAmy1* in the transgenics, in line 9.4 the opposite was observed. However, this line also had higher α-amylase content than its null. Line 9.10 was notable in that the expression of *TaAmy1* was extremely low in both the transgenics and the nulls. This lines also had the highest expression of the *Atgai* transgene (Figure 4.4, A), but no corresponding reduction in α-amylase content was observed.

The expression of *TaAmy2* was also analysed in these lines, using forward primer Amy2_F_ext and reverse primer Amy2_R_ext (Appendix 1). However, there was no consistency of *TaAmy2* expression between lines, no correlation of expression patterns between transgenics and nulls (Figure 4.7, B) and no overall correlation between *TaAmy2* expression and α-amylase levels in these lines.

4.2.4 Analysis of transgenic lines expressing the *Atgai* gene under control of the embryo- and aleurone-specific *HvBeg1* promoter

4.2.4.1 GFP visualisation of *HvBeg1* activity

GFP was examined in grains at 21 and 35 dpa (according to section 2.7) from plants expressing *HvBeg1:Atgai* to confirm earlier studies in our laboratory which showed promoter activity beginning at 26 dpa. Whilst restricted to the expected target tissues in the grain, faint GFP expression was observed at 21 dpa in the aleurone layer and scutellum (Figure 4.8) and when younger grains were studied GFP was observed as early as 16 dpa. As mentioned in section 4.2.3.1 whilst growing conditions were consistent between experiments, the difference observed in the timing of promoter activity may be due to external environmental factors affecting the quality of growing conditions between experiments. However, due to time and resource constraints it also wasn't possible to further characterise the temporal activity of this promoter across multiple experiments. Promoter activity was also studied at germination and GFP was visible from 24 hours after imbibition (Figure 4.9) up to four days post germination. In these lines GFP was visible in the aleurone and the scutellum of the germinating grain, but not in the embryonic axis.

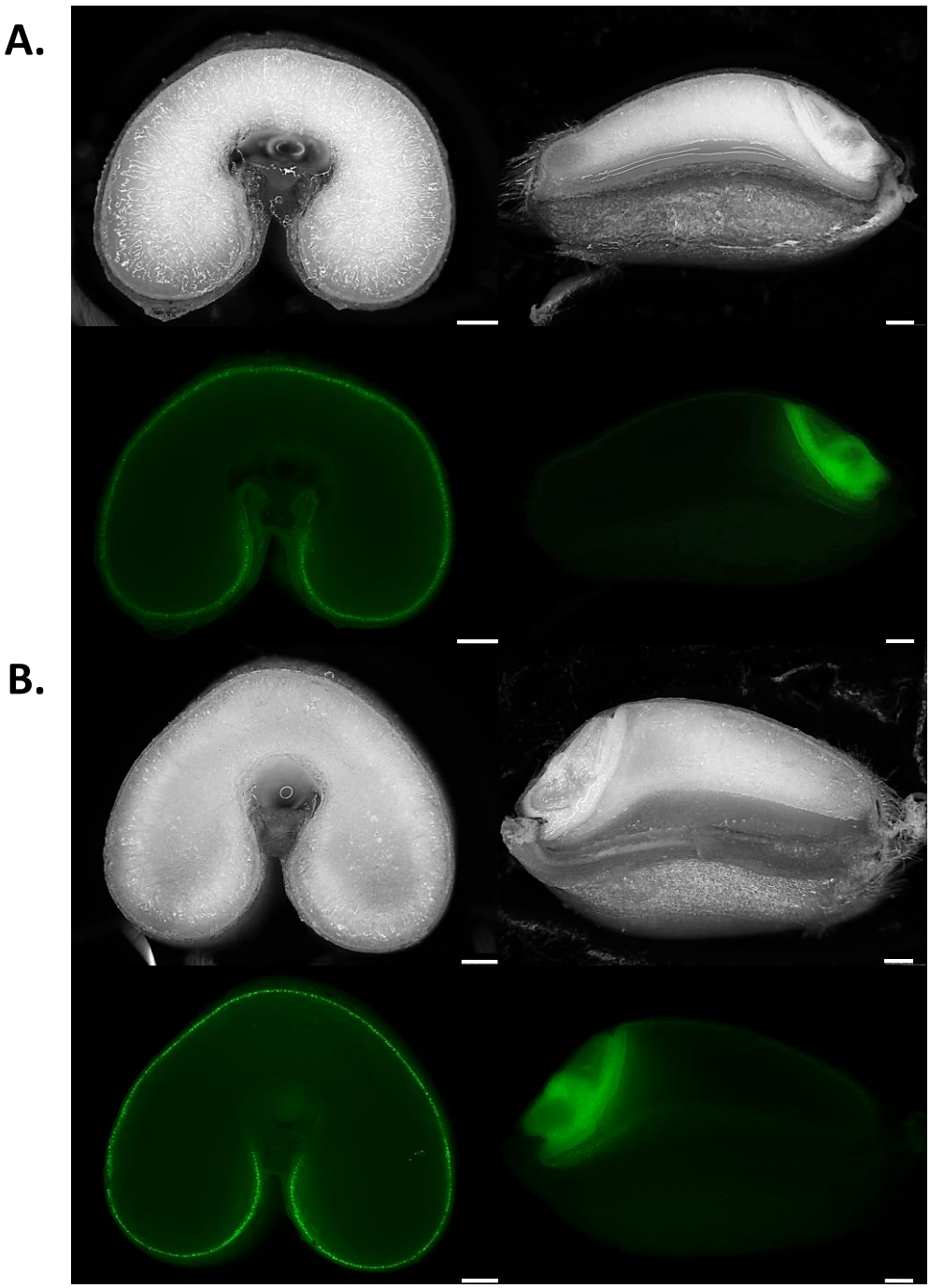


Figure 4.8: Activity of embryo and aleurone specific promoter in wheat grain
Transverse sections highlighting the aleurone layer and longitudinal sections highlighting the embryo are presented in bright field (top panel) and under a GFP filter set (excitation/ emission) (bottom panel) at 21 dpa (A) and 35 dpa (B) for typical transgenic lines harbouring GFP under control of the barley *HvBeg1* promoter. Scale bars represent 500µm for each image.



Figure 4.9: Activity of embryo and aleurone specific promoter in germinating grain

Transverse and longitudinal sections highlighting the aleurone layer and scutellum are presented in bright field (top panels) and under a GFP filter set (excitation/ emission) (bottom panels) at 24 hrs post imbibition for typical transgenic lines harbouring GFP under control of the barley *HvBeg1* promoter. Scale bars represent 500µm for each image.

4.2.4.2 *HvBeg1::Atgai* transgene expression

As described in section 4.2.3.2, to confirm expression of the introduced transgene, transcript levels of the *Atgai* gene were measured in cDNA synthesised (section 2.2.6) from RNA extracted as described in sections 2.2.4 and 2.2.5 from 35-dpa grains. These grains were harvested from ear two from three biological replicates from each of the seven independent lines in the experiment and their respective nulls and the wild-type control. The qRT-PCR was performed on this material according to section 2.2.7 using primers gai_qPCR-F and gai_qPCR-R. The expression of the transgene (Figure 4.10, A) was normalised against the expression of three endogenous genes – *Ta2526,*

TaGapDH and *TaSDH* (section 2.2.7 and appendix 1). The data presented in figure 4.10 is an average of the NRQs of three biological replicates, except for lines 10.8 and 10.11 where cDNA synthesis of one replicate failed. The qRT-PCR was performed on all plants in the experiment, including the null and wild-type plants as controls. However as mentioned in section 4.2.3.2, no expression of the transgene was observed in any of the control material (including the NRT controls) and as such these are excluded from the figures as presented.

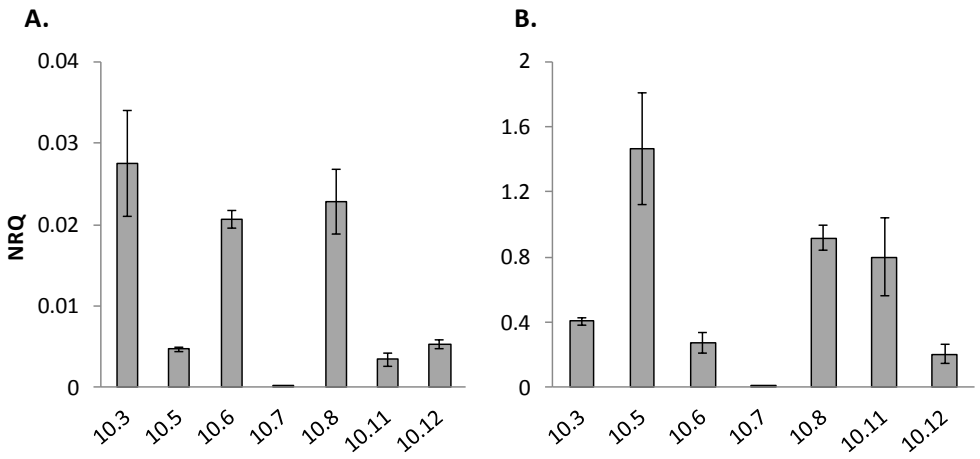


Figure 4.10: NRQs of *Atgai* and *GFP* in *HvBeg1:Atgai* transgenic lines
Average of normalised expression levels of the *Atgai* (A) and *GFP* (B) genes in 35 dpa grain as measured in three biological replicates for each transgenic line. Vertical error bars denote SEM.

It should be noted that in these lines as well, whilst detectable, *Atgai* NRQs were very low compared with the other transgenes examined within this project and ranged from 0.0034 to 0.027. It should also be noted that in line 10.7, *Atgai* expression was not detected in all three biological replicates (Figure 4.10, A), although all were PCR positive for the gene. *GFP* transcript levels were also measured on the same material using forward primer GFP_qPCR_F and reverse primer GFP_qPCR_R and are presented in figure 4.10, B. *GFP* expression levels in these lines were between 13 to 300 times higher than those observed for *Atgai*. Whilst the expression of *GFP* in these lines is not as high as

that seen for plants with the *HvChi26* promoter (Figure 4.4, B), these expression levels of *GFP* indicate that the promoter used is functional. This again suggests that potentially sequence conformation or *cis*-acting factors may be affecting expression of the *Atgai* gene. It is possible that *Atgai* expression in these lines is so low as to be non-functional, as for the *HvChi26::Atgai* lines. It should also be noted that qRT-PCR did not detect GFP expression in line 10.7, even though weak GFP expression was observed by UV examination (section 2.7). These results imply that in this line there might be other factors affecting the expression of the two transgenes and subsequent data for this line should be viewed with this in mind.

4.2.4.3 Analysis of *HvBeg1::Atgai* effect on yield

To study effects of expressing *HvBeg1::Atgai* on grain yield, mature grains harvested from three ears of each plant in the experiment was assessed as described in section 4.2.3.3. The data presented in Figure 4.11, A-E shows the average values for three biological replicates of each line. Whilst for the majority of lines the measurements for diameter (Figure 4.11, F) are also based on three biological replicates each, for the null plants of line 10.3 and the transgenic plants of 10.6 this is an average of two replicates only. In both lines one replicate did not produce enough grains to enable robust data analysis and thus were excluded. For all of the yield variables measured the differences between the transgenic, null and wild-type plants were assessed at the population level using ANOVA. Using LSD at 5% no significant differences were observed between the three genotypes for any of the variables studied (data not shown). This result agrees with the hypothesis that insensitivity to GA in the embryo and aleurone layer should not affect grain yield.

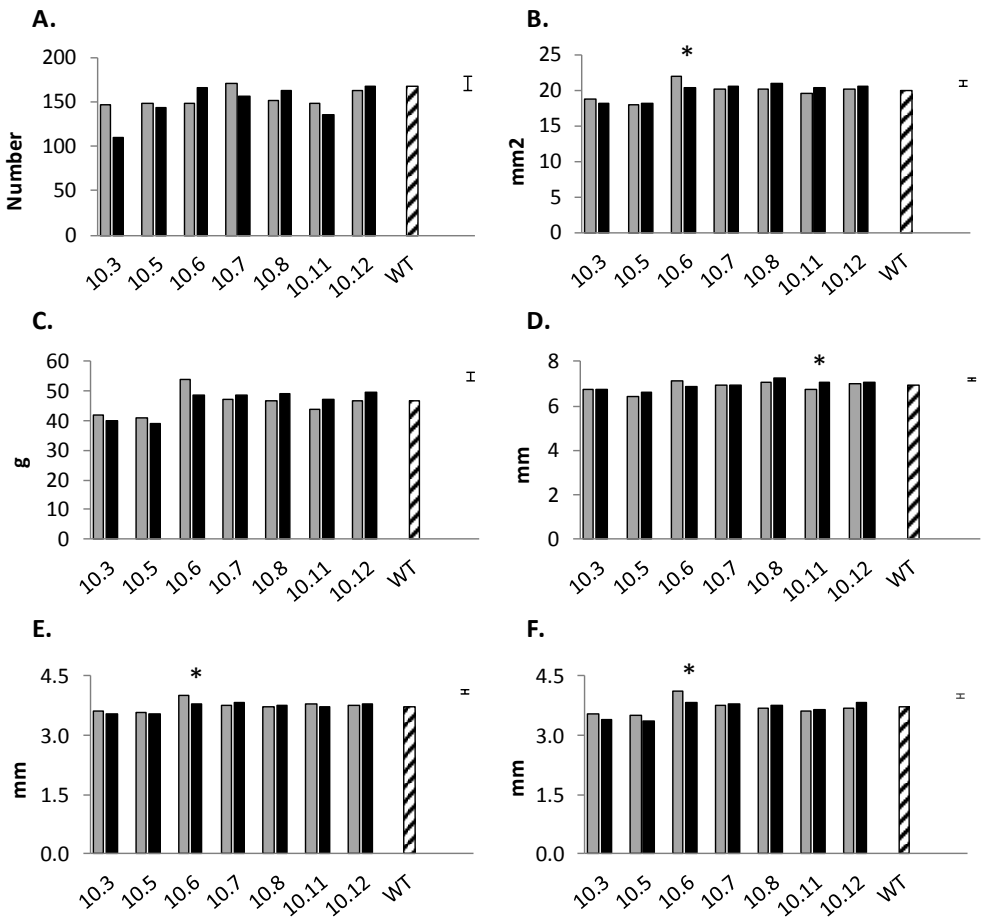


Figure 4.11: Analysis of yield components of *HvBeg1::Atgai* transgenic lines
Averages are presented for several variables: grain number (A), grain surface area (B), TGW (C), grain length (D), grain width (E) and grain diameter (F) for measurements on mature grains. Grey bars – transgenic lines, black bars – null segregants and hatched bars – WT. * denotes significant difference between a transgenic and its null using least significant difference (LSD) at 5%: p value at – *: ≤ 0.05. Vertical error bars denote SED on 1, 28 df in A-E and 1, 26 df in F.

The differences between the transgenic lines and their respective nulls were also analysed using ANOVA. Grain numbers, averaged from three ears, showed a broad range from a low of 109.7 (null, line 10.3) to a high of 170.7 (transgenic, line 10.7), but no significant differences were observed between the transgenics and nulls in any of the lines (Figure 4.11, A), indicating that, as expected, expression of this construct does not affect grain number. The average TGW also showed a wide range with a low of 38.93 g (null, line 10.5)

and a high of 53.79 g (transgenic, line 10.6). However, again no significant differences were observed between the transgenics and nulls in any of the lines (Figure 4.11, C). For grain surface area, width and diameter measurements, whilst the majority of lines did not show a significant difference, in line 10.6 the transgenic grains had a significantly larger area ($p = 0.024$ F-test = 5.69), width ($p = 0.038$, F-test = 4.76) and diameter ($p = 0.047$, F-test = 4.36) than its null (Figure 4.11, B, E and F). Whilst, in line 10.11 the transgenic grains had significantly lower length (Figure 4.11, D) than its null ($p = 0.037$, F-test = 4.81), grain length measurements did not show a significant difference in any other line. Taken as a whole for this construct, as for the *HvChi26::Atgai* lines, there was no evidence that the *HvBeg1::Atgai* affected either grain yield or grain morphology.

4.2.4.4 Analysis of *HvBeg1::Atgai* effect on quality

To study the effects of expressing *HvBeg1::Atgai* on grain quality; hardness, moisture content and α-amylase content were assessed. Grain hardness and moisture were measured using the SKCS system as described in section 2.4.1 and differences between transgenics and their respective nulls analysed using ANOVA at 5% LSD. The data presented in figure 4.12, A and B represents the average of three biological replicates of each line, with the exception of the null line 10.3 and transgenic line 10.6 where only two replicates were available. Grain hardness did not show any significant differences in the majority of the lines except line 10.6 (Figure 4.12, A). In this line the transgenic plants had a significantly lower hardness index than the null plants ($p = 0.008$, F-test = 8.37). Whilst the moisture content of all lines in this experiment was in the normal range (11 -14%), only lines 10.5 and 10.11 displayed significant differences (Figure 4.12, B), with transgenic grains in line 10.5 having a lower moisture content than their null ($p = 0.007$, F-test = 8.43), and in line 10.11 transgenics having higher moisture content than the nulls ($p < 0.001$, F-test = 26.05).

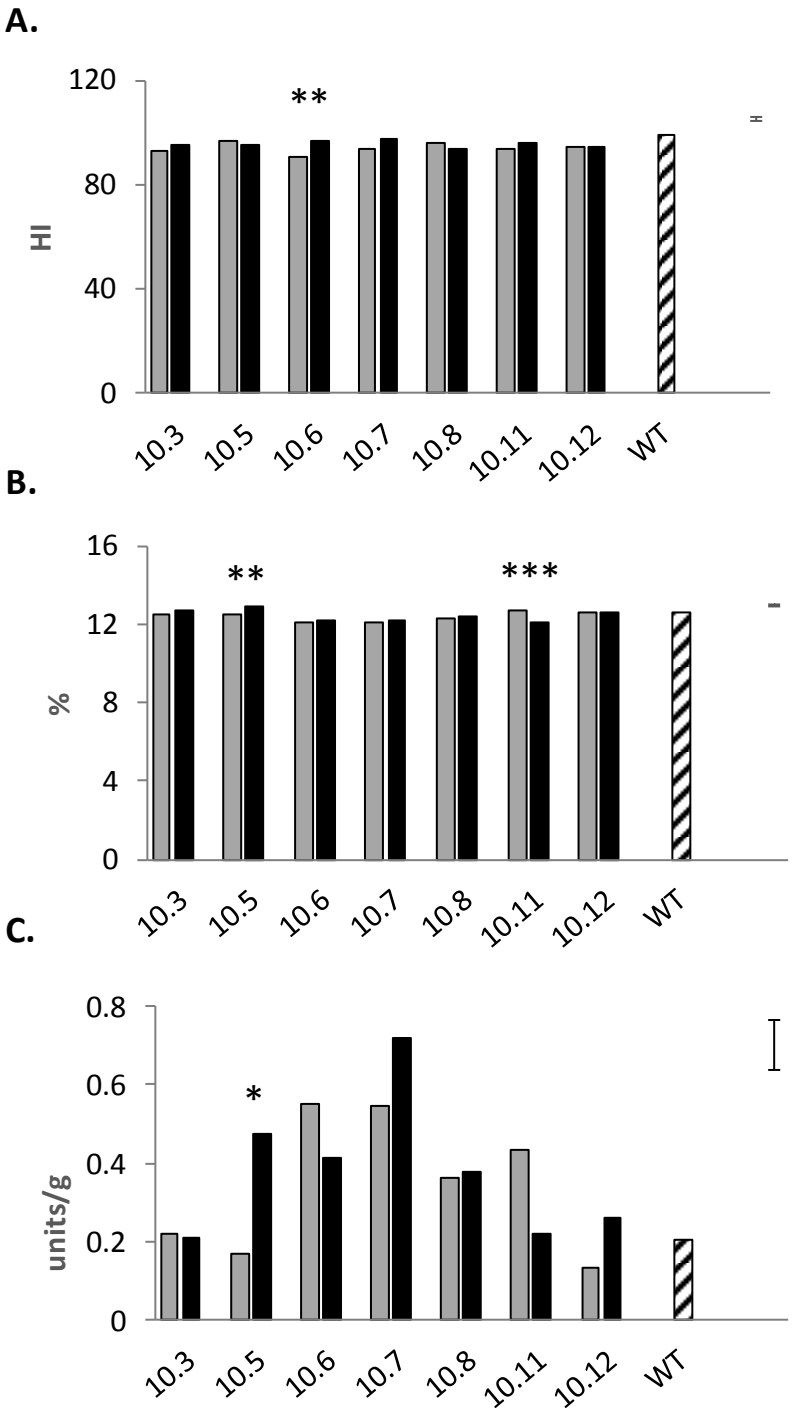


Figure 4.12: Analysis of quality components of *HvBeg1::Atgai* transgenic lines

Averages are presented for several variables: grain hardness (A), moisture content (B) and α-amylase (C) for measurements on mature grains. Grey bars – transgenic lines, black bars – null segregants and hatched bars – WT. * denotes significant difference between a transgenic and its null using LSD at 5%: p value at – *: ≤ 0.05, **: ≤ 0.005 and ***: ≤ 0.001. Vertical error bars denote SED on 1, 26 df in A and B, and 1, 28 df in C.

Grains crushed during the SKCS analysis were collected and milled to a fine flour and α-amylase activity measured on 25 mg of this material according to section 2.4.2. The data presented in figure 4.12, C shows CU for each line and is an average of three biological replicates. It should be noted that as described in section 4.2.3.4, the level of α-amylase enzyme in the wild-type control was much lower (0.21 CU/g) in this experiment compared with the rest of the studies in this project. The α-amylase content in the rest of the lines showed a broad range with the highest value being 0.72 CU/g (null, line 10.7) and the lowest 0.13 CU/g (transgenic, line 10.12) (Figure 4.12, C). We hypothesised that insensitivity to GA in the embryo and aleurone layer would result in a reduction in the α-amylase content and in order to test this the differences between the transgenics and their respective nulls were analysed using ANOVA. As shown in section 4.2.4.2 (Figure 4.10, A) line 10.3 has the highest expression of the *Atgai* transgene. However, this did not result in a corresponding reduction in the α-amylase content in this line compared to its null. Whilst there was large variation in the α-amylase content in the different lines studied, only line 10.5 ($p = 0.046$, F-test = 4.36) showed a significant difference. In this line the transgenic plants had lower α-amylase levels than its null, although this line had a relatively low level of expression of the *Atgai* transgene (Figure 4.10, A). These results also indicate that either GA insensitivity in the embryo and aleurone layer does not have any effect on α-amylase production or as with *HvCHI26::Atgai* the low level of *Atgai* transgene expression is making this construct ineffective. In the latter case the variation in α-amylase content in these lines could again be a result of the stochastic nature of this enzyme activity in grain.

4.2.4.5 *HvBeg1::Atgai* effect on endogenous gene expression

As the α-amylase levels in these plants were highly variable, as in plants expressing *HvChi26::Atgai*, the expression levels of the two endogenous α-amylase genes – *TaAmy1* and *TaAmy2* – were measured. These measurements

were performed according to section 2.2.7 and on the same 35 dpa cDNA used to measure transgene expression (section 4.2.4.2). The expression of the two genes (Figure 4.13, A and B) was normalised against the expression of three endogenous genes – *Ta2526, TaGapDH* and *TaSDH* (section 2.2.7 and appendix 1). The data presented in figure 4.13 (A and B) is an average of the NRQs of three biological replicates, except for lines 10.8 and 10.11 where cDNA synthesis of one replicate failed.

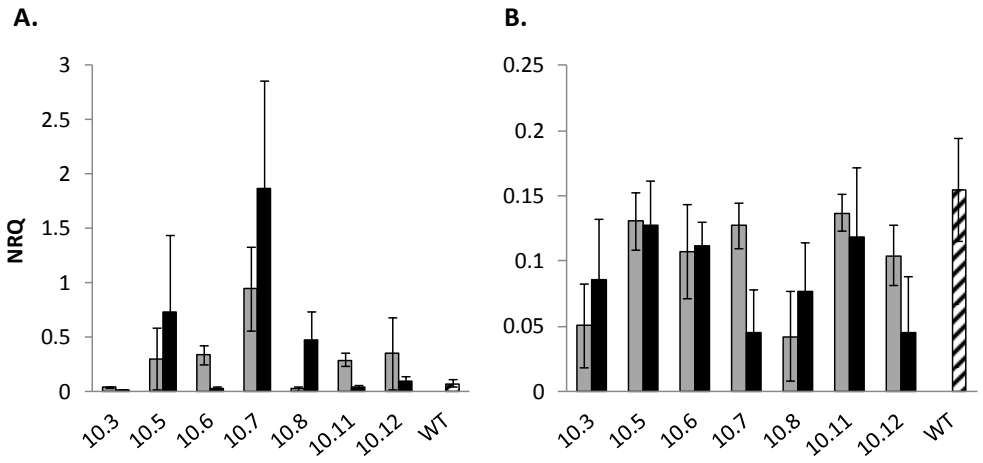


Figure 4.13: NRQs of *TaAmy1* and *TaAmy2* in *HvBeg1::Atgai* transgenic lines

Endogenous levels of the *TaAmy1* (A) and *TaAmy2* (B) genes at 35 dpa. Grey bars – transgenic lines, black bars – null segregants and hatched bars – WT. Vertical error bars denote SEM.

The qRT-PCR for *TaAmy1* was performed using primers TaAmy1_F2 and TaAmy_R2 (section 4.2.3.5) and revealed significant variation within biological replicates and across and within lines (Figure 4.13). Line 10.7 which did not express either of the two transgenes (Figure 4.10) showed the highest levels of endogenous *TaAmy1* in both the transgenics and nulls (Figure 4.13, A). This line also had the highest α-amylase content (Figure 4.12, C) and the high levels of *TaAmy1* could explain this result. Whilst the expression of *TaAmy1* overall showed no trend and there was no consistency between lines, in the majority

of the lines the expression of *TaAmy1* was comparable between the transgenics and their nulls. However, in lines 10.6 and 10.11 there was an increase in *TaAmy1* levels in the transgenics, and in line 10.8 transgenics there was a reduction compared to the nulls. As shown in section 4.2.4.2, line 10.8 also had a relatively high expression of the *Atgai* transgene (Figure 4.10, A), but no corresponding reduction in α-amylase content was observed.

The expression of *TaAmy2* was analysed using primers Amy2_F_ext and Amy2_R_ext (section 4.2.3.5) and was found to be comparable between the transgenics, nulls and the wild-type control, except in line 10.7 (Figure 4.13, B). In this line the expression was elevated in the transgenics, but this did not correspond with the α-amylase results for this line (Figure 4.12, C). As mentioned in section 4.2.4.2 and shown in Figure 4.10, this line does not express either of the two transgenes and thus the increase in *TaAmy2* expression is unlikely to be due to over expression of *HvBeg1::Atgai*.

4.3 Conclusions

The aim of the work described in this chapter was to introduce GA insensitivity in the embryo and aleurone layer of developing wheat grain in order to study the effect on grain yield and quality. This was performed using two expression constructs – *HvChi26::gai* and *HvBeg1::gai*. We hypothesised that insensitivity to GA in these two tissues, the sites of GA and α-amylase production would reduce the amount of α-amylase in the grain without affecting yield. However, as was demonstrated this was not the case. In plants expressing *HvChi26::gai*, whilst no substantial effects were observed on any yield parameters measured, and grain morphology was unaffected, none of the transgenic lines showed a statistically significant reduction in α-amylase levels compared to their nulls. Indeed, in two of the lines α-amylase levels were higher in the transgenic plants than in the null controls, but this did not correspond with the expression of the endogenous *TaAmy* genes. In all lines the expression of the *Atgai* transgene was very low compared to other transgenes studied in this project. This low expression of the transgene could mean that the construct is non-functional in these plants, which could explain the lack of a phenotype. In plants expressing *HvBeg1::gai*, whilst again there were no effects on yield or grain morphology, α-amylase levels were reduced in only one line. In the rest of the lines there was a large variation in α-amylase, but none of the differences between the transgenics and their nulls were statistically significant. The expression of the *TaAmy* endogenous genes again did not match the α-amylase levels. In these plants as well the expression of the *Atgai* transgene was extremely low, indicating that the transgene may also be non-functional, explaining the lack of a phenotype.

This low level of expression of the *Atgai* transgene in both constructs indicates two possibilities: the first being that the wrong tissues was analysed for this study. The material used for transcript analysis was 35 days old whole grains of which the embryo and aleurone layer are a small part and the major portion is

the endosperm. It is possible that the levels of the transgene appear low only due to the fact that it is expressed in a small proportion of the grain. However, if this was true we should have seen a similar pattern in the expression of the *GFP* gene but this was not the case. The levels of expression of *GFP* were extremely high in both constructs compared to *Atgai*. The other possibility is that the *Atgai* gene is unable to be transcribed in wheat. However, the expression of this gene was also studied in another construct (see chapter 6) where the level of expression is higher than the lines studied here. This indicates that there might be other factors such as transcriptional silencing or post-transcriptional gene silencing for the low levels of expression seen in these lines and not the functionality of the gene. Methylation in promoter regions, histones or coding sequences can influence gene expression at both the transcriptional and post transcriptional level (Rajeevkumar *et al.*, 2015). Multicopy integration of the transgene at random locations has also been suggested to lead to silencing (Mishiba *et al.*, 2005). It is also possible that the *de novo* methylation of one transgene by a second transgene under control of the same promoter leading to silencing (Fagard and Vaucheret, 2000). Another possibility for the low levels of expression of the transgene in these plants is post transcriptional gene silencing due to *cis*-inactivation where transcripts do not accumulate in spite of continuous transcription (Rajeevkumar *et al.*, 2015).

If either of the possible gene silencing mechanisms are acting in these plants and the AtGAI protein is not being produced the aleurone layer would still able to perceive GA and produce the α-amylase enzyme. This also explains why we don't see any impact on the expression of the endogenous *TaAmy* genes which should have been downregulated by the presence of the gai DELLA protein. In addition, the variation in α-amylase activity seen in these lines may be a result of the stochastic nature of this enzyme.

Chapter 5. Effects of manipulating GA in the pericarp and seed coat layers of developing wheat grain

5.1 Introduction

In a grain the endosperm and embryo are surrounded by the maternal pericarp and seed coat tissues which are derived from the ovary wall. In cereals the testa is the true seed coat and in wheat its cuticle is made up of two layers which are believed to develop from the inner integument (Morrison, 1975). In a developing grain the integument layers are two cells thick and whilst the outer integument degenerates by five to six dpa, the inner integument persists. By 11 dpa the cell contents of the outer layer of the inner integument collapse and a semi-permeable cuticle is formed over most of the surface of the grain, except in the region of the crease where this layer is discontinuous. Condensed tannins accumulate in this layer late in grain development giving red wheat its characteristic colour and there is a strong correlation between increased pigmentation and reduced levels of preharvest sprouting (PHS) (Evers and Millar, 2002, WheatBP, 2016). In a developing grain the inner integument may be a site for GA biosynthesis as it has been shown in pea to contain 13-hydroxylase and 20-oxidase activity and it accumulates bioactive GAs (Rodrigo *et al.*, 1997).

The tissue of the caryopsis that lies outside the seed coat is the pericarp which originates as a component of the carpel wall and thus is also maternal in origin (Section 1.2 - Figures 1.4 & 1.5). During the early stages of development this tissue comprises of several layers of parenchymatic cells, a two layer chlorenchyma and the inner epidermis. However, by around 15 dpa it gets reduced to several layers of cuticle and at maturity the pericarp consists mainly of dry empty cells, some of which are distorted, with many intercellular spaces.

The inner epidermis of the pericarp comprises an incomplete layer of tube cells and a layer of cross cells which are unique to grasses. In wheat, these cells form a complete layer over most of the surface of the wheat grain by attaching to the cuticle of the testa (Winton and Winton, 1932, Evers and Millar, 2002). During early development, there are small starch granules in the parenchymatous cells between the inner and outer epidermal layers, however in a mature grain this layer has undergone autolysis and its products used by the developing endosperm. This loss of the parenchyma breaks the attachment of the testa with the cross cells over the surface of the grain and they remain attached only in the region of the crease (Evers and Millar, 2002). As discussed in section 1.3.5, GA signalling and inactivating genes are expressed highly in the pericarp layers of developing grains, whilst the biosynthesis genes only show low levels of expression (Pearce *et al.*, 2015).

Expressing the GA biosynthesis gene (*AtGA20ox1*) in the pericarp and the inner integument layer using promoters that are switched on in the early stages of grain development may help to determine whether GA biosynthesis occurs in these tissues and if their expansion is regulated by this hormone. These plants could also help to determine if the seed coat potentially restricts grain size, and does increasing GA biosynthesis in these tissues allow the production of larger grain, without adverse effects on flour quality. The two promoters selected for this study were the barley Germin F (*HvGerF*) which is active in the pericarp from 5-35 dpa and the wheat Dihydroflavanol-4-reductase (*TaDFR-D*) promoter which is active in the inner integument from 7-25 dpa (Table 3.1) (Figure 5.1).

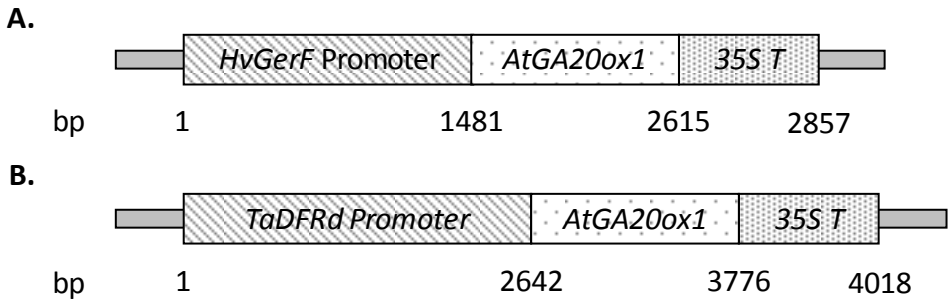


Figure 5.1: Basic structure of *HvGerF::AtGA20ox1* and *TaDFRd::AtGA20ox1*
Basic structure of constructs *HvGerF::AtGA20ox1* (A) and *TaDFR-D::AtGA20ox1* (B). The position of junctions between elements is given in bp. The CaMV 35S terminator is labelled 35S T.

Germins are known to occur only in cereals and have been characterised as oxalate-oxidases (OxOs) (Lane *et al.*, 1993, Lane, 2002). Wu *et al*. (2000) isolated five germin genes (*GerA*, *-B*, *-D*, *-E* and *-F*) from barley and showed four of these to be expressed in the testa/pericarp tissues. These genes are closely related to the rice *germin 1* but are different from the wheat embryo OxO and other barley OxOs (Wu *et al.*, 2000). These authors also isolated the 5' upstream sequence of the *GerB* and *GerF* genes which showed a 93.3% (1352 bp) identity including a 225-bp long intron in both genes at the same site. They also transiently expressed the beta-glucuronidase gene using the *GerB* (847 bp) and *GerF* (899 bp) promoters in the epicarp, pericarp + testa and endosperm of 1-20 dpa barley grains. In spite of having highly conserved promoter sequences the two genes show a difference in both their temporal and tissue-specific expression. The *GerF* promoter was highly active in the testa, and to a lower level in the epicarp tissue, whereas the *GerB* promoter displayed weak activity only in the testa and was absent from the epicarp; neither promoter was active in the endosperm (Wu *et al.*, 2000). In another study both genes were also shown to be expressed in seedlings and spikes, but to different extents, and whilst *GerB* had high expression in coleoptiles and primary leaves, *GerF* was expressed in seedling roots, developing spikes and pericarp/testa (Federico *et al.*, 2006). Deletion studies performed on both promoters by these authors showed that only 97 bp of the conserved proximal promoter sequence was

enough to drive GFP expression in epicarp, coleoptile and spikes, but to a reduced extent (Federico *et al.*, 2006). For the present study 1480 bp of 5'UTR of the *HvGerF* gene was isolated by PCR based on the sequence published by Wu *et al*., (2000) (GenBank, AF250935) and promoter activity studied in three independent lines expressing nuclear-targeted GFP under control of this promoter (Figure 1.15). GFP activity was observed in the inner integument and pericarp tissues from five to 35 dpa in all lines. Promoter activity was not observed in any of the non-target tissues except for low-level expression of GFP in the glumes of two line (Vaughan, S., unpublished data).

The second promoter described in this chapter is associated with the wheat DFR gene, the product of which is involved in flavonoid biosynthesis, where it catalyses the reduction of dihydroflavonols to leucoanthocyanidins (Holton and Cornish, 1995). The wheat *DFR* gene was first isolated from developing grains of blue-grained wheat and consisted of 1062 bp ORF, predicting a protein of 354 amino acids and 38.3 kDa. This sequence displayed significant identity with the DFRs of barley (94%), rice (83%) and maize (84%) (Yang *et al.*, 2003a). Three *DFR* homoeologous genes located on the long arm of wheat chromosomes 3A, 3B and 3D were isolated from Chinese Spring by Himi and Noda (2004). These authors also studied the expression of these three genes and found that whilst in the grain *TaDFR-B* and *-D* showed higher expression than *TaDFR-A*, in leaves and roots *TaDFR-B* showed the highest expression. In whole grains the maximum expression was seen at five dpa and in the seed coat at 10 dpa. They also showed that the 5' upstream region of these genes included two (*TaDFR-A* and *-D*) or three (*TaDRD-B*) combinations of a G-box core element and a binding site for a Myb-type transcription factor P. All three promoters also contained two core elements (AAAG) for Dof (DNA binding one zinc finger) transcription factors known to be involved in tissue specificity and a TACpyAT element. In addition, the promoter of *TaDFR-A* also contained a core element for SBF-1 factor (GGTTAA), which has been implicated in organ-specificity. These differences seen in the promoter sequences of these genes may account for the different patterns of gene expression (Himi and Noda,

2004). For this study the *TaDFR-D* promoter was isolated using genome walking from wheat cv. Cadenza generating a 2750 bp fragment (Vaughan, S. unpublished data). This represented 109 bp of *TaDFR* CDS which displayed 96.3%, 95.4% and 96.3% identity to the previously published (Himi and Noda, 2004) homoeologous *TaDFR-A* (GenBank, AB162138), *-B* (GenBank, AB162139) and *-D* (GenBank, AB162140) CDS, respectively. Furthermore, 550 bp of 5' upstream sequences also displayed 75.6%, 75.3% and 97.7% identity with the three homologues *TaDFR-A, -B* and *-D* confirming that the isolation of the *TaDFR-D* promoter. A further 2091 bp of associated 5' upstream sequence was also isolated and this extended and verified sequence, based on a single fragment and sequenced in both directions was submitted to Genbank under the accession HM564398. This is the source of the *TaDFR-D* promoter used in this study. Promoter activity was studied during grain development using three independent lines expressing nuclear-targeted GFP under control of the *TaDFR-D* promoter (Figure 1.15). The promoter was found to be highly active in only the inner integument layer of the grains from seven to 25 dpa. However, in one line low levels of GFP were also observed in some of the glumes (Vaughan, S., unpublished data).

5.2 Results and Discussion

5.2.1 Production of homozygous material

To select homozygous material for this study, 24 T1 plants from seven independent lines of *HvGerF::AtGA20ox1* and six lines of *TaDFR-D::AtGA20ox1* were genotyped as described in Chapter 3. TaqMan assays (section 2.2.3) were performed on T1 plants of both constructs using forward primer Q_At20ox1-F, reverse primer Q_At20ox1-R and hybridization probe Q_At20ox1-probe (Appendix 1). For both constructs, three plants were chosen from each independent line as potential homozygotes. The T2 progenies of the plants harbouring construct *HvGerF::AtGA20ox1* were analysed by PCR (section 2.2.2) using forward primer GerF-F and reverse primer 20ox-R (Appendix 1). The same analysis was also performed on T2 *TaDFR-D::AtGA20ox1* transgenic lines using forward primer DFRd-F and reverse primer 20ox-R (Appendix 1). Homozygous T2 plants were subsequently selected and an experiment performed with three biological replicates on four independent lines for each construct.

5.2.2 Experimental design

Studies on developing grains were performed to examine the effects of expressing the *AtGA20ox1* gene in the pericarp and seed coat layers of the grain using transgenic wheat lines harbouring the *HvGerF::AtGA20ox1* and *TaDFR-D::AtGA20ox1* constructs generated as described in section 2.1. A single RCBD experiment was setup as described in section 2.1.1 with three replicates of four independent lines of each construct. In this experiment for each line two plants were grown in 20-cm pots and each plant cut back to five tillers. From ears two, three and four, of both plants in each replicate block, grains were harvested at 10, 20, 30, 40, 50 and 60 dpa from the six ears which were each assigned a time point in a randomised manner. These were harvested to study grain development. Grains harvested at 10 dpa were also utilised to measure

transcript levels of the transgene. From ear five, grains were harvested at two time points (10 and 20 dpa – four grains each) to visualise GFP (section 2.7) to study promoter activity. Grains from ear one of each plant in a pot in each replicate were harvested and pooled at maturity to measure final yield and analyse various quality parameters.

5.2.3 Analysis of transgenic lines expressing the *AtGA20ox1* gene under control of the pericarp-specific *HvGerF* promoter

5.2.3.1 GFP visualisation of *HvGerF* activity

GFP was examined in grains at 10 and 20 dpa as described in section 2.7. These two time points were chosen to confirm the earlier studies in our laboratory which showed promoter activity from five to 35 dpa. In these studies at 10 dpa (Figure 5.2, A) GFP activity was observed in the inner integument and not the pericarp layer. However, at 20 dpa (Figure 5.2, B) GFP activity was now observed in both the inner integument and pericarp layers. Unfortunately, due to time constraints it wasn't possible to further characterise the spatial activity of this promoter across multiple experiments. Promoter activity was also studied at germination, but no GFP was visible in any tissues of the grain or emerging seedling from 24 hours after imbibition to up to four days post germination.

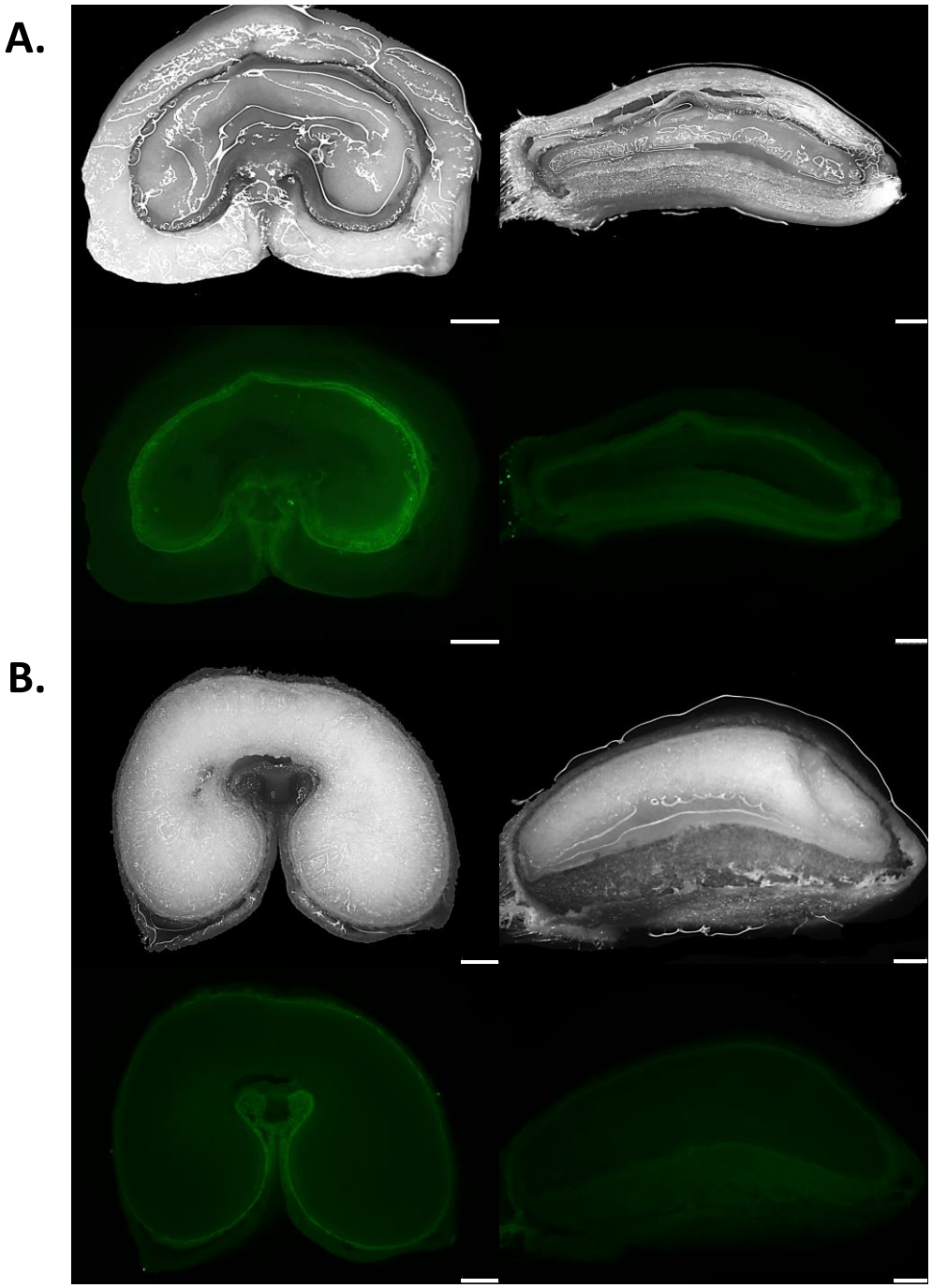


Figure 5.2: Activity of inner integument and pericarp-specific promoter in wheat grain

Transverse and longitudinal sections highlighting the inner integument and pericarp layers are presented in bright field (top panel) and under a GFP filter set (excitation/ emission) (bottom panel) at 10 dpa (A) and 20 dpa (B) for typical transgenic lines harbouring GFP under control of the barley *HvGerF* promoter. Scale bars represent 500µm for each image.

5.2.3.2 *HvGerF::AtGA20ox1* transgene expression

To confirm expression of the introduced transgene, transcript levels of the *AtGA20ox1* gene were measured in cDNA synthesised (section 2.2.6) from RNA extracted as described in sections 2.2.4 and 2.2.5 from 10 dpa grains. These grains were harvested from either ear two, three or four from three biological replicates from each of the four independent lines in the experiment and their respective nulls and the wild type control. qRT-PCR was performed on this material according to section 2.2.7 using forward primer q_At20ox1_F1 and reverse primer q_At20ox1_R1 (Appendix 1). The expression of the transgene (Figure 5.3) was normalised against the expression of two endogenous genes – *Ta2526* and *TaGapDH* (section 2.2.7 and appendix 1). The data presented in Figure 5.3 is an average of the normalised relative quantifications (NRQs) of three biological replicates, except for line 3.8. In this line both plants in one replicate block died and due to this reason all further measurement for this line are based on two biological replicates only. The qRT-PCR was performed on all plants in the experiment, including the null and wild-type plants as controls. No expression of the transgene was observed in any of the control material (including the NRT controls) and as such these are excluded from the figures as presented.

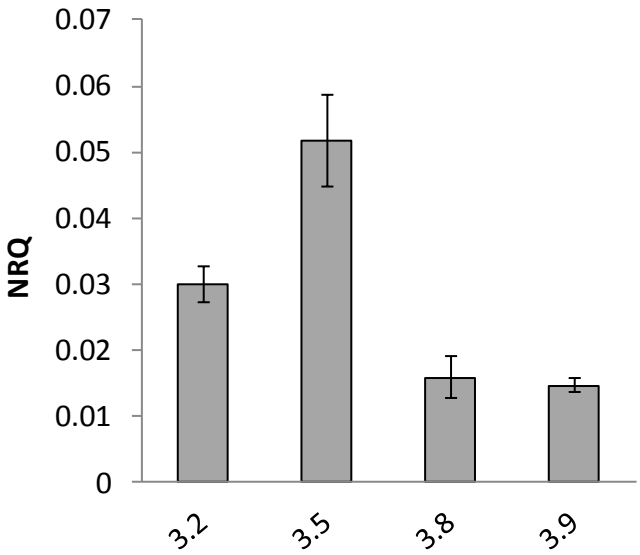


Figure 5.3: NRQs of *AtGA20ox1* in *HvGerF::AtGA20ox1* transgenic lines

Average of normalised expression levels of the *AtGA20ox1* at 10 dpa grains as measured in three biological replicates for each transgenic line. Vertical error bars denote SEM.

The expression of the *AtGA20ox1* transgene did not show a large degree of variation between the four independent lines studied (Figure 5.3) with the difference between the highest and lowest NRQs being only 0.037. Whilst the highest level of transgene expression at 0.052 was observed in line 3.5, the lowest was seen in line 3.9 at 0.015. The expression levels of this gene were comparable to other transgenes studied in this project.

5.2.3.3 Analysis of *HvGerF::AtGA20ox1* effects on yield

To study effects of expressing *AtGA20ox1* in the pericarp on grain yield, mature grains harvested from one ear (taken as a standardised proxy for total yield) of two plants per replicate block were assessed according to the methods described in sections 2.3 and 2.4.1. The MARVIN digital seed counter was used to count the number of grains and measure their surface area, length and

width. These grains were then weighed to calculate TGW. The measurements for diameter were obtained from SKCS as described in section 2.4.1. The data presented in figure 5.4 show the average values for three biological replicates for each line, except the transgenic plants of line 3.8 for which the data are based on two replicates only. For all of the yield variables measured the difference between the transgenic, null and wild type was assessed at the population level using ANOVA. Using LSD at 5% significant differences were observed between the three genotypes for all of the yield parameters measured except grain width and diameter (data not shown). For number of grains, TGW and area significant differences were observed between all three genotypes with the transgenics displaying the lowest values, followed by the nulls and the wild-type. The grain length of the transgenic lines was also significantly shorter than both the nulls and the wild-type with these two genotypes not showing a significant difference. These results indicate that increasing GA in the pericarp layer of the grain could be having a negative effect on grain yield.

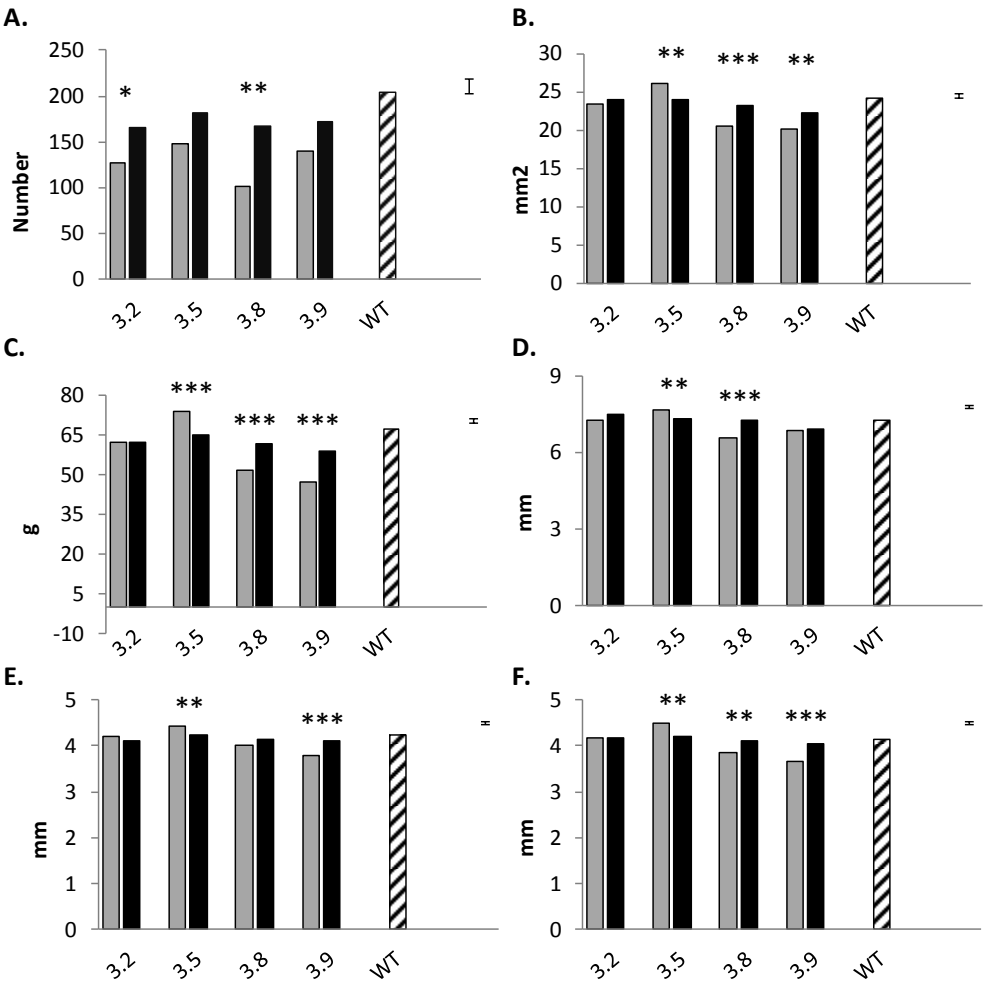


Figure 5.4: Analysis of yield components in *HvGerF::AtGA20ox1* transgenic lines

Averages are presented for several variables: grain number (A), grain surface area (B), TGW (C), grain length (D), grain width (E) and grain diameter (F) for measurements on mature grains. Grey bars – transgenic lines, black bars – null segregants and hatched bars – WT. * denotes significant difference between a transgenic and its null using LSD at 5%: p value at – *: ≤ 0.05, **: ≤ 0.005 ***: ≤ 0.001. Vertical error bars denote SED on 1, 16 df.

The differences between the transgenic lines and their respective nulls were also analysed using ANOVA. Grain number showed a broad range from a low of 101 (transgenic, line 3.8) to a high of 204.33 (wild-type), where significant differences were observed in two lines (Figure 5.4, A). The transgenics plants of line 3.2 (p = 0.047, F-test = 4.65) and line 3.8 (p = 0.002, F-test = 13.56) had fewer grains than their nulls. There was also a wide range in average TGW for

these lines, from a low of 47.40 g (transgenic, line 3.9) to a high of 73.52 g (transgenic, line 3.5). Significant differences were observed in TGW for three of the four lines (Figure 5.4, C), with line 3.5 ($p < 0.001$, F-test =21.57) being heavier than its null and lines 3.8 ($p < 0.001$, F-test = 29.89) and 3.9 ($p < 0.001$, F-test = 40.91) being lighter. As discussed in section 5.2.3.2 (Figure 5.3) line 3.5 had the highest expression of the *AtGA20ox1* transgene. In terms of grain surface area and diameter (Figure 5.4, B and F) the same pattern as TGW was seen with the transgenics of line 3.5 [area ($p = 0.001$, F-test = 15.39), diameter ($p = 0.004$, F-test = 10.99)] having larger grains than its null and lines 3.8 [area ($p < 0.001$, F-test = 26.06), diameter ($p = 0.009$, F-test = 8.76)] and 3.9 [area ($p = 0.002$, F-test = 13.49), diameter ($p < 0.001$, F-test = 20.02)] smaller. However, for grain length (Figure 5.4, D), whilst transgenic line 3.5 ($p = 0.009$, F-test = 8.76) was longer than its nulls and 3.8 ($p < 0.001$, F-test = 31.94) smaller, line 3.9 showed no significant difference. Whereas for grain width whilst again transgenic line 3.5 ($p = 0.008$, F-test = 9.06) was wider than its null, line 3.8 showed no difference and transgenic line 3.9 was smaller ($p < 0.001$, F-test = 20.39). Taken together, these results show an inconsistency in grain yields between the different transgenic lines. Whilst two of the four lines display a reduction in yield, it should be noted that one of these lines also had the fewest number of grains, and two plants in this line in one replicate block died indicating that there might be other issues contributing to the health of these plants thus impacting the yield. The contrasting results of the other two line (3.5 and 3.8) with one showing an increase in yield and the other a reduction compared to their nulls leads to a difficulty in making any definite conclusions about the effects of the expression of *AtGA20ox1* gene in the pericarp and inner integument on grain yield.

5.2.3.4 Analysis of *HvGerF::AtGA20ox1* effects on quality

To study the effect of expressing *AtGA20ox1* gene in the pericarp on grain quality, grain hardness and grain moisture content were assessed using the

SKCS system as described in section 2.4.1. The data presented in figure 5.5 represents the average of three biological replicates of each line except the transgenic of line 3.8. For both grain hardness and moisture content the differences between the transgenic, null and wild type were assessed at the population level by ANOVA using LSD at 5%. For grain hardness no differences were observed between any of the three genotypes. However, differences were observed in grain moisture content at the genotype level with the transgenic grains showing the lowest moisture content followed by the nulls and the wild type having the highest value.

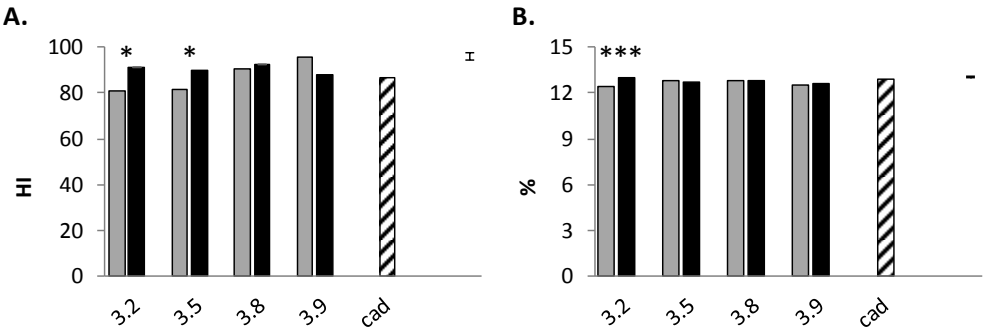


Figure 5.5: Analysis of quality components on *HvGerF::AtGA20ox1* transgenic lines

Averages are presented for: grain hardness (A) and moisture content (B) for measurements on mature grains. Grey bars – transgenic lines, black bars – null segregants and hatched bars – WT. * denotes significant difference between a transgenic and its null using LSD at 5%: p value at – *: ≤ 0.05 and ***: ≤ 0.001. Vertical error bars denote SED on 1, 16 df.

The differences between the individual transgenic lines and their respective nulls were also analysed by ANOVA and grain hardness (Figure 5.5, A) showed significant differences in two lines. In both line 3.2 ($p = 0.016$, F-test = 7.22) and 3.5 ($p = 0.040$, F-test = 5.00) the transgenics had lower hardness index than the nulls. The moisture content (Figure 5.5, B) in these lines, whilst being in the normal range (11 -14%), showed a significant difference in line 3.2 ($p < 0.001$, F-test = 27.36) with the transgenics having lower moisture content.

5.2.4 Analysis of transgenic lines expression the *AtGA20ox1* gene under control of the inner integument-specific *TaDFR-D* promoter

5.2.4.1 GFP visualisation of *TaDFR-D* activity

GFP was examined in grains at 10 and 20 dpa as described in section 2.7. These two time points were chosen to confirm the earlier studies in our laboratory which showed promoter activity from seven to 25 dpa. GFP activity was observed in only the inner integument layer of the grains at both 10 and 20 dpa (Figure 5.6). Promoter activity was also studied at germination, but no GFP was visible in any tissues of the grain or emerging seedling from 24 hours after imbibition to up to four days post germination.

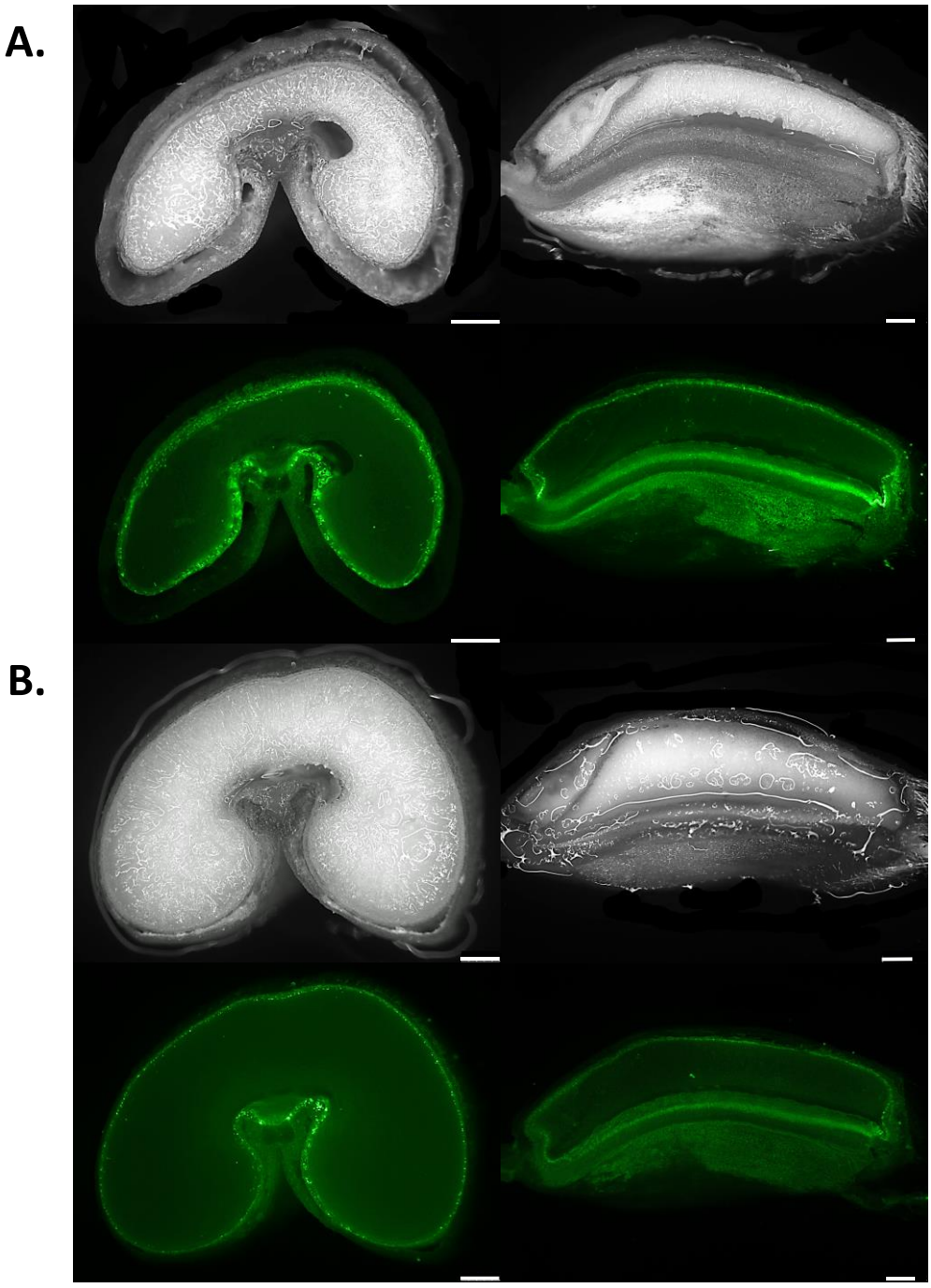


Figure 5.6: Activity of inner integument-specific promoter in wheat grain
Transverse and longitudinal sections highlighting the inner integument layer are presented in bright field (top panel) and under a GFP filter set (excitation/ emission) (bottom panel) at 10 dpa (A) and 20 dpa (B) for typical transgenic lines harbouring GFP under control of the wheat *TaDFR-D* promoter. Scale bars represent 500µm for each image.

5.2.4.2 *TaDFR-D::AtGA20ox1* transgene expression

To confirm expression of the introduced transgene, transcript levels of the *AtGA20ox1* gene were measured in cDNA synthesised (section 2.2.6) from RNA extracted as described in sections 2.2.4 and 2.2.5 from 10 dpa grains. These grains were harvested from either ear two, three or four from three biological replicates from each of the four independent lines in the experiment and their respective nulls and the wild type control. qRT-PCR was performed on this material according to section 2.2.7 using forward primer q_At20ox1_F1 and reverse primer q_At20ox1_R1 (Appendix 1). The expression of the transgene (Figure 5.7) was normalised against the expression of three endogenous genes – *Ta2526, TaSDH* and *TaGapDH* (section 2.2.7 and appendix 1). The data presented in Figure 5.7 is an average of the normalised relative quantifications (NRQs) of three biological replicates, except for line 4.4 where cDNA synthesis of one replicate failed. The qRT-PCR was performed on all plants in the experiment, including the null and wild type plants as controls. No expression of the transgene was observed in any of the control material (including the NRT controls) and as such these are excluded from the figures as presented.

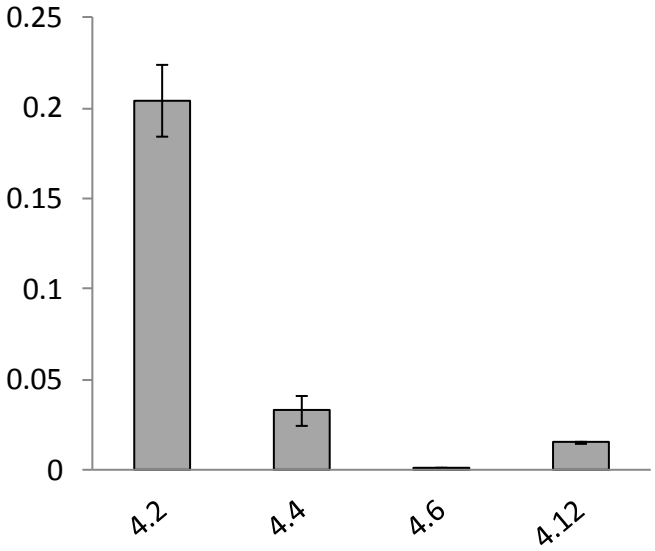


Figure 5.7: NRQs of *AtGA20ox1* in *TaDFR-D::AtGA20ox1* transgenic lines
Average of normalised expression levels of the *AtGA20ox1* at 10 dpa grains as measured in three biological replicates for each transgenic line. Vertical error bars denote SEM.

The expression of the *AtGA20ox1* transgene showed a large degree of variation between the four independent lines studied (Figure 5.7) with the highest NRQ at 0.204 (line 4.2) and lowest at 0.001 (line 4.6) showing a 270-fold difference between these two lines. Line 4.2 also had significantly higher gene expression than the other two lines with it being six and 14-fold higher than lines 4.4 and 4.12 respectively. The expression levels of this gene were broadly comparable to the rest of the transgenes studied in this project.

5.2.4.3 Analysis of the effect *TaDFR-D::AtGA20ox1* on yield

To study effects of expressing *AtGA20ox1* in the inner integument on grain yield, mature grains harvested from one ear (taken as a standardised proxy for total yield) of two plants per replicate block were assessed according to the methods described in sections 2.3 and 2.4.1. Yield measurements were performed as discussed in section 5.2.3.3 and the data presented in figure 5.8

shows the average values for three biological replicates of each line. For all of the yield variables measured, the difference between the transgenic, null and wild type was assessed at the population level using ANOVA. Using LSD at 5% significant differences were observed between the three genotypes for TGW, area and length with the transgenics displaying the lowest values, followed by the nulls and the wild-type. Grain diameter also showed a significant difference at the genotype level with the null grains being larger than those from the transgenics. These results indicate expressing the *AtGA20ox1* in the inner integument could be having a negative effect on grain yield.

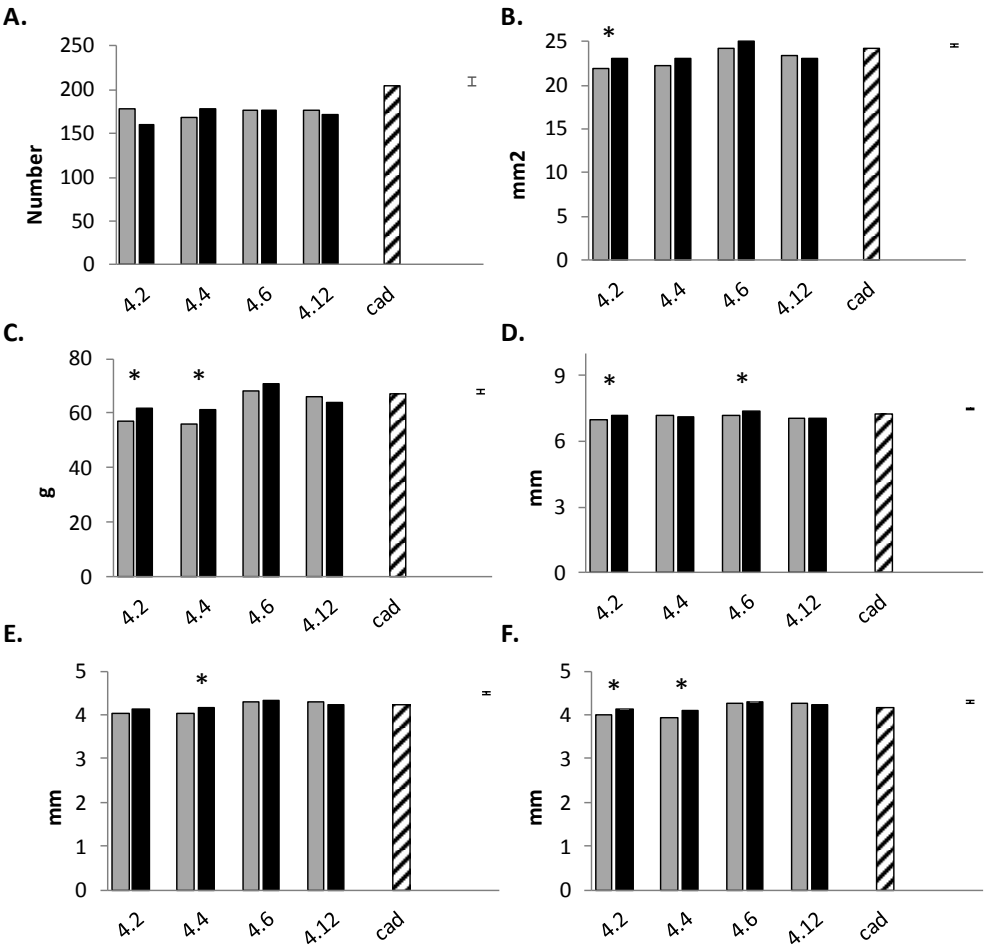


Figure 5.8: Analysis of yield components in *TaDFR-D::AtGA20ox1* transgenic lines

Averages are presented for several variables: grain number (A), grain surface area (B), TGW (C), grain length (D), grain width (E) and grain diameter (F) for measurements on mature grains. Grey bars – transgenic lines, black bars – null segregants and hatched bars – WT. * denotes significant difference between a transgenic and its null using LSD at 5%: p value at – *: ≤ 0.05. Vertical error bars denote SED on 1, 16 df.

The differences between the transgenic lines and their respective nulls were also analysed using ANOVA. Grain number between the different lines was fairly uniform with no significant differences observed in any lines (Figure 5.8, A). Whilst the TGW and diameter for these lines did not display a wide range, significant differences were observed in two lines (Figure 5.4, C and F), with the transgenics of both lines 4.2 [TGW ($p = 0.028$, F-test = 5.84), diameter ($p = 0.018$, F-test = 6.96)] and 4.4 [TGW ($p = 0.012$, F-test = 7.96), diameter ($p = 0.10$,

F-test = 8.55)] being lighter and smaller than their nulls. The grain surface area and width (Figure 5.8, B and E) showed a significant difference in one line each with the transgenic lines 4.2 (p = 0.038, F-test = 5.12) and 4.4 (p = 0.032, F-test = 5.54) being smaller and thinner, respectively, than their nulls. However, for grain length (Figure 5.8, D) differences were observed in two lines, with both lines 4.2 (p = 0.030, F-test = 5.66) and 4.6 (p = 0.011, F-test = 8.15) being shorter than their nulls. Taken together, these results show a slight reduction in grain yields in the different transgenic lines as three of the four lines displayed a reduction in the different yield variables measured. However, it should be noted that only one line (4.2) displayed a reduction in both the weight and size of the grains. These results indicate, although not very strongly, that the expression of the *AtGA20ox1* gene in the inner integument could be leading to a reduction in grain yields.

5.2.4.4 Analysis of *TaDFR-D::AtGA20ox1* effects on grain quality

To study the effect of expressing *AtGA20ox1* in the inner integument on grain quality, grain hardness and grain moisture content were assessed using the SKCS system, as described in section 2.4.1, and the data presented in figure 5.9 represents the average of three biological replicates for each line. For both grain hardness and moisture content the differences between the transgenic, null and wild type were assessed at the population level by ANOVA using LSD at 5%. For grain hardness no differences were observed between any of the three genotypes; however, differences were observed in grain moisture content with null grains showing a significant reduction in moisture content compared to both the wild type and the transgenics, which did not show any variance between genotypes.

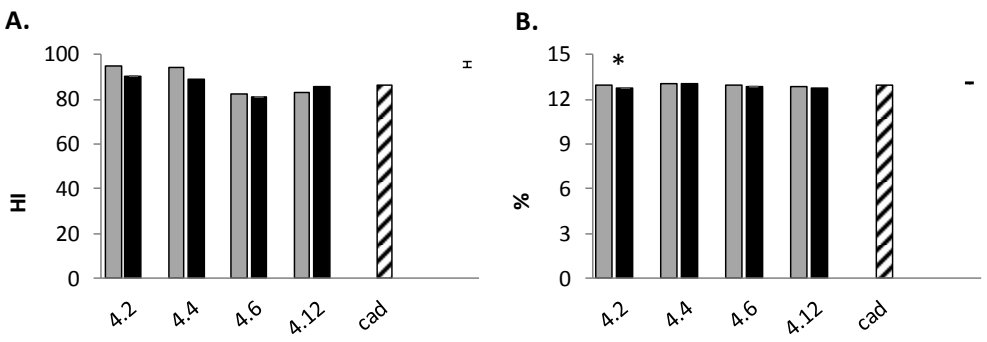


Figure 5.9: Analysis of quality components on *TaDFR-D::AtGA20ox1* transgenic lines

Averages are presented for: grain hardness (A) and moisture content (B) for measurements on mature grains. Grey bars – transgenic lines, black bars – null segregants and hatched bars – WT. * denotes significant difference between a transgenic and its null using LSD at 5%: p value at – *: ≤ 0.05. Vertical error bars denote SED on 1, 16 df.

The differences between the transgenics and their respective nulls for the individual lines were also analysed by ANOVA and grain hardness (Figure 5.9, A), showed no differences in any of the lines. However, the moisture content (Figure 5.9, B) in these lines whilst being in the normal range (11 -14%), showed a significant difference in line 4.2 ($p = 0.017$, F-test = 7.11) with the transgenics having higher moisture content than the null.

5.2.5 Analysis of *HvGerF::AtGA20ox1* and *TaDFR-D::AtGA20ox1* effects on grain development

Any potential effect on grain expansion of modifying GA biosynthesis in the pericarp and inner integument layers might have been obscured by analysing grain at maturity if grain size is limited by other factors such as grain filling. This was addressed by analysing the grain throughout development. Grains were harvested at 10, 20, 30, 40, 50 and 60 dpa (from ears two, three and four of two plants per replicate block) and assessed according to the method described in section 2.3 using the MARVIN digital seed counter as described in section 5.2.3.3. The data presented in this section is an average of three biological replicates for all lines except line 3.8 where only two replicates were available.

In order to analyse grain development and to account for the complex design of this experiment, in collaboration with a statistician – Dr Stephen Powers, a linear mixed model was fitted to the data using the method of residual maximal likelihood (REML) (section 2.6). During the course of this experiment it was observed that the transgenic plants harbouring the *HvGerF::AtGA20ox1* construct (section 5.2.3.3, Figure 5.4, A) had an unusually high number of aborted grains and the effects of reduced grain number on the remaining yield variables were also tested in this model. For the total number of grains ($p < 0.001$, F-test = 267.20) and weight ($p < 0.001$, F-test = 104.90) highly significant results were observed, and as can be expected for these variables the linear effect of the number of aborted seeds was important. However, no interactions related to the number of aborted seeds were observed for any of the other yield variables measured.

The linear mixed model fitted for average weight per grain ($p = 0.003$. F-test = 2.02) and average area per grain ($p = 0.005$, F-test = 1.92) revealed a significant interaction between line and time factors and a nonlinear model was fitted in order to extract more information than may be afforded by linear modelling.

An ad hoc model (Figure 5.10) was developed, based on the observation that both the increasing and decreasing weight followed a logistic trend.

$$y = \left(\frac{A}{(1 + e^{-B(t-M)})}\right)\left(\frac{1}{(1 + e^{C(t-N)})} + L\right)$$

Figure 5.10: Formula to fit nonlinear model

The formula for fitting nonlinear models of average weight and area per grain. y = average weight or area per grain; t = time in dpa; A = a shape parameter for growth; B = effective rate of growth; C = the effective rate of drying down; M = estimated time (dpa) to 50% of maxima; N = time to 50% of the decrease from maxima to final weight or area; L = a constant added to the second logistic.

The model was fitted using nonlinear least squares, to estimate parameters along with standard errors. A "parallel curves" analysis was then used to consider which of the parameters (A, B, C, M, N and L) were required to be estimated separately for each of the 17 lines in the experiment, thus allowing them to be compared as regards these parameters. The F-test was used to assess competing models, and forward selection of more complex models was used to build a parsimonious final model.

5.2.5.1 Average weight per grain

The parallel curves analysis of average weight per grain revealed that separate L (constant added to the second logistic) parameters ($F(16,278) = 27.03$, $p <$

0.001), followed by separate N (time to 50% of the decrease from maxima to final weight) ($F(16,262) = 2.58$, $p < 0.001$) parameters were significant in improving the overall fit. Following these parametric expansions, the shape parameter for growth – A, the effective rate of growth – B, the corresponding effective rate of drying down – C and the time to 50% of maximal weight – M, were all found to be not significantly different ($F(16,246) = 1.28$, $p = 0.210$; $F(16, 246) = 0.41$, $p = 0.979$; $F(16, 246) = 0.03$, $p = 0.989$, $F(16, 246) = 0.63$, $p = 0.858$, respectively) across the lines (Table 5.1). These results imply that there were differences in growth due to the differences seen in times to 50% of the decrease from maxima to final weight (N) and in the parameter (L) giving the final weight, whereas the rate of the growth up to the maximal average weight and then down from this were the same for all lines (Table 5.1). The estimated residual variance (s^2) from fitting the model was 0.00004717 on 262 df, and the estimated variance accounted for (R^2) by the model was 92.9%.

Table 5.1: Estimates of parameters of average weight per grain in *HvGerF::AtGA20ox1* and *TaDFR-D::AtGA20ox1* transgenic lines

Estimates of the parameters obtained from the nonlinear model for average weight per grain. Standard errors are given in parenthesis. 3; *HvGerF::AtGA20ox1* and 4; *TaDFR-D::AtGA20ox1*. T; transgenics and N; nulls.

Parameter / Line		*A*	*B*	*C*	*M*	*N*	*N* for T-N	*L*	*AL*[†]
3.2	**T**	0.04772 (0.00254)	0.12153 (0.00598)	0.89 (0.59)	16.256 (0.434)	49.21 (5.89)	0.25	1.2789 (0.0942)	0.06103 (0.00242)
	N					48.96 (7.72)		1.462 (0.100)	0.06979 (0.00241)
3.5	**T**					50.18 (1.37)	0.75	1.823 (0.118)	0.08701 (0.00245)
	N					49.43 (4.24)		1.514 (0.104)	0.07227 (0.00243)
3.8	**T**					42.60 (19.60)	-5.2	1.155 (0.104)	0.05511 (0.00317)
	N					47.80 (16.40)		1.463 (0.094)	0.06980 (0.00244)
3.9	**T**					48.00 (14.90)	-1.04	0.982 (0.078)	0.04684 (0.00241)
	N					49.04 (7.13)		1.296 (0.094)	0.06183 (0.00242)
4.2	**T**					48.24 (0.81)	-0.92	1.315 (0.098)	0.06274 (0.00246)
	N					49.16 (6.20)		1.315 (0.095)	0.06275 (0.00242)
4.4	**T**					49.37 (4.69)	0.14	1.187 (0.091)	0.05665 (0.00243)
	N					49.23 (5.73)		1.503 (0.103)	0.07170 (0.00242)
4.6	**T**					49.54 (3.44)	1.34	1.533 (0.105)	0.07315 (0.00243)
	N					48.20 (13.30)		1.647 (0.104)	0.07861 (0.00242)
4.12	**T**					49.88 (0.99)	0.31	1.532 (0.106)	0.07313 (0.00244)
	N					49.57 (3.19)		1.483 (0.103)	0.07075 (0.00243)
WT						50.79 (5.79)		1.585 (0.111)	0.07565 (0.00249)

[†]*Final Average weight per grain;*

The time taken to reach 50% of the decrease from maxima to final weight (N) showed a large variation among the lines with the wild-type taking the longest (50.79 dpa) and the transgenic line 3.8 the shortest (42.6 dpa) time. In plants harbouring the *HvGerF::AtGA20ox1* construct differences were seen between the transgenics and their nulls in three of the four lines. Whilst the transgenic line 3.5 displayed the longest time amongst all lines from this construct (50.18 dpa), this was only 0.75 days longer than its null. However, this did result in an increase in final grain weight (AL) in the transgenic line (0.08701 g) compared to its null (0.07565 g). In contrast to this the transgenics of lines 3.8 and 3.9 both took a shorter time to reach 50% of the decrease from maxima to final weight compared to their respective nulls, resulting in lower final weight in both transgenic lines (Table 5.1). These results emulate those seen for total yield measurements in section 5.2.3.3 (Figure 5.4).

However, in lines harbouring the *TaDFR-D::AtGA20ox1* construct the differences between the transgenics and their nulls in the time taken to reach 50% of the decrease from maxima to final weight did not display the same effects on final weight as those seen in the *HvGerF::AtGA20ox1* lines. Here the transgenic line 4.6 in spite of taking 1.34 days longer than its null to reach 50% of the decrease from maxima to final weight had slightly lower final weight. Whereas in line 4.4, both genotypes took approximately the same time to reach this stage, however the transgenics weighed substantially lower than the null (Table 5.1).

For each line, the time at which maximal weight is reached and its value were also obtained from the model (Table 5.2). The maximal weight per grain was compared to the final weight and as table 5.2 shows this difference was consistent for all the lines in the experiment. The differences between the time to maximal weight and time to reach 50% of the decrease from maxima to final weight were also consistent in these lines, implying that the rate of drying down was similar across all lines and the differences observed in final weight were possibly due to the differences in the time taken to reach maximal weight.

Table 5.2: Estimates of time to maximal weight per grain in *HvGerF::AtGA20ox1* and *TaDFR-D::AtGA20ox1* transgenic lines

The estimated time (t_{max}) at which maximal average weight per grain (y_{max}) is reached. The difference between maximum and final weight (y_{max} - AL) and time taken from maximal to 50% of final weight (N - t_{max}) are also shown. Standard errors are given in parenthesis. 3; *HvGerF::AtGA20ox1* and 4; *TaDFR-D::AtGA20ox1*. T; transgenics and N; nulls.

Parameter / Line		t_{max}	y_{max}	y_{max} - AL	N - t_{max}
3.2	**T**	44.1	0.10470 (0.01770)	0.04367	5.11
	N	43.9	0.11306 (0.01900)	0.04327	5.06
3.5	**T**	45.2	0.13031 (0.01625)	0.0433	4.98
	N	44.4	0.11568 (0.01799)	0.04341	5.03
3.8	**T**	38.2	0.09531 (0.01036)	0.0402	4.4
	N	42.9	0.11251 (0.02528)	0.04271	4.9
3.9	**T**	42.9	0.09051 (0.02109)	0.04367	5.1
	N	43.9	0.10540 (0.01774)	0.04357	5.14
4.2	**T**	43.2	0.10592 (0.01610)	0.04318	5.04
	N	44.1	0.10634 (0.01837)	0.04359	5.06
4.4	**T**	44.2	0.10053 (0.01647)	0.04388	5.17
	N	44.2	0.11504 (0.01864)	0.04334	5.03
4.6	**T**	44.5	0.11658 (0.01754)	0.04343	5.04
	N	43.4	0.12122 (0.02540)	0.04261	4.8
4.12	**T**	44.8	0.11671 (0.01604)	0.04358	5.08
	N	44.5	0.11426 (0.01703)	0.04351	5.07
WT		45.6	0.11953 (0.01252)	0.04388	5.19

The fitted curves for each construct are shown in figures 5.11 and 5.12 along with the plotted means (n = 3) for combinations of lines and time points. The strong growth in average weight per grain for transgenic line 3.5 can be seen in comparison to its null. The relatively quick growth of transgenic line 3.8 compared to its null and the rest of the lines can also be seen, resulting in much lower final weight. The curves indicate that the strength of the interaction seen between lines and time was largely due to the distinct trends shown by transgenic lines 3.5 and 3.8 (Figure 5.11) and the slight differences observed in the growth rates of the lines harbouring the *TaDFR-D::AtGA20ox1* construct compared to the wild-type (Figure 5.12).

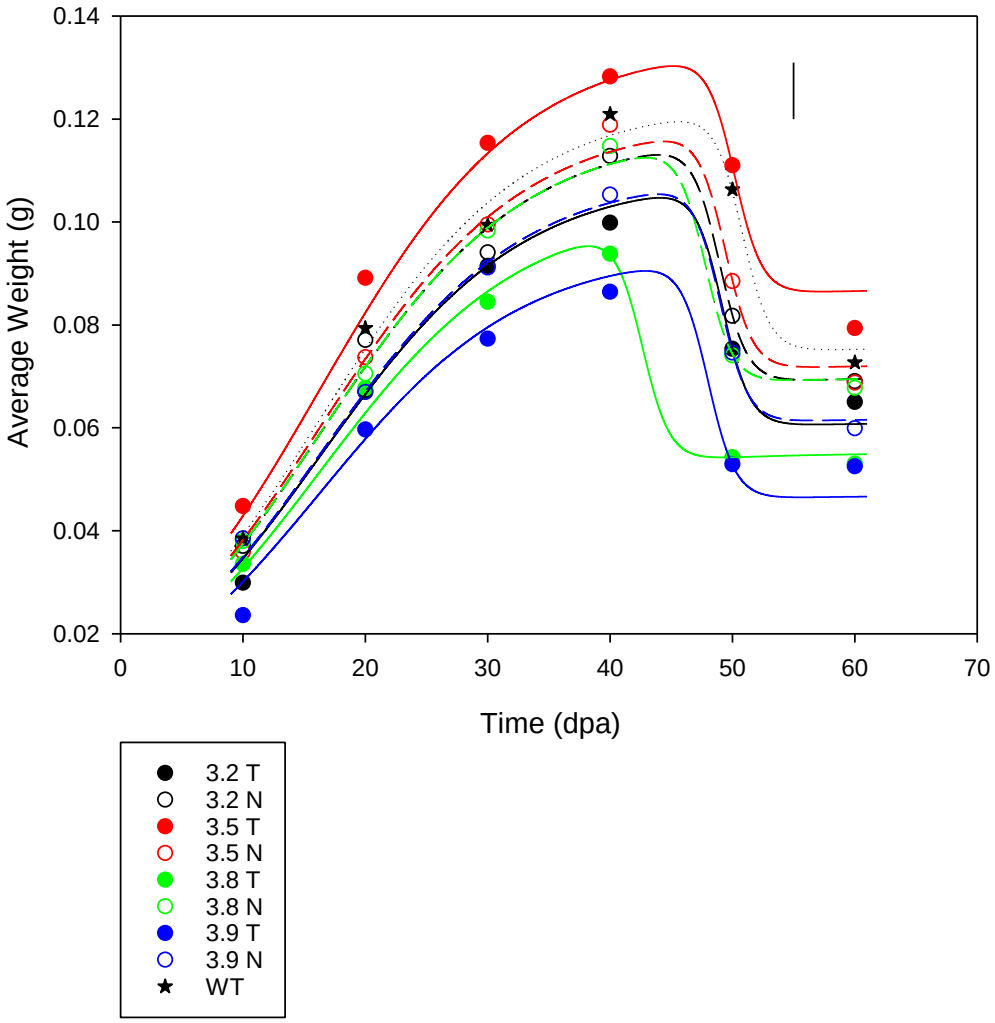


Figure 5.11: Fitted curves for average weight per grain of *HvGerF::AtGA20ox1* transgenic lines

The fitted curves with the plotted means (n = 3) for combinations of lines and time points. Vertical error bar represents LSD at the 5% (0.010971 on 193 df) for the comparison of the means between lines given the ANOVA. T; transgenics and N; nulls.

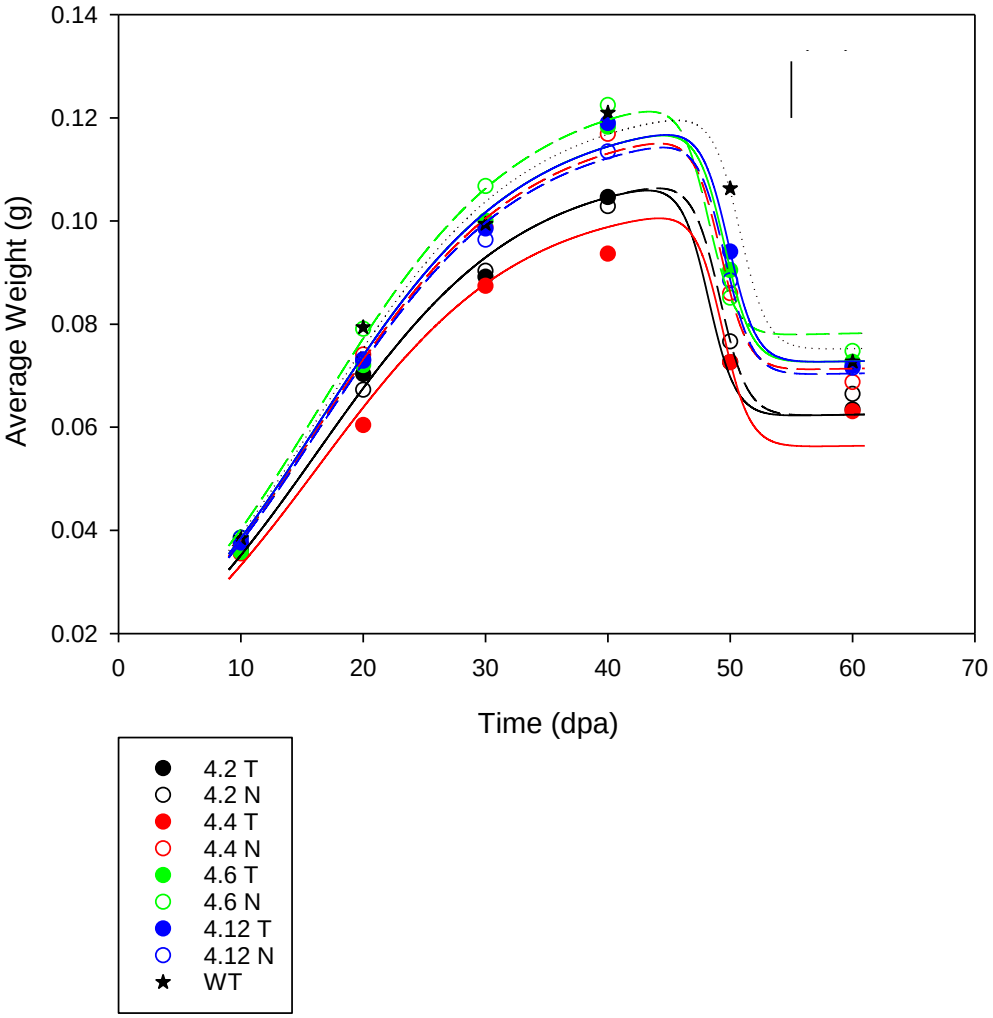


Figure 5.12: Fitted curves for average weight per grain of *TaDFR-D::AtGA20ox1* transgenic lines

The fitted curves with the plotted means (n = 3) for combinations of lines and time points. Vertical error bar represents LSD at the 5% (0.010971 on 193 df) for the comparison of the means between lines given the ANOVA. T; transgenics and N; nulls.

5.2.5.2 Average area per grain

The parallel curve analysis of average area per grain revealed that separate A (a shape parameter for growth) parameters ($F(16,278) = 21.19$, $p < 0.001$), followed by separate B (effective rate of growth) parameters ($F(16,262) = 3.62$, $p < 0.001$) were significant in improving the overall fit. Following these parametric expansions, the rate of drying down – C, the time to 50% of maximal area – M, time to 50% of the decrease from maximal to final area – N and the constant added to the second logistic – L were all found to be not significantly different ($F(16,246) = 1.64$, $p=0.057$; $F(16, 246) = 1.06$, $p = 0.385$; $F(16, 246) = 0.47$, $p = 0.960$, $F(16, 246) = 0.38$, $p = 0.986$, respectively) across the lines (Table 5.3). These results imply that the lines differed more in the rate of increase in average area per seed, with both A and B parameters being estimated as separate for the lines, rather than in the decrease in area through drying down, with C, M, N and L parameters being retained as common over the lines. The estimated residual variance (s^2) from fitting the model was 3.019 on 262 df, and the estimated variance accounted for (R^2) by the model was 89.9%.

Table 5.3: Estimates of parameters of average area per grain in *HvGerF::AtGA20ox1* and *TaDFR-D::AtGA20ox1* transgenic lines

Estimates of the parameters obtained from the nonlinear model for average area per grain. Standard errors are given in parenthesis. 3; *HvGerF::AtGA20ox1* and 4; *TaDFR-D::AtGA20ox1*. T; transgenics and N; nulls.

Parameter / Line		*A*	*B*	*C*	*M*	*N*	*L*	$AL^{\dagger}$	$AL^{\dagger}$ for T-N
3.2	**T**	11.686 (0.866)	0.1031 (0.0201)	0.400 (0.118)	6.195 (0.351)	48.49 (0.56)	1.952 (0.146)	22.813 (0.696)	-1.455
	N	12.431 (0.826)	0.1467 (0.0251)					24.268 (0.581)	
3.5	**T**	14.360 (1.020)	0.1090 (0.0177)					28.025 (0.685)	2.53
	N	13.059 (0.976)	0.0964 (0.0178)					25.495 (0.749)	
3.8	**T**	10.176 (0.680)	0.1796 (0.0437)					19.865 (0.607)	-4.171
	N	12.312 (0.853)	0.1245 (0.0219)					24.036 (0.616)	
3.9	**T**	10.207 (0.698)	0.1426 (0.0288)					19.927 (0.558)	-2.545
	N	11.511 (0.783)	0.1370 (0.0251)					22.472 (0.582)	
4.2	**T**	11.622 (0.780)	0.1445 (0.0261)					22.689 (0.573)	-0.601
	N	11.930 (0.850)	0.1150 (0.0212)					23.290 (0.641)	
4.4	**T**	11.839 (0.877)	0.1027 (0.0199)					23.113 (0.699)	-1.765
	N	12.743 (0.909)	0.1116 (0.0197)					24.878 (0.660)	
4.6	**T**	12.987 (0.997)	0.0902 (0.0173)					25.354 (0.802)	-0.082
	N	13.029 (0.909)	0.1191 (0.0202)					25.436 (0.637)	
4.12	**T**	13.100 (1.000)	0.0910 (0.0173)					25.568 (0.796)	0.978
	N	12.596 (0.923)	0.1034 (0.0190)					24.590 (0.700)	
WT		13.874 (0.981)	0.0826 (0.0150)					27.084 (0.943)	

†*Final Average area per grain;*

The average final area per grain (Table 5.3) also showed a large degree of variation amongst all lines with the transgenic line 3.5 having the highest (28.025 mm^2) and transgenic line 3.8 (19.865 mm^2) having the lowest area. In plants harbouring the *HvGerF::AtGA20ox1* construct differences were seen between the transgenics and their nulls in all four lines. Whilst the transgenic line 3.5 had a larger area than its null, corresponding with it being heavier (Table 5.1) the other three lines in this construct displayed the opposite result with all transgenics being smaller than their respective nulls. There were less substantial differences in average area per grain for the majority of lines harbouring the *TaDFR-D::AtGA20ox1* construct, except in line 4.4 where the transgenic grains were smaller than the nulls. This corresponded with the differences seen in grain weight in this line.

For each line, the time at which maximal area was reached and its value were also obtained from the model (Table 5.4). The maximal area per grain was compared to the final area per grain and as table 5.4 shows for the majority of lines this reduction in grain area was consistent. However, the transgenic lines 3.8 and 3.9 which had smaller final areas compared to their nulls also showed a lower reduction in size during drying down. In addition to that, the transgenic line 3.5 which had a larger area than its null showed a bigger reduction in grain size implying that these grains possibly displayed the capacity to expand their size, although they were unable to maintain this increase. Whilst accepting that two lines (3.8 and 3.9) show opposing results to line 3.5 – which displayed the highest expression of the *AtGA20x1* transgene amongst these lines (Figure 5.3), there is a possibility that the expression of this gene in the pericarp and inner integument layers could lead to an increase in the size of the grain. The lines harbouring the *TaDFR-D::AtGA20ox1* construct did not display any substantial differences in grain size between the various transgenics and their nulls.

Table 5.4: Estimates of time to maximal size per grain in *HvGerF::AtGA20ox1* and *TaDFR-D::AtGA20ox1* transgenic lines

The estimated time (t_{max}) at which maximal average area per grain (y_{max}) is reached. The difference between maximum and final area (y_{max} - AL) is also shown. Standard errors are given in parenthesis. 3; *HvGerF::AtGA20ox1* and 4; *TaDFR-D::AtGA20ox1*. T; transgenics and N; nulls.

Line \ Parameter		t_{max}	y_{max}	y_{max} - AL
3.2	**T**	39.3	33.120 (0.550)	10.307
	N	37.3	36.181 (0.607)	11.913
3.5	**T**	39.0	40.919 (0.567)	12.894
	N	39.6	36.724 (0.551)	11.229
3.8	**T**	35.9	29.831 (0.728)	9.966
	N	38.3	35.489 (0.579)	11.453
3.9	**T**	37.5	29.667 (0.589)	9.74
	N	37.7	33.384 (0.591)	10.912
4.2	**T**	37.4	33.802 (0.600)	11.113
	N	38.7	34.172 (0.564)	10.882
4.4	**T**	39.3	33.538 (0.550)	10.425
	N	38.9	36.406 (0.564)	11.528
4.6	**T**	39.9	36.205 (0.551)	10.851
	N	38.5	37.430 (0.575)	11.994
4.12	**T**	39.6	36.552 (0.549)	10.984
	N	39.3	35.708 (0.554)	11.118
WT		40.2	38.168 (0.644)	11.084

The fitted curves for each construct are shown in figures 5.13 and 5.14 along with the plotted means (n = 3) for combinations of lines and time points. The differences seen in the rate of increase in area in the various lines harbouring the *HvGerF::AtGA20ox1* construct compared to their nulls and the wild-type

can be seen in these curves (Figure 5.13). The curves also indicate that there were only slight differences in the growth rates of the lines harbouring the *TaDFR-D::AtGA20ox1* construct compared to the wild-type (Figure 5.14).

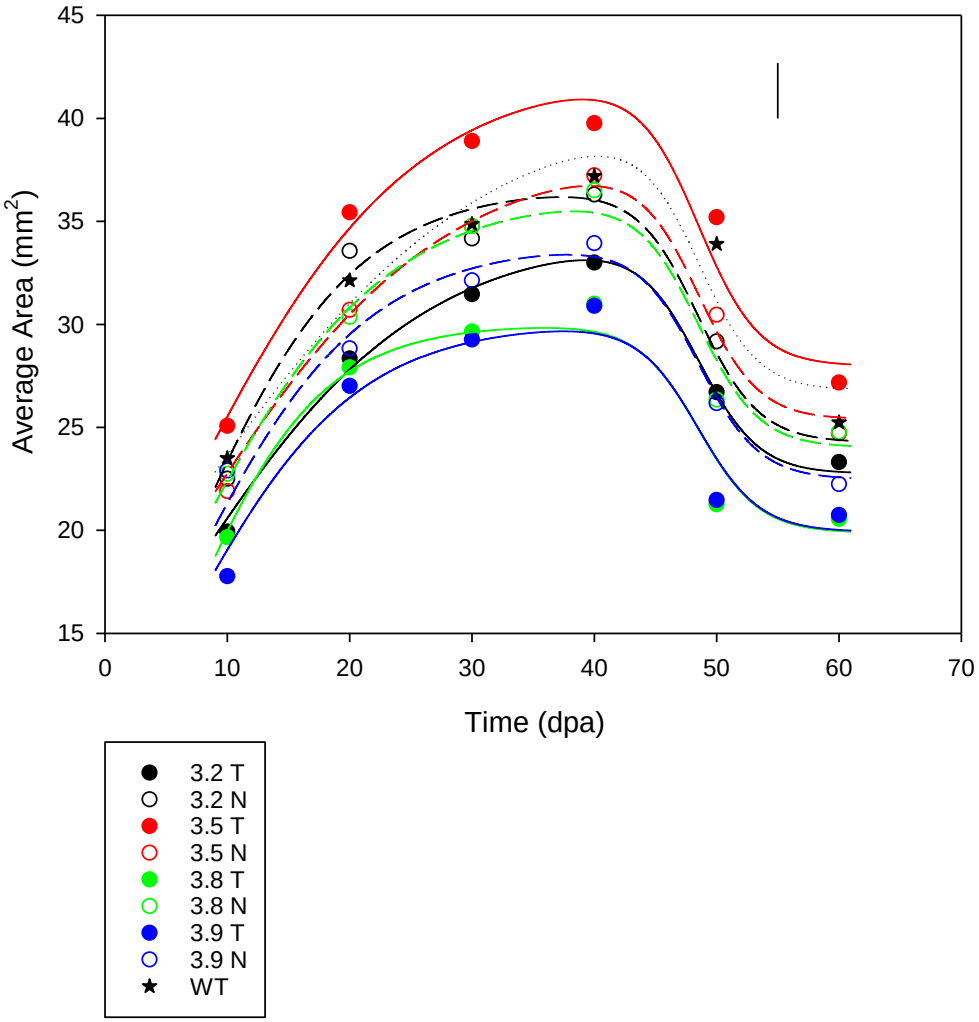


Figure 5.13: Fitted curves for average area per grain of *HvGerF::AtGA20ox1* transgenic lines

The fitted curves with the plotted means (n = 3) for combinations of lines and time points. Vertical error bar represents LSD at the 5% (2.6889 on 180 df) for the comparison of the means between lines given the ANOVA. T; transgenics and N; nulls.

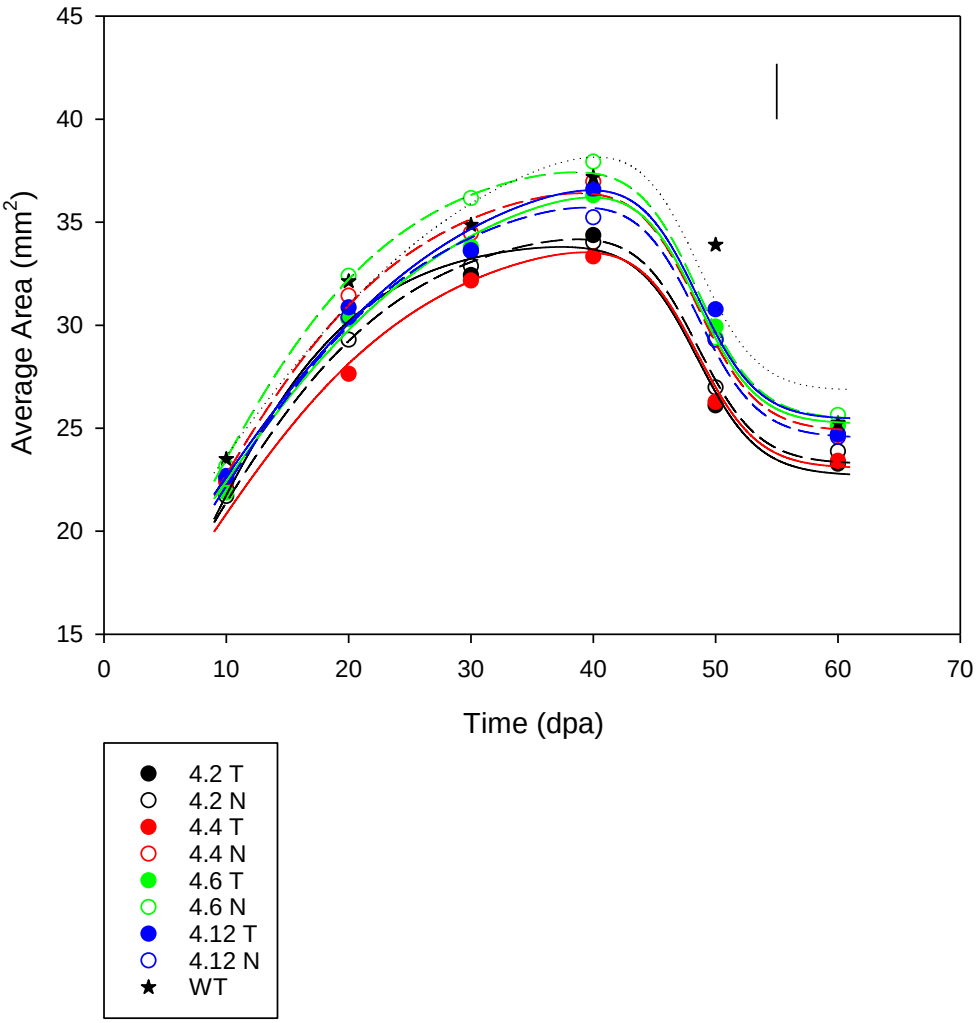


Figure 5.14: Fitted curves for average area per grain of *TaDFR-D::AtGA20ox1* transgenic lines

The fitted curves with the plotted means (n = 3) for combinations of lines and time points. Vertical error bar represents LSD at the 5% (2.6889 on 180 df) for the comparison of the means between lines given the ANOVA. T; transgenics and N; nulls.

The modelling also showed that the average time between reaching the peak in area per seed and the peak in weight per seed to be 4.6 - 6.6 days for the majority of lines studied except for line 3.8 which also displayed reduced yield and high number of aborted grains. This line displayed only 2.3 days between these two stages resulting in a shorter grain filling period again indicating other factors being involved in the reduction of yield in this line.

5.3 Conclusions

The work described in this chapter examined the effects of expressing the *AtGA20ox1* gene in the pericarp and inner integument layers of the grain using two promoters, *HvGerF* and *TaDFR-D*. This work was carried out to determine if the seed coat layers restrict grain size and if expressing a GA biosynthetic gene in these tissues results in the production of larger grain. However, no clear conclusions could be made regarding this. In plants harbouring the *HvGerF::AtGA20ox1* construct whilst three of the four transgenic lines displayed a yield phenotype, they showed contrasting results. Two of these lines showed a reduction in both weight and grain size; however, one of these lines also had an unusually high number of aborted grains. We know from previous work that a reduction in grain number can lead to an increase in size due to the extra resources available to the remaining grains. Since the line in this experiment does not display this phenotype it implies that there might be other factors affecting the health of these plants, which also resulted in the death of two plants in a replicate block. In contrast the plants harbouring the *TaDFR-D::AtGA20ox1* construct did not show any substantial differences in grain yield. Whilst reduction in some yield variables was observed in the transgenics of three of the lines, this was only weakly significant.

The growth of these grains was also studied during development in order to test if any potential effect on grain expansion of modifying GA biosynthesis in these tissues might have been lost at maturity due to other factors such as unavailability of extra resources. For plants transformed with construct *HvGerF::AtGA20ox1*, the line showing increased yield compared to its null, took a longer time to reach 50% of its final weight, whereas the lines showing a reduction in weight took a shorter time compared to their respective nulls. These two lines also had the lower maximum weight during development and took fewer days to reach it, whereas the line with increased yield had higher maximum weight and took longer to reach it, when compared to each of their

nulls. The plants transformed with the *TaDFR-D::AtGA20ox1* construct when studied during development did not display any substantial differences among the lines, except in one case where the transgenic took a longer time than its null to reach both its maximal and 50% of final weight, but this did not result in an increase in final or maximal weights.

The measurements for grain size also displayed similar results with the plants in both constructs following the same pattern as for grain weight. The higher yielding *HvGerF::AtGA20ox1* line also displayed the bigger grain area, and those lines with low yield had smaller grain areas. These lines also displayed a difference in the grain size reduction from maximum to final with the smaller grains showing a smaller reduction, and the grains in the line with increased yield showing a larger reduction in size between these two stages. For plants transformed with *TaDFR-D::AtGA20ox1* there were less substantial differences in this parameter, with only one line showing a significantly smaller size compared to its null and showing a smaller reduction in size from maximum to final.

The consistency in the grain filling period in the majority of the lines of both constructs indicates that the differences seen in the rate of increase in area and days taken to reach the 50% of the decrease from maxima to final weight could possibly be the main factors contributing to the differences seen in yields. These results indicate that the grains that took longer to reach their maximal weight displayed a different growth pattern and were able to expand for a longer time thus resulting in an increase in final size and weight. However, the line which showed the maximum yield whilst taking the longest to reach both maximal and final weights, also showed the biggest reduction in grain size from maximum to final implying that final yield may be limited by lack of source inputs.

However, based on the results from these two constructs it is difficult to make definite conclusions about the role of GA in the seed coat layers and its effects on grain size and development.

Chapter 6. The effect of manipulating GA in the endosperm of developing wheat grain

6.1 Introduction

In grasses the endosperm is a persistent seed structure mainly comprising of starch and forms the majority of the mature seed, which is in contrast to many species including *Arabidopsis* (Sabelli and Larkins, 2009). In the mature endosperm starch granules are embedded in a matrix of storage proteins and these provide nutrition to the germinating embryo, and developing seedling, following hydrolysis by enzymes such as α-amylase (Olsen *et al.*, 1999, Evers and Millar, 2002).

An efficient system of assimilate transfer from vegetative tissues into seeds is an important determinant of yield and in grasses this system is facilitated by the Endosperm transfer cells (ETC) – a modified part of the aleurone layer that differentiates prior to endosperm cellularisation (Sabelli and Larkins, 2009, Thiel, 2014). The ETC are adapted for transport of solutes, mainly sucrose and amino acids to the developing seed and their main distinguishing feature is the presence of extensive cell wall ingrowths to increase the surface of plasma membrane available for transport (Pate and Gunning, 1972, Thompson *et al.*, 2001). In barley and wheat, ETCs are located along the crease and allow the rapid transport of solutes at symplastic/apoplastic bottlenecks such as the interface between maternal vascular tissue and the endosperm (Offler *et al.*, 2003).

There is available evidence that GA is synthesised in the endosperm of several plant species and it was first reported that the endosperm of *Marah macrocarpus* contains high amounts of bioactive GA-like compounds (Corcoran and Phinney, 1962). The early GA biosynthetic enzymes CPS and KS were first identified in extracts from the endosperm and embryo of *Marah macrocarpus*

(MacMillan *et al.*, 1997) and KS and GA 20-oxidase were extracted from the endosperm of pumpkin (Lange, 1994, Saito *et al.*, 1995). The presence of bioactive GAs in the endosperm of young pea seeds (Rodrigo *et al.*, 1997) and the expression of early GA biosynthesis genes and *TaGA3ox1* in the endosperm of developing wheat grain (Pearce *et al.*, 2015) also provide evidence that GA biosynthesis occurs in this tissue.

Work in our laboratory has shown that decreasing the level of GA in the endosperm throughout grain development can decrease the α-amylase content of the grain, improving flour quality, but also that this can have negative impacts on grain size (Vaughan, S. unpublished data). Our hypothesis was that by using a promoter which is active only late in grain development to decrease the amount of GA we may be able to improve grain quality without impacting grain size. For this study the wheat *Tritin* promoter (*TaTri*) was chosen to test this hypothesis as it does not display activity until approximately 25 dpa.

Tritin belongs to the ribosome-inactivating protein (RIP) family, members of which are toxic proteins that catalytically inactivate prokaryotic or eukaryotic ribosomes (Bass *et al.*, 1992, Dang and Van Damme, 2015). They mainly function as *N*-glycosidases to remove a specific adenine residue from a universally conserved sarcin/ricin loop in 23S/25S/28S rRNA (Endo *et al.*, 1987, de Virgilio *et al.*, 2010). Tritin is a Type I RIP present in wheat seeds and was first identified as a component of a wheat-germ protein-synthesising system that caused inhibition of protein synthesis in an ascites cell-free system (Stewart *et al.*, 1977). The *Tritin* gene first isolated from wheat by Habuka *et al*., (1993) consisted of a 5' UTR sequence (991 bp), an open reading frame (828 bp) and 3' UTR sequence (431 bp). This gene showed 88% homology (Habuka *et al.*, 1993) to barley RIP gene which is known to accumulate in the starchy endosperm during late seed development (Leah *et al.*, 1991). The 5' UTR sequence along with several TATA boxes also contained three sequences that were homologous to the binding sequence of the maize transcriptional

activator protein, Opaque-2. This gene is thought to activate the expression of maize RIP, thus a similar DNA-binding protein may also control the expression of the *Tritin* gene (Habuka *et al.*, 1993). These authors also confirmed a previous report by Reisbig and Bruland (1983) that wheat has three *Tritin* genes. Altenbach and Kothari (2004) studied transcripts of wheat endosperm genes under different temperature regimes and found differences in the expression pattern of *Tritin*. They found that under 24/17^{o}C temperature regime this gene is expressed at 28 and 34 dpa, whereas under 37/28^{o}C regime it is expressed as early as 8 dpa. *Tritin* has also been shown to be expressed during late stage of senescence of wheat coleoptiles and may be involved in programme cell death (Sawasaki *et al.*, 2008). For this study the *TaTri* promoter was isolated using genome walking from wheat cv. Cadenza. This generated a single 1769 bp fragment which represented 401 bp of CDS and 1368 bp of 5' UTR. The CDS matched the *TaTri* sequence previously identified by Habuka *et al*. (1993) (D13795), except for one base, which did not result in an amino acid substitution. In the 5' UTR, the first 988 bp also displayed 99.3% identity to this previously published sequence. Along with this, an additional 380 bp was isolated, resulting in a 1368 bp promoter. This extended and verified sequence, based on a single fragment and sequenced in both directions, was submitted to Genbank under the accession HM564397 and is the source of the *TaTri* promoter used in this study. Promoter activity was studied during grain development in our laboratory using three independent lines harbouring the *TaTri* promoter directing nuclear-targeted GFP expression (Figure 1.15). This promoter was found to be highly active in the endosperm in all lines examined from 25 dpa onwards through to maturity. No promoter activity was observed in any non-target tissues examined.

We also hypothesised that conferring GA increase and GA insensitivity specifically in the endosperm transfer layer would enable us to examine the role of this tissue in grain development and its role in determining grain yield and quality. For this study the wheat *Endosperm 1* (*TaEND1*) promoter was selected for this purpose. The *END1* gene encodes a non-specific lipid transfer

protein and was first identified in barley ETC (Doan *et al.*, 1996, Lopato *et al.*, 2014). *In situ* hybridization studies performed by Doan *et al*. (1996) showed the expression of the barley *END1* to be only in the coenocyte above the nucellar projection during the free-nuclear stage of endosperm development. Once cellularization is complete, *END1* was shown to accumulate in the endosperm transfer cells and a few layers of ventral starchy endosperm. Using northern blot hybridization these authors also observed *END1* transcripts from 5-30 dpa in the grain, with it increasing from 5 dpa to 8 dpa, remaining steady between 8-25 dpa and decreasing from 25- to 30 dpa. Drea *et al*. (2005) performed similar studies on the *END1* orthologue from wheat and showed that its expression matched that shown in barley. Li *et al*. (2008) cloned a homologue of the wheat *END1*, *TaPR60* and showed it to accumulate in the developing grain from the end of cellularization till maturity. They also studied the promoter of a rice orthologue (*OsPR602*) and showed that in rice promoter activity was observed in the ETC, the starchy endosperm and in the maternal vascular tissue adjacent to the ETC and vascular tissue of the lemma and palea. However, in barley the activity of this promoter was restricted to the ETC and adjacent layers of the starchy endosperm, matching the expression of *END1* shown by Doan *et al*. (1996). An orthologue of *TaPR60* from *Triticum durum* (*TdPR60*) was transformed into wheat, barley and rice with a gene promoter:GUS fusion. While in wheat and barley the expression of this construct was restricted to the endosperm transfer layer, in rice expression was seen in the starchy endosperm during early grain filling (Kovalchuk *et al.*, 2009). These authors were unable to identify any identical or near identical *cis*-elements in the *TaPR60* and *OsPR602* promoters. The *TaEND1* promoter used in this study was isolated from a vector supplied by John Doan (James Hutton Institute, UK) under an MTA and its activity was further studied during grain development in our lab. This was done using nine independent lines harbouring 2143 bp of the promoter directing nuclear targeted GFP expression (Figure 1.15). GFP activity was observed only in the ETC from 7 dpa to 40 dpa. No GFP was observed in any non-target tissues examined.

For this study the expression of a GA inactivating gene from bean (*PcGA2ox1*) was driven by the *TaTri* promoter (Figure 6.1, A) to decrease the amount of GA in developing grains to improve grain quality without impacting grain size. In addition, in the endosperm transfer layer the *Atgai* gene was expressed to help understand the role of GA signalling in the developing grain, while the GA biosynthesis gene (*AtGA20ox1*) was expressed to increase the level of GA and determine if this increase enhances grain size, using the *TaEND1* promoter (Figure 6.1, B and C).

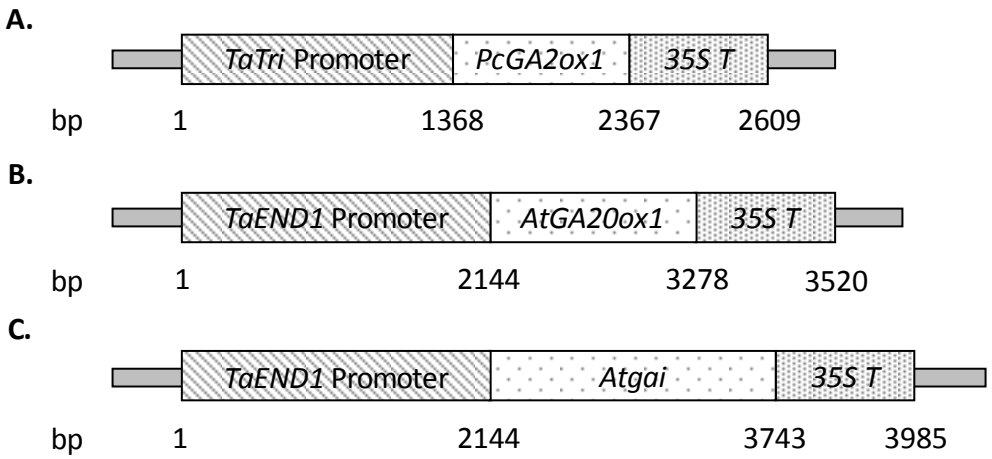


Figure 6.1: Basic structure of *TaTri::PcGA2ox1, TaEND1::AtGA20ox1* and *TaEND1::Atgai*

Basic structure of constructs *TaTri::PcGA2ox1* (A)*, TaEND1::AtGA20ox1* (B) and *TaEND1::Atgai* (C). The position of junctions between elements is given in base pairs (bp). The CaMV35S terminator is labelled 35S T.

6.2 Results and discussion

6.2.1 Production of homozygous material

To select homozygous material for this study 24 T1 plants from five lines of *TaTri::PcGA2ox1*, six lines of *TaEND1::AtGA20ox1* and four lines of *TaEND1::Atgai* were genotyped as described in Chapter 3. TaqMan assays (section 2.2.3) were performed on T1 plants of *TaTri::PcGA2ox1* using forward primer Q_Pc2ox-F, reverse primer Q_Pc2ox-R and hybridization probe Q_Pc2ox-probe (Appendix 1). The same analysis was also performed on T1 plants of *TaEND1::AtGA20ox1* using forward primer Q_At20ox-F, reverse primer Q_At20ox-R and hybridization probe Q_At20ox-probe (Appendix 1) and on T1 plants of *TaEND1::Atgai* using forward primer Q_GAI-F, reverse primer Q_GAI-R and hybridization probe Q_GAI-probe (Appendix 1). For all constructs, three plants were chosen from each independent line as potential homozygotes. The T2 progenies of the plants harbouring construct *TaTri::PcGA2ox1* were analysed by PCR (section 2.2.2) using forward primer Tri-F and reverse primer 2ox-R (Appendix 1). As discussed in chapter 3, for this construct homozygous T2 plants were identified in four of the five lines tested, and two of these lines were confirmed by southern analysis (section 2.3.8) to be clonal. An experiment was performed on the remaining three independent lines with three biological replicates each.

The T2 progenies of *TaEND1::AtGA20ox1* were also analysed by PCR, using forward primer END1-F and reverse primer 20ox-R (Appendix 1), and homozygous plants identified in five of the six lines tested. Homozygous T2 plants were selected from four of these lines and an experiment performed with three biological replicates for each line. The same analysis was also performed on T2 *TaEND1::Atgai* transgenic lines, using forward primer END1-F and reverse primer Gai-R (Appendix 1), and homozygous material identified in three of the four lines tested. For this construct the experiment was set-up using all four independent lines though one of them (line 11.7) was

hemizygous. Whilst for this line only positive plants were chosen for this study it is possible that they were still hemizygous and some of the grains harvested were negative for the transgene and subsequent data should be viewed with this in mind.

6.2.2 Experimental design

6.2.2.1 *TaTri::PcGA2ox1*

Grain yield and quality studies were performed to examine the effects of expressing the *PcGA2ox1* gene in the endosperm of the grain using transgenic wheat lines harbouring the *TaTri::PcGA2ox1* construct generated as described in section 2.1. A single RCBD experiment was setup as described in section 2.1.1 with three replicates of each line. In this experiment single plants were grown in 15-cm pots and cut back to five tillers per plant. From ears four and five; grains were harvested at maturity to measure yield and analyse various quality parameters. Grains from ears two and three were harvested at 35 and 49 dpa, respectively, to measure transcript levels and grains from ear one were harvested at three time points (14, 35 and 42 dpa – four grains each) to visualise GFP (section 2.7) to confirm promoter activity.

6.2.2.2 *TaEND1::AtGA20ox1* and *TaEND1::Atgai*

The effects of GA increase and insensitivity in the endosperm transfer layer were examined through an extensive yield and development study using transgenic wheat lines harbouring the *TaEND1::AtGA20ox1* and *TaEND1::Atgai* constructs generated as described in section 2.1. A single RCBD experiment was set-up as described in section 2.1.1 with three replicates of four independent lines of each construct. In this experiment six plants were grown per line in each replicate block with two plants in a 20-cm pot and each plant cut back to five tillers. Of the six plants in each replicate, plant one was used for development

studies, plants two and six for yield and quality analysis and plants three, four and five for GA hormone analysis. For the development studies from plant one, grains were harvest at two time points (14 and 28 dpa – four grains each) to visualise GFP (section 2.7) to study promoter activity. From ears two, three and four of plant one, grains were harvested at 14 and 28 dpa to measure various transcript levels. In each replicate the grains at the two time points were harvested from a different ear; replicate one: 14 dpa – ear two, 28 dpa – ear three; replicate two: 14 dpa – ear three, 28 dpa – ear four: replicate three: 14 dpa – ear four, 28 dpa – ear two. From plants two and six all grains were harvested for yield and quality analysis. For hormone measurements, grains were harvested at 28 dpa from ears two and three of plants three, four and five and the samples pooled for each replicate.

6.2.3 GFP visualisation of promoter activity

6.2.3.1 *TaTri* activity

GFP was examined in grains at 14, 35 and 42 dpa as described in section 2.7. These three time points were chosen to confirm the earlier studies in our laboratory which showed promoter activity beginning at 25 dpa. Whilst GFP was not visible in any tissues of the grain at 14 dpa, it was present in the starchy endosperm at both 35 (Figure 6.2) and 42 dpa. Promoter activity was further studied in germinating grain for all lines studied and no GFP was observed in any grain tissues from 24 hours after imbibition up to four days post germination.

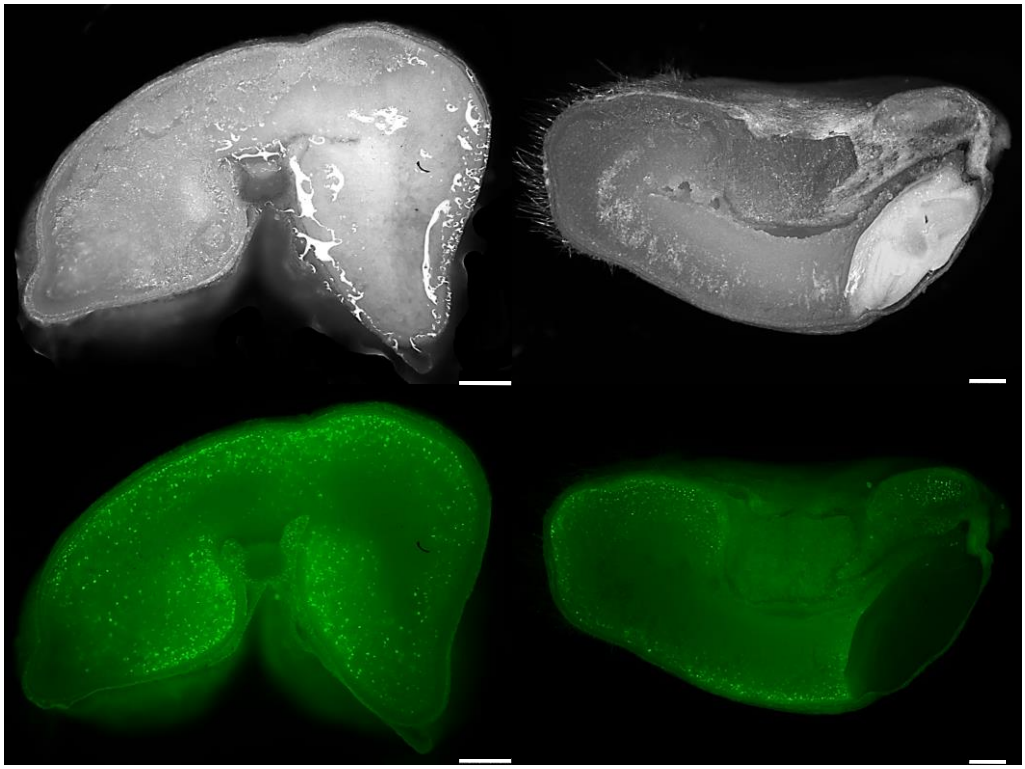


Figure 6.2: Activity of endosperm specific promoter in wheat grain
Transverse and longitudinal sections highlighting the endosperm are presented in bright field (top panel) and under a GFP filter set (excitation/ emission) (bottom panel) at 35 dpa for typical transgenic lines harbouring GFP under control of the wheat *TaTri* promoter. Scale bars represent 500µm for each image.

6.2.3.2 *TaEND1* activity

GFP was examined in grains at 14 and 28 dpa as described in section 2.7. These two time points were chosen to confirm the earlier studies in our laboratory which showed promoter activity from seven to 40 dpa. Whilst GFP was visible in the ETC cells at both 14 and 28 dpa, no other obvious morphological effects were observed in this tissue for either construct (Figure 6.3). Promoter activity was further studied in germinating grain for all lines studied and no GFP was observed in any grain tissues from 24 hours after imbibition up to four days post germination.

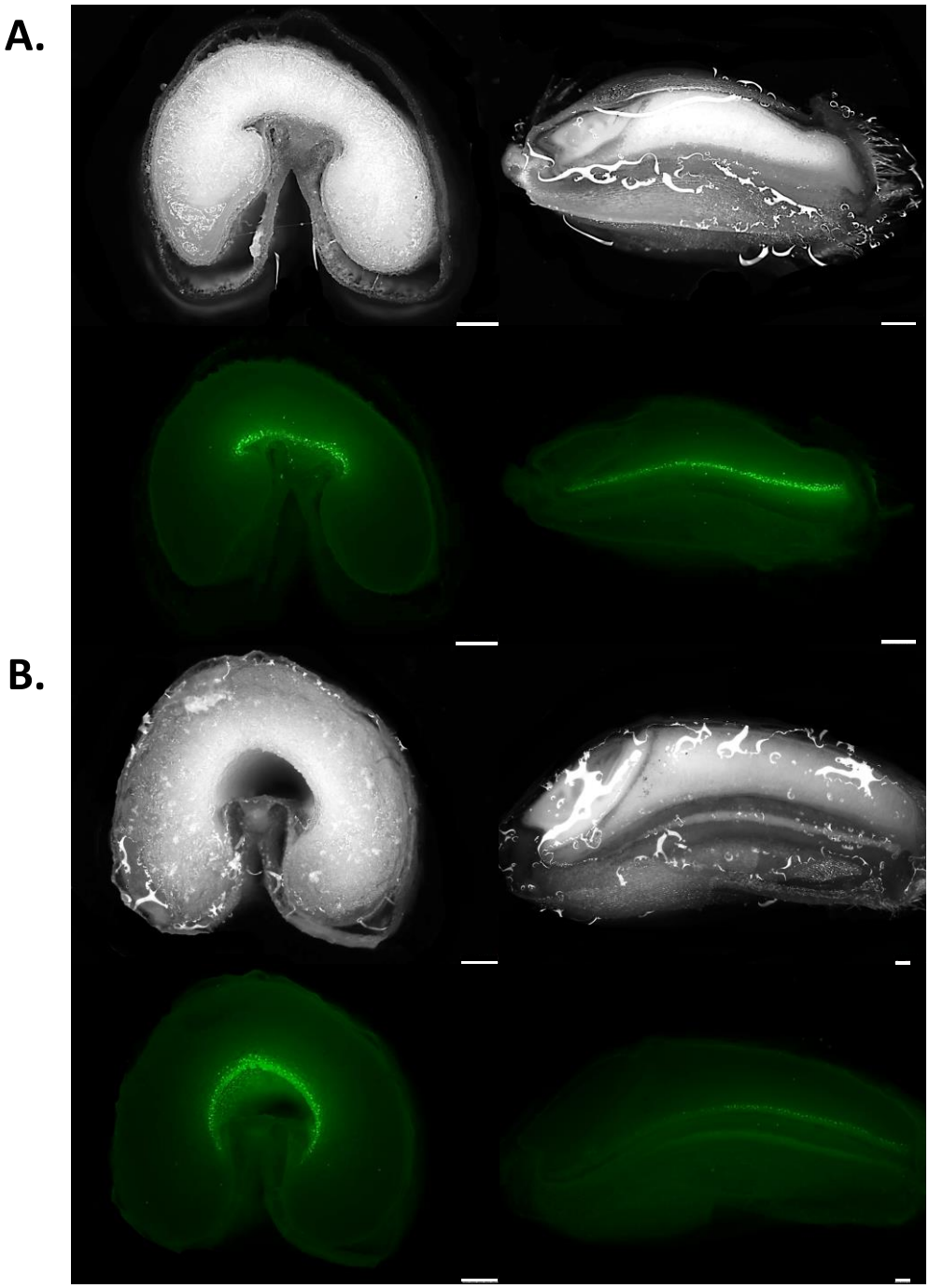


Figure 6.3: Activity of endosperm transfer layer specific promoter in wheat grain

Transverse and longitudinal sections highlighting the endosperm transfer layer are presented in bright field (top panel) and under a GFP filter set (excitation/ emission) (bottom panel) at 14 dpa (A) and 28 dpa (B) for typical transgenic lines harbouring GFP under control of the wheat *TaEND1* promoter. Scale bars represent 500µm for each image.

6.2.4 Analysis of transgenic lines expressing the *PcGA2ox1* gene under control of the endosperm-specific *TaTri* promoter

6.2.4.1 *TaTri::PcGA2ox1* transgene expression

To confirm expression of the introduced transgene, transcript levels of the *PcGA2ox1* gene were measured in cDNA synthesised (section 2.2.6) from RNA extracted as described in sections 2.2.4 and 2.2.5 from 35 and 49 dpa grains. These grains were harvested from ears two and three, respectively, from three biological replicates from each of the three independent lines in the experiment and their respective nulls and the wild-type control. The qRT-PCR was performed on this material according to section 2.2.7 using forward primer Q_Pc2ox-F and reverse primer Q_Pc2ox-R (Appendix 1). The expression of the transgene (Figure 6.4, A and B) was normalised against the expression of two endogenous genes – *Ta2526* and *TaGapDH* (section 2.2.7 and appendix 1). The data presented in figure 6.4 is an average of the NRQs of three biological replicates for each line at both time points. The qRT-PCR was performed on all plants in the experiment, including the null and wild type plants as controls. No expression of the transgene was observed in any of the controls (including the NRT controls) and, as such, these are excluded from the figures presented.

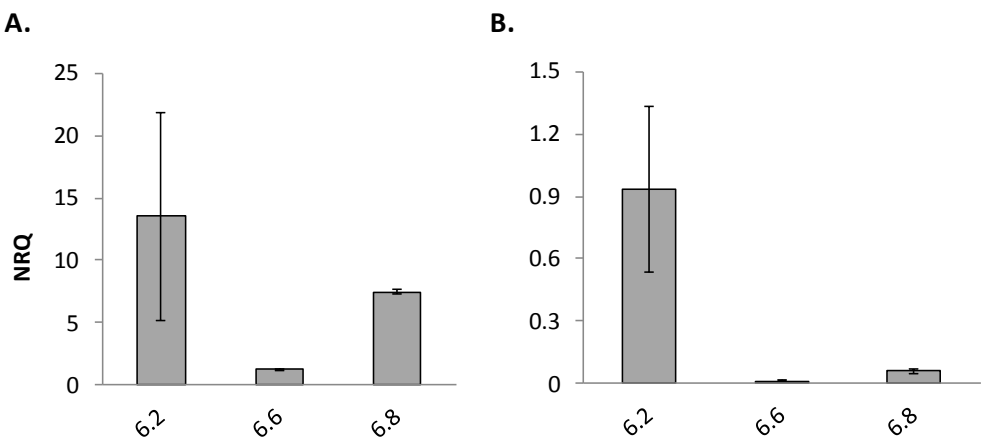


Figure 6.4: NRQs of *PcGA2ox1* gene in *TaTri::PcGA2ox1* transgenic lines
Average of normalised expression levels of the *PcGA2ox1* in 35 dpa (A) and 49 dpa (B) grain as measured in three biological replicates for each transgenic line. Vertical error bars denote SEM.

The expression of the *PcGA2ox1* transgene showed a large degree of variation between the three independent lines at both time points studied (Figure 6.4, A and B). At 35 dpa, there were up to 10-fold differences between lines, with line 6.2 displaying amongst the highest transgene expression observed in this project (Figure 6.4, A). At 49 dpa, whilst still detectable, the expression levels of the transgene saw a 15- to 124-fold reduction compared to 35 dpa (Figure 6.4, B) with line 6.8 showing the biggest decrease. At both time points the highest level of transgene expression was seen in line 6.2 and the lowest in line 6.6.

6.2.4.2 Analysis of *TaTri::PcGA2ox1* effects on yield

To study effects of expressing *PcGA2ox1* gene in the endosperm on grain yield, mature grains harvested from two ears (taken as a standardised proxy for total yield) of each plant was assessed according to the methods described in sections 2.3. The MARVIN digital seed counter was used to count the number of grains and measure their surface area, length and width. These grains were then weighed to calculate TGW. The data presented in figure 6.5 shows the

average values for three biological replicates of each line except the null plants of line 6.8. In this line one replicate did not produce enough grains to enable robust data analysis and was therefore excluded from further analysis. For all of the yield variables measured the difference between the transgenic, null and wild type was assessed at the population level using ANOVA. Using LSD at 5%, no significant differences were observed between the three genotypes for any of the yield parameters measured. This result agrees with the hypothesis that GA reduction in the endosperm late in grain development would not have a significant effect on grain yield.

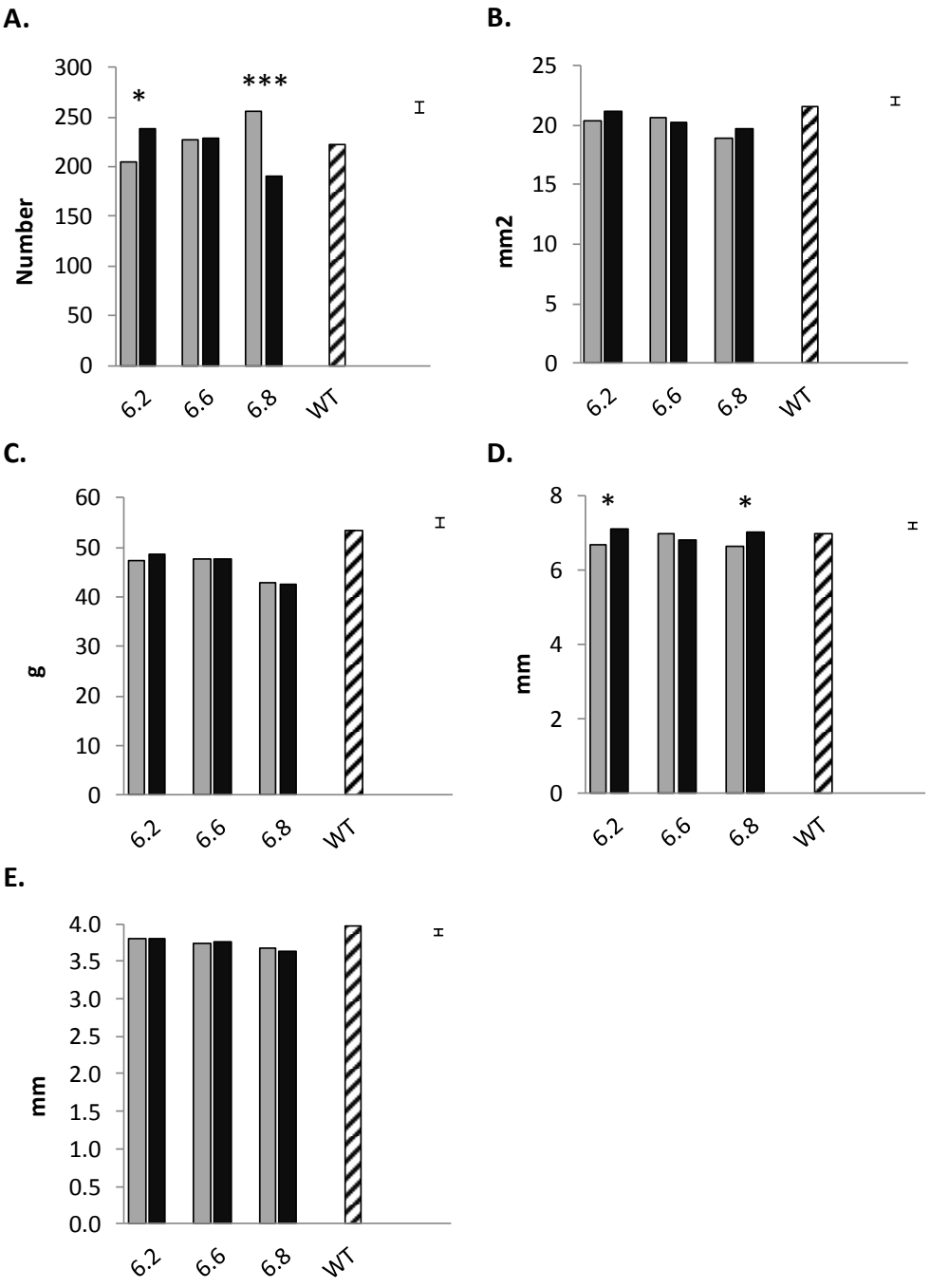


Figure 6.5: Analysis of yield components in *TaTri::PcGA2ox1* transgenic lines

Averages are presented for several variables: grain number (A), grain surface area (B), TGW (C), grain length (D) and grain width (E) for measurements on mature grains. Grey bars – transgenic lines, black bars – null segregants and hatched bars – WT. * denotes significant difference between a transgenic and its null using LSD at 5%: p value at – *: ≤ 0.05 and ***: ≤ 0.001. Vertical error bars denote SED on 1, 11 df.

The differences between the transgenic lines and their respective nulls were also analysed using ANOVA. Grain number was highly variable in this experiment, from a low of 190.7 in nulls of line 6.8 to a high of 256.7 in transgenics also of line 6.8 (Figure 6.5, A). This difference in grain number in this line was statistically significant using LSD at 5% ($p < 0.001$, F-test = 26.07). Whilst line 6.6 did not show any differences between the null and transgenic lines, in line 6.2 the pattern was reversed and the transgenic plants had fewer grains than their nulls ($p = 0.02$, F-test = 7.34). This contrasting result for grain number in two out of three lines, both of which strongly express the transgene, suggests that that the expression of *TaTri::PcGA2ox1* may not be the primary cause of these results. The average TGW also showed a wide range from a low of 42.4 g (null, line 6.8) to a high of 53.26 g (wild type). However, no significant differences were observed between the transgenics and nulls in any of the lines (Figure 6.5, C). Likewise, measurements of grain surface area and width also showed no significant differences between or within any of the lines (Figure 6.5, B and E). Grain length measurements showed a statistically significant difference in lines 6.2 ($p = 0.036$, F-test = 5.71) and 6.8 ($p = 0.048$, F-test = 4.94) where both sets of transgenic grains were significantly shorter than their null counterparts. As described in section 6.2.4.1 (Figure 6.4) these two lines also had the highest expression of the *PcGA2ox1* gene out of the three lines. Taken as a whole these results indicate that while the variations seen in grain number were not a result of the expression of *TaTri::PcGA2ox1*, the reduction in grain length in two lines was. We hypothesised that reduction in GA levels late in grain development should not affect its size; however, the examination of these lines implies that this was not the case. As previously mentioned as a population the transgenic lines did not show a significant difference in grain size compared to the nulls. However, when within lines differences were analysed two of the three transgenic lines did show a reduction in grain length and the only line which did not show any change also had the lowest expression of the *PcGA2ox1* gene. Indeed, these results do indicate that expression of the *PcGA2ox1* gene even this late in grain development can affect its size, however

this result was based on only three independent lines and must be viewed with this in mind.

6.2.4.3 Analysis of *TaTri::PcGA2ox1* effects on quality

To study the effect of expressing the *PcGA2ox1* gene in the endosperm on grain quality, the α-amylase and nitrogen contents of the grains were assessed. Grains measured in the yield study were milled to a fine flour and the α-amylase activity measured on 25 mg of this material according to section 2.4.2. The data presented in figure 6.6, A shows CU for each line and is an average of three biological replicates except the nulls of line 6.8. There was an overall trend towards increased α-amylase in the transgenics compared to their null. Taking the data at the population level when analysed by ANOVA using LSD at 5% (section 2.6), significant correlations were observed on the basis of genotype with the nulls having significantly lower α-amylase than both the transgenics and the wild type suggesting that that the *TaTri::PcGA2ox1* construct was not having a positive effect on grain quality. However, within individual lines only a weakly significant difference ($p = 0.074$, F-test = 3.90) was observed for line 6.6. This could potentially be due to the high expression of the *PcGA2ox1* transgene leading to an increase in the transcripts of endogenous genes resulting in overcompensation and increased GA levels.

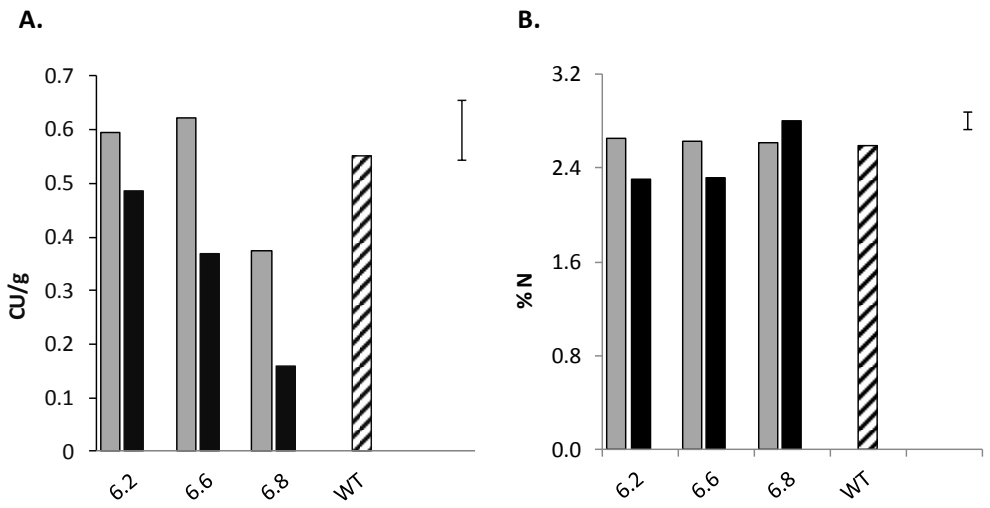


Figure 6.6: Analysis of quality components in *TaTri::PcGA2ox1* transgenic lines

Averages are presented for: α-amylase (A) and grain nitrogen content (B) for measurements on mature grains. Grey bars – transgenic lines, black bars – null segregants and hatched bars – WT. Vertical error bars denote SED on 1, 11 df.

The percentage of nitrogen in the grains was also measured (as a proxy for protein content) according to section 2.4.3. When the nitrogen content between the transgenics, null and wild-type grains were assessed at the population level no differences were observed between the three genotypes. There were no statistically significant differences between the transgenics and their respective nulls for any of the lines after analysis by ANOVA using LSD at 5%, indicating that the transgene was having no effect on grain protein accumulation in these lines.

6.2.4.4 *TaTri::PcGA2ox1* effect on endogenous gene expression

To further understand the increase in the α-amylase levels in these plants the expression levels of the two endogenous α-amylase genes – *TaAmy1* and *TaAmy2* – were measured. As mentioned in section 6.2.4.3 the high expression of the *PcGA2ox1* transgene (Figure 6.4) could lead to the up-regulation of GA-biosynthetic genes. To explore this further the expression of the endogenous

developing-endosperm-specific gene, *TaGA20ox3* was also measured. These measurements were performed according to section 2.2.7 and on the same 35 and 49 dpa cDNA used for the analysis described in section 6.2.4.1. At both time points the expression of the three genes was normalised against the expression of two endogenous genes – *Ta2526* and *TaGapDH* (section 2.2.7 and appendix 1) and the data presented in figure 6.7 is an average of the NRQs of three biological replicates for each line.

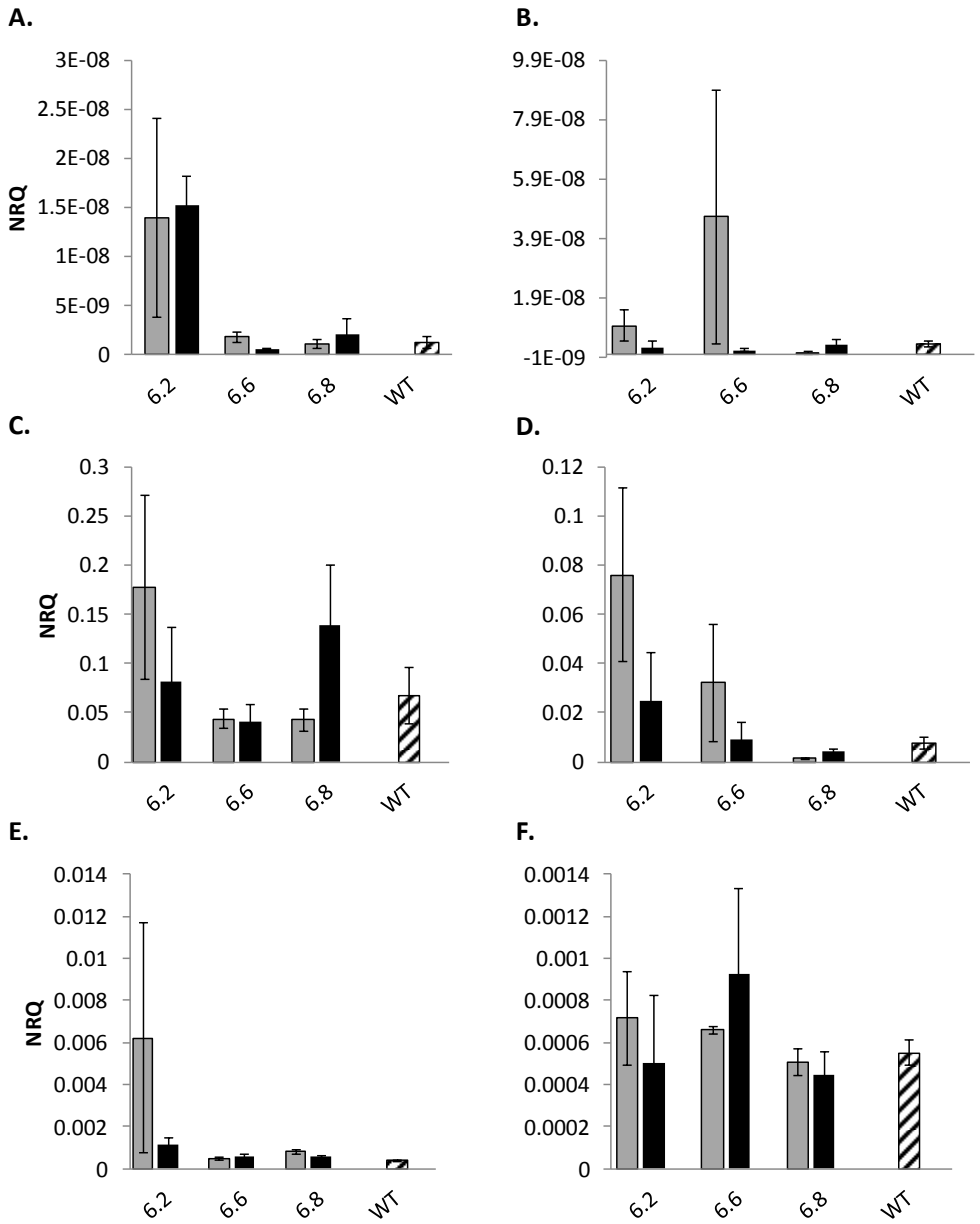


Figure 6.7: NRQs of *TaAmy1*, *TaAmy2* and *TaGA20ox3* genes in *TaTri::PcGA2ox1* transgenic lines

Endogenous levels of the *TaAmy1* (A and B). *TaAmy2* (C and D) and *TaGA20ox3* (E and F) genes at 35 dpa (A, C and E) and 49 dpa (B, D and F). Grey bars – transgenic lines, black bars – null segregants and hatched bars – WT. Vertical error bars denote SEM.

The qRT-PCR for *TaAmy1,* performed using forward primer TaAmy1_F2 and reverse primer TaAmy1_R2 (Appendix 1), showed a large degree of variation within biological replicates and across and within lines. The expression of *TaAmy1* in these lines at both 35 and 49 dpa (Figure 6.7, A and B) was extremely

low. At 35 dpa, whilst overall there were no changes in the expression of *TaAmy1* between the transgenics and their null, in line 6.2 it was highly upregulated in both compared to the rest of the lines and the wild type control (Figure 6.7, A). At 49 dpa, whilst the expression of *TaAmy1* was again very low it was upregulated in the transgenics of line 6.2 and 6.6 (Figure 6.7, B). The relatively high expression of this gene in the transgenics could explain the slight increase in the α-amylase content in these lines.

The expression levels of *TaAmy2,* analysed using forward primer Amy2_F_ext and reverse primer Amy2_R_ext (Appendix 1), showed no overall trend with no consistency between lines at either 35 and 49 dpa (Figure 6.7, C and D). At 35 dpa, whilst accepting considerable variation between replicates, in line 6.2 the expression of this gene was slightly upregulated compared to its null. However, in line 6.8 it was reduced and there was no change in line 6.6 (Figure 6.7, C). At 49 dpa in lines 6.2 and 6.6 the expression of *TaAmy2* was elevated in the transgenic lines, however in line 6.8 there was a slight reduction.

The expression level of *TaGA20ox3,* measured using forward and reverse primers Ta20ox3-F and Ta20ox3-R respectively (Appendix 1), revealed that at both time points, and for the majority of lines, the expression of this gene showed no differences between the transgenics, nulls and the wild-type plants (Figure 6.7, E and F). However, again whilst accepting considerable variation between replicates, at 35 dpa *TaGA20ox3* expression was elevated in the transgenics of line 6.2. As was shown in section 6.2.4.1 (Figure 6.4) this line had the highest expression of the *PcGA2ox1* transgene and this could possibly be causing the feedback regulation of the *TaGA20ox3* gene resulting in its increase. However, no increase in the expression of *TaGA20ox3* was seen in the other two transgenic lines at either time point.

Whilst there were slight differences in the expression of the three endogenous genes studied in this section it should be noted that there were large variations observed in the biological replicates in the majority of the lines for all genes. Due to this it is difficult to make definite conclusions about the effects of the

expression of the *PcGA2ox1* transgene on the expression of these genes or its role in the feedback regulation of GA biosynthetic genes.

6.2.5 Analysis of transgenic lines expressing the *AtGA20ox1* gene under control of the ETC-specific *TaEND1* promoter

6.2.5.1 *TaEND1::AtGA20ox1* transgene expression

To confirm expression of the introduced transgene, transcript levels of the *AtGA20ox1* gene were measured in cDNA synthesised (section 2.2.6) from RNA extracted as described in sections 2.2.4 and 2.2.5 from 14 and 28 dpa grains. These grains were harvested from three biological replicates from each of the four independent lines in the experiment and their respective nulls and the wild type control. The qRT-PCR was performed on this material according to section 2.2.7 using forward primer q_At20ox1_F1 and reverse primer q_At20ox1_R1 (Appendix 1). The expression of the transgene at 14 dpa was normalised against the expression of three endogenous genes – *Ta2526, TaGapDH* and *TaSDH* (Figure 6.8, A) and against two endogenous genes - *Ta2526* and *TaSDH* at 28 dpa (Figure 6.8, B) (section 2.2.7 and appendix 1). The data presented in figure 6.8 is an average of the NRQs of three biological replicates, except for line 2.12. In this line one plant flowered three weeks after the rest of the population and was thus discarded and the data presented is based on two replicates. The qRT-PCR was performed on all plants in the experiment, including the null and wild-type plants as controls. No expression of the transgene was observed in any of the control material (including the NRT controls) and as such these are excluded from the figures as presented.

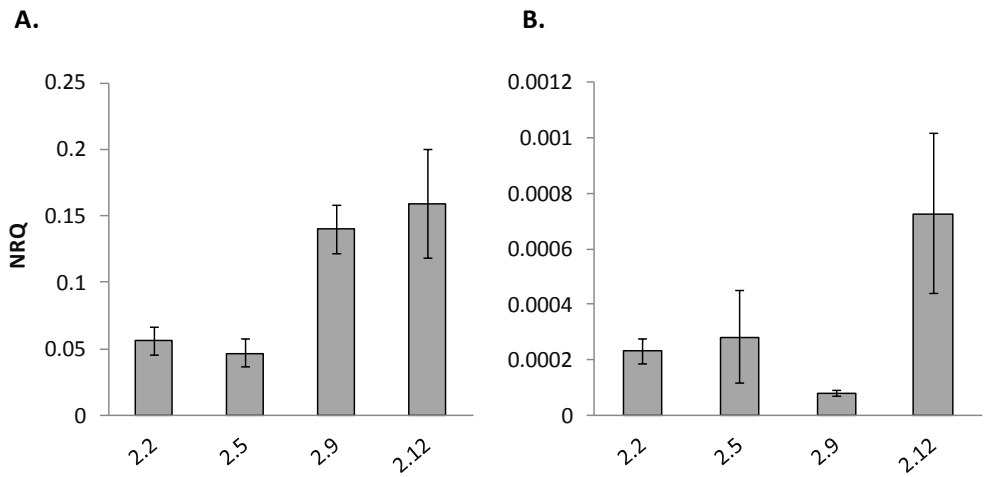


Figure 6.8: NRQs of *AtGA20ox1* in *TaEND1::AtGA20ox1* transgenic lines
Average of normalised expression levels of the *AtGA20ox1* at 14 dpa (A) and 28 dpa (B) grains as measured in three biological replicates for each transgenic line. Vertical error bars denote SEM.

The expression of the *AtGA20ox1* transgene showed a large degree of variation between the four independent lines at both time points studied (Figure 6.8, A and B). However, at both time points the highest level of transgene expression was observed in line 2.12. At 14 dpa, the highest expression at 0.16 was in line 2.12 and the lowest at 0.05 was in line 2.5 (Figure 6.8, A). Whilst this level of expression was lower than that seen for *PcGA2ox1* expressed from the *TaTri* promoter (Figure 6.4 in section 6.2.4.1), it was comparable to the rest of the transgenes studied in this project. At 28 dpa (Figure 6.8, B) the expression levels of this gene saw a huge reduction compare to 14 dpa with line 2.9 showing the biggest decrease, with a 1788-fold change.

6.2.5.2 Analysis of *TaEND1::AtGA20ox1* effects on yield

To study effects of expressing *AtGA20ox1* in the grain ETC on grain yield, mature grains harvested from five ears (taken as a standardised proxy for total yield) of two plants per replicate were assessed according to the methods described in sections 2.3 and 2.4.1. The MARVIN digital seed counter was used

to count grain number and measure their surface area, length and width. These grains were then weighed to calculate TGW. The measurements for diameter were obtained from SKCS as described in section 2.4.1. The data presented in figure 6.9 shows the average values for three biological replicates – the grains from plants two and six of each replicate block were pooled together to form one sample resulting in three biological replicates. For all of the yield variables measured the difference between the transgenic, null and wild type was assessed at the population level by ANOVA using LSD at 5%. Whilst no significant differences were observed between the three genotypes for TGW, area and length, the null lines did have significantly more grains than the transgenics, although neither line showed a difference to the wild type. The width and diameter of the transgenic grains was larger than both the nulls and the wild type, but they also had the least number of grains of the three genotypes which could, in part, explain the increase in grain width.

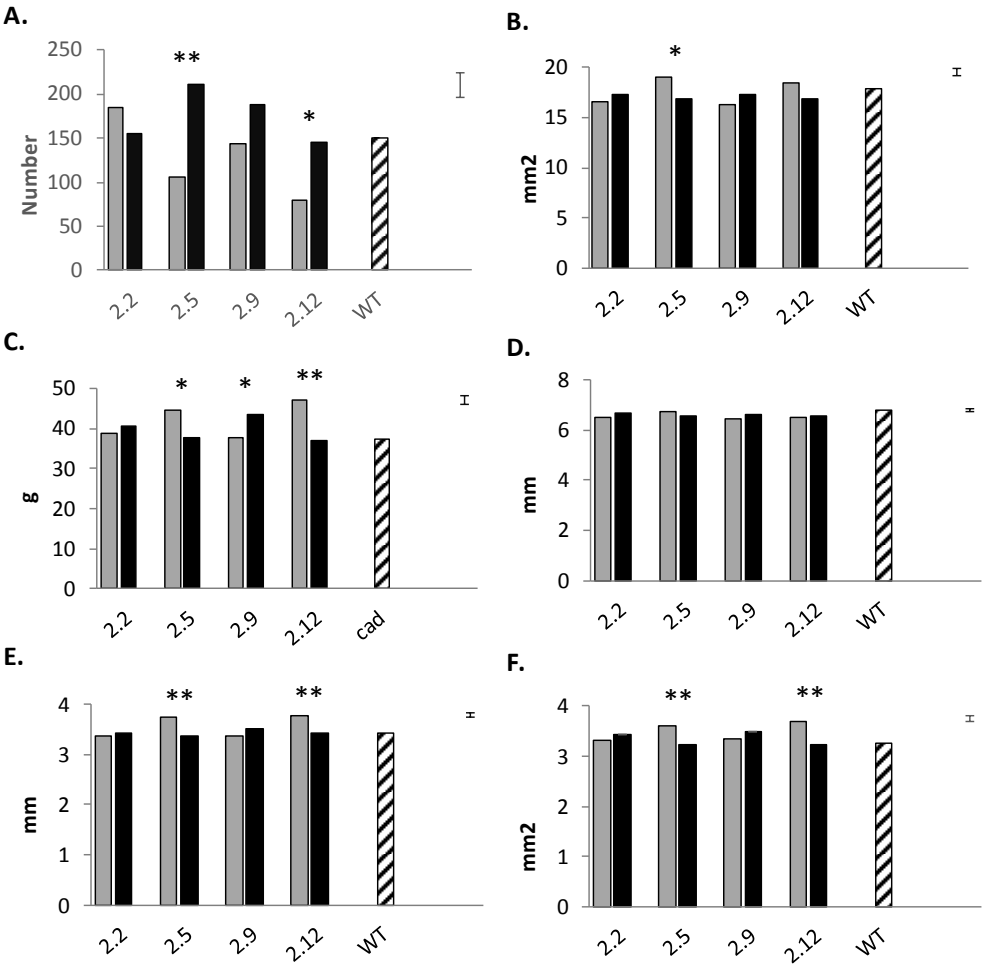


Figure 6.9: Analysis of yield components in *TaEND1::AtGA20ox1* transgenic lines

Averages are presented for several variables: grain number (A), grain surface area (B), TGW (C), grain length (D), grain width (E) and grain diameter (F) for measurements on mature grains. Grey bars – transgenic lines, black bars – null segregants and hatched bars – WT. * denotes significant difference between a transgenic and its null using LSD at 5%: p value at – *: ≤ 0.05 and **: ≤ 0.005. Vertical error bars denote SED on 1, 16 df.

The differences between the transgenic lines and their respective nulls were also analysed using ANOVA. Grain number showed a broad range from a low of 80 (transgenic, line 2.12) to a high of 210 (null, line 2.5) where significant differences were observed in both these lines (Figure 6.9, A) and the transgenics plants had fewer grains than their nulls (line 2.5: p = 0.004, F-test = 11.45 and line 2.12: p = 0.047, F-test = 4.61). During the course of this

experiment it was observed that the transgenic plants had an unusually high number of aborted grains. There are no reports of, nor did we observe, the *TaEND1* promoter being active in tissues other than the ETC and thus expression should have been restricted to the grain and therefore only after anthesis. We assume, therefore, that the transgene expression was not responsible for the reduced grain set. There was also a wide range in average TGW for these lines, from a low of 37.68 g (transgenic, line 2.9) to a high of 46.93 g (transgenic, line 2.12). Significant differences were observed in TGW for three of the four lines (Figure 6.9, C), with lines 2.5 ($p = 0.019$, F-test = 6.83) and 2.12 ($p = 0.001$, F-test = 4.15) both being heavier than their nulls and line 2.9 ($p = 0.039$, F-test = 5.05) being lighter. In terms of grain surface area, only line 2.5 was significantly different from its null, (Figure 6.9, B) with the transgenic grains having significantly larger area than the null ($p = 0.015$, F-test = 7.47). Grain width and diameter (Figure 6.9, E and F) also showed significant differences in lines 2.5 and 2.12 where grains from both transgenic lines were wider than those from the respective nulls (line 2.5: $p = 0.002$, F-test = 12.85 and line 2.12: $p = 0.005$, F-test = 10.62) and had a bigger diameter (line 2.5: $p = 0.008$, F-test = 9.24 and line 2.12: $p = 0.003$, F-test = 12.23). However, grain length in all lines showed no significant differences using LSD at 5% or 10% (Figure 6.9, E). Taken together, these results show an increase in size and weight of the transgenics grains of two lines, indicating that the *TaEND1::AtGA20ox1* construct could be having a positive effect on grain yields. However, the transgenics in these two lines also showed a significant reduction in the number of grains produced potentially increasing the amount of resources available to the remaining grains and this may, in part, explain the increase in grain size and weight. Unfortunately, due to time and resource constraints it wasn't possible to study these lines in detail in an experiment where the source and sink were manipulated to investigate the possible cause of the changes in grain yield.

6.2.5.3 Analysis of *TaEND1::AtGA20ox1* effects on quality

To study the effect of expressing *AtGA20ox1* in the grain ETC on grain quality, grain hardness, grain moisture content and the α-amylase content of flour were assessed. Grain hardness and moisture were measured using the SKCS system as described in section 2.4.1 and the data presented in figure 6.10 A and B represents the average of three biological replicates for each line. For both grain hardness and moisture content the differences between the transgenic, null and wild type was assessed at the population level by ANOVA using LSD at 5%. For both these variables all three genotypes were significantly different from each other. The transgenic grains had the lowest hardness index and moisture content followed by the null, with the wild type having the highest averages for both. The differences between the transgenics and their respective nulls were also analysed by ANOVA and both grain hardness and moisture content showed significant differences in lines 2.5 and 2.12. In both these lines the transgenic grains had a significantly lower hardness index than the nulls (line 2.5: $p < 0.001$, F-test = 16.84 and line 2.12: $p = 0.006$, F-test = 10.04). Whilst the moisture content of all lines in this experiment was in the normal range (11 -14%), again lines 2.5 and 2.12 showed significant differences with the transgenics having lower moisture content than their respective nulls (line 2.5: $p = 0.002$, F-test = 14.31 and line 2.12: $p = 0.009$, F-test = 8.70). These two lines also showed an increase in grain size (Figure 6.9) and these results match those seen in previous work in our laboratory where increase in grain size was accompanied with a reduction in hardness index and moisture content.

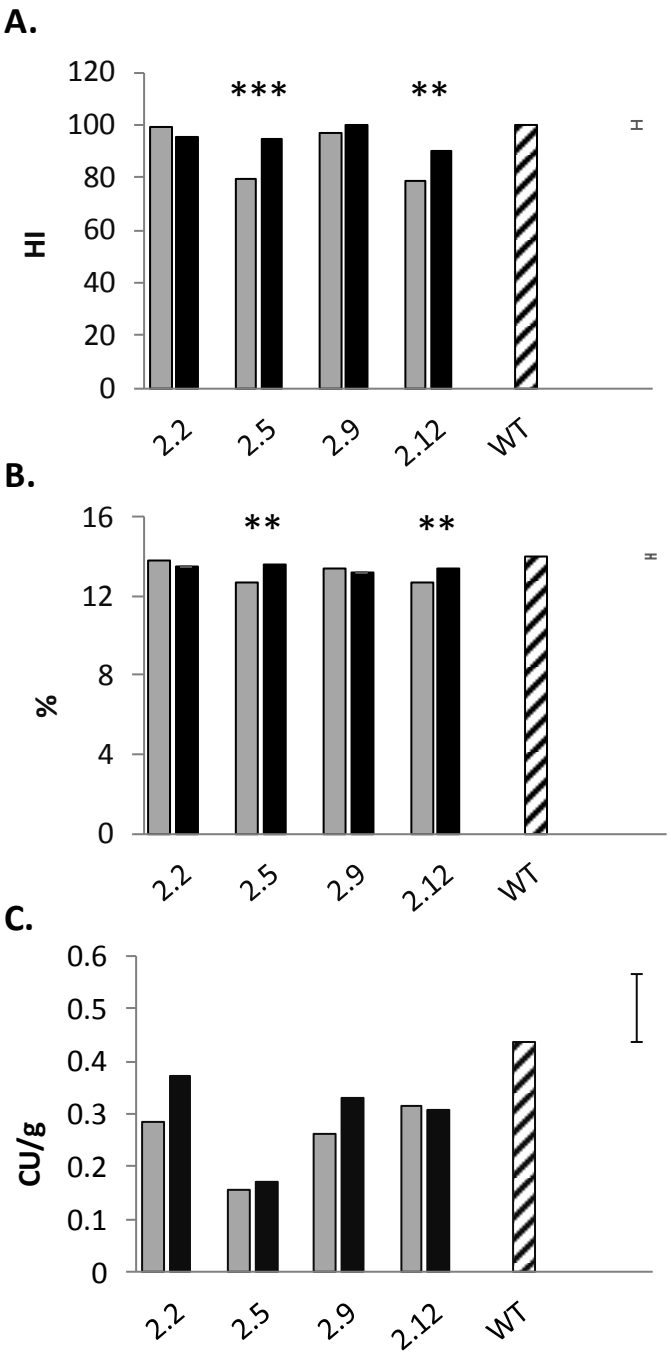


Figure 6.10: Analysis of quality components on *TaEND1::AtGA20ox1* transgenic lines

Averages are presented for several variables: grain hardness (A), moisture content (B) and α-amylase (C) for measurements on mature grains. Grey bars – transgenic lines, black bars – null segregants and hatched bars – WT. * denotes significant difference between a transgenic and its null using LSD at 5%: p value at – **: ≤ 0.005 and ***: ≤ 0.001. Vertical error bars denote SED on 1, 16 df.

Grains crushed during the SKCS analysis were collected and milled to a fine flour and α-amylase measured on 25 mg of this material according to section 2.4.2. Figure 6.10 C shows CU for each line as the average of three biological replicates. The α-amylase content in these lines showed a large degree of variation with a low of 0.16 CU/g (transgenic, line 2.5) to a high of 0.44 CU/g (wild type). However, when the transgenics, nulls and the wild type were assessed at the population level with ANOVA, using LSD at 5%, no significant differences were observed between the three genotypes. The differences between the transgenics and their nulls were also analysed by ANOVA and no significant differences were observed in any of the lines. These results indicate that expressing the *AtGA20ox1* gene in the endosperm transfer layer does not affect the α-amylase content of flour.

6.2.5.4 Analysis of *TaEND1::AtGA20ox1* effects on GA levels

To examine the effects of the *TaEND1::AtGA20ox1* construct on GA levels 28 dpa grain were analysed for GA content. These grains were harvested from ears two and three of plants three, four and five from each replicate block. All grains harvested from a replicate block were pooled to form one sample. Lines 2.5 and 2.12 which displayed increased grain weight (Figure 6.9) were chosen for this study, although due to time and resource constraints, only one replicate of the transgenic, its null and a wild type was analysed from each line. The data presented in table 6.1 shows the levels (ng/g of dry weight) of multiple GAs which were extracted and quantified as described in section 2.5.

Table 6.1: GA concentrations in grain from *TaEND1::AtGA20ox1* transgenic lines

Levels of different GAs (ng/gDW) measured in 28 dpa grains from one replicate each. Rows in bold represent bioactive GAs. T: transgenic and N: null.

Line / GA	2.5		2.12		WT
	T	N	T	N	
GA_{12}	0.09	0.10	0.11	0.09	0.24
GA_{53}	0.16	0.14	0.12	0.23	0.22
GA_{44}	0.61	1.05	0.88	1.14	2.73
GA_{19}	4.30	5.60	6.60	7.00	14.6
GA_{20}	0.06	0.11	0.09	0.10	0.28
GA_1	*	**0.78**	**0.72**	**0.85**	**1.26**
GA_8	0.33	0.48	0.26	0.25	0.67
GA_{29}	0.48	0.54	0.58	0.55	0.82
GA_3	**0.57**	**0.49**	**0.48**	**0.51**	**0.59**
GA_{15}	0.29	0.39	0.49	0.54	2.74
GA_{24}	0.25	0.15	0.53	0.57	1.98
GA_9	0	0.02	0.06	0.02	0.88
GA_4	**0**	**0**	**0**	**0**	**0.08**
GA_{34}	0.07	0.36	0.37	0.18	0.40
GA_{54}	**5.80**	**22.10**	**12.10**	**26.50**	**143.0**

** Sample not measured*

Overall for all of the GAs measured the wild type grains contained higher amounts compared to the transgenics and the nulls of both lines 2.5 and 2.12. As discussed in section 1.3.1 plants contain two parallel pathways (13-hydroxylation and non-13-hydroxylation) to produce bioactive GAs. Wheat predominantly contains 13-hydroxy GAs which produce GA_1 as the main bioactive GA in this species. As table 6.1 shows the levels of GA_1 and its precursor GAs (GA_{53}, GA_{44}, GA_{19} and GA_{20}) were higher in the wild type compared to the rest of the lines. In the transgenic line 2.5 the HPLC fraction containing GA_1 was lost and thus this GA could not be quantified for this sample; however, in the transgenic line 2.12 its level was lower compared to the null. Whilst the majority of precursor GAs (GA_{44}, GA_{19} and GA_{20}) also showed a reduction in the transgenic lines compared to the nulls, GA_{53} only

displayed this difference in line 2.12, where the levels of this GA in the null were comparable to the wild-type.

As with the 13-hydroxy GAs, the non-13-hydroxy GA precursors (GA_{12}, GA_{15}, GA_{24} and GA_9) were also present in a higher quantity in the wild type grains, with GA_9 showing the biggest difference (35 times higher in wild type). Unlike the 13-hydroxy GA precursors, these GAs did not show the same reduction in the transgenic lines compared to their nulls. GA_4, the bioactive product of the non-13-hydroxylation pathway, whilst present at very low levels in the wild type grains was not detected in the transgenics or nulls of both lines. However, the inactive GA_{34} was detected in all lines, though again at a higher level in the wild type grains, and showed no pattern between the transgenic and null lines. The other two inactive GAs (GA_8 and GA_{29}) were also higher in the wild type plants, and also did not display any differences between the transgenic lines and their nulls. The third bioactive GA – GA_3 – however was present equally in all five samples, though at a lower level than GA_1.

GA_{54} (1-hydroxy-GA_4) which has some biological activity, about 10% that of GA_1, is present at very high concentrations in the endosperm of developing wheat grains. This was the only bioactive GA which showed a consistent difference in the transgenics and nulls of both lines 2.5 and 2.12. Whilst in both genotypes it was lower than the wild type grains, in the transgenics it showed a bigger reduction. When comparing the transgenics and their nulls, line 2.5 showed a bigger difference with the transgenic having 3.8 times lower amount of this GA and transgenic line 2,12 showing a 2.1 times reduction.

Whilst accepting that both the transgenics and nulls show a reduction in GA concentration compared to the wild-type, the transgenic lines also show a reduction compared to their nulls, although this was not always consistent between the two lines. These results, though based on only one sample of each line, indicate that the expression of the *AtGA20ox1* transgene did not lead to an increase in GA levels, but in fact produced a slight reduction.

6.2.5.5 Analysis of *TaEND1::AtGA20ox1* effects on endogenous gene expression

To understand the changes in the GA levels in these lines the expression levels of the GA biosynthetic gene *TaGA20ox3* were measured. These measurements were performed according to section 2.2.7 and on the same 14 and 28 dpa cDNA used for the analysis described in section 6.2.5.1 The expression of the transgene at 14 dpa was normalised against the expression of three endogenous genes - *Ta2526, TaGapDH* and *TaSDH* (Figure 6.11, A) and against two endogenous genes - *Ta2526* and *TaSDH* at 28 dpa (Figure 6.11, B) (section 2.2.7 and appendix 1). The data presented in figure 6.11 is an average of the NRQs of three biological replicates, except for transgenics of line 2.12 at both 14 and 28 dpa which is based on two replicates only.

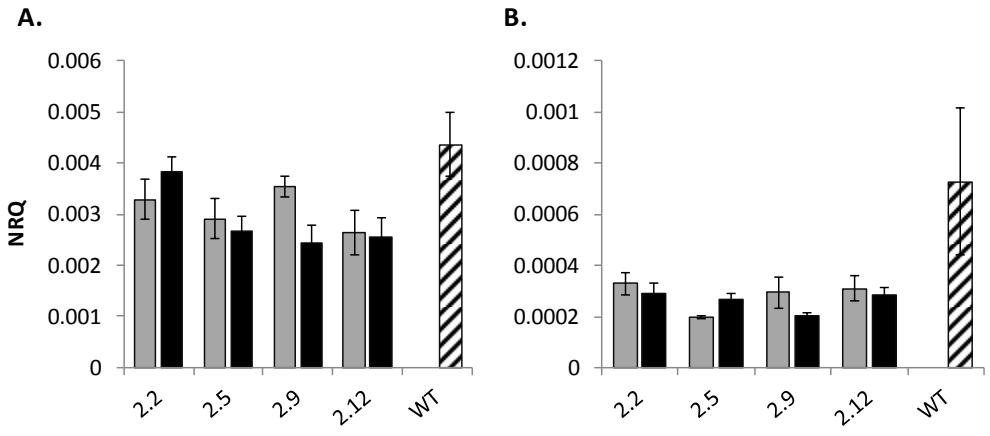


Figure 6.11: NRQs of *TaGA20ox3* in *TaEND1::AtGA20ox1* transgenic lines
Expression levels of the native *TaGA20ox3* gene at 14 dpa (A) and 28 dpa (B). Grey bars – transgenic lines, black bars – null segregants and hatched bars – WT. Vertical error bars denote SEM.

The qRT-PCR for *TaGA20ox3* was performed using primers Ta20ox3-F and Ta20ox3-R (Appendix 1) and overall there was a trend towards lower expression of this gene in all lines compared to the wild-type plants at both time points. At 14 dpa (Figure 6.11, A) in the majority of the lines the

transgenics showed higher expression of *TaGA20ox3* compared to the nulls and only in line 2.2 did the null show an elevation in gene expression. However, at 28 dpa (Figure 6.11, B) this was not consistent between the different lines. At this time point the transgenics line 2.5 showed a reduction in the expression of *TaGA20ox3* compared to the null, transgenic line 2.9 showed an increase and the other two line (2.2 and 2.12) showed no difference. Whilst there was a reduction in the expression of *TaGA20ox3* at 28 dpa in all lines compared to the wild-type, it should be noted that there was large variation observed in the biological replicates of the wild-type at this time point. In addition to that, there was also inconsistency in *TaGA20ox3* expression in the different lines and due to this it is difficult to make definite conclusions about the effects of the expression of the *AtGA20ox1* transgene on the expression of *TaGA20ox3* or its effects on the reduction in GA hormone content in the two lines studied in section 6.2.5.4 (Table 6.1).

6.2.6 Analysis of transgenic lines expressing the *Atgai* gene under control of the ETC-specific *TaEND1* promoter

6.2.6.1 *TaEND1::Atgai* transgene expression

To confirm expression of the introduced transgene, transcript levels of the *Atgai* gene were measured in cDNA synthesised (section 2.2.6) from RNA extracted as described in sections 2.2.4 and 2.2.5 from 14 and 28 dpa grains. These grains were harvested from three biological replicates from each of the four independent lines in the experiment and their respective nulls and the wild type control. The qRT-PCR was performed on this material according to section 2.2.7 using forward and reverse primers gai_qPCR-F and gai_qPCR-R respectively (Appendix 1). The expression of the transgene at both 14 and 28 dpa was normalised against the expression of three endogenous genes – *Ta2526, TaGapDH* and *TaSDH* (Figure 6.12, A and B) (section 2.2.7 and appendix

1). The qRT-PCR was performed on all plants in the experiment, including the null and wild-type plants as controls. No expression of the transgene was observed in any of the control material (including the NRT controls) and as such these are excluded from the figures as presented. The data presented in figure 6.12 A for 14 dpa are an average of the NRQs of three biological replicates, except for line 11.7 where cDNA synthesis of one replicate failed. For 28 dpa data are presented only for lines 11.4 and 11.7 (Figure 6.12, B). Lines 11.5 and 11.8 did not pass the qRT-PCR quality control checks as the *Atgai* gene was either not amplified or the amplification was very late in the qRT-PCR cycling. In the samples where *Atgai* was amplified there was a large degree of variation between each of the technical replicates and thus the data was deemed unreliable and not included.

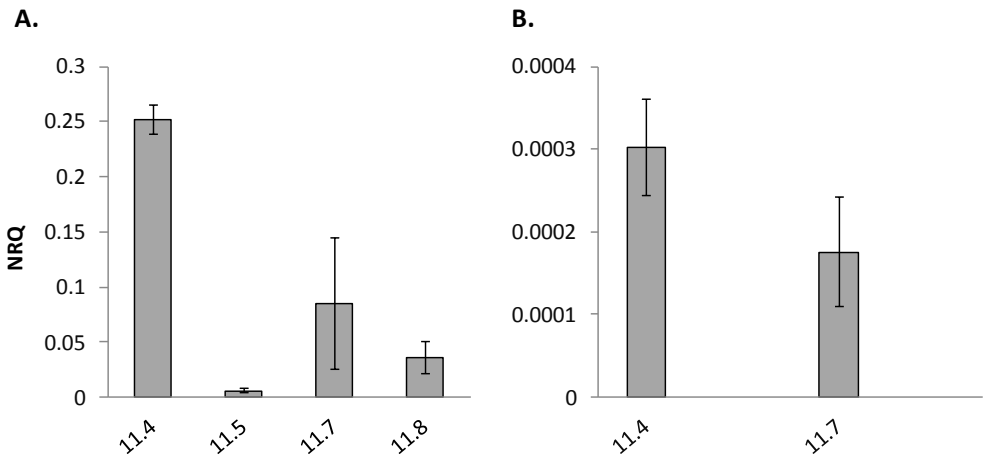


Figure 6.12: NRQs of *Atgai* in *TaEND1::Atgai* transgenic lines
Average of normalised expression levels of the *Atgai* at 14 dpa (A) and 28 dpa (B) grains as measured in three biological replicates for each transgenic line. Vertical error bars denote SEM.

At 14 dpa the expression of the *Atgai* transgene showed a large degree of variation between the four independent lines with the highest expression at 0.25 in line 11.4 and the lowest at 0.006 in line 11.5 (Figure 6.12, A). This level of expression was comparable to that of *AtGA20ox1* at 14 dpa (Figure 6.8, A),

indicating that the *TaEND1* promoter was equally functional at this time point in both the constructs. Likewise, at 28 dpa (Figure 6.12, B) the levels of expression in lines 11.4 and 11.7 were also comparable to those found for *AtGA20ox1* in figure 6.8 B. However as previously mentioned *Atgai* expression at 28 dpa in lines 11.5 and 11.8 was very low, making the data generated unreliable. In lines 11.4 and 11.7 the expression of this gene from 14 to 28 dpa saw an 837 and 485-fold reduction, respectively.

6.2.6.2 Analysis of *TaEND1::Atgai* effects on yield

To study effects of expressing *Atgai* in the grain ETC on grain yield, mature grains harvested from five ears (taken as a standardised proxy for total yield) of two plants per line were assessed according to the methods described in sections 2.3 and 2.4.1. Yield measurements were performed as discussed in section 6.2.5.2. The data presented in figure 6.13 shows the average values of three biological replicates each variable – the grains from plants two and six of each replicate block were pooled together to form one sample resulting in three biological replicates. For all of the yield variables measured the difference between the transgenic, null and wild type was assessed at the population level by ANOVA using LSD at 5%. No significant differences were observed between the three genotypes for grain number; however, differences were observed for the remaining variables. The average TGW, width and diameter showed a statistically significant increase in the nulls compared to both the transgenics and the wild type, whereas no differences were observed between the other two genotypes for these variables. Whilst the transgenics had smaller average length compared to only the nulls, they also had smaller area than both the nulls and wild type. Taken together these results indicate that the *TaEND1::Atgai* construct may be having a negative effect on grain yield.

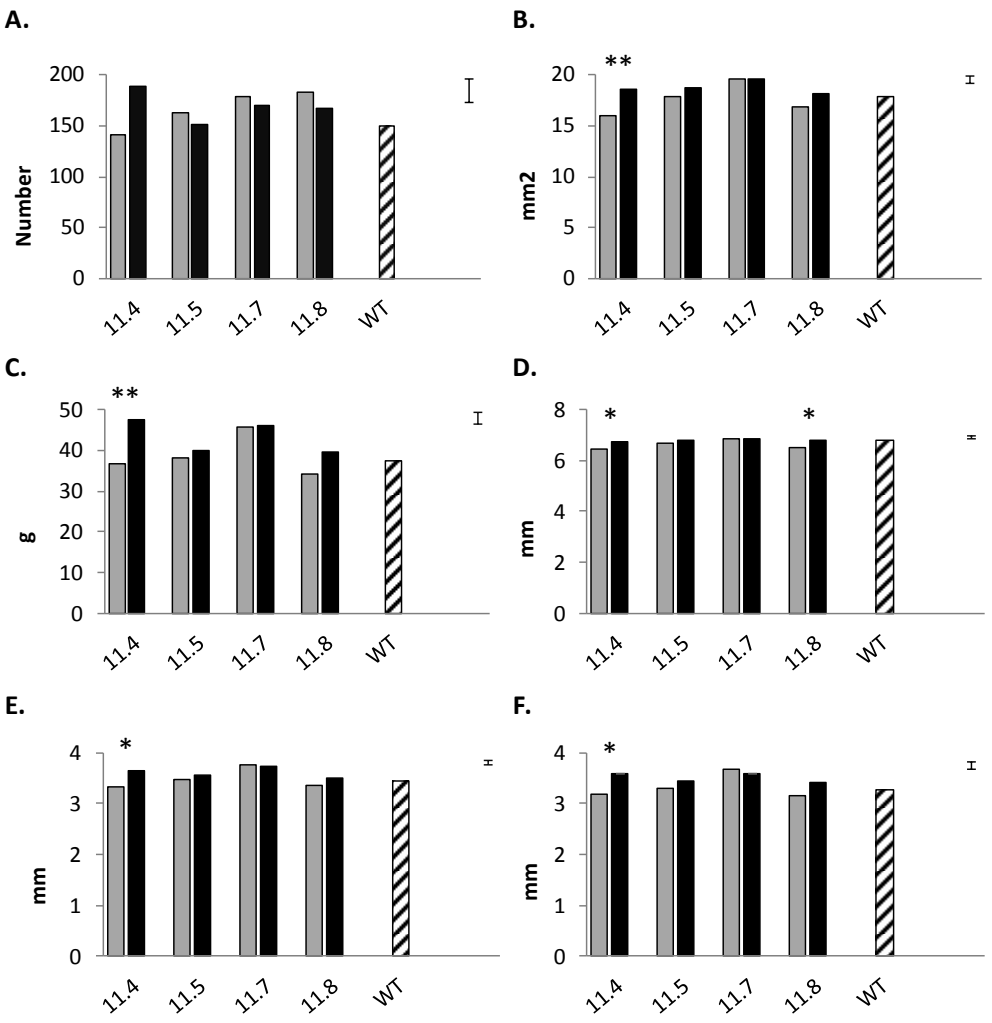


Figure 6.13: Analysis of yield components on *TaEND1::Atgai* transgenic lines

Averages are presented for several variables: grain number (A), grain surface area (B), TGW (C), grain length (D), grain width (E) and grain diameter (F) for measurements on mature grains. Grey bars – transgenic lines, black bars – null segregants and hatched bars – WT. * denotes significant difference between a transgenic and its null using LSD at 5%: p value at – *: ≤ 0.05 and **: ≤ 0.005. Vertical error bars denote SED on 1, 16 df.

The differences between the transgenic lines and their respective nulls were also analysed using ANOVA. Grain number, was fairly uniform for this construct and did not show large variation and no significant differences were observed in any of the lines (Figure 6.13, A). Whilst the average TGW showed a wide range from a low of 34.02 g (transgenic, line 11.8) to a high of 47.35 g (null, line 11.4) significant differences were observed only in line 11.4 (Figure 6.13, C) where the nulls were heavier than the transgenics (p = 0.006, F-test = 9.92). For

average grain area the majority of lines did not show a significant difference (Figure 6.13, B), except for line 11.4 (in which transgene expression was the highest) where the transgenic grains were significantly smaller (p = 0.005, F-test = 10.65) than their respective nulls. Grain width and diameter (Figure 6.13, E and F) also showed significant differences in line 11.4 where the transgenic grains were thinner (p = 0.022, F-test = 6.48) and had a smaller diameter (p = 0.019, F-test = 6.83) than the null. Grain length showed significant differences in two lines, with the transgenics of both lines 11.4 and 11.8 (both lines: p = 0.032, F-test = 5.49) being smaller than their respective nulls (Figure 6.13, D). These results show a reduction in the size and weight of transgenics of two lines indicating that expressing the *Atgai* in the endosperm transfer layer could be having a negative effect on grain yields.

6.2.6.3 Analysis of *TaEND1::Atgai* effects on quality

To study the effect of expressing the *Atgai1* gene in the ETC on grain quality, grain hardness, grain moisture content and the α-amylase content of flour were assessed. Grain hardness and moisture were measured using the SKCS system as described in section 2.4.1 and the differences between the transgenic, null and wild type was assessed at the population level by ANOVA using LSD at 5%. Whilst for hardness index only the nulls and transgenics were significantly different from each other, the moisture content was different between all three genotypes. The null grains showed a statistically significant reduction in hardness index compared to the transgenics and they also had the lowest moisture content followed by the transgenics, with the wild type having the highest average. The differences between the transgenics and their respective nulls were also analysed by ANOVA and for the majority of lines no significant differences were observed for either grain hardness or moisture content (Figure 6.14, A and B). The exception to this was again line 11.4 where the transgenic grains had a significantly higher moisture content than the nulls (p = 0.004, F-test = 10.94).

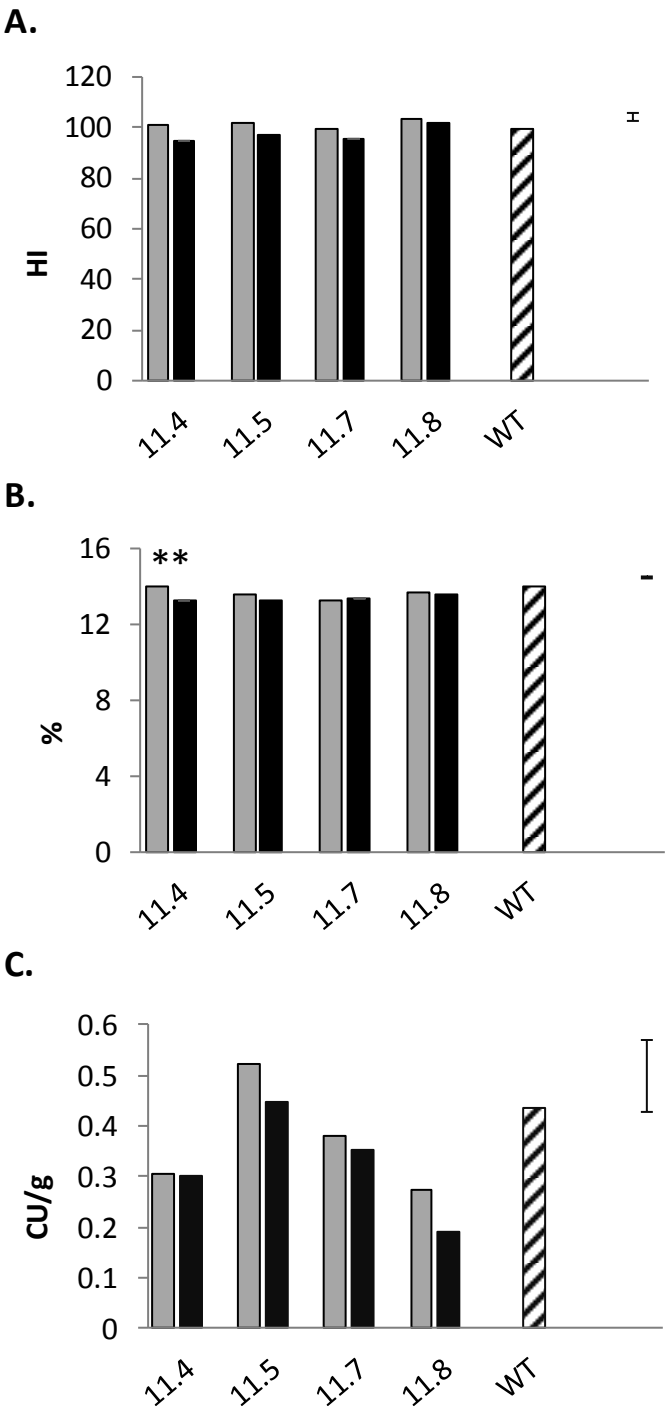


Figure 6.14: Analysis of quality components on *TaEND1::Atgai* transgenic lines

Averages are presented for several variables: grain hardness (A), moisture content (B) and α-amylase (C) for measurements on mature grains. Grey bars – transgenic lines, black bars – null segregants and hatched bars – WT. * denotes significant difference between a transgenic and its null using LSD at 5%: p value at – **: ≤ 0.005. Vertical error bars denote SED on 1, 16 df.

Grains crushed during the SKCS analysis were collected and milled to a fine flour and α-amylase measured on 25 mg of this material according to section 2.4.2. The data presented in figure 6.14, C shows CU for each line and is an average of three biological replicates. The α-amylase content in these lines showed a large degree of variation with a low of 0.19 CU/g (null, line 11.8) to a high of 0.52 CU/g (transgenic, line 11.5). However, when the transgenics, nulls and the wild type were assessed at the population level with ANOVA, using LSD at 5%, no significant differences were observed between the three genotypes (data not shown). The differences between the transgenics and their nulls were also analysed by ANOVA and no significant differences were observed in any of the lines. These results indicate that expressing the *Atgai* gene in the transfer layers of the endosperm does not affect the α-amylase content of flour.

6.2.6.4 Analysis of *TaEND1::Atgai* effects on GA levels

The effect of the *TaEND1::Atgai* construct on GA levels was determined in whole grains at 28 dpa. The grains used for this analysis were harvested and pooled as described in section 6.2.5.4. Lines 11.4 and 11.8 which displayed changes in yield (Figure 6.13) were chosen for this study. However, due to time and resource constraints only one replicate per line of the transgenic, its null and a wild type was analysed. The data presented in table 6.2 shows the levels (ng/g of dry weight) of multiple GAs which were extracted and quantified as described in section 2.5. As table 6.2 shows, only negligible differences were observed in the GA levels between the wild type and the transgenics and nulls of both lines 11.4 and 11.8. GA_1 was present as the main bioactive GA in all lines with its level being the highest amongst the bioactive GAs. Whilst in line 11.4 the levels of this GA were comparable between the transgenic and its null, in line 11.8 it showed a reduction in the nulls. The 13-hydroxy precursor GAs (GA_{53}, GA_{44}, GA_{19} and GA_{20}) also showed a reduction in the nulls of 11.8, however GA_{44} and GA_{19} showed an increase in the null of 11.4. This line also showed an increase in the levels of GA_3 (bioactive) compared to its transgenic

and the rest of the lines, whereas the null of 11.8 showed an increase in the levels of GA_4 (bioactive).

Table 6.2: GA concentrations in grains of *TaEND1::Atgai* transgenic lines

Levels of different GAs (ng/gDW) measured in 28 dpa grains from one replicate each. Rows in bold represent bioactive GAs. T: transgenic and N: null.

Line / GA	11.4		11.8		WT
	T	N	T	N	
GA_{12}	0.18	0.18	0.20	0.21	0.24
GA_{53}	0.19	0.21	0.22	0.16	0.22
GA_{44}	2.89	3.21	2.66	2.07	2.73
GA_{19}	11.20	15.20	11.60	8.30	14.6
GA_{20}	0.29	0.30	0.28	0.18	0.28
GA_1	**1.15**	**1.17**	**1.13**	**0.99**	**1.26**
GA_8	0.60	0.47	0.58	0.47	0.67
GA_{29}	0.64	0.65	0.63	0.60	0.82
GA_3	**0.66**	**1.00**	**0.53**	**0.53**	**0.59**
GA_{15}	2.61	2.32	2.30	2.01	2.74
GA_{24}	1.75	1.70	1.58	1.68	1.98
GA_9	0.09	0.17	0.09	0.12	0.88
GA_4	**0.07**	**0.05**	**0.12**	**0.20**	**0.08**
GA_{34}	0.53	0.44	0.51	0.32	0.40
GA_{54}	**128.4**	**109.9**	**113.9**	**94.5**	**143.0**

The non-13-hydroxy GA precursors displayed inconsistent results between the lines with GA_{15} being lower in both the nulls and GA_9 being higher compared to the transgenics and GA_{24} being lower only in the null of 11.8. Two of the three inactive GAs measured – GA8 and GA34 – showed an increase in the transgenics of both lines compared to the nulls, whilst the third, GA_{29} showed no differences, although it was lower than the wild-type. The levels of GA_{54} were also higher in the wild type compared to the rest of the lines, although

this difference was not as substantial as that seen for the *TaEND1::AtGA20ox1* construct (Table 6.1). As previously mentioned, GA_{54} has some biological activity and the transgenics of both lines had higher levels of this GA compared to both their respective nulls. These results, though also only based on one sample of each line, whilst being inconsistent between the lines for the majority of GAs measured do show an increase in the endosperm specific bioactive GA_{54} in the transgenic lines compared to their nulls. This indicates that the expression of the *Atgai* transgene could be the reason for this increase, implying that GA insensitivity in the ETC of grains could result in an increase in GA content.

6.2.6.5 Analysis of *TaEND1::Atgai* effects on endogenous gene expression

To understand if GA insensitivity has any effects on the expression of GA biosynthetic genes, the expression levels of the *TaGA20ox3* were measured. These measurements were performed according to section 2.2.7 and on the same 14 and 28 dpa cDNA used in section 6.2.6.1 The expression of the transgene at 14 and 28 dpa was normalised against the expression of three endogenous genes - *Ta2526, TaGapDH* and *TaSDH* (Figure 6.15, A and B) (section 2.2.7 and appendix 1). The data presented in figure 6.15 is an average of the NRQs of three biological replicates, except for the transgenics of line 11.7 and nulls of line 11.8 at 14 dpa and the nulls of 11.5 and 11.8 at 28 dpa, where cDNA synthesis of one replicate failed.

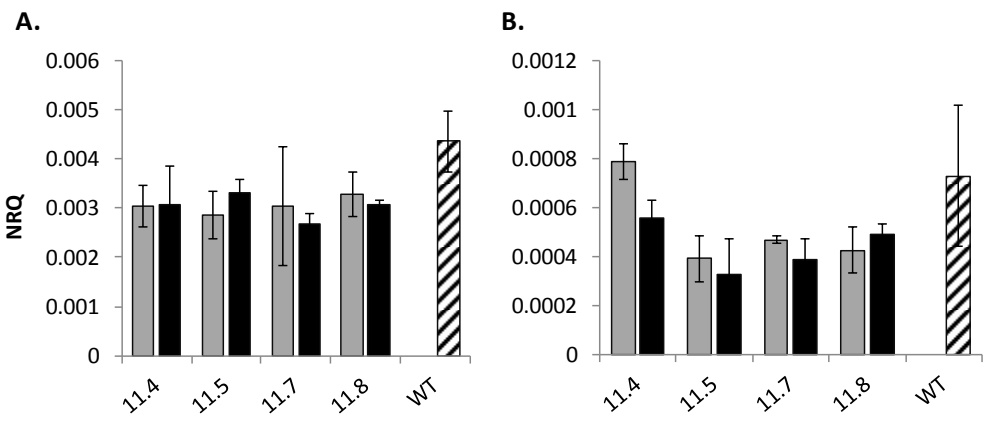


Figure 6.15: NRQs of *TaGA20ox3* in *TaEND1::Atgai* transgenic lines
Endogenous levels of the *TaGA20ox3* gene at 14 dpa (A) and 28 dpa (B). Grey bars – transgenic lines, black bars – null segregants and hatched bars – WT. Vertical error bars denote SEM.

The expression levels of *TaGA20ox3* were measured using primers Ta20ox3-F and Ta20ox3-R (Appendix 1) as in section 6.2.5.5. At 14 dpa (Figure 6.15, A) whilst the expression of *TaGA20ox3* did not show any significant differences between the transgenics and nulls in any of the lines, it did show a slight overall reduction compared to the wild type. As shown in section 6.2.6.1 (Figure 6.12, A) line 11.4 had the highest expression of the *Atgai* transgene. However, this did not result in an increase in the level of *TaGA20ox3* expression at this time point. At 28 dpa (Figure 6.15, B) the expression of this gene was more varied between the four lines, however for the majority of lines no substantial differences were observed between the transgenics and their nulls. However, the transgenics of line 11.4 did show a slight increase in the expression of *TaGA20ox3* compared to its null. This line also had the highest expression of the *Atgai* transgene at 28 dpa (Figure 6.12, B), along with the increase in transcripts of *TaGA20ox3* could be the reason for the increase in GA_{54} content in these lines (Table 6.2). However, with only one line showing a slight increase in *TaGA20ox3* levels, and the fact that the *Atgai* gene is expressed only in the transfer cells of the grain and the analysis presented here was performed on whole grains, there is insufficient evidence to suggest that *Atgai* is regulating expression of this gene.

6.3 Conclusions

The effects of manipulating GA content and GA insensitivity in the endosperm of developing grains as described in this chapter were investigated using three different constructs – *TaTri::PcGA2ox1, TaEND1::AtGA20ox1* and *TaEND1::Atgai*. We hypothesised that decreasing the amount of GA late in grain development through the *TaTri::PcGA2ox1* construct had the potential to improve grain quality without impacting grain size. In addition we hypothesised that the *TaEND1::Atgai* and *TaEND1::AtGA20ox1* constructs would respectively help in understanding the role of GA signalling in the developing grain and determine if an increase in GA in the ETC enhances grain size.

Two of the three homozygous transgenic lines obtained with the *TaTri::PcGA2ox1* construct contained shorter grains than their nulls indicating that expressing the *PcGA2ox1* gene even relatively late in grain development can affect grain size. In addition, these transgenic lines did not show any significant differences in the α-amylase levels compared to the nulls indicating that expression of the *PcGA2ox1* gene in the endosperm is not affecting grain quality. To analyse if expressing a GA inactivating gene in the endosperm has any effects on the expression of biosynthetic genes the levels of *TaGA20ox3* were measured and no effects were observed. These results indicate that expressing *PcGA2ox1* even late in grain development can lead to a decrease in grain size without having a positive effect on quality.

Plants in the two constructs designed to manipulate GA content and perception in the endosperm transfer layer displayed a grain yield phenotype. Whilst in lines harbouring the *TaEND1::AtGA20ox1* construct there was an increase in grain size, those transformed with *TaEND1::Atgai* displayed the opposite result. However, the *TaEND1::AtGA20ox1* lines also showed a reduction in grain number which may have influenced grain size due to increased availability of resources. Neither construct conferred any change in the α-amylase content

in the transgenic lines consistent with the endosperm transfer layer not being involved in the production of this enzyme, but also suggesting that changes made to GA levels and perception in this tissue do not significantly affect the induction of α-amylase elsewhere in the grain.

The levels of the GA hormone were also measured in the transgenics and their nulls of two lines from each construct. As mentioned this was performed on only one sample for each line. Whilst the transgenics from the lines transformed with *TaEND1::AtGA20ox1* displayed a slight reduction in GA content compared to the null, there was a huge overall reduction in both transgenics and nulls in both lines compared to the wild-type and the *TaEND1::Atgai* plants. Both the transgenics and nulls for the *TaEND1::AtGA20ox1* construct contained about half the amount of GA_1 – the main bioactive GA in wheat – compared to the wild type grains. However, the transgenic line had a lower amount than the null. A huge overall reduction was also observed in the levels of the bioactive GA_{54} in both the transgenics and nulls, though again the transgenics contained lower amounts than their respective nulls. Previous work in our laboratory has shown that the expression of the *AtGA20ox1* gene in the endosperm can result in an acceleration of growth rates of grains (Vaughan, S. unpublished data). The grains in the transgenic lines of this construct could possibly be exhibiting an accelerated growth pattern resulting in them being physiologically older than the nulls at 28 dpa. The levels of GA in the grain are at their peak at 21 dpa and gradually decline to 28 dpa, after which they show a sharp decline in older grains (Lenton, J. unpublished data). If the transgenic grains studied here are indeed older than their nulls this could explain the reduction seen in GA levels.

The lines harbouring the *TaEND1::Atgai* construct also had lower levels of GA compared to the wild type; however this reduction was not as substantial as that seen in lines with the *TaEND1::AtGA20ox1* construct. The levels of the main bioactive GA, GA_1, showed an inconsistent pattern between the transgenics and nulls of the two lines with it showing an increase in only one of

the transgenic lines. However, the levels of GA_{54} were increased in both the transgenic lines compared to the nulls, indicating that expressing *Atgai* results in the accumulation of this hormone in these lines. The expression of the endogenous biosynthetic gene *TaGA20ox3* was measured in these lines to examine if expressing *Atgai* was leading to an up-regulation in endogenous GA biosynthetic genes. The expression levels of *TaGA20ox3* did not display any consistent changes in the transgenic lines compared to both the nulls and wild type control, so that altered expression of this gene does not account for the observed differences in GA levels, although there may be effects on expression of other genes in the GA biosynthetic pathway.

As mentioned above, the levels of GAs were overall substantially lower in the lines of the *TaEND1::AtGA20ox1* construct compared to the wild type and lines of the *TaEND1::Atgai* construct. This points to the possibility of an experimental or methodological error during either harvest, extraction or measurement of these samples. These plants were all grown together in the same glasshouse in one large randomised experiment thus facing the same environmental conditions during development. The GA measurements were all performed on plants from the same replicate block, with grains harvested from two ears on three plants each, resulting in a large pool constituting each sample. The grains were pooled in order to eliminate any variation brought about by possible errors while staging the ears. The presence of a large pool of grains from multiple ears in each sample also removes the possibility of mistakes made during harvest as a reason for these inexplicable GA results. The second possibility of errors during the extraction or measurement process is also unlikely as the lines of the *TaEND1::AtGA20ox1* construct were analysed in the same batch as the wild-type and lines of *TaEND1::Atgai* construct analysed separately. These observations indicate that the GA levels determined in these lines are reliable. It is difficult to account for the extremely low GA levels in grains from both transgenic and null lines from transformation with the *TaEND1::AtGA20ox1* construct. Since these results are based on only one

sample each there is a need to confirm them by measuring the other two replicates and the other two lines from the experiment.

Chapter 7. Effects of manipulating gibberellin metabolism in both the endosperm and scutellum of developing grains

7.1 Introduction

Transgenic lines expressing the *AtGA20ox1* in the endosperm using the *high molecular weight glutenin subunit* promoter (*TaHMW-GS*) (Lamacchia *et al.*, 2001) (Figure 7.1, A) and the *PcGA2ox1* gene in the embryo and scutellum using the maize *globulin 1* promoter (*ZmGlb1*) (Belanger and Kriz, 1989) (Figure 7.1, B) were previously examined in our laboratory. The lines that were engineered to produce increased levels of GA in the endosperm showed an increase in grain size, but also an increase in α-amylase content, reducing the flour quality. This was reversed in the lines engineered, to decrease GA content in the embryo and scutellum, resulting in smaller grains than controls and with reduced α-amylase content in the mature grain. To further investigate these findings and refine our ability to manipulate grain size and quality the work outlined in this chapters studies the effects of crossing these lines to combine the two genotypes.

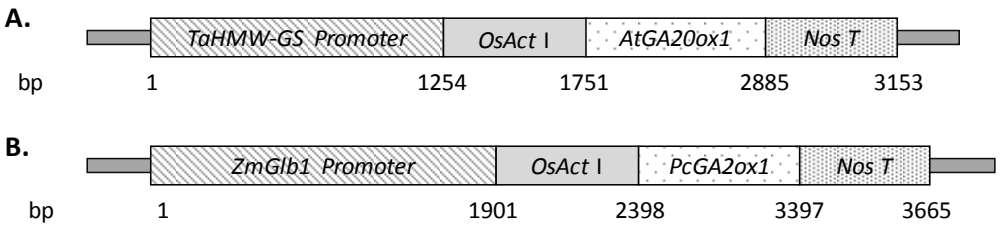


Figure 7.1: Basic schematic of *TaHMW-GS::AtGA20ox1* and *ZmGlb1::PcGA2ox1*

Basic schematic of constructs *TaHMW-GS::AtGA20ox1* (A) and *ZmGlb1::PcGA2ox1* (B). The position of junctions between elements is given in bp. The rice Actin intron is labelled *OsAct I* and the Nopaline synthase terminator labelled *Nos T*.

Prolamins which are one of the major seed storage proteins in wheat comprise of monomeric gliadins and polymeric glutenins, which includes both low (LMW-GS) and high (HMW-GS) molecular-weight glutenin subunits (Shewry and Tatham, 1990). The *HMW-GS* promoters have a major, 38 bp, regulatory enhancer (Thomas and Flavell, 1990) the location of which is highly conserved in all promoters beginning at position -185 to -189 (Shewry *et al.*, 1999). In addition this promoter also contains a G-box like motif which, in combination with the enhancer element, increases promoter activity, but is not essential for it (Norre *et al.*, 2002). The promoter sequences of *HMW-GS* genes are highly conserved in the Triticeae family and studies have shown that the sequences are more conserved in the orthologous genes than they are in the different paralogues in wheat (Anderson *et al.*, 2002, Makai *et al.*, 2015).

The seed specificity of the *HMW-GS* promoter was first shown in tobacco plants by driving the expression of the bacterial chloramphenicol acetyl transferase (CAT) gene (Colot *et al.*, 1987, Thompson *et al.*, 1985). These two studies also showed that the CAT activity was confined to the endosperm of the tobacco seeds. Robert *et al.* (1989) were the first to show in tobacco that only 433 bp of the upstream DNA sequence is required for endosperm-specific activity. Halford *et al.* (1989) further refined this to a 277-bp region upstream of the transcription start site of the *Glu-1D-5* gene that was required for tissue specific expression in tobacco. When using a 1253 bp promoter fragment, including all of the known regulatory elements to drive expression of the *UidA* (GUS) reporter gene, promoter activity was first observed in the centre of the lobes of wheat grains at 10-12 dpa and had spread throughout the endosperm by 21 dpa (Lamacchia *et al.*, 2001). In another study using 425 bp of the promoter sequence, transgene expression was also observed in the aleurone layer along with the endosperm of wheat grains from seven to 24 dpa (Furtado *et al.*, 2009). However, in the Lamacchia *et al.* (2001) study no transgene expression was observed in the aleurone layer. The ability of the *HMW-GS* promoter to be active in the aleurone layer when using a truncated version suggests that *cis*-elements acting as repressors of aleurone expression are located upstream

from the 425 bp sequence used by Furtado *et al*. (2009). Furthermore, it has been shown that the seed specificity of this promoter is lost when expressed in rice (Furtado *et al.*, 2008) which is likely to be due to the absence of species-specific transcription factors necessary for faithful expression in the heterologous system.

TaHMW-GS promoter activity was also studied during wheat grain development in our laboratory using eight independent transgenic lines expressing nuclear targeted GFP (Figure 1.15) under control of 1247 bp of the *TaHMW-GS* (Lamacchia *et al.*, 2001). In these lines strong GFP expression was observed in the endosperm of all lines from four dpa until about 53 dpa. However, confocal analysis revealed that there were often significant levels of GFP expression in non-target tissues (leaves, glumes, roots & pollen) in some of these lines. This backed up previous studies in our laboratory using the *TaHMW-GS* promoter to direct the expression of the GUS reporter where it was observed that this promoter occasionally confers constitutive-like expression, possibly due to truncations of the promoter fragment incorporated during biolistics (Vaughan, S. unpublished data).

The promoter utilised for the second construct in this study is associated with the maize *7S Globulin 1* gene (*ZmGlb1*). Glb1 is one of the most abundant proteins in maize embryos known to be positively regulated by ABA (Kriz *et al.*, 1990), however it is not essential for embryo development or germination as homozygosity for the null allele has no effect on development (Schwartz, 1979). The *Glb1* gene was shown to be expressed in the maize embryo with its levels rising from 18-24 dpa and then declining to reach a steady state from 30-42 dpa (Belanger and Kriz, 1989). These authors also observed low levels of *Glb1* transcripts in mature grains. However, they were unable to determine if this was due to continued transcription of the gene or due to mRNA stability. A 1.4-kb fragment of *Glb1* promoter was shown to drive the expression of the GUS reporter gene in the embryos of developing tobacco seeds at 15 dpa, but not in seedlings, leaves or roots. Expression was also observed in mature seeds,

but only upon ABA treatment (Liu and Kriz, 1996). Promoter deletion studies performed by Liu *et al*. (1998) showed that a 272-bp fragment in the presence of ABA was enough to drive expression of the GUS reporter gene in maize cultured cells. These authors also showed that using a longer undeleted sequence of 1391 bp resulted in a relatively lower level of GUS expression in maize cultured cells, indicating the presence of a silencer element in the promoter between -1391 and -805. ABA-responsive elements (ABREs) similar to those seen in the *Em* gene in wheat have also been identified in the promoter sequence of *Glb1* at positions -118 (Em1a), -76 (Em1b) and -161 (Em2) (Belanger and Kriz, 1991). Mutations in the Em1a element in the promoter region resulted in the abolition of GUS expression in maize cultured cells upon ABA treatment, indicating the importance of this element in regulating gene expression (Liu *et al.*, 1998). Studies in our laboratory using the *ZmGlb1* promoter to direct expression of the *UidA* gene in wheat revealed strong expression in the scutellum of developing grains. Expression was also observed to a lesser extent in the endosperm transfer layer of developing grains (Vaughan, S. unpublished data).

7.2 Results and discussion

7.2.1 Production of hybrid plants

T4 homozygous plants of transgenic lines harbouring the *TaHMW-GS::AtGA20ox1* and *ZmGlb1::PcGA2ox1* constructs were crossed according to the methods described in section 2.8. For each construct the two best lines (in terms of grain size and reduced α-amylase content) were selected as parental material and two-way crosses carried out, resulting in four crosses (Table 7.1).

Table 7.1: Crossing plan for hybrid wheat lines
Four hybrid lines (A-D) were generated by crossing two lines each harbouring either the construct *TaHMW-GS::AtGA20ox1* or *ZmGlb1::PcGA2ox1*.

Cross	Parent lines	
	TaHMW-GS::AtGA20ox1 **X**	***ZmGlb1::PcGA2ox1***
A	44.72	40.49
B	44.75	40.49
C	44.72	40.47
D	44.75	40.47

To select F1 hybrids harbouring both constructs, several grains harvested from each of the four crosses were analysed by PCR (section 2.2.2) using forward primer At20ox1-F and reverse primer At20ox1-R (Appendix 1) to genotype for the presence of *AtGA20ox1* and primers Pc2ox-F and Pc2ox-R (Appendix 1) to genotype for *PcGA2ox1*. Whilst the majority of plants tested were positive for both transgenes, a few plants only possessed one, indicating incomplete emasculation of the female parent and self-pollination had occurred on some occasions. One F1 plant positive for both the transgenes from each of the four independent crosses was selected and its F2 segregating progenies further analysed.

7.2.2 Production of homozygous material

7.2.2.1 Identifying segregating genotypes

The aim of this study was to identify in the F2 segregating progeny of each cross (Table 7.1) material homozygous for both *AtGA20ox1* and *PcGA2ox1*, homozygous for *PcGA2ox1,* homozygous for *AtGA20ox1* and null (Table 7.2) so as to compare the effects of these transgene combinations on grain size and quality in identical backgrounds and across generations.

Table 7.2: Genotypes identified for yield and quality study
The four genotypes identified from the F2 segregating progenies to be utilised for yield and quality studies. The labels shown will be used to describe each genotype in the subsequent sections.

Genotype identified	Genotype Label
Contains both *PcGA2ox1* and *AtGA20ox1* – double homozygote	**1**
Contains *PcGA2ox1* only	**2**
Contains *AtGA20ox1* only	**3**
Null	**4**

To identify these different genotypes in the segregating F2 population, 48 plants from each of the four crosses were grown according to section 2.1 and genotyped by PCR analysis (section 2.2.2) using primers described in section 7.2.1. The expected Mendelian segregation ratio for the F2 population where both parents were homozygous for the transgene is shown in table 7.3. PCR analysis was performed on 48 plants per cross as, due to the hexaploid nature of wheat, statistically there is expected to be a 1 in 48 chance of identifying a plant homozygous or null for both genes.

Table 7.3: Mendelian segregation ratio in the F2 generation
The expected segregation of F2 plants and the genotypes recognised by PCR analysis.

Zygosity	PCR genotype	Expected segregation ratio
Homozygous for both genes	+ve for both genes	1
Homozygous for one gene and hemizygous for the other		4
Hemizygous for both genes		4
Homozygous for one gene and null for the other	+ve for only one gene	2
Hemizygous for one gene and null for the other		4
Null for both the genes	Null	1

The data presented in table 7.4 shows the results obtained from the PCR analysis of the segregating F2 progeny of each cross. In three of the four crosses the segregation of the genotypes identified matched closely to that of the expected segregation shown in table 7.3. Whilst in cross A, C and D the number of plants for each genotype approximately matched the expected segregation, in cross B this was not the case. In this cross there was a larger number of plants that contained both the *AtGA20ox1* and *PcGA2ox1* transgenes resulting in fewer plants that contained only one (Table 7.4).

Table 7.4: PCR analysis of segregating F2 progeny
PCR analysis showing the number of plants identified for each of the four genotypes in each cross.

Cross	Genotype			
	+ve for both genes	+ve only *AtGA20ox1*	+ve only *PcGA2ox1*	null for both genes
A	25	9	11	3
B	33	5	7	3
C	26	9	9	4
D	26	7	10	5

7.2.2.2 TaqMan Assays to identify homozygous material

To select homozygous material for the four genotypes described in table 7.2 to be used in this study, the F2 segregating plants were further analysed by TaqMan assay (section 2.2.3 and chapter 3). This was performed using forward primer Q_At20ox-F, reverse primer Q_At20ox-R and hybridization probe Q_At20ox-probe to amplify *AtGA20ox1* and primers Q_Pc2ox-F and Q_Pc2ox-R and probe Q_Pc2ox-probe to amplify *PcGA2ox1* (Appendix 1). The ΔCt for each sample for both transgenes was calculated against the Ct values of the endogenous control gene amplified using primers HvCon2-F and HvCon2-R and probe HvCon2-probe (Appendix 1) as described in chapter 3. The assay was performed on all 48 F2 progeny for each cross, but as null segregants do not register in this assay they are not represented in the resultant graphs. The resultant TaqMan assay identified putative homozygotes for each of the target genotypes (Table 7.2) for all four initial crosses (Figures 7.2 - 7.5) where plants were selected based on their relative ΔCt values. For these plants zygosity selections were based only on ΔCts and not the normalised values as previous results showed this was the more reliable parameter. For each of the four crosses, plants that had a low ΔCt value for both of the transgenes were selected as putative double homozygotes (*AtGA20ox* and *PcGA2ox* – genotype 1), plants with a low ΔCt value for only a single transgene were selected as

putative homozygotes for each individual gene (Genotypes 2 and 3) and a null line (Genotype 4) was also taken through from each cross as a control.

However, the selection of homozygous material in these lines was not always straightforward due to the presence of two transgenes. In crosses B and C all plants selected displayed ΔCt values within an acceptable range for the different genotypes required (Figures 7.3 and 7.4). However, in cross A, of the three plants selected as potential double homozygotes (Figure 7.2), only two plants displayed a low ΔCt value for both the transgenes. Plant A7 whilst having a low ΔCt for *PcGA2ox1*, displayed a high *AtGA20ox1* ΔCt (outside of the desired 1 cycle range). However, in spite of this, this plant was selected as it displayed the best result compared to the remaining plants in this cross. In cross D, whilst plants were identified as double homozygous and only homozygous for *AtGA20ox1* (Figure 7.5), a plant could not be identified as only homozygous for *PcGA2ox1*, as all plants that displayed a low ΔCt value for *PcGA2ox1* were also positive for the *AtGA20ox1* gene. The plant with the lowest ΔCt for *PcGA2ox1,* whilst also being null for *AtGA20ox1,* was therefore selected as putative for this genotype.

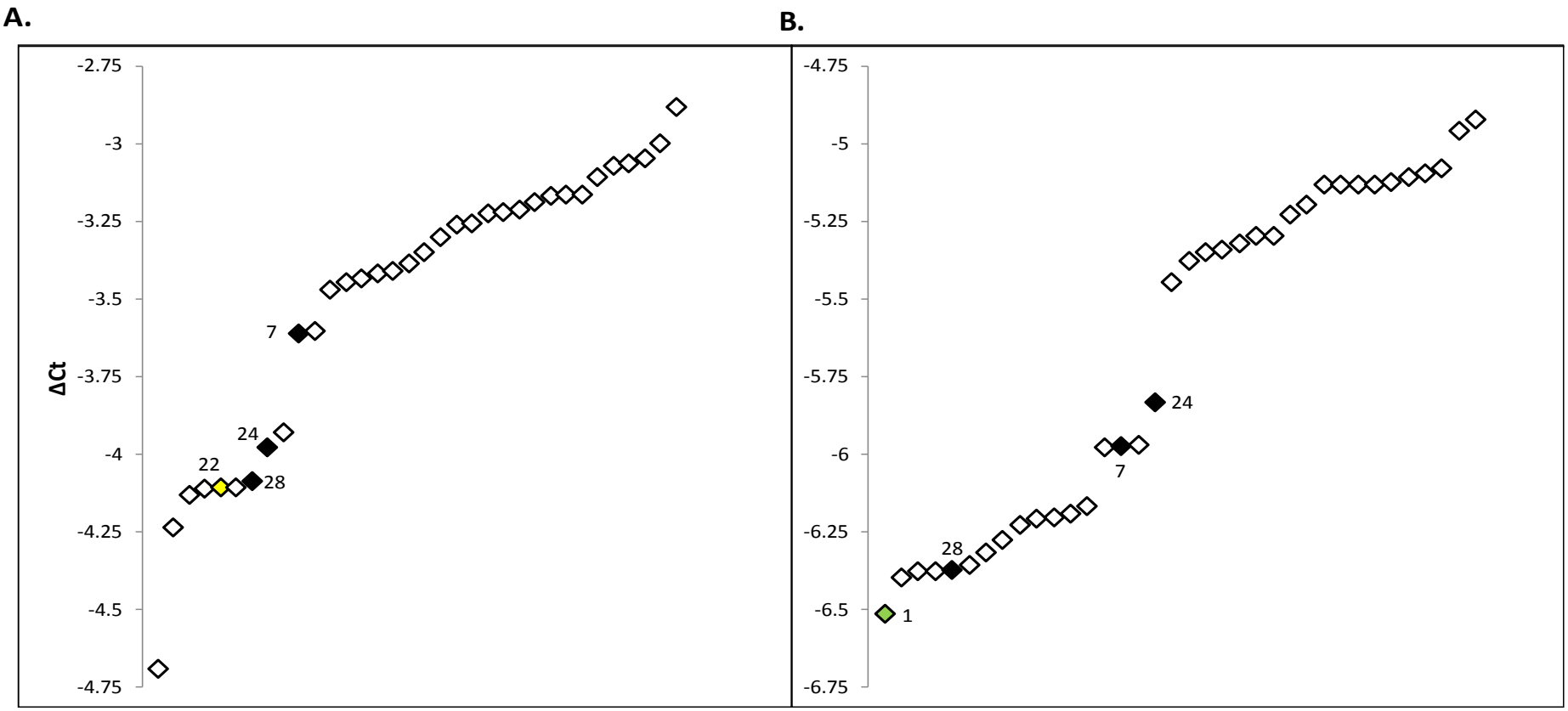


Figure 7.2: TaqMan assay for F2 progeny resulting from cross A

ΔCt for *AtGA20ox1* (A) and *PcGA2ox1* (B) in cross A. Each box contains values for positive progeny for that transgene. Coloured plots represent those plants selected as potential homozygotes for further analysis - Black diamonds: putative homozygotes for both transgenes; yellow diamond: putative homozygote for *AtGA20ox1*, green diamond: putative homozygote for *PcGA2ox1*. Specific plant numbers are indicated in each plot.

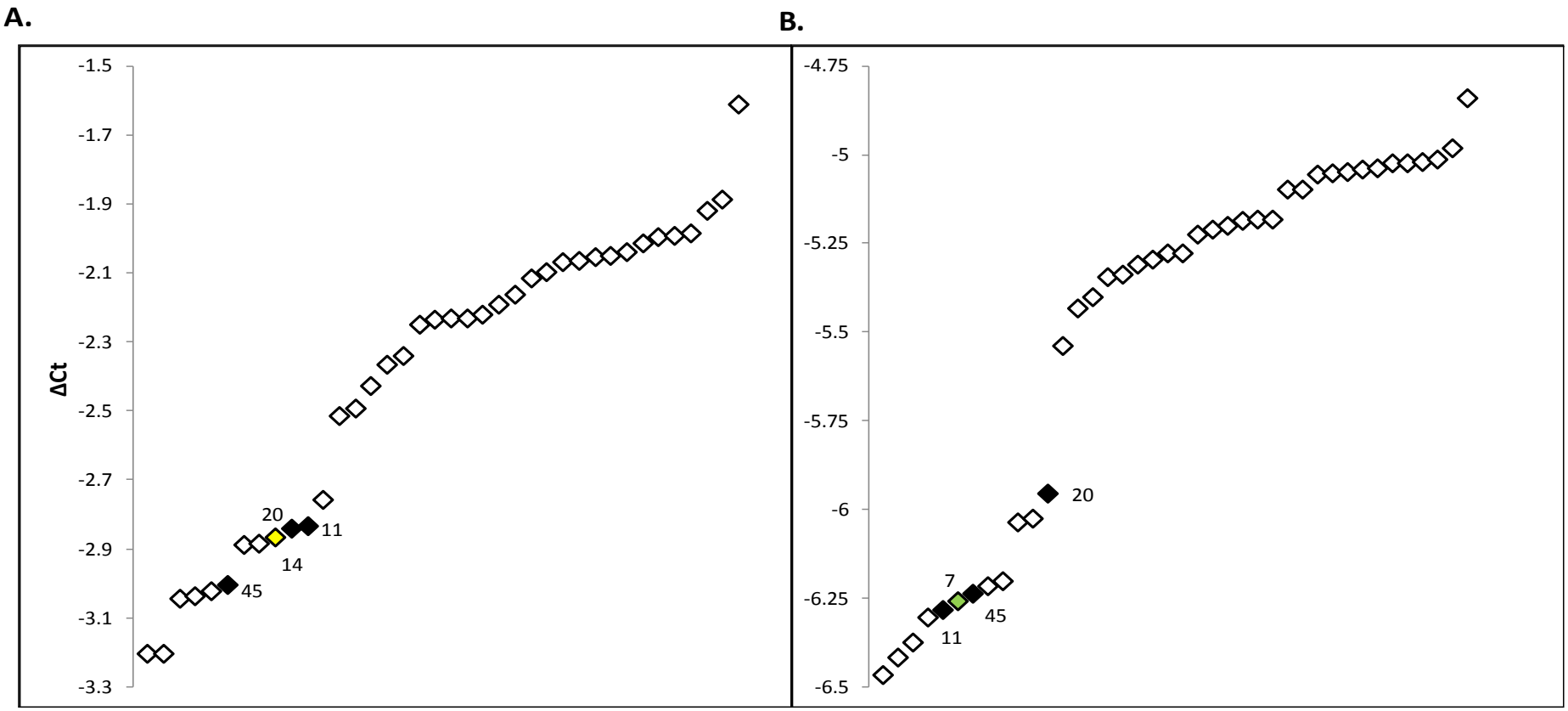


Figure 7.3: TaqMan assay for F2 progeny resulting from cross B

ΔCt for *AtGA20ox1* (A) and *PcGA2ox1* (B) in cross B. Each box contains values for positive progeny for that transgene. Coloured plots represent those plants selected as potential homozygotes for further analysis - Black diamonds: putative homozygotes for both transgenes; yellow diamond: putative homozygote for *AtGA20ox1*, green diamond: putative homozygote for *PcGA2ox1*. Specific plant numbers are indicated in each plot.

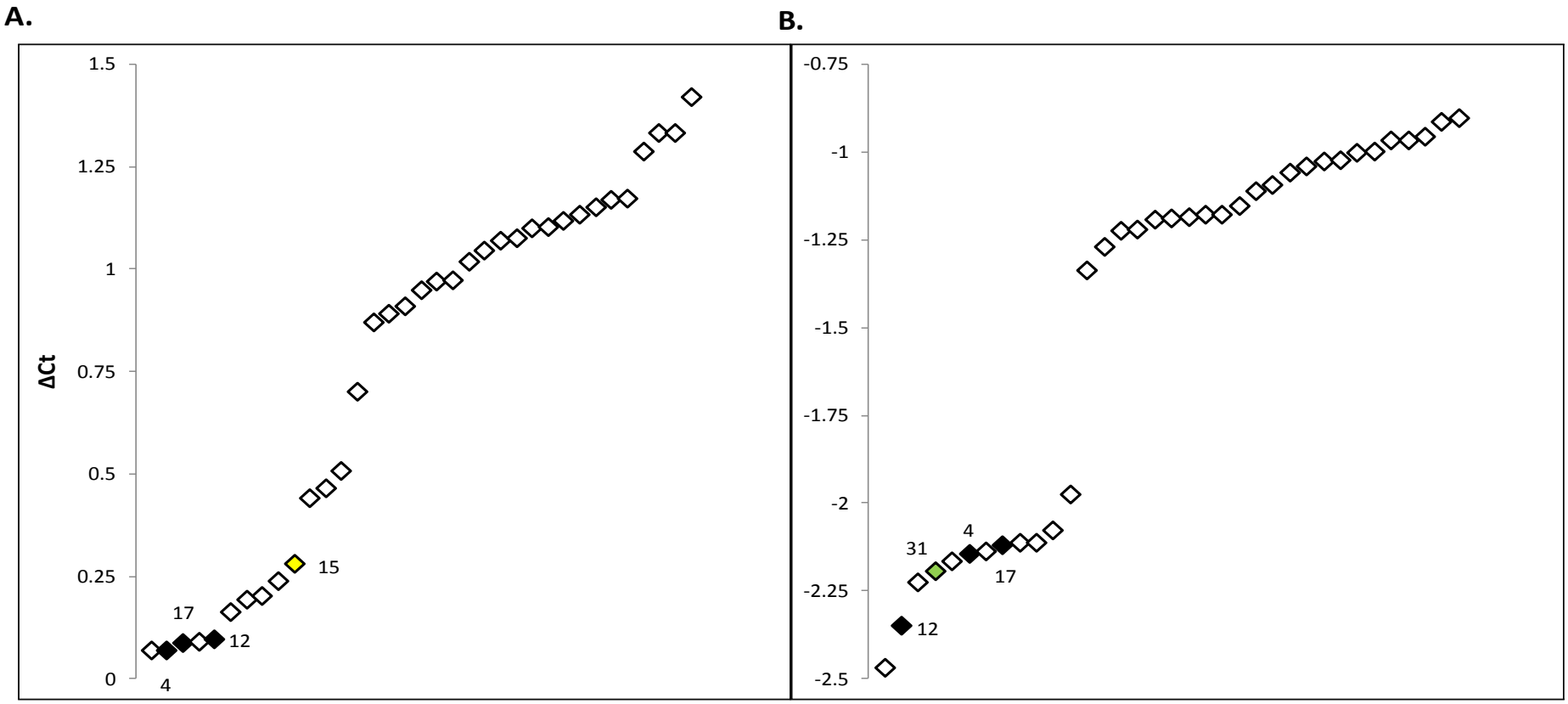


Figure 7.4: TaqMan assay for F2 progeny resulting from cross C

ΔCt for *AtGA20ox1* (A) and *PcGA2ox1* (B) in cross C. Each box contains values for positive progeny for that transgene. Coloured plots represent those plants selected as potential homozygotes for further analysis - Black diamonds: putative homozygotes for both transgenes; yellow diamond: putative homozygote for *AtGA20ox1*, green diamond: putative homozygote for *PcGA2ox1*. Specific plant numbers are indicated in each plot.

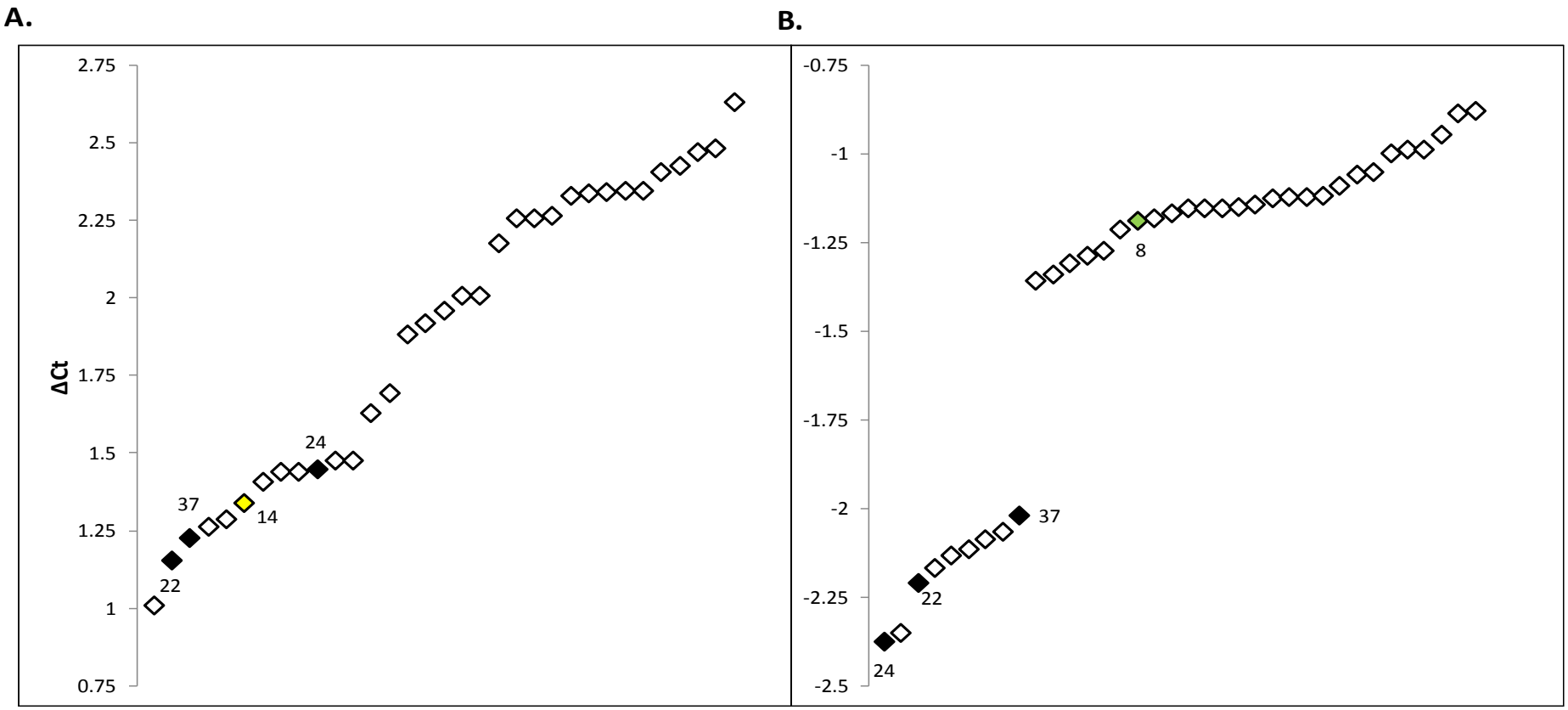


Figure 7.5: TaqMan assay for F2 progeny resulting from cross D

ΔCt for *AtGA20ox1* (A) and *PcGA2ox1* (B) in cross D. Each box contains values for positive progeny for that transgene. Coloured plots represent those plants selected as potential homozygotes for further analysis - Black diamonds: putative homozygotes for both transgenes; yellow diamond: putative homozygote for *AtGA20ox1*, green diamond: putative homozygote for *PcGA2ox1*. Specific plant numbers are indicated in each plot.

7.2.2.3 PCR analysis to confirm zygosity of F3 plants

For each of the four crosses, 24 F3 progenies from those F2 lines putatively assigned as homozygous for both *AtGA20ox1* and *PcGA2ox1*, homozygous for *PcGA2ox1,* homozygous for *AtGA20ox1* or null were genotyped. These plants were examined by PCR analysis (section 2.2.2) using primers as described in section 7.2.1. This analysis was performed to confirm the zygosity assessment using the TaqMan assays (Figures 7.2 - 7.5). As table 7.5 shows not all the plants selected through the TaqMan assay displayed the expected genotype. Unfortunately, from cross A plant A28 died and as discussed in section 7.2.2.2 this was one of two plants that displayed the best ΔCt results for both the transgenes. The other two plants selected – A7 and A24 – were each homozygous for only one transgene and hemizygous for the other, resulting in this cross not having a double homozygote. In cross D, plant D8 was selected as the best option for a *PcGA2ox1* homozygous genotype (Section 7.2.2.2, Figure 7.5) but as table 7.4 shows this plant was not homozygous for the *PcGA2ox1* gene. However, the expected genotypes were confirmed for all lines selected for crosses B and C enabling a full analysis of this material representing the full complement of four genotypes in the same background for two sets of parental material. Table 7.5 shows the zygosity analysis for each line that was taken through to yield and quality experiments.

Table 7.5: Zygosity analysis and genotype confirmation in F3 transgenic lines

Results of PCR on F3 generation plants to confirm TaqMan assay results. Rows in bold represent lines taken through for further experimentation.

Line	Zygosity				Genotype
	PcGA2ox1		***AtGA20ox1***		
	+ve	**-ve**	**+ve**	**-ve**	
A 7	24	0	22	2	*PcGA2ox1* homozygous / *AtGA20ox1* hemizygous
A 24	15	9	24	0	*PcGA2ox1* hemizygous / *AtGA20ox1* homozygous
A 1	**24**	**0**	**0**	**24**	***PcGA2ox1* homozygous / *AtGA20ox1* null (A2)**
A 22	**0**	**24**	**24**	**0**	***PcGA2ox1* null / *AtGA20ox1* homozygous (A3)**
A12	**0**	**24**	**0**	**24**	**Null (A4)**
B 20	**24**	**0**	**24**	**0**	***PcGA2ox1* homozygous / *AtGA20ox1* homozygous (B1)**
B 11	24	0	24	0	*PcGA2ox1* homozygous / *AtGA20ox1* homozygous
B 45	24	0	24	0	*PcGA2ox1* homozygous / *AtGA20ox1* homozygous
B 7	**24**	**0**	**0**	**24**	***PcGA2ox1* homozygous / *AtGA20ox1* null (B2)**
B 14	**0**	**24**	**24**	**0**	***PcGA2ox1* null / *AtGA20ox1* homozygous (B3)**
B18	**0**	**24**	**0**	**24**	**Null (B4)**
C 4	**24**	**0**	**24**	**0**	***PcGA2ox1* homozygous / *AtGA20ox1* homozygous (C1)**
C 12	24	0	24	0	*PcGA2ox1* homozygous / *AtGA20ox1* homozygous
C 17	24	0	24	0	*PcGA2ox1* homozygous / *AtGA20ox1* homozygous
C 31	**24**	**0**	**0**	**24**	***PcGA2ox1* homozygous / *AtGA20ox1* null (C2)**
C 15	**0**	**24**	**24**	**0**	***PcGA2ox1* null / *AtGA20ox1* homozygous (C3)**
C13	**0**	**24**	**0**	**24**	**Null (C4)**
D 24	**24**	**0**	**24**	**0**	***PcGA2ox1* homozygous / *AtGA20ox1* homozygous (D1)**

D 22	24	0	24	0	*PcGA2ox1* homozygous / *AtGA20ox1* homozygous
D 37	24	0	24	0	*PcGA2ox1* homozygous / *AtGA20ox1* homozygous
D 8	19	5	0	24	*PcGA2ox1* hemizygous / *AtGA20ox1* null
D 14	**0**	**24**	**24**	**0**	***PcGA2ox1* null / *AtGA20ox1* homozygous (D3)**
D7	**0**	**24**	**0**	**24**	**Null (D4)**

7.2.3 Experimental design of grain yield and quality studies in *TaHMW-GS::AtGA20ox1* X *ZmGlb1::PcGA2ox1* hybrid lines

Yield and quality studies were performed to examine the effects of co-expressing the *AtGA20ox1* and *PcGA2ox1* genes in wheat grain, expressed in the endosperm and embryo, respectively. Double homozygotes were assessed alongside sister lines expressing either the *AtGA20ox1* or *PcGA2ox1* genes with null segregants and a wild-type Cadenza as a control. A single RCBD experiment was setup as described in section 2.1.1 with three replicates of the different genotypes described in Table 7.5 along with a wild-type control. In this experiment two plants were grown in 20-cm pots for each line and cut back to five tillers each. One plant in each pot was left till maturity and all five ears harvested to measure yield and analyse various quality parameters. Grains from ears two and three of the second plant were harvested at 14 and 42 dpa to measure transcript levels of the transgene. These two ears were each assigned a time point in a randomised manner.

7.2.4 Transgene expression of *AtGA20ox1* and *PcGA2ox1*

To confirm expression of the introduced transgenes transcript levels of the two genes were measured in cDNA synthesised (section 2.2.6) from RNA extracted as described in sections 2.2.4 and 2.2.5 from 14 and 42 dpa grains. Due to time and resource constraints this analysis was performed only on samples harvested from crosses B and C where all four homozygous genotypes were available. These grains were harvested from either ear two or three from three biological replicates of the different genotypes and the wild type control. qRT-PCR was performed on this material according to section 2.2.7 using forward primer q_At20ox1_F1 and reverse primer q_At20ox1_R1 (Appendix 1) to amplify the *AtGA20ox1* transgene and primers Q_Pc2ox-F2 and Q_Pc2ox-R2 (Appendix 1) to amplify *PcGA2ox1*. The expression of both the transgenes at each time point (Figure 7.6) was normalised against the expression of three endogenous genes – *Ta2526*, *TaSDH* and *TaGapDH* (section 2.2.7 and appendix 1). The data presented in figure 7.6 is an average of the NRQs of three biological replicates, except for lines B2 and C4 at 42 dpa, where cDNA synthesis of one sample in each failed. The qRT-PCR was performed on all four genotypes of both the crosses and the wild type control. However, as no expression of either transgene was observed in the nulls or the wild type control these are marked with 'X's in the figures presented (Figure 7.6). Since lines B2, B3, C2 and C3 contain only one of the two transgenes absence of expression for the other transgene is also represented by an 'X' in figure 7.6.

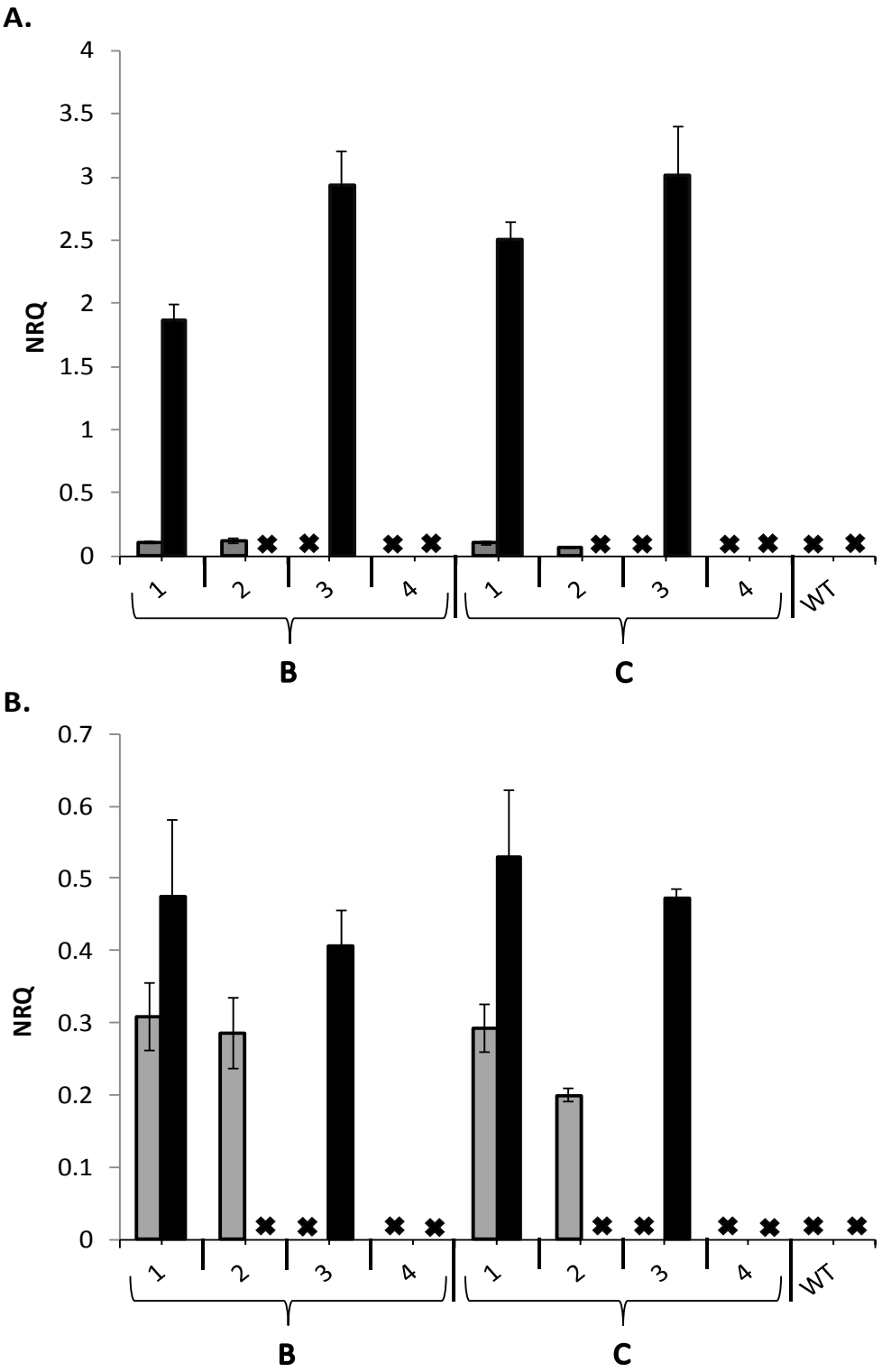


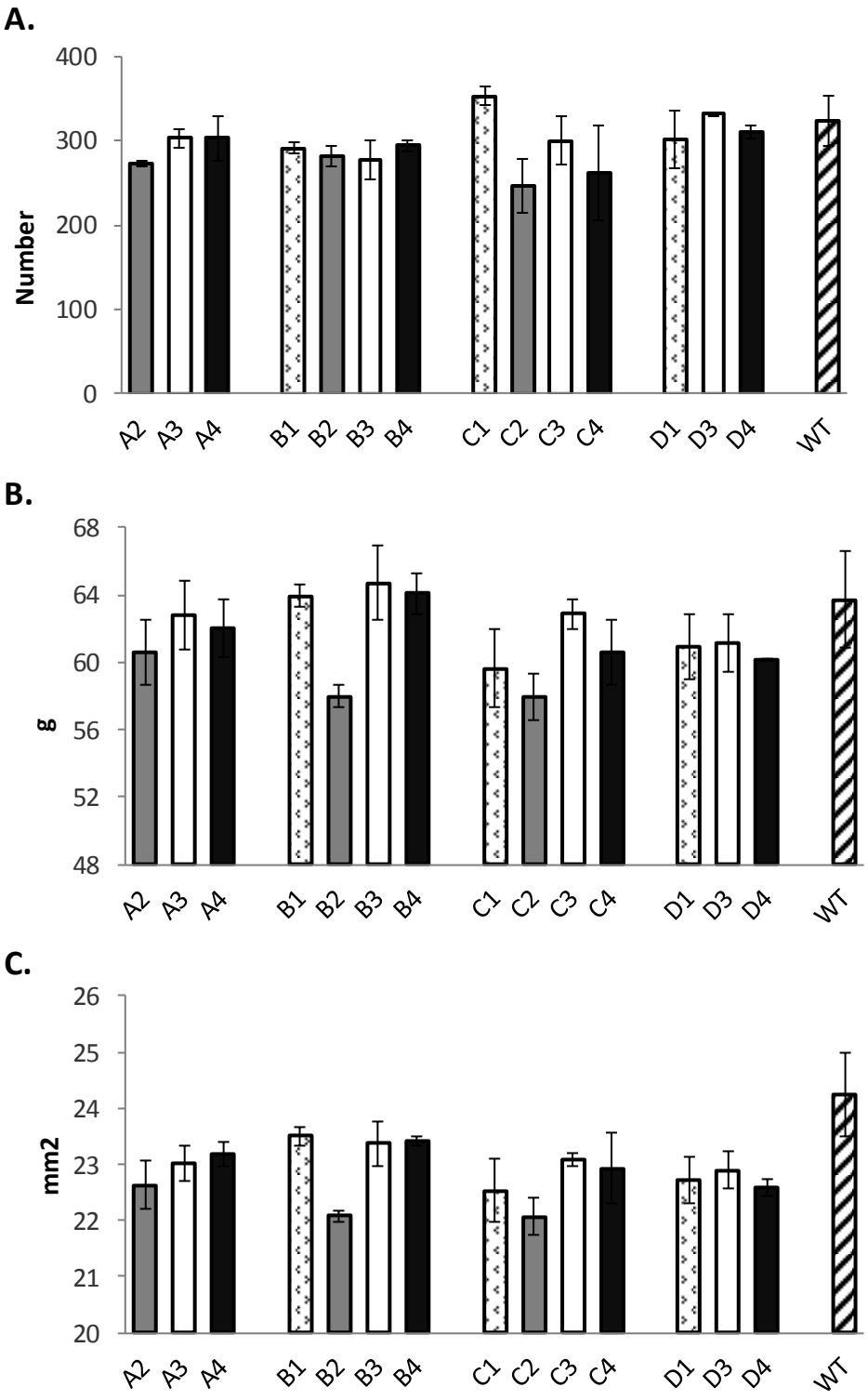
Figure 7.6: NRQs of *AtGA20ox1* and *PcGA2ox1* expression in *TaHMW-GS::AtGA20ox1* X *ZmGlb1::PcGA2ox1* transgenic lines.

Average of normalised expression levels at 14 dpa (A) and 42 dpa (B) grains as measured in three biological replicates of each genotype in cross B, C and wild type. 1: double homozygote, 2: *PcGA2ox1* only, 3: *AtGA20ox1* only and 4: null. Grey bars – *PcGA2ox1* expression, black bars – *AtGA20ox1* expression and X – no expression. Vertical error bars denote SEM.

As previously described, lines B1 and C1 express both transgenes; B2 and C2 express only *PcGA2ox1*; B3 and C3 only *AtGA20ox1* and lines C4, B4 and wild-type express neither. Whilst the expression of the *PcGA2ox1* transgene was lower than that of *AtGA20ox1* at both 14 dpa (Figure 7.6, A) and 42 dpa (Figure 7.6, B), neither gene displayed large biological variation, within or between crosses. The expression of both *PcGA2ox1* and *AtGA20ox1* in these plants at both time points was similar to that seen in the parent lines previously studied in our laboratory. In the current experiment the difference in expression levels between the two transgenes was much bigger at 14 dpa with the expression of *AtGA20ox1* being highest in line C3 at 3.04 and the expression of *PcGA2ox1* lowest in line C2 at 0.069, showing a 44-fold difference. However, at 42 dpa only a 2.65-fold difference was observed with line C1 showing the highest expression of *AtGA20ox1* at 0.53 and line C2 the lowest expression of *PcGA2ox1* at 0.2.

7.2.5 Analysis of *TaHMW-GS::AtGA20ox1* X *ZmGlb1::PcGA2ox1* effects on yield

To study the effects of co-expressing the *AtGA20ox1* and *PcGA2ox1* transgenes on grain yield, mature grain harvested from five ears (taken as a standardised proxy for total yield) was assessed according to the methods described in sections 2.3 and 2.4.1. The MARVIN digital seed counter was used to count the number of grains and measure their surface area, length and width. These grains were then weighed to calculate TGW. The measurements for diameter were obtained from SKCS as described in section 2.4.1. The data presented in figure 7.7, A-F shows the average values for three biological replicates of each line. Due to the unbalanced nature of this experiment, REML (section 2.6) was used to analyse the significance of differences between the different genotypes and to extract within-line variance components. For all variables, the plants were assessed using LSD at 5% at the overall population level based on the presence or absence of each transgene.


A.
Number
400
300
200
100
0
A2 A3 A4 B1 B2 B3 B4 C1 C2 C3 C4 D1 D3 D4 WT
B.
g
68
64
60
56
52
48
A2 A3 A4 B1 B2 B3 B4 C1 C2 C3 C4 D1 D3 D4 WT
C.
mm2
26
25
24
23
22
21
20
A2 A3 A4 B1 B2 B3 B4 C1 C2 C3 C4 D1 D3 D4 WT

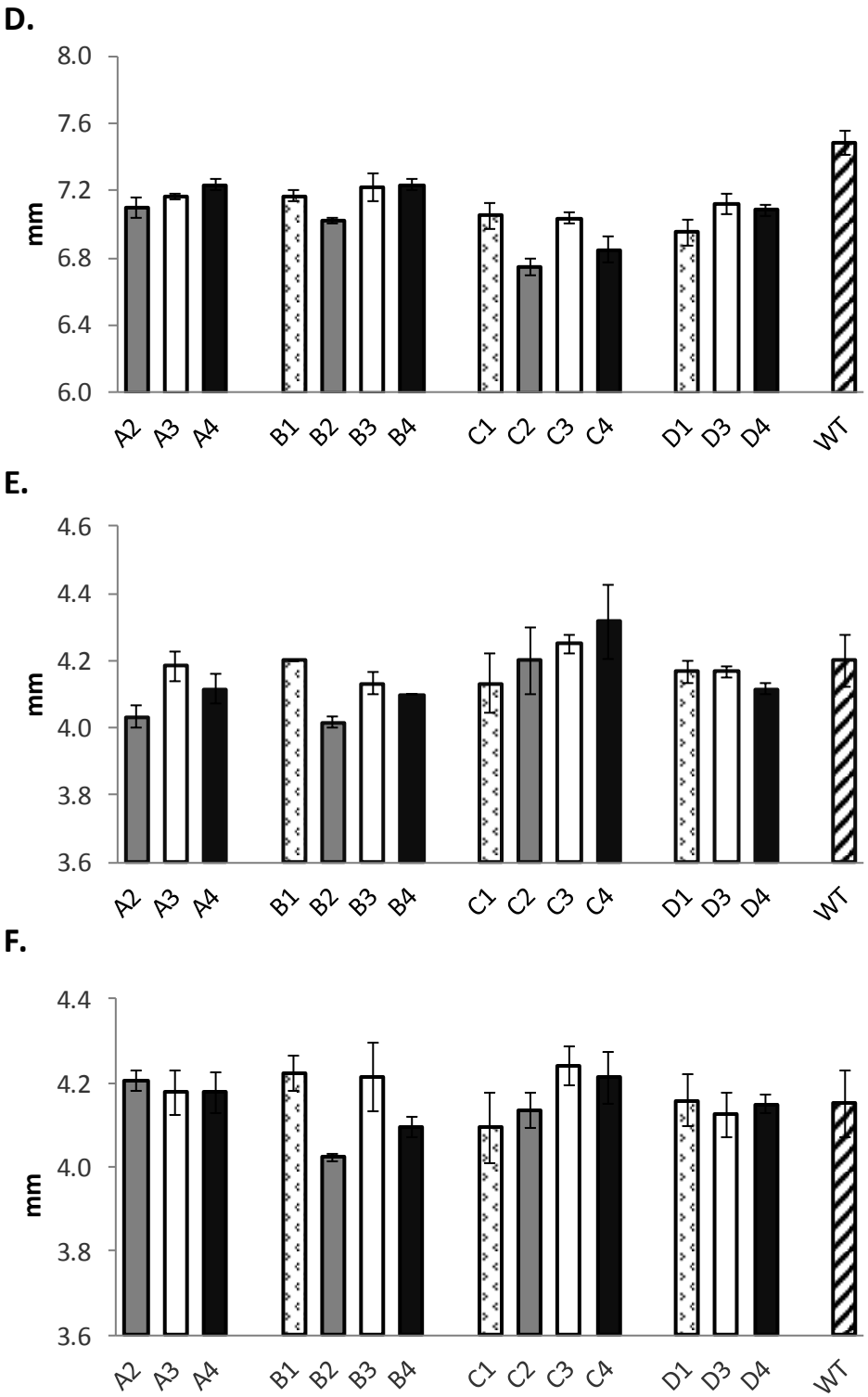


Figure 7.7: Analysis of yield components on *TaHMW-GS::AtGA20ox1* X *ZmGlb1::PcGA2ox1* hybrid lines

Averages are presented for several variables: grain number (A), TGW (B) grain surface area (C) grain length (D), grain width (E) and grain diameter (F) for measurements on mature grains. Dotted bars: 1 - double homozygote, grey bars: 2 - *PcGA2ox1* only, white bars: 3 - *AtGA20ox1* only, black bars: 4 - null and hatched bars: WT. Vertical error bars represent SEM. Note that for clarity the scale of the *y*-axis has been expanded in panels B-F.

The grain number (Figure 7.7, A) for the various lines when analysed at the population level showed no significant differences and in cross A, B and D this was similar in all lines within each cross; however, in cross C the double homozygote displayed a higher number of grains compared to the rest of the lines in this cross. For TGW (Figure 7.7, B) significant differences were observed when plants were analysed at the population level and those expressing the *PcGA2ox1* gene ($p = 0.025$, F-test = 5.59), when averaged, weighed significantly less than those not expressing this gene. However, when looking at the four genotypes (Table 7.2) individually within each cross, whilst the *PcGA2ox1* only lines displayed a trend towards a reduction in TGW compared to the other lines in the cross, the double homozygotes did not. The double homozygote in the three crosses, where present, displayed TGW higher than the *PcGA2ox1* only lines and similar to the *AtGA20ox1* only and null lines within the cross. These results indicate that whilst the expression of the *PcGA2ox1* transgene results in the reduction of grain weight, co-expression of the *AtGA20ox1* gene is able to counteract this effect, resulting in grains in the double homozygote with comparable weights to their *AtGA20ox1* only and nulls plants.

The surface area measurements (Figure 7.7, C) were also analysed to study overall effects of the two transgenes by REML using LSD at 5%. When analysed at the population levels the wild type plants were an outlier and these grains had a significantly larger area than the rest of the plants ($p = 0.002$, F-test = 12.26). For this variable as well plants that expressed the *PcGA2ox1* gene, when averaged, had a significantly smaller area than those not expressing this gene ($p = 0.025$, F-test = 5.58). However, again, when looking at the individual genotypes within each cross, similar trends as those seen for TGW were observed. The *PcGA2ox1* only lines showed a reduction in area compared to the other lines in the cross, which was not displayed by the double homozygotes. The area of the double homozygotes in each cross was similar to the *AtGA20ox1* only and null lines in that cross. Taken together these results also indicate that the *PcGA2ox1* genes appears to apply the most influence on grain size and the presence of the *AtGA20ox1* gene is able to negate this effect.

The measurements for length (Figure 7.7, D) when assessed by REML using LSD at 5% showed the largest variation between the different genotypes. The wild-type grains again appeared to be an outlier and were significantly larger than the rest of the plants ($p < 0.001$, F-test = 53.07). For grain length as well plants expressing *PcGA2ox1*, when averaged, had smaller length than those not containing this transgene ($p = 0.002$, F-test = 11.60). Differences were also observed when grain lengths in plants expressing the *AtGA20ox1* gene were averaged, with these plants having smaller grains than plants not expressing this gene ($p = 0.01$, F-test = 7.52). However, when looking at the individual genotypes, cross B and C both displayed similar trends as those seen for TGW and area with the *PcGA2ox1* only lines having shorter grain and the double homozygote having similar length to the rest of the lines in the cross. In addition, in cross C significant difference was observed ($p = 0.15$, F-test = 4.12) where plants that expressed the *AtGA20ox1* gene had significantly longer grains than those without the gene, with both the double homozygote and *AtGA20ox1* only lines being larger than *PcGA2ox1* only and null lines. However, in cross D the double homozygote did not display the same level of recovery in length as that shown by those in cross B and C, containing smaller grain than the *AtGA20ox1* only and null lines. Taken together these results also indicate that whilst the presence of the *PcGA2ox1* gene results in a reduction in grain length the co-expression of the *AtGA20ox1* gene is able to negate this effect and in cross C appears to be having a positive effect, resulting in significantly larger grains.

The measurements for grain width and diameter (Figure 7.7, E and F) when analysed at the population level did not display any significant differences and in cross C the double homozygote showed a reduction in both variables compared to the rest of the lines in that cross. This could possibly be due to the increase in grain number seen in this line (Figure 7.7 A) potentially reducing the amount of resources available to the grains. However, for both grain width and diameter cross B displayed similar trends as those seen for the other yield variables measured. Here the *PcGA2ox1* only and null lines were smaller than

the double homozygote and *AtGA20ox1* only lines, implying that the *PcGA2ox1* gene has similar effect on grain width and diameter as it does on other yield variables, and the *AtGA20ox1* gene is at least in part able to overcome this.

7.2.5 Analysis of *TaHMW-GS::AtGA20ox1* X *ZmGlb1::PcGA2ox1* effects on quality

7.2.5.1 Grain hardness and moisture content

The grains analysed in section 7.2.3.3 were further assessed for grain quality by measuring their grain hardness and moisture content using the SKCS system as described in section 2.4.1. The data presented in figure 7.8 A and B shows the average values for three biological replicates for each line. These results were also analysed by REML (section 2.6) as described in section 7.2.5 and for both variables, the plants were assessed at the overall population level based on the presence or absence of each transgene. Grain hardness measurements (Figure 7.8, A) were assessed to study the overall effects of the two transgenes using LSD at 5% and significant differences were observed for the effect of *AtGA20ox1* within crosses B and D ($p = 0.009$, F-test = 4.58). In both these crosses the double homozygote and *AtGA20ox1* only plants displayed a significant reduction in hardness index compared to the other lines in the cross. In cross C an inverse trend to that observed for grain width and diameter was seen with the double homozygote having the highest hardness index, although this was not significant. These results agree with previous work done on the *ZmGlb1::PcGA2ox1* parent lines where transgenic grains which showed reduction in width also displayed an increase in hardness index and moisture content. These lines also showed a change in the cellular structure of the grains where the transgenic lines showed the presence of a larger number of smaller cells, possibly resulting in the changes seen in grain hardness and moisture content.

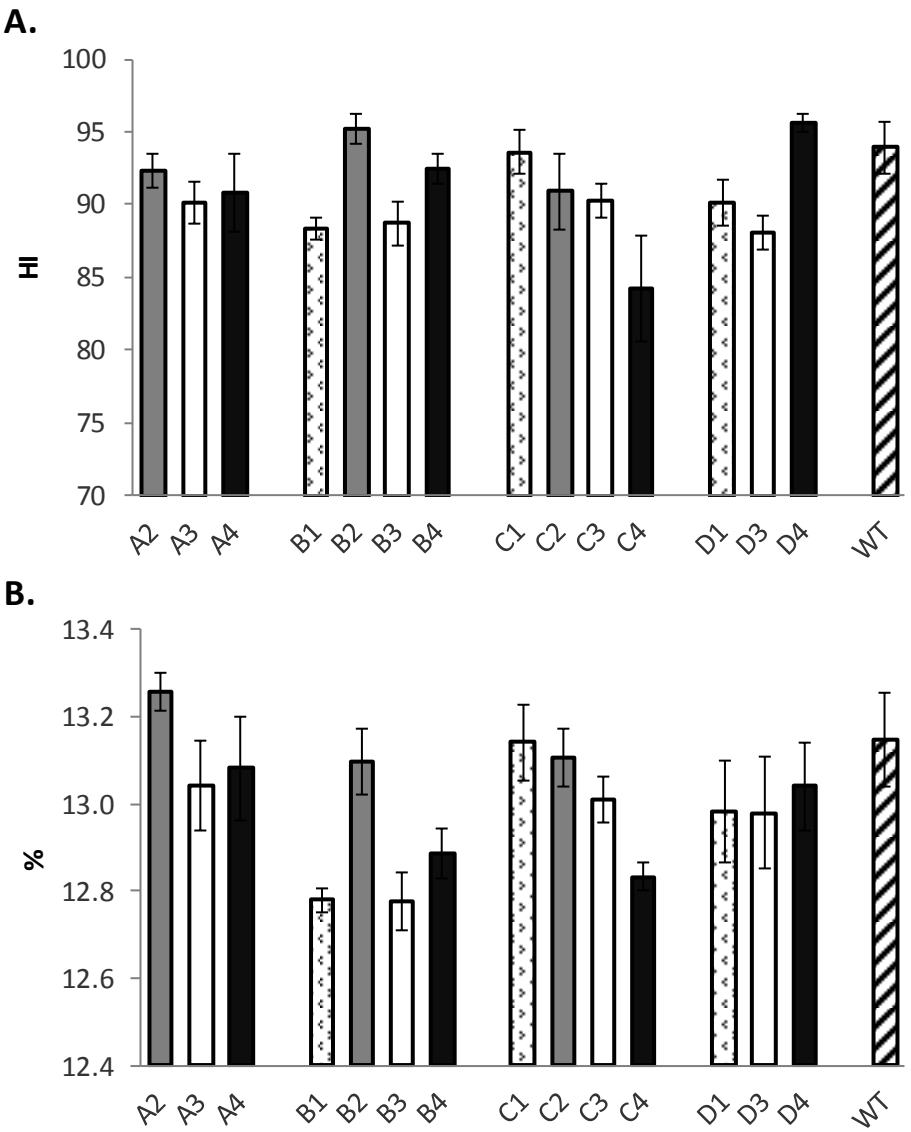


Figure 7.8: Analysis of grain hardness and moisture content on *TaHMW-GS::AtGA20ox1 X ZmGlb1::PcGA2ox1* hybrid lines

Averages are presented for: grain hardness (A) and moisture content (B) for measurements on mature grains. Dotted bars: 1 - double homozygote, grey bars: 2 - *PcGA2ox1* only, white bars: 3 - *AtGA20ox1* only, black bars: 4 - null and hatched bars: WT. Vertical error bars represent SEM. Note that for clarity the scale of the *y*-axis has been expanded.

The moisture content (Figure 7.8, B) in these lines showed an effect of *PcGA2ox1* where plants expressing this gene had higher moisture than those not expressing this gene ($p = 0.007$, F-test= 8.45). When looking at the

individual genotypes within each cross similar trends as those seen for grain hardness were observed. In crosses B and D the double homozygote and *AtGA20ox1* only plants displayed a significant reduction in moisture content compared to the other lines in the cross. In addition cross C also displayed the same trend with the double homozygote displaying an increase in moisture content compared to the rest. Taken together these results indicate that lines which display a reduction in width also show an accompanying increase in grain hardness and moisture content, although this relationship has not been analysed statistically.

7.2.5.2 α-amylase and nitrogen content

Grains crushed during the SKCS analysis of crosses B and C were collected and α-amylase and nitrogen content of these were assessed. These crushed grains were milled to a fine flour and α-amylase measured on 25 mg of this material according to section 2.4.2. The data presented in figure 7.9 A are an average of three biological replicates for each line. The α-amylase content across the different lines showed a broad range with the highest value being 0.56 CU/g (wild-type) and the lowest 0.13 CU/g (line B2 – *PcGA2ox1* only) (Figure 7.9, A). The different genotypes were assessed at the population level by ANOVA using LSD at 5% and the wild-type was an outlier having significantly higher α-amylase compared to the rest of the plants ($p = 0.030$, F-test = 5.64). Within each cross, whilst cross B displayed a trend towards a reduction in α-amylase in lines that expressed the *PcGA2ox1* gene, cross C did not show this. In cross B, both the double homozygote and *PcGA2ox1* only plants had lower α-amylase compared to the *AtGA20ox1* only and null lines. Whereas in cross C only the double homozygote line had lower α-amylase than the *AtGA20ox1* only and null plants. However, no statistical significance was observed for the differences between any of the genotypes in either construct. The reduction in α-amylase levels in both double homozygotes compared to the nulls and *AtGA20ox1* only lines though not significant does present an interesting result.

However, all lines also showed a large degree of biological variation, possibly due to the stochastic nature of the α-amylase enzyme resulting in a difficulty in making definite conclusions about the effects of the two transgenes on α-amylase.

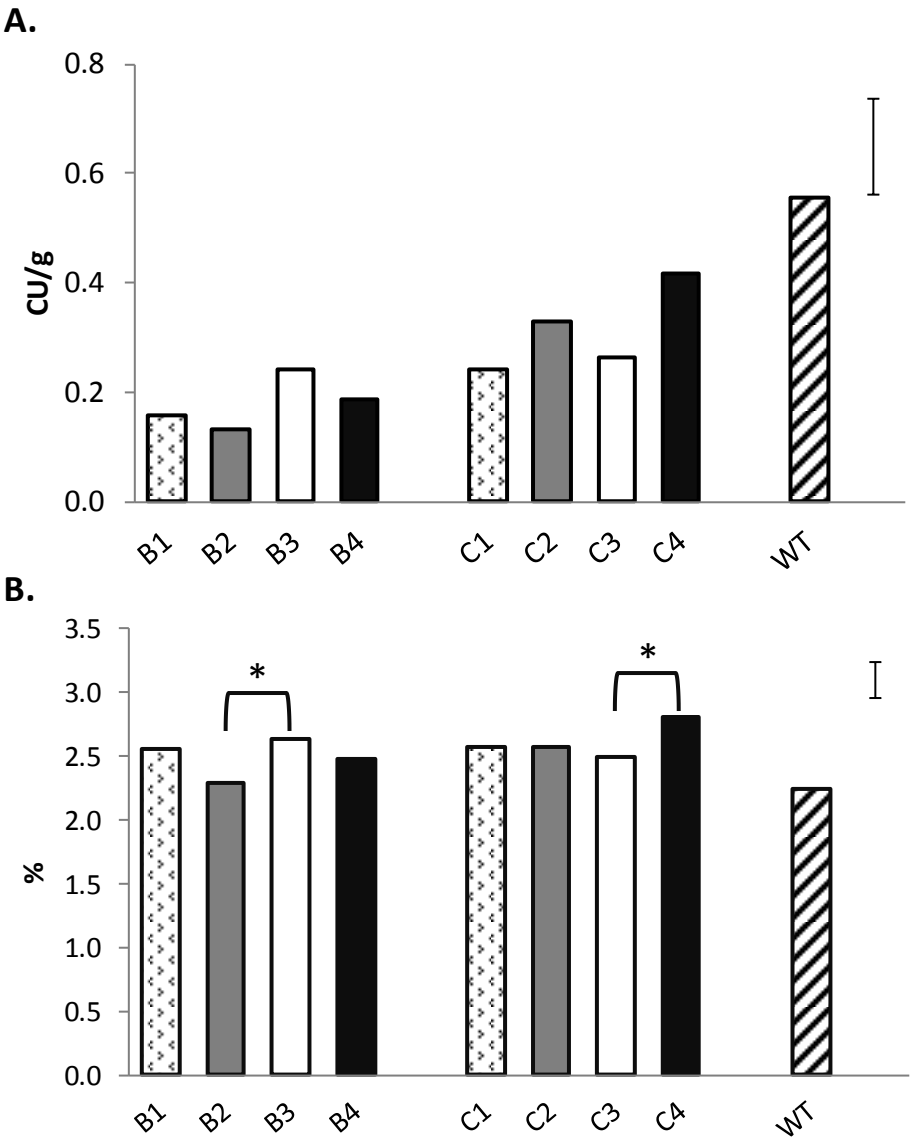


Figure 7.9: Analysis of α-amylase and nitrogen of *TaHMW-GS::AtGA20ox1* X *ZmGlb1::PcGA2ox1* hybrid lines

Averages are presented for α-amylase (A) and nitrogen content (B) on mature grains. Dotted bars: 1 - double homozygote, grey bars: 2 - *PcGA2ox1* only, white bars: 3 - *AtGA20ox1* only, black bars: 4 - null and hatched bars: WT. * denotes significant difference between a transgenic and its null using LSD at 5%: p value at – *: ≤ 0.05. Vertical error bars represent SED on 20 df.

The percentage of nitrogen in the grains was also measured (as a proxy for protein content) according to section 2.4.3 (Figure 7.9, B). The difference between the hybrid plants and wild type was assessed at the population level by ANOVA using LSD at 5%. For this variable as well the wild-type was an outlier and had significantly lower nitrogen content compared to the rest of the plants ($p = 0.007$, F-test = 9.52). Significant differences ($p = 0.049$, F-test = 3.03) were also observed between the different genotypes within the crosses. Whilst the *PcGA2ox1* only line in cross B had significantly lower nitrogen than the *AtGA20ox1* only line, in cross C the *AtGA20ox1* only line showed a significant reduction compared to the null. The inconsistency in these results indicate that possibly the expression of the two transgenes was not having an effect on the nitrogen levels in the grain.

7.3 Conclusions

The aim of the work described in this chapter was to examine the effects of co-expressing the *AtGA20ox1* and *PcGA2ox1* transgenes in the endosperm and embryo, respectively, of developing grains. Hybrid plants were generated by crossing T4 homozygous lines harbouring each construct and the resulting progeny taken through three generations to produce homozygous material representing four genotypes (1: *AtGA20ox1* + *PcGA2ox1*, 2: *PcGA2ox1* only, 3: *AtGA20ox1* only and 4: null) for each cross. A TaqMan assay was successful in identifying all the desired genotypes in two of the four crosses (B and C), whilst in the remaining two only three of the four genotypes could be identified.

Whilst grains in the parent lines harbouring the *TaHMW-GS::AtGA20ox1* construct displayed a 8.3 - 12.5% increase in weight compared to the wild-type (Vaughan, S. unpublished data), this result was not observed in the hybrid lines. However, all of the *AtGA20ox1* only lines displayed a trend towards an increase in weight compared to their nulls. In this experiment the *PcGA2ox1* transgene appeared to be negatively influencing grain weight with the *PcGA2ox1* only lines being lighter than their nulls. However, co-expression of the *AtGA20ox1* transgene was able to overcome this negative effect in the double homozygotes with their weights being similar to the null lines. The *PcGA2ox1* transgene also appeared to have a similar effect on area with the *PcGA2ox1* only being smaller than the nulls and, also for this variable, the *AtGA20ox1* transgene was able to overcome this negative effect in the double homozygote with their size being comparable to the *AtGA20ox1* only and null plants. The measurements of grain length whilst displaying similar trends as those observed for TGW and area, showed a statistically significant increase in length in the double homozygote and *AtGA20ox1* only lines in one cross when compared to their null and *PcGA2ox1* only lines.

Whilst the *PcGA2ox1* gene appears to be influencing grain size, its effects on grain quality were inconsistent. Grains in the parent lines harbouring the *ZmGlb1::PcGA2ox1* construct displayed a 4 - 20-fold reduction in α-amylase compared to the wild-type (Vaughan, S. unpublished data). The hybrid lines examined here also had lower levels of α-amylase than the wild-type. However, when compared to their nulls, this reduction was nonsignificant. Whilst the *PcGA2ox1* only and *AtGA20ox1* only lines showed inconsistency in the α-amylase in the two crosses, the double homozygotes in both crosses displayed a reduction compared to their nulls. In one cross the *PcGA2ox1* only line showed lower levels of α-amylase compared to its null and *AtGA20ox1* only had higher, whereas this result was reversed in the other cross. Although the double homozygote displayed an interesting trend, the inconsistency in the other lines makes it difficult to make any definite conclusions about the effects of the two transgenes on α-amylase levels.

In previous studies performed in our laboratory on the parent lines used for this study, all comparisons of transgenic material were made against wild-type plants as null segregants were unavailable. The hybrid lines in this experiment, whilst displaying the stability of the two transgenes over several generations, did not show the same phenotypes as those seen in the parent lines compared to the wild-type. However, studies performed in the present experiment, and indeed others in this thesis indicate that the wild-type is usually an outlier compared to the rest of the lines for the majority of variables measured. Hence for each transgenic line a segregating null provides a more reliable and robust comparison point. Thus, in this experiment when comparing the double homozygotes to their nulls, whilst being nonsignificant the changes seen in grain size and α-amylase levels displayed interesting trends.

Chapter 8. General Discussion

Manipulation of the GA biosynthesis and signalling pathways is known to significantly alter plant phenotype (Peng *et al.*, 1997, Coles *et al.*, 1999, Hedden, 2003), and previous work in our laboratory has shown that in wheat it also affects grain size and quality (Vaughan, S., unpublished work). Whilst GA is known to play a role in determining fruit size in a number of species (Groot *et al.*, 1987, Serrani *et al.*, 2007, Zhang *et al.*, 2007, Casanova *et al.*, 2009), this was the first report of it being involved in regulating grain size in wheat. In this work it was shown that whilst an increase in GA content during development resulted in bigger grains and an increase in α-amylase levels, a reduction in GA caused a reduction in grain size and a decrease in α-amylase levels, indicating the need for a more refined system to maintain the yield improvements without the concomitant reduction in quality. The aim of this study was to further characterise the effects of temporal and spatial manipulation of GA in specific tissues of the developing grain to understand what role GA plays during development, and utilise this to increase the yield potential of wheat, along with improving grain quality. We hypothesised that manipulating GA levels in the endosperm and seed coat layers during different stages of development could increase grain size without having a negative impact on quality, whilst insensitivity to GA in the embryo and aleurone layers could improve quality without impacting grain size. To test this, several transgenic lines were generated where using tissue-specific promoters GA biosynthesis, inactivation or signalling was modified during particular stages of grain development in specific tissues (Table 3.1). To confirm the expression patterns of the six promoters used in this study, each promoter was also linked to the H2B nuclear targeted GFP reporter gene.

Prior to any experimental analysis of these constructs it was essential to identity homozygous material to ensure that all grains of each independent line were of the same, and known, genotype. The development of a qPCR based

method – TaqMan assay – resulted in the successful identification of homozygous material as early as the T1 generation. The 90% success rate (Table 3.4) of this method significantly helped in reducing the time and costs involved compared to using conventional methods of PCR to identify homozygous material, which can often take up to three or four generations.

In the embryo and aleurone layers of developing grains, insensitivity to GA was introduced by expressing a gain-of function mutant DELLA from Arabidopsis (*Atgai*) known to be resistant to GA induced degradation. It is known that GA produced by the germinating embryo is perceived by the aleurone layer resulting in the production of the α-amylase enzyme (Kaneko *et al.*, 2003). Previous work in our laboratory showed that in a developing grain as well, it is mainly GA produced by the embryo that induces the production of α-amylase. The aleurone layers of DELLA gain-of-function mutants are known to require 100-fold more GA than wild-type plants to induce the expression of α-amylase genes showing a reduced sensitivity to GA (Gale and Marshall, 1973, Ho *et al.*, 1981, Chandler *et al.*, 2002). We hypothesised that insensitivity to GA in the two layers involved in the production of α-amylase would result in a change in the amount of this enzyme without having any impact on yield. Surprisingly, whilst the yield, grain hardness and moisture content in these lines were largely unaffected (Figures 4.5 and 4.11) the levels of α-amylase were inconsistent across the different lines in both constructs (Figures 4.6 and 4.12). When the mutant DELLA gene was expressed in the aleurone layer only (using *HvChi26* promoter), the majority of lines showed no change in α-amylase, however two lines showed an increase. Whereas when the mutant DELLA gene was expressed in both the embryo and aleurone layers (using *HvBeg1* promoter) whilst one line showed a reduction in α-amylase, no change was seen in the rest.

The reason for the inconsistent α-amylase phenotype could be the extremely low levels of transgene expression seen in all lines harbouring both constructs, possibly resulting in them being non-functional in these plants. If the transgene

in these lines was non-functional the variation seen in α-amylase activity may be a result of the stochastic nature of this enzyme. Amongst grains from the same ear α-amylase levels can be highly variable with some having extremely high levels and some very low (Gale *et al.*, 1987, Mrva and Mares, 2001, Flintham *et al.*, 2011) which could be contributing to the large variation and inconsistency we see in these lines. Although this gain-of-function DELLA gene has been shown to be functional in a tissue specific manner in *Arabidopsis* roots (Ubeda-Tomas *et al.*, 2008) and in cereals by Fu *et.al*, (2001) who showed that its constitutive expression in rice plants results in the reduction of α-amylase production in the grains. However, it is possible that though this gene worked in rice and *Arabidopsis* it may not be functional in wheat. It would be interesting to perform a western blot analysis or immunolocalization of the DELLA protein in order to confirm that the transgene is translated. It could also be beneficial to utilise a different gain-of function DELLA gene, possibly *Rht-1* to ensure that GA insensitivity is achieved in the embryo and aleurone layers and study the effects on α-amylase levels in those transgenic lines. Promoter deletion studies could also be performed on the promoters currently used to test for the presence of elements that might be leading to the suppression of the *Atgai* gene. It would also be useful to characterise new promoters active in the embryo and aleurone layers as another method of achieving GA insensitivity.

Another possibility for the lack of a phenotype in these lines could be the existence of an alternative GA signalling mechanism in the aleurone layer. Before the GID1-DELLA GA signalling model was established there were believed to be gibberellin-binding-proteins (GBPs) in the aleurone of cereals which were first reported by Jelsema *et al*. (1977) in the aleurone of homogenates of wheat seed. It was later shown that α-amylase is induced in aleurone protoplasts by a GA derivative that is impervious to plasma membranes (Hooley *et al.*, 1991). Gilroy and Jones (1994) later showed that GA microinjected to cytoplasm of barley aleurone protoplasts failed to induce α-amylase, whereas external GA_3 application resulted in the production of α-amylase. Several GBPs were also detected in the plasma membranes of oat

aleurone layer suggesting that GA perception occurs on the external face of the plasma membrane inducing α-amylase production (Hooley *et al.*, 1993, Lovegrove *et al.*, 1998). These characteristics of GBPs cannot be explained regarding the GA receptor GID1 or DELLA proteins which both localise to the nucleus and not the plasma membrane (Ueguchi-Tanaka *et al.*, 2005). Though these results suggest the potential existence of an alternative GA perception mechanism mediated by GBPs (Hartweck and Olszewski, 2006), Yano *et al*., (2015) observed that none of the six *RAmy* genes in rice were enhanced by GA in the *gid1* mutant seeds whereas all are enhanced in the wild type. In the GA untreated *slr1* mutant the six *RAmy* genes were expressed at the same level as GA treated wild type seeds. They also performed an analysis of GA-related gene expression using microarrays and then confirmed by qRT-PCR that all GA up and down regulated genes are also regulated by the GID1_DELLA system. They believe these results show that GID1-DELLA is the only GA perception system involved in GA dependant gene expression in aleurone cells. However, if the *Atgai* gene is functional in the transgenic lines discussed in this thesis, it does raise the possibility of the existence of an alternative or additional GA signalling mechanism active in the aleurone layer. This is an interesting prospect and something that needs to be investigated further.

To further understand the role of GA in influencing grain size and quality GA content or perception was manipulated in the endosperm of developing grains. This tissue is known to produce high levels of GA during development, and whilst the purpose of this is still unknown it is possible that it is involved in regulating grain size. In order to test this, plants were generated where a GA inactivating gene from bean (*PcGA2ox1*) was expressed in the endosperm of grain at a late stage in development, as previous work in our laboratory showed that when this was done throughout grain development it tended to improve grain quality but reduced grain size. The promoter chosen for this study (*TaTri*) was active at a stage in development when grain size is believed to have been determined and a reduction in GA should have no further effect on grain physiology. However, two of the three lines studied, which also had high

transgene expression (Figure 6.4), displayed a reduction in grain length (Figure 6.5) and α-amylase levels remained unchanged (Figure 6.6). These results, though based on a very small population, imply that expressing a GA inactivating gene even at such a late stage in grain development may have a negative impact on grain size, and thus yields. It would be useful to measure the levels of the GA hormone in these transgenic lines to ensure that expressing *PcGA2ox1* is also resulting in a reduction of bioactive GAs. If this is indeed true, these results suggest GA may have a more enduring role in determining grain size throughout development and is something that needs to be investigated further. However, in order to be certain of the phenotype observed here these results need to be confirmed looking at a much larger number of independent lines, and if possible over several experiments. It would also be beneficial to study the cellular morphology of these grains to determine whether the changes observed in grain size were due to a change in cell size or cell number, to help in understanding how GA regulates grain size. In previous work in our laboratory it was observed that the grains with a reduction in size comprised of more but smaller cells compared to the wild-type. It would be interesting to determine if the same changes are observed in these lines and could provide an indication of GA having an impact on cell fate much later in grain development than previously thought.

The effects of manipulating GA levels in the grain were tested further in plants generated to express a GA biosynthesis gene from Arabidopsis (*AtGA20ox1*) in the developing endosperm transfer layer of the grain using the *TaEND1* promoter. GA insensitivity was also introduced in this layer utilising the same promoter to examine the role of GA signalling in the endosperm. Interestingly, whilst two lines expressing *AtGA20ox1* showed an increase in grain size (Figure 6.9), lines expressing *Atgai* had the opposite phenotype with two of the four lines examined showing a slight reduction in yield (Figure 6.13). Lines expressing *AtGA20ox1* which displayed an increase in grain yield also showed changes in grain hardness and moisture content with these variables being significantly reduced in both lines. Whereas the line expressing *Atgai* which

showed a reduction in both grain weight and size, showed an increase in moisture content. These results agree with previous work done in our laboratory where grains with an increase in size show a reduction in hardness and moisture content, and smaller grains show an opposite result. It would be interesting to study the cellular morphology of these grains to further investigate what effects manipulating GA levels has on cell size and cell number and how this impacts grain hardness and the grains ability to retain moisture. Whilst there were changes in grain morphology, no change in α-amylase content was observed in either construct (Figure 6.10 and 6.14) implying that this tissue does not have as much of an influence as the embryo in the production of this enzyme. The results from these two constructs further indicate that GA produced by the endosperm whist having an impact on grain morphology, does not influence the production of α-amylase. However, the effects on yield were only observed in two of the four lines harbouring each construct respectively making it difficult to make any definite conclusions about the effect of these transgenes on grain size. Particularly since in the lines expressing *AtGA20ox1* the increase in yield was seen in lines that also had a reduction in grain number, possibly resulting in the availability of extra resources to the remaining grains resulting in increased size and weight.

Gain-of-function DELLA mutants have been shown to accumulate bioactive GAs in vegetative tissues (Appleford and Lenton, 1991) along with the high expression of feedback regulated genes (Dill and Sun, 2001, Silverstone *et al.*, 2001). In order to test if the lines expressing *Atgai* in the endosperm transfer layer also displayed similar results the expression levels of the *TaGA20ox3* gene and the concentration of GA were measured. The expression of the *TaGA20ox3* gene was unchanged in the transgenic lines (Figure 6.15) when compared to their nulls implying that either the transgene may not be regulating the expression of this gene, or that this gene is not feedback regulated in the grain. Some preliminary work has suggested that in the endosperm of wheat grains GA biosynthetic genes may not be feedback regulated (Lenton, J., unpublished data). However, an increase in the levels of the bioactive GA_{54} (Table 6.2) were

seen in the transgenic lines compared to their nulls implying that possibly GA insensitivity in the endosperm transfer layer is leading to the accumulation of this hormone. This also implies that even though no changes in the expression of *TaGA20ox3* were observed in these lines, GA insensitivity could be having an effect on the expression of other genes in the GA biosynthetic pathway resulting in GA accumulation. However, these results are based on only one sample from two lines in the experiment leading to a difficulty in making definite conclusions about the effects of GA insensitivity in the endosperm transfer layer. In order to confirm these results this analysis needs to be performed on the full set of replicate samples from this experiment.

The concentration of GA was also measured in the lines expressing *AtGA20ox1* in the endosperm transfer layer. Differences were observed between the transgenic and null plants with both transgenic lines having lower amounts of GA_{54} than their nulls (Table 6.1). Whilst the overexpression of GA biosynthetic 20-oxidase genes has been shown to result in increasing GA production (Huang *et al.*, 1998, Coles *et al.*, 1999), the transgenic lines studied here displayed the opposite result. Previous work in our laboratory has shown that expressing *AtGA20ox1* in the endosperm can result in grains developing at a faster rate compared to the wild-type (Vaughan, S. unpublished data). It is possible that the transgenic lines studied here could be displaying a similar phenotype resulting in the grains studied being physiologically older than their nulls, and thus displaying lower levels of GA. Several biomarkers have been characterised for studying different aging signals in developing seeds (Fu *et al.*, 2015) and it would be useful to confirm the theory that expression of *AtGA20ox1* is accelerating the growth of the transgenic lines by utilising one of these markers. However, as with the *TaEND1::Atgai* lines these results are also based on one sample for each for the two transgenic lines studied and the analysis needs to be performed on the full set of replicates to confirm these findings.

Whilst the transgenic lines expressing the *AtGA20ox1* gene in the endosperm transfer cells displayed a reduction in GA levels compared to the nulls, both

these genotypes showed a large reduction compared to the wild-type and *TaEND1::Atgai* plants. This reduction in GA levels in the transformed plants could possibly be the result of somaclonal variations. Plant tissue culture comprises of two phases, dedifferentiation – formation of callus – and re-differentiation – regeneration into plants. This process can be stressful for the plant cells and result in genetic or epigenetic alterations in the plants which can be inherited stably (Wang *et al.*, 2013b). If these alterations occur early during the tissue culture process they can be clonally multiplied and result in the same genetic change in a number of individuals (Brettell and Dennis, 1991, Kohli *et al.*, 2004). The lines studied here whilst being generated from separate calluses during the tissue culture process, could possibly have developed similar epigenetic alterations which could explain the reduction in GA content seen in the transgenics and nulls of two independent lines.

The role of GA in determining grain size was also studied by expressing *AtGA20ox1* in the seed coat layers of the developing grain under control of the *HvGerF* and *TaDFRd* promoters. The aim of this study was to understand whether the seed coat restricts grain size and if increasing GA biosynthesis in these layers may affect this. Plants where the biosynthesis gene was expressed in the inner integument layer using the *TaDFRd* promoter displayed a slight reduction in final yields though this was only weakly significant (Figure 5.7). However, lines with gene expression in the pericarp and inner integument layers using the *HvGerF* promoter displayed contrasting results compared to each other (Figure 5.4). In plants harbouring the *HvGerF::AtGA20ox1* construct whilst two of the four lines studied showed significant reduction in both grain size and weight, one line showed an increase. We also hypothesised the possibility that the increase in GA levels in these layers could result in an increase in grain size during development, as the developing grain fills with water. However, these grains then may not be able to sustain this increase in size due to a lack of resources resulting in an inability to 'fill' the grain to its full potential. In order to test this hypothesis changes in grain size were studied during development and nonlinear models generated for grain weight and

surface area. These results mirrored those seen for final yield with developmental differences seen in plants that showed significant changes in final yield. Lines expressing the *AtGA20ox1* gene in the inner integument displayed only slight variation in development compared to the wild-type and no differences were observed between the transgenics and their nulls (Figures 5.11 and 5.13). One line which had the highest expression of the *AtGA20ox1* gene (Figure 5.3) in the pericarp and inner integument layers displayed a difference in growth rate and a longer grain filling period compared to its null, resulting in an increase in final grain size and weight (Figures 5.10 and 5.12). Whereas, one line which had lower levels of transgene expression displayed slower growth rate and a shorter grain filling than its null resulting in reduced grain size and weight. Though this transgenic line also had an unusually high number of aborted grains, possibly indicating towards other factors apart from the expression of the transgene leading to the change in grain size (Figure 5.4). Unfortunately, the weak phenotype seen in the lines expressing *AtGA20ox1* in the inner integument layer and the contrasting phenotype in lines expressing this gene in the pericarp and inner integument layers result in a difficulty in making any definite conclusions about what effect, if any the transgene is having on grain development. Whilst the inner integument layer has been shown to be a site of GA biosynthesis in certain species (Rodrigo *et al.*, 1997, Nadeau *et al.*, 2011) it is possible that in wheat expression of the *AtGA20ox1* is not resulting in an increase in production of bioactive GAs. Whereas the pericarp layer shows high levels of expression of GA signalling and inactivating genes along with very low levels of biosynthesis genes (Pearce *et al.*, 2015), implying that GA may not be produced here, however, it could be moving into this tissue and its concentration regulated. In the pericarp layer it is also possible that expressing the *AtGA20ox1* gene is not resulting in an increase in the production of bioactive GAs. However, in order to make any conclusions about this it would be necessary to further study gene expression and levels of GA in these transgenic lines. Though if this analysis is performed on whole grains it is possible that any changes occurring in the inner integument or the pericarp layers might be lost as these tissues only constitute a small proportion

of the grain. Isolating these tissues using techniques such as laser capture microdissection to perform gene expression analysis could be a useful way of overcoming this issue. In addition, techniques such as Fluorescence Resonance Energy Transfer (FRET) using intracellular GA biosensors that detect the presence and possibly the concentration of bioactive GAs (Miyamoto *et al.*, 2012) could be used to study the levels of this hormone in the different tissues of the grain.

The work described in this thesis was developed based on previous work in our laboratory which looked at lines expressing *AtGA20ox1* in the endosperm using the *TaHMW-GS* promoter and lines expressing *PcGA2ox1* in the embryo using the *ZmGlb1* promoter. Lines engineered to increase levels of GA in the endosperm showed an increase in grain size and α-amylase and lines with reduced GA in the embryo showed a reduction in grain size and α-amylase. Hybrid plants were generated by crossing these lines to further investigate these results. The studies performed on the parent lines compared the transgenic lines to the wild-type control as segregating nulls were unavailable and it is important to note that the studies performed in this thesis have consistently shown that the wild-type 'control' is an outlier for most of the analyses undertaken. The segregating nulls represent a more biologically robust internal baseline and for this reason, in the hybrid lines double homozygotes, lines homozygous for only one of the two transgenes and null segregants were identified and retained to allow comparison of all four genotypes in identical genetic backgrounds. Whilst these lines did not display the same significant results observed in the parent lines compared to the wild-type, similar trends were observed for both grain size and α-amylase levels in lines expressing only one transgene when compared to their nulls (Figures 7.7 and 7.9). In addition, the double homozygote plants displayed similar grain size phenotype to the *AtGA20ox1* only plants showing a slight increase in size and a reduction in α-amylase levels, when compared to their nulls. These results confirm the stability of the two transgenes (and their expression) over several generations and also confirm inheritance of the phenotypes seen in the parent

lines. Whilst these results do show interesting trends, they are based on only two lines and it would be beneficial to repeat these studies on more lines over multiple experiments.

All transgenic lines described in this thesis were generated by direct gene transfer using particle bombardment. This process is known to generate large transgenic loci and as shown in Chapter 3 can result in plants with up to 20 transgene copies. These insertions can be highly variable and can contain either single copies, tandem or inverted repeats, concatemers, intact transgenes, truncated and rearranged sequences or interspersed genomic DNA. In contrast plants generated through *Agrobacterium*-mediated transformations contain low copy numbers of the transgene (Kohli *et al.*, 2010), though they can also contain unwanted 'plasmid backbone' sequences that get integrated into the host genome (Sparks *et al.*, 2014). The presence of multiple copies of the transgene at several different loci can result in differing transgene segregation ratios across generations and variable gene expression within populations of plants generated from the same transformation event; as was observed in the majority of studies performed in this thesis. The transgenic lines studied in this project all displayed a range of phenotypes within each construct. Along with this there were also indications of possible silencing of the transgene and somaclonal variations. Presence of multiple copies of the transgene is not believed to result in increased amount of transcript and has also been shown to induce silencing due to DNA methylation at the transgene locus (Gelvin *et al.*, 1983, Meyer *et al.*, 1992). Apart from this the stability of the transgene is also affected by other factors such as position effects, whereby the specific nature of genomic DNA surrounding the site of insertion may affect transgene expression (Wilson *et al.*, 1990). Analysis of transgene loci in several species has also revealed that many integrated transgenes contain minor rearrangements, however the impact of these rearrangements is underestimated as unexplained phenotypes are assumed to be an epigenetic phenomenon (Kohli *et al.*, 2010). Whilst generating transgenic plants using *Agrobacterium*-mediation transformation may help alleviate some of the

issues faced in plants generated through biolistics, it could be more beneficial to utilise site directed nuclease based techniques such as CRISPR/Cas9 or TALENs (transcription activator-like effector nucleases) to modify gene expression. These techniques offer the advantage of gene modifications occurring only at the target site (Xiong *et al.*, 2015) thus avoiding off target effects such as those possibly seen in the lines studied here. In addition, CRISPR/Cas9 also offers the ability to introduce multiple gene interruptions simultaneously (Wang *et al.*, 2013a), allowing the disruption of several genes in a plant through a single transformation. This in combination with the advances made in recent years in the sequencing of the wheat genome, making available sequences of native genes allows for their targeted disruption, thus to some extent alleviating the need to use overexpression constructs. It would be interesting to target the expression of different genes in the GA biosynthetic and signalling pathways using CRISPR/Cas9 in a tissue specific manner (Stolfi *et al.*, 2014) and study its effects on grain development. The availability of the wheat genome sequence also allows for the opportunity to mine for and characterise different promoters that could be used to target gene expression during grain development.

The work in this thesis displayed changes in grain size in lines where GA content was manipulated in the endosperm indicating towards the involvement of GA produced in this tissue in grain size regulation. It would be interesting to study these lines in an experiment where the source and sink were manipulated. This experiment could help determine if the increase in grain size seen due to excess GA is pushed further when extra resources are available or if there is a limit to this. This could also help determine if the reduced grain size seen in lines with decreased GA content can be rescued by the availability of extra resources. The work presented here also supported previous findings that GA produced by the endosperm might not play a role in the production of the α-amylase enzyme. Though, due to time constrains these studies were performed on a small number of independent lines and in order to make any definite conclusions need to be repeated looking at more lines, possibly over multiple experiments.

In addition, plants where GA perception was manipulated in the embryo and aleurone layers did not display any substantial changes in grain size or α-amylase levels, however these lines need to be characterised further by determining the functionality of the transgene to be able to make any conclusions about them.

Whilst a role for GA was observed in grain development in these studies, the role of GA in grain quality was harder to establish, implying that possibly manipulating this hormone to improve grain quality might not the right strategy. However, the lines which expressed *AtGA20ox1* in the endosperm transfer layer displayed an increase in grain size without any negative impact on grain quality and provide an interesting avenue for further investigations into using this to improve grain yields. Additionally, the lines harbouring the various constructs described here provide a new resource that could be further characterised possibly using next generation sequencing technologies to help further understand grain development.

Chapter 9. References

ABE, A., TAKAGI, H., FUJIBE, T., AYA, K., KOJIMA, M., SAKAKIBARA, H., UEMURA, A., MATSUOKA, M. & TERAUCHI, R. 2012. Osga20ox1, a candidate gene for a major qtl controlling seedling vigor in rice. *Theoretical and Applied Genetics,* 125**,** 647-657.

ACRECHE, M. M. & SLAFER, G. A. 2006. Grain weight response to increases in number of grains in wheat in a mediterranean area. *Field Crops Research,* 98**,** 52-59.

ALABADI, D., GALLEGO-BARTOLOME, J., ORLANDO, L., GARCIA-CARCEL, L., RUBIO, V., MARTINEZ, C., FRIGERIO, M., IGLESIAS-PEDRAZ, J. M., ESPINOSA, A., DENG, X. W. & BLAZQUEZ, M. A. 2008. Gibberellins modulate light signaling pathways to prevent arabidopsis seedling de-etiolation in darkness. *Plant J,* 53**,** 324-35.

ALBERTS, B., JOHNSON, A., LEWIS, J., RAFF, M., ROBERTS, K. & WALTER, P. 2002. Control of gene expression. *Molecular biology of the cell, 4th edition.* New York: Garland Science.

ALTENBACH, S. B. & KOTHARI, K. M. 2004. Transcript profiles of genes expressed in endosperm tissue are altered by high temperature during wheat grain development. *Journal of Cereal Science,* 40**,** 115-126.

ANAND, A., TRICK, H. N., GILL, B. S. & MUTHUKRISHNAN, S. 2003. Stable transgene expression and random gene silencing in wheat. *Plant Biotechnology Journal,* 1**,** 241-251.

ANDERSON, O. D., LARKA, L., CHRISTOFFERS, M. J., MCCUE, K. F. & GUSTAFSON, J. P. 2002. Comparison of orthologous and paralogous DNA flanking the wheat high molecular weight glutenin genes: Sequence conservation and divergence, transposon distribution, and matrix-attachment regions. *Genome,* 45**,** 367-380.

ANTOINE, C., PEYRON, S., LULLIEN-PELLERIN, V., ABECASSIS, J. & ROUAU, X. 2004. Wheat bran tissue fractionation using biochemical markers. *Journal of Cereal Science,* 39**,** 387-393.

APPLEFORD, N. E. J., EVANS, D. J., LENTON, J. R., GASKIN, P., CROKER, S. J., DEVOS, K. M., PHILLIPS, A. L. & HEDDEN, P. 2006. Function and transcript analysis of gibberellin-biosynthetic enzymes in wheat. *Planta,* 223**,** 568-82.

APPLEFORD, N. E. J. & LENTON, J. R. 1991. Gibberellins and leaf expansion in near-isogenic wheat lines containing rht1 and rht3 dwarfing alleles. *Planta,* 183**,** 229-236.

AYA, K., UEGUCHI-TANAKA, M., KONDO, M., HAMADA, K., YANO, K., NISHIMURA, M. & MATSUOKA, M. 2009. Gibberellin modulates anther

development in rice via the transcriptional regulation of gamyb. *Plant Cell,* 21**,** 1453-1472.

AZIZ, P. 1972. Histogenesis of carpel in triticum-aestivum l. *Botanical Gazette,* 133**,** 376-386.

BABIO, N., BALANZA, R., BASULTO, J., BULLO, M. & SALAS-SALVADO, J. 2010. Dietary fibre: Influence on body weight, glycemic control and plasma cholesterol profile. *Nutricion Hospitalaria,* 25**,** 327-340.

BAILLY, C. 2004. Active oxygen species and antioxidants in seed biology. *Seed Science Research,* 14**,** 93-107.

BALDEV, B., LANG, A. & AGATEP, A. O. 1965. Gibberellin production in pea seeds developing in excised pods - effect of growth retardant amo-1618. *Science,* 147**,** 155-&.

BARRON, C., SURGET, A. & ROUAU, X. 2007. Relative amounts of tissues in mature wheat (triticum aestivum l.) grain and their carbohydrate and phenolic acid composition. *Journal of Cereal Science,* 45**,** 88-96.

BASKIN, J. M. & BASKIN, C. C. 2003. New approaches to the study of the evolution of physical and physiological dormancy, the two most common classes of seed dormancy on earth. *In:* NICOLAS, G., BRADFORD, K. J., COME, D. & PRITCHARD, H. W. (eds.) *Biology of seeds: Recent research advances.* Cambridge: Cabi Publishing.

BASS, H. W., WEBSTER, C., OBRIAN, G. R., ROBERTS, J. K. M. & BOSTON, R. S. 1992. A maize ribosome-inactivating protein is controlled by the transcriptional activator opaque-2. *Plant Cell,* 4**,** 225-234.

BAULCOMBE, D. C., HUTTLY, A. K., MARTIENSSEN, R. A., BARKER, R. F. & JARVIS, M. G. 1987. A novel wheat alpha-amylase gene (alpha-amy3). *Molecular & General Genetics,* 209**,** 33-40.

BECHTEL, D. B., ABECASSIS, J., SHEWRY, P. R. & EVERS, A. D. 2009. Chapter 3: Development, structure, and mechanical properties of the wheat grain. *Wheat: Chemistry and technology.* AACC International, Inc.

BECHTEL, D. B., GAINES, R. L. & POMERANZ, Y. 1982. Early stages in wheat endosperm formation and protein body initiation. *Annals of Botany,* 50**,** 507-518.

BELANGER, F. C. & KRIZ, A. L. 1989. Molecular characterization of the major maize embryo globulin encoded by the glb1 gene. *Plant Physiology,* 91**,** 636-643.

BELANGER, F. C. & KRIZ, A. L. 1991. Molecular-basis for allelic polymorphism of the maize globulin-1 gene. *Genetics,* 129**,** 863-872.

BELITZ, H. D., GROSCH, W. & SCHIEBERLE, P. 2009. Cereals and cereal products. *In:* BELITZ, H. D., GROSCH, W. & SCHIEBERLE, P. (eds.) *Food chemistry.* Berlin: springer.

BENFEY, P. N. & CHUA, N. H. 1990. The cauliflower mosaic virus-35s promoter - combinatorial regulation of transcription in plants. *Science,* 250**,** 959-966.

BENNETT, M. D., SMITH, J. B. & BARCLAY, I. 1975. *Early seed development in the triticeae*, Royal Society.

BENTSINK, L., JOWETT, J., HANHART, C. J. & KOORNNEEF, M. 2006. Cloning of dog1, a quantitative trait locus controlling seed dormancy in arabidopsis. *Proceedings of the National Academy of Sciences of the United States of America,* 103**,** 17042-17047.

BENTSINK, L. & KOORNNEEF, M. 2008. Seed dormancy and germination. *The Arabidopsis Book / American Society of Plant Biologists,* 6**,** e0119.

BERJAK, P. 2006. Unifying perspectives of some mechanisms basic to desiccation tolerance across life forms. *Seed Science Research,* 16**,** 1-15.

BETHKE, P. C., LIBOUREL, I. G. L. & JONES, R. L. 2007. Nitric oxide in seed dormancy and germination. *Annual plant reviews volume 27: Seed development, dormancy and germination.* Blackwell Publishing Ltd.

BEWLEY, J. D. 1997. Seed germination and dormancy. *Plant Cell,* 9**,** 1055-1066.

BEWLEY, J. D. & BLACK, M. 1994. Seeds: Physiology of development and germination, second edition. *Seeds: Physiology of development and germination, Second edition***,** xv+445p.

BHALLA, P. L. 2006. Genetic engineering of wheat - current challenges and opportunities. *Trends in biotechnology,* 24**,** 305-11.

BHATNAGAR, S. P. & CHANDRA, S. 1975. Reproductive-biology of triticum .3. Unfertilized ovule and embryo sac - fertilization - post-fertilization changes in embryo sac and transformation of pistil into caryopsis in relation to time. *Phytomorphology,* 25**,** 471-477.

BIHMIDINE, S., HUNTER, C. T., III, JOHNS, C. E., KOCH, K. E. & BRAUN, D. M. 2013. Regulation of assimilate import into sink organs: Update on molecular drivers of sink strength. *Frontiers in Plant Science,* 4.

BLACKWOOD, A. D., SALTER, J., DETTMAR, P. W. & CHAPLIN, M. F. 2000. Dietary fibre, physicochemical properties and their relationship to health. *Journal of the Royal Society for the Promotion of Health,* 120**,** 242-247.

BONNETT, O. T. 1966. *Inflorescences of maize, wheat, rye, barley, and oats: Their initiation and development,* [Urbana, Ill.], University of Illinois, College of Agriculture, Agricultural Experiment Station.

BORRAS, L., SLAFER, G. A. & OTEGUI, M. E. 2004. Seed dry weight response to source-sink manipulations in wheat, maize and soybean: A quantitative reappraisal. *Field Crops Research,* 86**,** 131-146.

BRADBURY, D., CULL, I. M. & MACMASTERS, M. M. 1956. *Structure of the mature wheat kernel: Gross anatomy and relationships of parts. I*.

BREATHNACH, R. & CHAMBON, P. 1981. Organization and expression of eukaryotic split genes-coding for proteins. *Annual Review of Biochemistry,* 50**,** 349-383.

BREMNER, P. M. & RAWSON, H. M. 1978. The weights of individual grains of the wheat ear in relation to their growth potential, the supply of assimilate and interaction between grains. *Australian Journal of Plant Physiology,* 5.

BRENNER, M. L. & CHEIKH, N. 1995. The role of hormones in photosynthate partitioning and seed filling. *In:* DAVIES, P. J. (ed.) *Plant hormones: Physiology, biochemistry and molecular biology.* Dordrecht: Springer Netherlands.

BRETTELL, R. I. S. & DENNIS, E. S. 1991. Reactivation of a silent ac following tissue-culture is associated with heritable alterations in its methylation pattern. *Molecular & General Genetics,* 229**,** 365-372.

BRIAN, P. W. & HEMMING, H. G. 1955. The effect of gibberellic acid on shoot growth of pea seedlings. *Physiologia Plantarum,* 8**,** 669-681.

BRIGGLE, L. W. & CURTIS, B. C. 1987. Wheat worldwide. *In:* HEYNE, E. G. (ed.) *Wheat and wheat improvement.* second ed. Madison, Wisconsin, USA: American society of Agronomy.

BUBNER, B. & BALDWIN, I. T. 2004. Use of real-time pcr for determining copy number and zygosity in transgenic plants. *Plant Cell Reports,* 23**,** 263-271.

BULEON, A., COLONNA, P., PLANCHOT, V. & BALL, S. 1998. Starch granules: Structure and biosynthesis. *International Journal of Biological Macromolecules,* 23**,** 85-112.

BURKE, T. W. & KADONAGA, J. T. 1996. Drosophila tfiid binds to a conserved downstream basal promoter element that is present in many tata-box-deficient promoters. *Genes & Development,* 10**,** 711-724.

BURNEY, J. A., DAVIS, S. J. & LOBELL, D. B. 2010. Greenhouse gas mitigation by agricultural intensification. *Proceedings of the National Academy of Sciences of the United States of America,* 107**,** 12052-12057.

CAL, M., WEI, J., LI, X. H., XU, C. G. & WANG, S. P. 2007. A rice promoter containing both novel positive and negative cis-elements for regulation of green tissue-specific gene expression in transgenic plants. *Plant Biotechnology Journal,* 5**,** 664-674.

CALDERINI, D. F., DRECCER, M. F. & SLAFER, G. A. 1997. Consequences of breeding on biomass, radiation interception and radiation-use efficiency in wheat. *Field Crops Research,* 52**,** 271-281.

CAMPBELL, W. P., LEE, J. W., OBRIEN, T. P. & SMART, M. G. 1981. Endosperm morphology and protein body formation in developing wheat-grain. *Australian Journal of Plant Physiology,* 8**,** 5-19.

CAO, D. N., HUSSAIN, A., CHENG, H. & PENG, J. R. 2005. Loss of function of four della genes leads to light- and gibberellin-independent seed germination in arabidopsis. *Planta,* 223**,** 105-113.

CASANOVA, L., CASANOVA, R., MORET, A. & AGUSTI, A. 2009. The application of gibberellic acid increases berry size of 'emperatriz' seedless grape. *Spanish Journal of Agricultural Research,* 7**,** 919-927.

CHALLINOR, A. J., WATSON, J., LOBELL, D. B., HOWDEN, S. M., SMITH, D. R. & CHHETRI, N. 2014. A meta-analysis of crop yield under climate change and adaptation. *Nature Climate Change,* 4**,** 287-291.

CHANDLER, P. M., HARDING, C. A., ASHTON, A. R., MULCAIR, M. D., DIXON, N. E. & MANDER, L. N. 2008. Characterization of gibberellin receptor mutants of barley (hordeum vulgare l.). *Molecular Plant,* 1**,** 285-294.

CHANDLER, P. M., MARION-POLL, A., ELLIS, M. & GUBLER, F. 2002. Mutants at the slender1 locus of barley cv himalaya. Molecular and physiological characterization. *Plant Physiology,* 129**,** 181-190.

CHEN, L., NISHIZAWA, T., HIGASHITANI, A., SUGE, H., WAKUI, Y., TAKEDA, K. & TAKAHASHI, H. 2001. A variety of wheat tolerant to deep-seeding conditions: Elongation of the first internode depends on the response to gibberellin and potassium. *Plant Cell and Environment,* 24**,** 469-476.

CHINNUSAMY, V., GONG, Z. Z. & ZHU, J. K. 2008. Abscisic acid-mediated epigenetic processes in plant development and stress responses. *Journal of Integrative Plant Biology,* 50**,** 1187-1195.

CHO, J. N., RYU, J. Y., JEONG, Y. M., PARK, J., SONG, J. J., AMASINO, R. M., NOH, B. & NOH, Y. S. 2012. Control of seed germination by light-induced histone arginine demethylation activity. *Developmental Cell,* 22**,** 736-748.

CHOI, H. W., LEMAUX, P. G. & CHO, M. J. 2003. Long-term stability of transgene expression driven by barley endosperm-specific hordein promoters in transgenic barley. *Plant Cell Reports,* 21**,** 1108-1120.

COLES, J. P., PHILLIPS, A. L., CROKER, S. J., GARCIA-LEPE, R., LEWIS, M. J. & HEDDEN, P. 1999. Modification of gibberellin production and plant development in arabidopsis by sense and antisense expression of gibberellin 20-oxidase genes. *Plant Journal,* 17**,** 547-556.

COLLEGE OF AGRICULTURE FOOD AND ENVIRONMENT, U. O. K. 2016. Seed development [Online]. Available: http://dept.ca.uky.edu/PLS440/schedule/seeddevelopment.pdf [Accessed].

COLOT, V., ROBERT, L. S., KAVANAGH, T. A., BEVAN, M. W. & THOMPSON, R. D. 1987. Localization of sequences in wheat endosperm protein genes which confer tissue-specific expression in tobacco. *Embo Journal,* 6**,** 3559-3564.

CORCORAN, M. R. & PHINNEY, B. O. 1962. Changes in amounts of gibberellin-like substances in developing seed of echinocystis, lupinus and phaseolus. *Physiologia Plantarum,* 15**,** 252-&.

CORDER, A. M. & HENRY, R. J. 1989. Carbohydrate-degrading enzymes in germinating wheat. *Cereal Chemistry,* 66**,** 435-439.

CURABA, J., MORITZ, T., BLERVAQUE, R., PARCY, F., RAZ, V., HERZOG, M. & VACHON, G. 2004. Atga3ox2, a key gene responsible for bioactive gibberellin biosynthesis, is regulated during embryogenesis by leafy cotyledon2 and fusca3 in arabidopsis. *Plant Physiology,* 136**,** 3660-3669.

CURTIS, T. & HALFORD, N. G. 2014. Food security: The challenge of increasing wheat yield and the importance of not compromising food safety. *Annals of Applied Biology,* 164**,** 354-372.

DAFTARY, R. D., POMERANZ, Y., SHOGREN, M. & FINNEY, K. F. 1968. Functional bread-making properties of wheat flour lipids .2. Role of flour lipid fractions in bread-making. *Food Technology,* 22**,** 79-&.

DAHIYA, N., TEWARI, R. & HOONDAL, G. S. 2006. Biotechnological aspects of chitinolytic enzymes: A review. *Applied Microbiology and Biotechnology,* 71**,** 773-782.

DAI, M. Q., ZHAO, Y., MA, Q. F., HU, Y., HEDDEN, P. F., ZHANG, Q. & ZHOU, D. X. 2007. The rice yabby1 gene is involved in the feedback regulation of gibberellin metabolism. *Plant Physiology,* 144**,** 121-133.

DANG, L. Y. & VAN DAMME, E. J. M. 2015. Toxic proteins in plants. *Phytochemistry,* 117**,** 51-64.

DANIELL, H. 2002. Molecular strategies for gene containment in transgenic crops. *Nature Biotechnology,* 20**,** 581-586.

DAVIERE, J. M. & ACHARD, P. 2013. Gibberellin signaling in plants. *Development,* 140**,** 1147-1151.

DAVIES, P. J. 1995. *The plant hormones: Their nature, occurrence, and functions*, Kluwer Academic Publishers, PO Box 989, 3300 AZ Dordrecht, Netherlands; Kluwer Academic Publishers, 101 Phillip Drive, Norwell, Massachusetts 02061, USA.

DAYAN, J. 2016. Gibberellin transport. *Annual plant reviews, volume 49.* John Wiley & Sons, Ltd.

DE LUCAS, M., DAVIERE, J. M., RODRIGUEZ-FALCON, M., PONTIN, M., IGLESIAS-PEDRAZ, J. M., LORRAIN, S., FANKHAUSER, C., BLAZQUEZ, M. A., TITARENKO, E. & PRAT, S. 2008. A molecular framework for light and gibberellin control of cell elongation. *Nature,* 451**,** 480-U11.

DE VIRGILIO, M., LOMBARDI, A., CALIANDRO, R. & FABBRINI, M. S. 2010. Ribosome-inactivating proteins: From plant defense to tumor attack. *Toxins,* 2**,** 2699-2737.

DEBEAUJON, I. & KOORNNEEF, M. 2000. Gibberellin requirement for arabidopsis seed germination is determined both by testa characteristics and embryonic abscisic acid. *Plant Physiology,* 122**,** 415-424.

DEGIDIO, M. G., MARIANI, B. M., NARDI, S., NOVARO, P. & CUBADDA, R. 1990. Chemical and technological variables and their relationships - a predictive equation for pasta cooking quality. *Cereal Chemistry,* 67**,** 275-281.

DELCOUR, J. A. & HOSENEY, R. C. 2010. Principles of cereal science and technology authors provide insight into the current state of cereal processing. *Cereal Foods World,* 55**,** 21-22.

DELROT, S. & BONNEMAIN, J. L. 1985. Mechanism and control of phloem transport. *Physiologie Vegetale,* 23**,** 199-220.

DEMEKE, T., HUCL, P., BAGA, M., CASWELL, K., LEUNG, N. & CHIBBAR, R. N. 1999. Transgene inheritance and silencing in hexaploid spring wheat. *Theoretical and Applied Genetics,* 99**,** 947-953.

DEPARTMENT OF ECONOMIC AND SOCIAL AFFAIRS, U. N. 2015. 2015 revision of world population prospects [Online]. Available: https://esa.un.org/unpd/wpp/ [Accessed].

DERVILLY, G., SAULNIER, L., ROGER, P. & THIBAULT, J. F. 2000. Isolation of homogeneous fractions from wheat water-soluble arabinoxylans. Influence of the structure on their macromolecular characteristics. *Journal of Agricultural and Food Chemistry,* 48**,** 270-278.

DEVOS, Y., DEMONT, M., DILLEN, K., REHEUL, D., KAISER, M. & SANVIDO, O. 2009. Coexistence of genetically modified (gm) and non-gm crops in the european union. A review. *Agronomy for Sustainable Development,* 29**,** 11-30.

DIAZ, I., VICENTE-CARBAJOSA, J., ABRAHAM, Z., MARTINEZ, M., ISABEL-LA MONEDA, I. & CARBONERO, P. 2002. The gamyb protein from barley interacts with the dof transcription factor bpbf and activates endosperm-specific genes during seed development. *Plant Journal,* 29**,** 453-464.

DILL, A., JUNG, H.-S. & SUN, T.-P. 2001. The della motif is essential for gibberellin-induced degradation of rga. *Proceedings of the National Academy of Sciences of the United States of America,* 98**,** 14162-7.

DILL, A. & SUN, T. P. 2001. Synergistic derepression of gibberellin signaling by removing rga and gai function in arabidopsis thaliana. *Genetics,* 159**,** 777-785.

DIRZO, R. & RAVEN, P. H. 2003. Global state of biodiversity and loss. *Annual Review of Environment and Resources,* 28**,** 137-167.

DIXON, K. W., MERRITT, D. J., FLEMATTI, G. R. & GHISALBERTI, E. L. 2009. Karrikinolide - a phytoreactive compound derived from smoke with

applications in horticulture, ecological restoration and agriculture. *Acta Horticulturae*, 155-170.

DOAN, D. N. P., LINNESTAD, C. & OLSEN, O. A. 1996. Isolation of molecular markers from the barley endosperm coenocyte and the surrounding nucellus cell layers. *Plant Molecular Biology,* 31, 877-886.

DONMEZ, E., SEARS, R. G., SHROYER, J. P. & PAULSEN, G. M. 2001. Genetic gain in yield attributes of winter wheat in the great plains. *Crop Science,* 41, 1412-1419.

DORAK, M. T. 2012. Real-time pcr [Online]. Available: http://www.dorak.info/genetics/realtime.html [Accessed].

DREA, S., LEADER, D. J., ARNOLD, B. C., SHAW, P., DOLAN, L. & DOONAN, J. H. 2005. Systematic spatial analysis of gene expression during wheat caryopsis development. *Plant Cell,* 17, 2172-2185.

DUBCOVSKY, J. & DVORAK, J. 2007. Genome plasticity a key factor in the success of polyploid wheat under domestication (vol 316, pg 1862, 2007). *Science,* 318, 393-393.

DUNCAN, J. D. & WEST, C. A. 1981. Properties of kaurene synthetase from marah-macrocarpus endosperm - evidence for the participation of separate but interacting enzymes. *Plant Physiology,* 68, 1128-1134.

E-OLIGOS. 2016. Taqman probes [Online]. Available: http://www.e-oligos.com/eoweb/products/eo-taqman.asp [Accessed].

EDNEY, M. J. 1996. Barley. *In:* HENRY, R. J. & KETTLEWELL, P. S. (eds.) *Cereal grain quality.* 1 ed. London: Chapman and Hall.

EEUWENS, C. J. & SCHWABE, W. W. 1975. Seed and pod wall development in pisum-sativum, l in relation to extracted and applied hormones. *Journal of Experimental Botany,* 26, 1-14.

ENDO, Y., MITSUI, K., MOTIZUKI, M. & TSURUGI, K. 1987. The mechanism of action of ricin and related toxic lectins on eukaryotic ribosomes - the site and the characteristics of the modification in 28-s ribosomal-rna caused by the toxins. *Journal of Biological Chemistry,* 262, 5908-5912.

ESTRADA-MELO, A. C., MA, C., REID, M. S. & JIANG, C. Z. 2015. Overexpression of an aba biosynthesis gene using a stress-inducible promoter enhances drought resistance in petunia. *Horticulture Research,* 2, 9.

EVANS, L. T. 1998. *Feeding the ten billion. Plants and population growth,* Cambridge, UK., Cambrudge University Press.

EVANS, L. T. & FISCHER, R. A. 1999. Yield potential: Its definition, measurement, and significance. *Crop Science,* 39, 1544-1551.

EVENSON, R. E. & GOLLIN, D. 2003. Assessing the impact of the green revolution, 1960 to 2000. *Science,* 300, 758-762.

EVERS, A. D. 1970. Development of the endosperm of wheat. *Annals of Botany,* 34, 547-&.

EVERS, T. & MILLAR, S. 2002. Cereal grain structure and development: Some implications for quality. *Journal of Cereal Science,* 36**,** 261-284.

FAGARD, M. & VAUCHERET, H. 2000. (trans)gene silencing in plants: How many mechanisms? *Annual Review of Plant Physiology and Plant Molecular Biology,* 51**,** 167-194.

FAO 2015. The state of food insecurity in the world.

FAOSTAT. 2016. Food and agriculture data [Online]. Available: http://faostat3.fao.org/home/E [Accessed].

FEDERICO, M. L., INIGUEZ-LUY, F. L., SKADSEN, R. W. & KAEPPLER, H. F. 2006. Spatial and temporal divergence of expression in duplicated barley germin-like protein-encoding genes. *Genetics,* 174**,** 179-190.

FELDMAN, M. 1995. Wheats. *In:* SMARTT J.; SIMMONDS, N. W. (ed.) *Evolution of crop plants.* Harlow, UK:: Longman Scientific and Technical.

FELDMAN, M. 2001. Origin of cultivated wheat. *In:* BONJEAN, A. P. A., W.J. (ed.) *The world wheat book: A history of wheat breeding.* Paris, France: Lavoisier Publishing,.

FENG, S. H., MARTINEZ, C., GUSMAROLI, G., WANG, Y., ZHOU, J. L., WANG, F., CHEN, L. Y., YU, L., IGLESIAS-PEDRAZ, J. M., KIRCHER, S., SCHAFER, E., FU, X. D., FAN, L. M. & DENG, X. W. 2008. Coordinated regulation of arabidopsis thaliana development by light and gibberellins. *Nature,* 451**,** 475-U9.

FESSELE, S., MAIER, H., ZISCHEK, C., NELSON, P. J. & WERNER, T. 2002. Regulatory context is a crucial part of gene function. *Trends in Genetics,* 18**,** 60-63.

FINCH-SAVAGE, W. E., CADMAN, C. S. C., TOOROP, P. E., LYNN, J. R. & HILHORST, H. W. M. 2007. Seed dormancy release in arabidopsis cvi by dry after-ripening, low temperature, nitrate and light shows common quantitative patterns of gene expression directed by environmentally specific sensing. *Plant Journal,* 51**,** 60-78.

FINCH-SAVAGE, W. E. & LEUBNER-METZGER, G. 2006. Seed dormancy and the control of germination. *New Phytologist,* 171**,** 501-523.

FINCHER, G. B. 1989. Molecular and cellular biology associated with endosperm mobilization in germinating cereal-grains. *Annual Review of Plant Physiology and Plant Molecular Biology,* 40**,** 305-346.

FINERAN, B. A., WILD, D. J. C. & INGERFELD, M. 1982. Initial wall formation in the endosperm of wheat, triticum-aestivum - a re-evaluation. *Canadian Journal of Botany-Revue Canadienne De Botanique,* 60**,** 1776-1795.

FINKELSTEIN, R. R. 2004. The role of hormones during seed development and germination. *Plant Hormones: Biosynthesis, Signal Transduction, Action***,** 513-537.

FINNEY, K. F. & BARMORE, M. A. 1948. Loaf volume and protein content of hard winter and spring wheats. *Cereal Chemistry,* 25**,** 291-312.

FISCHER, R. A. 2007. Understanding the physiological basis of yield potential in wheat. *Journal of Agricultural Science,* 145**,** 99-113.

FIXEN, K. R., THOMAS, S. C. & TONG, C. B. S. 2012. Blue light inhibition of tuberization in a day-neutral potato. *Journal of Plant Growth Regulation,* 31**,** 342-350.

FLEET, C. M., YAMAGUCHI, S., HANADA, A., KAWAIDE, H., DAVID, C. J., KAMIYA, Y. & SUN, T. P. 2003. Overexpression of atcps and atks in arabidopsis confers increased ent-kaurene production but no increase in bioactive gibberellins. *Plant Physiology,* 132**,** 830-839.

FLINTHAM, J. E., BORNER, A., WORLAND, A. J. & GALE, M. D. 1997. Optimizing wheat grain yield: Effects of rht (gibberellin-insensitive) genes. *The Journal of Agricultural Science,* 128**,** 11-25.

FLINTHAM, J. E., HOLDSWORTH, M. J., JACK, P. L., KETTLEWELL, P. S. & PHILLIPS, A. L. 2011. An integrated approach to stabilising hagberg falling number in wheat: Screens, genes and understanding. Project report.

FOOTITT, S., MULLER, K., KERMODE, A. R. & FINCH-SAVAGE, W. E. 2015. Seed dormancy cycling in arabidopsis: Chromatin remodelling and regulation of dog1 in response to seasonal environmental signals. *Plant Journal,* 81**,** 413-425.

FORESIGHT 2011. The future of food and farming, final project report. *Foresight projects.* The Government Office for Science, London.

FOULKES, M. J., SNAPE, J. W., SHEARMAN, V. J. & SYLVESTER-BRADLEY, R. 2007. Physiological processes associated with winter wheat yield potential progress. *Wheat Production in Stressed Environments,* 12**,** 591-597.

FU, X. D., RICHARDS, D. E., AIT-ALI, T., HYNES, L. W., OUGHAM, H., PENG, J. R. & HARBERD, N. P. 2002. Gibberellin-mediated proteasome-dependent degradation of the barley della protein sln1 repressor. *Plant Cell,* 14**,** 3191-3200.

FU, X. D., SUDHAKAR, D., PENG, J. R., RICHARDS, D. E., CHRISTOU, P. & HARBERD, N. P. 2001. Expression of arabidopsis gai in transgenic rice represses multiple gibberellin responses. *Plant Cell,* 13**,** 1791-1802.

FU, Y. B., AHMED, Z. & DIEDERICHSEN, A. 2015. Towards a better monitoring of seed ageing under ex situ seed conservation. *Conservation Physiology,* 3.

FUJIOKA, S., YAMANE, H., SPRAY, C. R., KATSUMI, M., PHINNEY, B. O., GASKIN, P., MACMILLAN, J. & TAKAHASHI, N. 1988. The dominant non-gibberellin-responding dwarf mutant (d8) of maize accumulates native gibberellins. *Proceedings of the National Academy of Sciences of the United States of America,* 85**,** 9031-9035.

FUKAZAWA, J., NAKATA, M., ITO, T., YAMAGUCHI, S. & TAKAHASHI, Y. 2010. The transcription factor rsg regulates negative feedback of ntga20ox1 encoding ga 20-oxidase. *Plant Journal,* 62**,** 1035-1045.

FUKAZAWA, J., TERAMURA, H., MURAKOSHI, S., NASUNO, K., NISHIDA, N., ITO, T., YOSHIDA, M., KAMIYA, Y., YAMAGUCHI, S. & TAKAHASHI, Y. 2014. Dellas function as coactivators of gai-associated factor1 in regulation of gibberellin homeostasis and signaling in arabidopsis. *Plant Cell,* 26**,** 2920-2938.

FURTADO, A., HENRY, R. J. & PELLEGRINESCHI, A. 2009. Analysis of promoters in transgenic barley and wheat. *Plant Biotechnology Journal,* 7**,** 240-253.

FURTADO, A., HENRY, R. J. & TAKAIWA, F. 2008. Comparison of promoters in transgenic rice. *Plant Biotechnology Journal,* 6**,** 679-693.

GALAU, G. A., JAKOBSEN, K. S. & HUGHES, D. W. 1991. The controls of late dicot embryogenesis and early germination. *Physiologia Plantarum,* 81**,** 280-288.

GALE, M. D., LAW, C. N., CHOJECKI, A. J. & KEMPTON, R. A. 1983. Genetic-control of alpha-amylase production in wheat. *Theoretical and Applied Genetics,* 64**,** 309-316.

GALE, M. D. & MARSHALL, G. A. 1973. Insensitivity to gibberellin in dwarf wheats. *Annals of Botany,* 37**,** 729-735.

GALE, M. D., SALTER, A. M. & LENTON, J. R. The induction of germination alpha-amylase during wheat grain development in unfavourable weather conditions. Fourth international symposium on pre-harvest sprouting in cereals., 1987 1987. Westview Press, Colorado, USA, 273-283.

GAN, Z., ELLIS, P. R. & SCHOFIELD, J. D. 1995. Gas cell stabilization and gas retention in wheat bread dough. *Journal of Cereal Science,* 21**,** 215-230.

GAO, X., HU, C. H., LI, H. Z., YAO, Y. J., MENG, M., DONG, J., ZHAO, W. C., CHEN, Q. J. & LI, X. Y. 2013. Factors affecting pre-harvest sprouting resistance in wheat (triticum aestivum l.): A review. *Journal of Animal and Plant Sciences,* 23**,** 556-565.

GAO, X. H., HUANG, X. Z., XIAO, S. L. & FU, X. D. 2008. Evolutionarily conserved della-mediated gibberellin signaling in plants. *Journal of Integrative Plant Biology,* 50**,** 825-834.

GARCIA, A. L., OTTO, B., REICH, S. C., WEICKERT, M. O., STEINIGER, J., MACHOWETZ, A., RUDOVICH, N. N., MOHLIG, M., KATZ, N., SPETH, M., MEUSER, F., DOERFER, J., ZUNFT, H. J. F., PFEIFFER, A. H. F. & KOEBNICK, C. 2007. Arabinoxylan consumption decreases postprandial serum glucose, serum insulin and plasma total ghrelin response in subjects with impaired glucose tolerance. *European Journal of Clinical Nutrition,* 61**,** 334-341.

GELVIN, S. B., KARCHER, S. J. & DIRITA, V. J. 1983. Methylation of the t-DNA in agrobacterium-tumefaciens and in several crown gall tumors. *Nucleic Acids Research,* 11**,** 159-174.

GILBERT, N. 2013. A hard look at gm crops. *Nature,* 497**,** 24-26.

GILROY, S. & JONES, R. L. 1994. Perception of gibberellin and abscisic-acid at the external face of the plasma-membrane of barley (hordeum-vulgare l) aleurone protoplasts. *Plant Physiology,* 104**,** 1185-1192.

GIROUX, M. J. & MORRIS, C. F. 1997. A glycine to serine change in puroindoline b is associated with wheat grain hardness and low levels of starch-surface friabilin. *Theoretical and Applied Genetics,* 95**,** 857-864.

GOMEZ-CADENAS, A., ZENTELLA, R., WALKER-SIMMONS, M. K. & HO, T. H. D. 2001. Gibberellin/abscisic acid antagonism in barley aleurone cells: Site of action of the protein kinase pkaba1 in relation to gibberellin signaling molecules. *Plant Cell,* 13**,** 667-679.

GOMEZ-MENA, C., DE FOLTER, S., COSTA, M. M. R., ANGENENT, G. C. & SABLOWSKI, R. 2005. Transcriptional program controlled by the floral homeotic gene agamous during early organogenesis. *Development,* 132**,** 429-438.

GOODING, M. J., UPPAL, R. K., ADDISU, M., HARRIS, K. D., UAUY, C., SIMMONDS, J. R. & MURDOCH, A. J. 2012. Reduced height alleles (rht) and hagberg falling number of wheat. *Journal of Cereal Science,* 55**,** 305-311.

GRAEBE, J. E., BOWEN, D. H. & MACMILLA.J 1972. Conversion of mevalonic acid into gibberellin a12-aldehyde in a cell-free system from cucurbita pepo. *Planta,* 102**,** 261-&.

GRAEBER, K., LINKIES, A., STEINBRECHER, T., MUMMENHOFF, K., TARKOWSKA, D., TURECKOVA, V., IGNATZ, M., SPERBER, K., VOEGELE, A., DE JONG, H., URBANOVA, T., STRNAD, M. & LEUBNER-METZGER, G. 2014. Delay of germination 1 mediates a conserved coat-dormancy mechanism for the temperature- and gibberellin-dependent control of seed germination. *Proceedings of the National Academy of Sciences of the United States of America,* 111**,** E3571-E3580.

GREBMER, K. V., SALTZMAN, A., BIROL, E., WIESMANN, D., PRASAI, N., YIN, S., YOHANNES, Y., MENON, P., THOMPSON, J. & SONNTAG, A. 2014. 2014 global hunger index: The challenge of hidden hunger. Bonn, Washington, D.C., and Dublin.

GRIFFITHS, J., MURASE, K., RIEU, I., ZENTELLA, R., ZHANG, Z. L., POWERS, S. J., GONG, F., PHILLIPS, A. L., HEDDEN, P., SUN, T. P. & THOMAS, S. G. 2006. Genetic characterization and functional analysis of the gid1 gibberellin receptors in arabidopsis. *Plant Cell,* 18**,** 3399-3414.

GROOS, C., GAY, G., PERRETANT, M. R., GERVAIS, L., BERNARD, M., DEDRYVER, F. & CHARMET, D. 2002. Study of the relationship between pre-harvest sprouting and grain color by quantitative trait loci analysis in a

whitexred grain bread-wheat cross. *Theoretical and Applied Genetics,* 104**,** 39-47.

GROOT, S. P. C., BRUINSMA, J. & KARSSEN, C. M. 1987. The role of endogenous gibberellin in seed and fruit-development of tomato - studies with a gibberellin-deficient mutant. *Physiologia Plantarum,* 71**,** 184-190.

GRUERE, G. & SENGUPTA, D. 2011. Bt cotton and farmer suicides in india: An evidence-based assessment. *Journal of Development Studies,* 47**,** 316-337.

GUAN, C. M., WANG, X. C., FENG, J., HONG, S. L., LIANG, Y., REN, B. & ZUO, J. R. 2014. Cytokinin antagonizes abscisic acid-mediated inhibition of cotyledon greening by promoting the degradation of abscisic acid insensitive5 protein in arabidopsis. *Plant Physiology,* 164**,** 1515-1526.

GUBLER, F., CHANDLER, P. M., WHITE, R. G., LLEWELLYN, D. J. & JACOBSEN, J. V. 2002. Gibberellin signaling in barley aleurone cells. Control of sln1 and gamyb expression. *Plant Physiology,* 129**,** 191-200.

GUBLER, F. & JACOBSEN, J. V. 1992. Gibberellin-responsive elements in the promoter of a barley high-pl alpha-amylase gene. *Plant Cell,* 4**,** 1435-1441.

GUBLER, F., KALLA, R., ROBERTS, J. K. & JACOBSEN, J. V. 1995. Gibberellin-regulated expression of a myb gene in barley aleurone cells - evidence for myb transactivation of a high-pl alpha-amylase gene promoter. *Plant Cell,* 7**,** 1879-1891.

GUBLER, F., WATTS, R. J., KALLA, R., MATTHEWS, P., KEYS, M. & JACOBSEN, J. V. 1997. Cloning of a rice cdna encoding a transcription factor homologous to barley gamyb. *Plant and Cell Physiology,* 38**,** 362-365.

HAAG, J. R. & PIKAARD, C. S. 2011. Multisubunit rna polymerases iv and v: Purveyors of non-coding rna for plant gene silencing. *Nature Reviews Molecular Cell Biology,* 12**,** 483-492.

HABUKA, N., KATAOKA, J., MIYANO, M., TSUGE, H., AGO, H. & NOMA, M. 1993. Nucleotide-sequence of a genomic gene encoding tritin, a ribosome-inactivating protein from triticum-aestivum. *Plant Molecular Biology,* 22**,** 171-176.

HALFORD, N. G., FORDE, J., SHEWRY, P. R. & KREIS, M. 1989. Functional-analysis of the upstream regions of a silent and an expressed member of a family of wheat seed protein genes in transgenic tobacco. *Plant Science,* 62**,** 207-216.

HANFT, J. M. & WYCH, R. D. 1982. Visual indicators of physiological maturity of hard red spring wheat. *Crop Science,* 22**,** 584-588.

HARTWECK, L. M. & OLSZEWSKI, N. E. 2006. Rice gibberellin insensitive dwarf1 is a gibberellin receptor that illuminates and raises questions about ga signaling. *Plant Cell,* 18**,** 278-282.

HASENEYER, G., RAVEL, C., DARDEVET, M., BALFOURIER, F., SOURDILLE, P., CHARMET, G., BRUNEL, D., SAUER, S., GEIGER, H. H., GRANER, A. & STRACKE, S. 2008. High level of conservation between genes coding for the gamyb transcription factor in barley (hordeum vulgare l.) and bread wheat (triticum aestivum l.) collections. *Theoretical and Applied Genetics,* 117**,** 321-331.

HAY, A., KAUR, H., PHILLIPS, A., HEDDEN, P., HAKE, S. & TSIANTIS, M. 2002. The gibberellin pathway mediates knotted1-type homeobox function in plants with different body plans. *Current Biology,* 12**,** 1557-1565.

HECK, G. R., CHAMBERLAIN, A. K. & HO, T. H. D. 1993. Barley embryo globulin-1 gene, beg1 - characterization of cdna, chromosome mapping and regulation of expression. *Molecular & General Genetics,* 239**,** 209-218.

HEDDEN, P. 2003. The genes of the green revolution. *TRENDS in Genetics,* 19**,** 5-9.

HEDDEN, P. 2016. Gibberellin biosynthesis in higher plants. *Annual plant reviews, volume 49.* John Wiley & Sons, Ltd.

HEDDEN, P. & CROKER, S. J. 1992. Regulation of gibberellin biosynthesis in maize seedlings. *Progress in Plant Growth Regulation,* 13**,** 534-544.

HEDDEN, P. & KAMIYA, Y. 1997. Gibberellin biosynthesis: Enzymes, genes and their regulation. *Annual Review of Plant Physiology and Plant Molecular Biology,* 48**,** 431-460.

HEDDEN, P. & PHILLIPS, A. L. 2000. Gibberellin metabolism: New insights revealed by the genes. *trends in plant science,* 5**,** 523-530.

HEDDEN, P. & PROEBSTING, W. M. 1999. Genetic analysis of gibberellin biosynthesis. *Plant Physiology,* 119**,** 365-370.

HEDDEN, P. & THOMAS, S. G. 2012. Gibberellin biosynthesis and its regulation. *Biochemical Journal,* 444**,** 11-25.

HELLIWELL, C. A., CHANDLER, P. M., POOLE, A., DENNIS, E. S. & PEACOCK, W. J. 2001a. The cyp88a cytochrome p450, ent-kaurenoic acid oxidase, catalyzes three steps of the gibberellin biosynthesis pathway. *Proceedings of the National Academy of Sciences of the United States of America,* 98**,** 2065-2070.

HELLIWELL, C. A., SHELDON, C. C., OLIVE, M. R., WALKER, A. R., ZEEVAART, J. A. D., PEACOCK, W. J. & DENNIS, E. S. 1998. Cloning of the arabidopsis ent-kaurene oxidase gene ga3. *Proceedings of the National Academy of Sciences of the United States of America,* 95**,** 9019-9024.

HELLIWELL, C. A., SULLIVAN, J. A., MOULD, R. M., GRAY, J. C., PEACOCK, W. J. & DENNIS, E. S. 2001b. A plastid envelope location of arabidopsis ent-kaurene oxidase links the plastid and endoplasmic reticulum steps of the gibberellin biosynthesis pathway. *Plant Journal,* 28**,** 201-208.

HENDERSON, J. T., LI, H. C., RIDER, S. D., MORDHORST, A. P., ROMERO-SEVERSON, J., CHENG, J. C., ROBEY, J., SUNG, Z. R., DE VRIES, S. C. &

OGAS, J. 2004. Pickle acts throughout the plant to repress expression of embryonic traits and may play a role in gibberellin-dependent responses. *Plant Physiology,* 134**,** 995-1005.

HEUN, M., SCHAFERPREGL, R., KLAWAN, D., CASTAGNA, R., ACCERBI, M., BORGHI, B. & SALAMINI, F. 1997. Site of einkorn wheat domestication identified by DNA fingerprinting. *Science,* 278**,** 1312-1314.

HILHORST, H. W. M. 1995. A critical update on seed dormancy .1. Primary dormancy. *Seed Science Research,* 5**,** 61-73.

HIMI, E. & NODA, K. 2004. Isolation and location of three homoeologous dihydroflavonol-4-reductase (dfr) genes of wheat and their tissue-dependent expression. *Journal of Experimental Botany,* 55**,** 365-375.

HIRANO, K., UEGUCHI-TANAKA, M. & MATSUOKA, M. 2008. Gid1-mediated gibberellin signaling in plants. *Trends in Plant Science,* 13**,** 192-199.

HO, L. C. 1988. Metabolism and compartmentation of imported sugars in sink organs in relation to sink strength. *Annual Review of Plant Physiology and Plant Molecular Biology,* 39**,** 355-378.

HO, T. H. D., NOLAN, R. C. & SHUTE, D. E. 1981. Characterization of a gibberellin-insensitive dwarf wheat, d6899 - evidence for a regulatory step common to many diverse responses to gibberellins. *Plant Physiology,* 67**,** 1026-1031.

HOCHHEIMER, A. & TJIAN, R. 2003. Diversified transcription initiation complexes expand promoter selectivity and tissue-specific gene expression. *Genes & Development,* 17**,** 1309-1320.

HOLDSWORTH, M. J., BENTSINK, L. & SOPPE, W. J. J. 2008a. Molecular networks regulating arabidopsis seed maturation, after-ripening, dormancy and germination. *New Phytologist,* 179**,** 33-54.

HOLDSWORTH, M. J., FINCH-SAVAGE, W. E., GRAPPIN, P. & JOB, D. 2008b. Post-genomics dissection of seed dormancy and germination. *Trends in Plant Science,* 13**,** 7-13.

HOLLAND, P. M., ABRAMSON, R. D., WATSON, R. & GELFAND, D. H. 1991. Detection of specific polymerase chain-reaction product by utilizing the 5'- 3' exonuclease activity of thermus-aquaticus DNA-polymerase. *Proceedings of the National Academy of Sciences of the United States of America,* 88**,** 7276-7280.

HOLTON, T. A. & CORNISH, E. C. 1995. Genetics and biochemistry of anthocyanin biosynthesis. *Plant Cell,* 7**,** 1071-1083.

HONG, Y. F., HO, T. H. D., WU, C. F., HO, S. L., YEH, R. H., LU, C. A., CHEN, P. W., YU, L. C., CHAO, A. L. & YU, S. M. 2012. Convergent starvation signals and hormone crosstalk in regulating nutrient mobilization upon germination in cereals. *Plant Cell,* 24**,** 2857-2873.

HOOLEY, R., BEALE, M. H. & SMITH, S. J. 1991. Gibberellin perception at the plasma-membrane of avena-fatua aleurone protoplasts. *Planta,* 183**,** 274-280.

HOOLEY, R., SMITH, S. J., BEALE, M. H. & WALKER, R. P. 1993. In-vivo photoaffinity-labeling of gibberellin-binding proteins in avena-fatua aleurone. *Australian Journal of Plant Physiology,* 20**,** 573-584.

HORVATH, H., JENSEN, L. G., WONG, O. T., KOHL, E., ULLRICH, S. E., COCHRAN, J., KANNANGARA, C. G. & VON WETTSTEIN, D. 2001. Stability of transgene expression, field performance and recombination breeding of transformed barley lines. *Theoretical and Applied Genetics,* 102**,** 1-11.

HOSHIKAWA, K. 1961. Studies on the ripening of wheat grain : 1. Embryological observations of the early development of the endosperm. *Japanese journal of crop science,* 29**,** 253-257.

HOU, X. L., LEE, L. Y. C., XIA, K. F., YEN, Y. Y. & YU, H. 2010. Dellas modulate jasmonate signaling via competitive binding to jazs. *Developmental Cell,* 19**,** 884-894.

HU, J. H., MITCHUM, M. G., BARNABY, N., AYELE, B. T., OGAWA, M., NAM, E., LAI, W. C., HANADA, A., ALONSO, J. M., ECKER, J. R., SWAIN, S. M., YAMAGUCHI, S., KAMIYA, Y. & SUN, T. P. 2008. Potential sites of bioactive gibberellin production during reproductive growth in arabidopsis. *Plant Cell,* 20**,** 320-336.

HUANG, S. S., RAMAN, A. S., REAM, J. E., FUJIWARA, H., CERNY, R. E. & BROWN, S. M. 1998. Overexpression of 20-oxidase confers a gibberellin-overproduction phenotype in arabidopsis. *Plant Physiology,* 118**,** 773-781.

HUBER, A. G. & GRABE, D. F. 1987. Endosperm morphogenesis in wheat - transfer of nutrients from the antipodals to the lower endosperm. *Crop Science,* 27**,** 1248-1252.

HUESING, J. E., ANDRES, D., BRAVERMAN, M. P., BURNS, A., FELSOT, A. S., HARRIGAN, G. G., HELLMICH, R. L., REYNOLDS, A., SHELTON, A. M., VAN RIJSSEN, W. J., MORRIS, E. J. & ELOFF, J. N. 2016. Global adoption of genetically modified (gm) crops: Challenges for the public sector. *Journal of Agricultural and Food Chemistry,* 64**,** 394-402.

HUI, L., DELMONTE, T. & RANADE, K. 2008. Genotyping using the taqman assay. *Current protocols in human genetics.* John Wiley and Sons, Inc.

HUNG, P. V., MAEDA, T. & MORITA, N. 2006. Waxy and high-amylose wheat starches and flours - characteristics, functionality and application. *Trends in Food Science & Technology,* 17**,** 448-456.

HWANG, Y. S., NICHOL, S., NANDI, S., JERNSTEDT, J. A. & HUANG, N. 2001. Aleurone- and embryo-specific expression of the beta-glucuronidase gene controlled by the barley chi26 and ltp1 promoters in transgenic rice. *Plant Cell Reports,* 20**,** 647-654.

IKEDA, A., UEGUCHI-TANAKA, M., SONODA, Y., KITANO, H., KOSHIOKA, M., FUTSUHARA, Y., MATSUOKA, M. & YAMAGUCHI, J. 2001. Slender rice, a constitutive gibberellin response mutant, is caused by a null mutation of the slr1 gene, an ortholog of the height-regulating gene gai/rga/rht/d8. *Plant Cell,* 13**,** 999-1010.

ITOH, H., TATSUMI, T., SAKAMOTO, T., OTOMO, K., TOYOMASU, T., KITANO, H., ASHIKARI, M., ICHIHARA, S. & MATSUOKA, M. 2004. A rice semi-dwarf gene, tan-ginbozu (d35), encodes the gibberellin biosynthesis enzyme, ent-kaurene oxidase. *Plant Molecular Biology,* 54**,** 533-547.

IZYDORCZYK, M. S. & BILIADERIS, C. G. 1993. Structural heterogeneity of wheat endosperm arabinoxylans. *Cereal Chemistry,* 70**,** 641-646.

IZYDORCZYK, M. S. & BILIADERIS, C. G. 1995. Cereal arabinoxylans: Advances in structure and physicochemical properties. *Carbohydrate Polymers,* 28**,** 33-48.

JACOBSEN, J. V., BARRERO, J. M., HUGHES, T., JULKOWSKA, M., TAYLOR, J. M., XU, Q. & GUBLER, F. 2013. Roles for blue light, jasmonate and nitric oxide in the regulation of dormancy and germination in wheat grain (triticum aestivum l.). *Planta,* 238**,** 121-138.

JACOBSEN, J. V. & CHANDLER, P. M. 1987. *Gibberellin and abscisic acid in germinating cereals*.

JAMIESON, P. D., MARTIN, R. J. & FRANCIS, G. S. 1995. Drought influences on grain-yield of barley, wheat, and maize. *New Zealand Journal of Crop and Horticultural Science,* 23**,** 55-66.

JELSEMA, C. L., RUDDAT, M., MORRE, D. J. & WILLIAMSON, F. A. 1977. Specific binding of gibberellin a-1 to aleurone grain fractions from wheat endosperm. *Plant and Cell Physiology,* 18**,** 1009-1019.

JENNINGS, A. C. & MORTON, R. K. 1963. Changes in nucleic acids and other phosphorus-containing compounds of developing wheat grain. *Australian Journal of Biological Sciences,* 16**,** 332-&.

JIA, S. R., WANG, F., SHI, L., YUAN, Q. H., LIU, W. G., LIAO, Y. L., LI, S. G., JIN, W. J. & PENG, H. P. 2007. Transgene flow to hybrid rice and its male-sterile lines. *Transgenic Research,* 16**,** 491-501.

KAMIYA, Y. & GARCIA-MARTINEZ, J. L. 1999. Regulation or gibberellin biosynthesis by light. *Current Opinion in Plant Biology,* 2**,** 398-403.

KANDA, T., SULLIVAN, K. F. & WAHL, G. M. 1998. Histone-gfp fusion protein enables sensitive analysis of chromosome dynamics in living mammalian cells. *Current Biology,* 8**,** 377-385.

KANEKO, M., ITOH, H., INUKAI, Y., SAKAMOTO, T., UEGUCHI-TANAKA, M., ASHIKARI, M. & MATSUOKA, M. 2003. Where do gibberellin biosynthesis and gibberellin signaling occur in rice plants? *Plant Journal,* 35**,** 104-115.

KANNO, Y., HANADA, A., CHIBA, Y., ICHIKAWA, T., NAKAZAWA, M., MATSUI, M., KOSHIBA, T., KAMIYA, Y. & SEO, M. 2012. Identification of an abscisic acid transporter by functional screening using the receptor complex as a sensor. *Proceedings of the National Academy of Sciences of the United States of America,* 109**,** 9653-9658.

KARLSSON, R., OLERED, R. & ELIASSON, A. C. 1983. Changes in starch granule size distribution and starch gelatinization properties during development and maturation of wheat, barley and rye. *Starke,* 35**,** 335-340.

KASAHARA, H., HANADA, A., KUZUYAMA, T., TAKAGI, M., KAMIYA, Y. & YAMAGUCHI, S. 2002. Contribution of the mevalonate and methylerythritol phosphate pathways to the biosynthesis of gibberellins in arabidopsis. *Journal of Biological Chemistry,* 277**,** 45188-45194.

KATHAGE, J. & QAIM, M. 2012. Economic impacts and impact dynamics of bt (bacillus thuringiensis) cotton in india. *Proceedings of the National Academy of Sciences of the United States of America,* 109**,** 11652-11656.

KATSUMI, M., FOARD, D. E. & PHINNEY, B. O. 1983. Evidence for the translocation of gibberellin-a3 and gibberellin-like substances in grafts between normal, dwarf1 and dwarf5 seedlings of zea-mays-l. *Plant and Cell Physiology,* 24**,** 379-388.

KAY, R., CHAN, A., DALY, M. & MCPHERSON, J. 1987. Duplication of camv-35s promoter sequences creates a strong enhancer for plant genes. *Science,* 236**,** 1299-1302.

KELLOGG, E. A. 2001. Evolutionary history of the grasses. *Plant Physiology,* 125**,** 1198-1205.

KENNEDY, G., NANTEL, G. & SHETTY, P. 2002. The scourge of "hidden hunger": Global dimensions of micronutrient deficiencies. *Food, Nutrition and Agriculture***,** 8-16.

KERSEY, P. J., ALLEN, J. E., ARMEAN, I., BODDU, S., BOLT, B. J., CARVALHO-SILVA, D., CHRISTENSEN, M., DAVIS, P., FALIN, L. J., GRABMUELLER, C., HUMPHREY, J., KERHORNOU, A., KHOBOVA, J., ARANGANATHAN, N. K., LANGRIDGE, N., LOWY, E., MCDOWALL, M. D., MAHESWARI, U., NUHN, M., ONG, C. K., OVERDUIN, B., PAULINI, M., PEDRO, H., PERRY, E., SPUDICH, G., TAPANARI, E., WALTS, B., WILLIAMS, G., TELLO-RUIZ, M., STEIN, J., WEI, S., WARE, D., BOLSER, D. M., HOWE, K. L., KULESHA, E., LAWSON, D., MASLEN, G. & STAINES, D. M. 2016. Ensembl genomes 2016: More genomes, more complexity. *Nucleic Acids Research,* 44**,** D574-D580.

KEW, R. B. G. 2016. Triticum aestivum (bread wheat) [Online]. Available: http://www.kew.org/science-conservation/plants-fungi/triticum-aestivum-bread-wheat [Accessed].

KICHEY, T., HIREL, B., HEUMEZ, E., DUBOIS, F. & LE GOUIS, J. 2007. In winter wheat (triticum aestivum l.), post-anthesis nitrogen uptake and remobilisation to the grain correlates with agronomic traits and nitrogen physiological markers. *Field Crops Research,* 102**,** 22-32.

KIM, W., LEE, Y., PARK, J., LEE, N. & CHOI, G. 2013. Honsu, a protein phosphatase 2c, regulates seed dormancy by inhibiting aba signaling in arabidopsis. *Plant and Cell Physiology,* 54**,** 555-572.

KING, K. E., MORITZ, T. & HARBERD, N. P. 2001. Gibberellins are not required for normal stem growth in arabidopsis thaliana in the absence of gai and rga. *Genetics,* 159**,** 767-776.

KING, R. W., MANDER, L. N., ASP, T., MACMILLAN, C. P., BLUNDELL, C. A. & EVANS, L. T. 2008. Selective deactivation of gibberellins below the shoot apex is critical to flowering but not to stem elongation of lolium. *Molecular Plant,* 1**,** 295-307.

KOEHLER, P. & WIESER, H. 2013. Chemistry of cereal grains. *In:* MARCO, G. & GANZLE, M. (eds.) *Handbook on sourdough biotechnology.* Springer.

KOHLI, A., MIRO, B. & TWYMAN, R. M. 2010. Transgene integration, expression and stability in plants: Strategies for improvements. *Transgenic Crop Plants, Vol 1: Principles and Development***,** 201-237.

KOHLI, A., PRYNNE, M. Q., MIRO, B., PEREIRA, A., TWYMAN, R. M., CAPELL, T. & CHRISTOU, P. 2004. Dedifferentiation-mediated changes in transposition behavior make the activator transposon an ideal tool for functional genomics in rice. *Molecular Breeding,* 13**,** 177-191.

KOK, E. J. & KUIPER, H. A. 2003. Comparative safety assessment for biotech crops. *Trends in Biotechnology,* 21**,** 439-444.

KOLOVOS, P., KNOCH, T. A., GROSVELD, F. G., COOK, P. R. & PAPANTONIS, A. 2012. Enhancers and silencers: An integrated and simple model for their function. *Epigenetics & Chromatin,* 5**,** 8.

KONDHARE, K. R., KETTLEWELL, P. S., FARRELL, A. D., HEDDEN, P. & MONAGHAN, J. M. 2013. The role of sensitivity to abscisic acid and gibberellin in pre-maturity alpha-amylase formation in wheat grains. *Journal of Cereal Science,* 58**,** 472-478.

KONG, L. G., GUO, H. H. & SUN, M. Z. 2015. Signal transduction during wheat grain development. *Planta,* 241**,** 789-801.

KOORNNEEF, M., BENTSINK, L. & HILHORST, H. 2002. Seed dormancy and germination. *Current Opinion in Plant Biology,* 5**,** 33-36.

KOORNNEEF, M., ELGERSMA, A., HANHART, C. J., VANLOENENMARTINET, E. P., VANRIJN, L. & ZEEVAART, J. A. D. 1985. A gibberellin insensitive mutant of arabidopsis-thaliana. *Physiologia Plantarum,* 65**,** 33-39.

KOORNNEEF, M. & VANDERVEEN, J. H. 1980. Induction and analysis of gibberellin sensitive mutants in arabidopsis-thaliana (l) heynh. *Theoretical and Applied Genetics,* 58**,** 257-263.

KOVALCHUK, N., SMITH, J., PALLOTTA, M., SINGH, R., ISMAGUL, A., ELIBY, S., BAZANOVA, N., MILLIGAN, A. S., HRMOVA, M., LANGRIDGE, P. & LOPATO, S. 2009. Characterization of the wheat endosperm transfer cell-specific protein tapr60. *Plant Molecular Biology,* 71**,** 81-98.

KRIZ, A. L. 1999. 7s globulins of cereals. *In:* SHEWRY, P. R. & CASEY, R. (eds.) *Seed proteins.* Dordrecht: Springer Netherlands.

KRIZ, A. R., WALLACE, M. S. & PAIVA, R. 1990. Globulin gene-expression in embryos of maize viviparous mutants - evidence for regulation of the glb1-gene by aba. *Plant Physiology,* 92**,** 538-542.

KUCERA, B., COHN, M. A. & LEUBNER-METZGER, G. 2005. Plant hormone interactions during seed dormancy release and germination. *Seed Science Research,* 15**,** 281-307.

KUROMORI, T., MIYAJI, T., YABUUCHI, H., SHIMIZU, H., SUGIMOTO, E., KAMIYA, A., MORIYAMA, Y. & SHINOZAKI, K. 2010. Abc transporter atabcg25 is involved in abscisic acid transport and responses. *Proceedings of the National Academy of Sciences of the United States of America,* 107**,** 2361-2366.

KUROMORI, T., SUGIMOTO, E. & SHINOZAKI, K. 2014. Intertissue signal transfer of abscisic acid from vascular cells to guard cells. *Plant Physiology,* 164**,** 1587-1592.

LAMACCHIA, C., SHEWRY, P. R., DI FONZO, N., FORSYTH, J. L., HARRIS, N., LAZZERI, P. A., NAPIER, J. A., HALFORD, N. G. & BARCELO, P. 2001. Endosperm-specific activity of a storage protein gene promoter in transgenic wheat seed. *Journal of Experimental Botany,* 52**,** 243-250.

LANE, B. G. 2002. Oxalate, germins, and higher-plant pathogens. *Iubmb Life,* 53**,** 67-75.

LANE, B. G., DUNWELL, J. M., RAY, J. A., SCHMITT, M. R. & CUMING, A. C. 1993. Germin, a protein marker of early plant development, is an oxalate oxidase. *Journal of Biological Chemistry,* 268**,** 12239-12242.

LANGE, M. J. P., LIEBRANDT, A., ARNOLD, L., CHMIELEWSKA, S. M., FELSBERGER, A., FREIER, E., HEUER, M., ZUR, D. & LANGE, T. 2013. Functional characterization of gibberellin oxidases from cucumber, cucumis sativus l. *Phytochemistry,* 90**,** 62-69.

LANGE, T. 1994. Purification and partial amino-acid-sequence of gibberellin 20-oxidase from cucurbita-maxima l endosperm. *Planta,* 195**,** 108-115.

LANGE, T. 1997. Cloning gibberellin dioxygenase genes from pumpkin endosperm by heterologous expression off enzyme activities in escherichia coli. *Proceedings of the National Academy of Sciences of the United States of America,* 94**,** 6553-6558.

LEAH, R., SKRIVER, K., KNUDSEN, S., RUUDHANSEN, J., RAIKHEL, N. V. & MUNDY, J. 1994. Identification of an enhancer silencer sequence

directing the aleurone-specific expression of a barley chitinase gene. *Plant Journal,* 6**,** 579-589.

LEAH, R., TOMMERUP, H., SVENDSEN, I. & MUNDY, J. 1991. Biochemical and molecular characterization of 3 barley seed proteins with antifungal properties. *Journal of Biological Chemistry,* 266**,** 1564-1573.

LEE, D. J. & ZEEVAART, J. A. D. 2005. Molecular cloning of ga 2-oxidase3 from spinach and its ectopic expression in nicotiana sylvestris. *Plant Physiology,* 138**,** 243-254.

LEE, D. J. & ZEEVAART, J. A. D. 2007. Regulation of gibberellin 20-oxidase1 expression in spinach by photoperiod. *Planta,* 226**,** 35-44.

LEE, L. G., CONNELL, C. R. & BLOCH, W. 1993. Allelic discrimination by nick-translation pcr with fluorogenic probes. *Nucleic Acids Research,* 21**,** 3761-3766.

LEE, S., KIM, S. G. & PARK, C. M. 2010. Salicylic acid promotes seed germination under high salinity by modulating antioxidant activity in arabidopsis. *New Phytologist,* 188**,** 626-637.

LEE, S. C., CHENG, H., KING, K. E., WANG, W. F., HE, Y. W., HUSSAIN, A., LO, J., HARBERD, N. P. & PENG, J. R. 2002. Gibberellin regulates arabidopsis seed germination via rgl2, a gai/rga-like gene whose expression is up-regulated following imbibition. *Genes & Development,* 16**,** 646-658.

LEUBNER-METZGER, G. 2001. Brassinosteroids and gibberellins promote tobacco seed germination by distinct pathways. *Planta,* 213**,** 758-763.

LEUBNER-METZGER, G. 2005. Beta-1,3-glucanase gene expression in low-hydrated seeds as a mechanism for dormancy release during tobacco after-ripening. *Plant Journal,* 41**,** 133-145.

LI, F., HAN, Y. Y., FENG, Y. A., XING, S. C., ZHAO, M. R., CHEN, Y. H. & WANG, W. 2013. Expression of wheat expansin driven by the rd29 promoter in tobacco confers water-stress tolerance without impacting growth and development. *Journal of Biotechnology,* 163**,** 281-291.

LI, M., SINGH, R., BAZANOVA, N., MILLIGAN, A. S., SHIRLEY, N., LANGRIDGE, P. & LOPATO, S. 2008. Spatial and temporal expression of endosperm transfer cell-specific promoters in transgenic rice and barley. *Plant Biotechnology Journal,* 6**,** 465-476.

LIM, P. E. & TATE, M. E. 1973. Phytases .2. Properties of phytase fractions f1 and f2 from wheat bran and myoinositol phosphates produced by fraction f2. *Biochimica Et Biophysica Acta,* 302**,** 316-328.

LIM, S., PARK, J., LEE, N., JEONG, J., TOH, S., WATANABE, A., KIM, J., KANG, H., KIM, D. H., KAWAKAMI, N. & CHOI, G. 2013. Aba-insensitive3, aba-insensitive5, and dellas interact to activate the expression of somnus and other high-temperature-inducible genes in imbibed seeds in arabidopsis. *Plant Cell,* 25**,** 4863-4878.

LINGLE, S. E. & CHEVALIER, P. 1985. Development of the vascular tissue of the wheat and barley caryopsis as related to the rate and duration of grain filling. *Crop Science,* 25**,** 123-128.

LINKIES, A. & LEUBNER-METZGER, G. 2012. Beyond gibberellins and abscisic acid: How ethylene and jasmonates control seed germination. *Plant Cell Reports,* 31**,** 253-270.

LIU, S., KRIZ, A., DUNCAN, D. & WIDHOLM, J. 1998. Abscisic acid-regulated glb1 transient expression in cultured maize p3377 cells. *Plant Cell Reports,* 17**,** 650-655.

LIU, S. Q. & KRIZ, A. 1996. Tissue-specific and aba-regulated maize glb1 gene expression in transgenic tobacco. *Plant Cell Reports,* 16**,** 158-162.

LIU, X. D., ZHANG, H., ZHAO, Y., FENG, Z. Y., LI, Q., YANG, H. Q., LUAN, S., LI, J. M. & HE, Z. H. 2013. Auxin controls seed dormancy through stimulation of abscisic acid signaling by inducing arf-mediated abi3 activation in arabidopsis. *Proceedings of the National Academy of Sciences of the United States of America,* 110**,** 15485-15490.

LIU, Y. X., KOORNNEEF, M. & SOPPE, W. J. J. 2007. The absence of histone h2b monoubiquitination in the arabidopsis hub1 (rdo4) mutant reveals a role for chromatin remodeling in seed dormancy. *Plant Cell,* 19**,** 433-444.

LIVAK, K. J., MARMARO, J. & TODD, J. A. 1995. Towards fully automated genome-wide polymorphism screening. *Nature Genetics,* 9**,** 341-342.

LIVAK, K. J. & SCHMITTGEN, T. D. 2001. Analysis of relative gene expression data using real-time quantitative pcr and the 2(t)(-delta delta c) method. *Methods,* 25**,** 402-408.

LODISH, H., BERK, A., ZIPURSKY, L. S., MATSUDAIRA, P., BALTIMORE, D. & DARNELL, J. 2000. Regulation of transcription initiation. *In:* FREEMAN, W. H. (ed.) *Molecular cell biology.* New York.

LOIT, E., MELNYK, C. W., MACFARLANE, A. J., SCOTT, F. W. & ALTOSAAR, I. 2009. Identification of three wheat globulin genes by screening a triticum aestivum bac genomic library with cdna from a diabetes-associated globulin. *Bmc Plant Biology,* 9**,** 11.

LOOSVELD, A., MAES, C., VAN CASTEREN, W. H. M., SCHOLS, H. A., GROBET, P. J. & DELCOUR, J. A. 1998. Structural variation and levels of water-extractable arabinogalactan-peptide in european wheat flours. *Cereal Chemistry,* 75**,** 815-819.

LOPATO, S., BORISJUK, N., LANGRIDGE, P. & HRMOVA, M. 2014. Endosperm transfer cell-specific genes and proteins: Structure, function and applications in biotechnology. *Frontiers in Plant Science,* 5.

LOVEGROVE, A., BARRATT, D. H. P., BEALE, M. H. & HOOLEY, R. 1998. Gibberellin-photoaffinity labelling of two polypeptides in plant plasma membranes. *Plant Journal,* 15**,** 311-320.

LOVEGROVE, A. & HOOLEY, R. 2000. Gibberellin and abscisic acid signalling in aleurone. *Trends in Plant Science,* 5**,** 102-110.

LUNN, G. D., KETTLEWELL, P. S., MAJOR, B. J. & SCOTT, R. K. 2001a. Effects of pericarp alpha-amylase activity on wheat (triticum aestivum) hagberg falling number. *Annals of Applied Biology,* 138**,** 207-214.

LUNN, G. D., MAJOR, B. J., KETTLEWELL, P. S. & SCOTT, R. K. 2001b. Mechanisms leading to excess alpha-amylase activity in wheat (triticum aestivum, l) grain in the uk. *Journal of Cereal Science,* 33**,** 313-329.

MACMILLAN, J. 2002. Occurrence of gibberellins in vascular plants, fungi, and bacteria (vol 20, pg 387, 2002). *Journal of Plant Growth Regulation,* 21**,** 242-243.

MACMILLAN, J., WARD, D. A., PHILLIPS, A. L., SANCHEZBELTRAN, M. J., GASKIN, P., LANGE, T. & HEDDEN, P. 1997. Gibberellin biosynthesis from gibberellin a(12)-aldehyde in endosperm and embryos of marah macrocarpus. *Plant Physiology,* 113**,** 1369-1377.

MACRITCHIE, F. 1981. Flour lipids - theoretical aspects and functional-properties. *Cereal Chemistry,* 58**,** 156-158.

MAGHIRANG, E. B. & DOWELL, F. E. 2003. Hardness measurement of bulk wheat by single-kernel visible and near-infrared reflectance spectroscopy. *Cereal Chemistry,* 80**,** 316-322.

MAGOME, H. & KAMIYA, Y. 2016. Inactivation processes. *Annual plant reviews, volume 49.* John Wiley & Sons, Ltd.

MAGOME, H., NOMURA, T., HANADA, A., TAKEDA-KAMIYA, N., OHNISHI, T., SHINMA, Y., KATSUMATA, T., KAWAIDE, H., KAMIYA, Y. & YAMAGUCHI, S. 2013. Cyp714b1 and cyp714b2 encode gibberellin 13-oxidases that reduce gibberellin activity in rice. *Proceedings of the National Academy of Sciences of the United States of America,* 110**,** 1947-1952.

MAKAI, S., EVA, C., TAMAS, L. & JUHASZ, A. 2015. Multiple elements controlling the expression of wheat high molecular weight glutenin paralogs. *Functional & Integrative Genomics,* 15**,** 661-672.

MARES, D. J. & GALE, M. D. 1990. Control of alpha-amylase synthesis in wheat grains. *Fifth International Symposium on Pre-Harvest Sprouting in Cereals***,** 183-194.

MARES, D. J., NORSTOG, K. & STONE, B. A. 1975. Early stages in development of wheat endosperm .1. Change from free nuclear to cellular endosperm. *Australian Journal of Botany,* 23**,** 311-326.

MARIN-DE LA ROSA, N., PFEIFFER, A., HILL, K., LOCASCIO, A., BHALERAO, R. P., MISKOLCZI, P., GRONLUND, A. L., WANCHOO-KOHLI, A., THOMAS, S. G., BENNETT, M. J., LOHMANN, J. U., BLAZQUEZ, M. A. & ALABADI, D. 2015. Genome wide binding site analysis reveals transcriptional coactivation of cytokinin-responsive genes by della proteins. *Plos Genetics,* 11**,** 20.

MARTIN, C. R., ROUSSER, R. & BRABEC, D. L. 1993. Development of a single-kernel wheat characterization system. *Transactions of the Asae,* 36**,** 1399-1404.

MARTIN, D. N., PROEBSTING, W. M. & HEDDEN, P. 1999. The slender gene of pea encodes a gibberellin 2-oxidase. *Plant Physiology,* 121**,** 775-781.

MASCLAUX-DAUBRESSE, C., DANIEL-VEDELE, F., DECHORGNAT, J., CHARDON, F., GAUFICHON, L. & SUZUKI, A. 2010. Nitrogen uptake, assimilation and remobilization in plants: Challenges for sustainable and productive agriculture. *Annals of Botany,* 105**,** 1141-1157.

MATSUSHITA, A., FURUMOTO, T., ISHIDA, S. & TAKAHASHI, Y. 2007. Agf1, an at-hook protein, is necessary for the negative feedback of atga3ox1 encoding ga 3-oxidase. *Plant Physiology,* 143**,** 1152-1162.

MCKERSIE, B. 2015. Planning for food security in a changing climate. *Journal of Experimental Botany,* 66**,** 3435-3450.

MESSEGUER, J., MARFA, V., CATALA, M. M., GUIDERDONI, E. & MELE, E. 2004. A field study of pollen-mediated gene flow from mediterranean gm rice to conventional rice and the red rice weed. *Molecular Breeding,* 13**,** 103-112.

MEYER, P., LINN, F., HEIDMANN, I., MEYER, H., NIEDENHOF, I. & SAEDLER, H. 1992. Endogenous and environmental-factors influence 35s promoter methylation of a maize a1 gene construct in transgenic petunia and its color phenotype. *Molecular & General Genetics,* 231**,** 345-352.

MIDDLETON, A. M., UBEDA-TOMAS, S., GRIFFITHS, J., HOLMAN, T., HEDDEN, P., THOMAS, S. G., PHILLIPS, A. L., HOLDSWORTH, M. J., BENNETT, M. J., KING, J. R. & OWEN, M. R. 2012. Mathematical modeling elucidates the role of transcriptional feedback in gibberellin signaling. *Proceedings of the National Academy of Sciences of the United States of America,* 109**,** 7571-7576.

MIRALLES, D. J. & SLAFER, G. A. 1995. Yield, biomass and yield components in dwarf, semi-dwarf and tall isogenic lines of spring wheat under recommended and late sowing dates. *Plant Breeding,* 114**,** 392-396.

MIRALLES, D. J. & SLAFER, G. A. 2007. Sink limitations to yield in wheat: How could it be reduced? *Journal of Agricultural Science,* 145**,** 139-149.

MISHIBA, K., NISHIHARA, M., NAKATSUKA, T., ABE, Y., HIRANO, H., YOKOI, T., KIKUCHI, A. & YAMAMURA, S. 2005. Consistent transcriptional silencing of 35s-driven transgenes in gentian. *Plant Journal,* 44**,** 541-556.

MITCHUM, M. G., YAMAGUCHI, S., HANADA, A., KUWAHARA, A., YOSHIOKA, Y., KATO, T., TABATA, S., KAMIYA, Y. & SUN, T. P. 2006. Distinct and overlapping roles of two gibberellin 3-oxidases in arabidopsis development. *Plant Journal,* 45**,** 804-818.

MITSUHARA, I., UGAKI, M., HIROCHIKA, H., OHSHIMA, M., MURAKAMI, T., GOTOH, Y., KATAYOSE, Y., NAKAMURA, S., HONKURA, R., NISHIMIYA, S.,

UENO, K., MOCHIZUKI, A., TANIMOTO, H., TSUGAWA, H., OTSUKI, Y. & OHASHI, Y. 1996. Efficient promoter cassettes for enhanced expression of foreign genes in dicotyledonous and monocotyledonous plants. *Plant and Cell Physiology,* 37**,** 49-59.

MIYAMOTO, T., DEROSE, R., SUAREZ, A., UENO, T., CHEN, M., SUN, T. P., WOLFGANG, M. J., MUKHERJEE, C., MEYERS, D. J. & INOUE, T. 2012. Rapid and orthogonal logic gating with a gibberellin-induced dimerization system. *Nature Chemical Biology,* 8**,** 465-470.

MORIONDO, M., GIANNAKOPOULOS, C. & BINDI, M. 2011. Climate change impact assessment: The role of climate extremes in crop yield simulation. *Climatic Change,* 104**,** 679-701.

MORRIS, C. F. & ROSE, S. P. 1996. Wheat. *In:* HENRY, R. J. & KETTLEWELL, P. S. (eds.) *Cereal grain quality.* 1 ed. London: Chapman and Hall.

MORRISON, I. N. 1975. Ultrastructure of cuticular membranes of developing wheat grain. *Canadian Journal of Botany-Revue Canadienne De Botanique,* 53**,** 2077-2087.

MORRISON, I. N. & OBRIEN, T. P. 1976. Cytokinesis in developing wheat-grain - division with and without a phragmoplast. *Planta,* 130**,** 57-67.

MORRISON, I. N., OBRIEN, T. P. & KUO, J. 1978. Initial cellularization and differentiation of aleurone cells in ventral region of developing wheat-grain. *Planta,* 140**,** 19-30.

MORRISON, W. R., MANN, D. L. & COVENTRY, W. S. A. M. 1975. Selective extraction and quantitative analysis of non-starch and starch lipids from wheat flour. *Journal of the Science of Food and Agriculture,* 26**,** 507-521.

MORRONE, D., CHEN, X. M., COATES, R. M. & PETERS, R. J. 2010. Characterization of the kaurene oxidase cyp701a3, a multifunctional cytochrome p450 from gibberellin biosynthesis. *Biochemical Journal,* 431**,** 337-344.

MOUNLA, M. A. K. 1978. Gibberellin-like substances in parts of developing barley-grain. *Physiologia Plantarum,* 44**,** 268-272.

MRVA, K. & MARES, D. J. 1996. Expression of late maturity a-amylase in wheat containing gibberellc acid insensitivity genes. *Euphytica,* 88**,** 69-76.

MRVA, K. & MARES, D. J. 2001. Induction of late maturity alpha-amylase in wheat by cool temperature. *Australian Journal of Agricultural Research,* 52**,** 477-484.

MRVA, K., WALLWORK, M. & MARES, D. J. 2006. Alpha-amylase and programmed cell death in aleurone of ripening wheat grains. *Journal of Experimental Botany,* 57**,** 877-885.

MURASE, K., HIRANO, Y., SUN, T. P. & HAKOSHIMA, T. 2008. Gibberellin-induced della recognition by the gibberellin receptor gid1. *Nature,* 456**,** 459-U15.

NADEAU, C. D., OZGA, J. A., KUREPIN, L. V., JIN, A., PHARIS, R. P. & REINECKE, D. M. 2011. Tissue-specific regulation of gibberellin biosynthesis in developing pea seeds. *Plant Physiology,* 156**,** 897-912.

NAKABAYASHI, K., BARTSCH, M., XIANG, Y., MIATTON, E., PELLENGAHR, S., YANO, R., SEO, M. & SOPPE, W. J. J. 2012. The time required for dormancy release in arabidopsis is determined by delay of germination1 protein levels in freshly harvested seeds. *Plant Cell,* 24**,** 2826-2838.

NAMBARA, E., OKAMOTO, M., TATEMATSU, K., YANO, R., SEO, M. & KAMIYA, Y. 2010. Abscisic acid and the control of seed dormancy and germination. *Seed Science Research,* 20**,** 55-67.

NELSON, D. C., RISEBOROUGH, J.-A., FLEMATTI, G. R., STEVENS, J., GHISALBERTI, E. L., DIXON, K. W. & SMITH, S. M. 2009. Karrikins discovered in smoke trigger arabidopsis seed germination by a mechanism requiring gibberellic acid synthesis and light. *Plant Physiology,* 149**,** 863-873.

NELSON, S. K. & STEBER, C. M. 2016. Gibberellin hormone signal perception: Down-regulating della repressors of plant growth and development. *Annual plant reviews, volume 49.* John Wiley & Sons, Ltd.

NESBITT, M. 1998. Where was einkorn wheat domesticated? *Trends in Plant Science,* 3**,** 82-83.

NETHERWOOD, T., MARTIN-ORUE, S. M., O'DONNELL, A. G., GOCKLING, S., GRAHAM, J., MATHERS, J. C. & GILBERT, H. J. 2004. Assessing the survival of transgenic plant DNA in the human gastrointestinal tract. *Nature Biotechnology,* 22**,** 204-209.

NODA, K., KAWABATA, C. & KANZAKI, K. 1994. Re-classification of developmental stage of wheat-grain. *Breeding Science,* 44**,** 115-120.

NONOGAKI, H. 2014. Seed dormancy and germination - emerging mechanisms and new hypotheses. *Frontiers in Plant Science,* 5**,** 14.

NORRE, F., PEYROT, C., GARCIA, C., RANCE, I., DREVET, J., THEISEN, M. & GRUBER, V. 2002. Powerful effect of an atypical bifactorial endosperm box from wheat hmwg-dx5 promoter in maize endosperm. *Plant Molecular Biology,* 50**,** 699-712.

OAKENFULL, D. G. & TOPPING, D. L. 1987. The nutritional-value of wheat bran. *Food Technology in Australia,* 39**,** 288-291.

ODELL, J. T., NAGY, F. & CHUA, N. H. 1985. Identification of DNA-sequences required for activity of the cauliflower mosaic virus-35s promoter. *Nature,* 313**,** 810-812.

OFFLER, C. E., MCCURDY, D. W., PATRICK, J. W. & TALBOT, M. J. 2003. Transfer cells: Cells specialized for a special purpose. *Annual Review of Plant Biology,* 54**,** 431-454.

OGAWA, M., HANADA, A., YAMAUCHI, Y., KUWALHARA, A., KAMIYA, Y. & YAMAGUCHI, S. 2003. Gibberellin biosynthesis and response during arabidopsis seed germination. *Plant Cell,* 15**,** 1591-1604.

OLSEN, O. A. 2001. Endosperm development: Cellularization and cell fate specification. *Annual Review of Plant Physiology and Plant Molecular Biology,* 52**,** 233-+.

OLSEN, O. A., LINNESTAD, C. & NICHOLS, S. E. 1999. Developmental biology of the cereal endosperm. *Trends in Plant Science,* 4**,** 253-257.

OLSZEWSKI, N., SUN, T.-P. & GUBLER, F. 2002. Gibberellin signaling: Biosynthesis, catabolism, and response pathways. *The Plant Cell,* 14**,** S61-S80.

ORLAND, E. W. 1917. Studies of inheritance in pisum. Ii. The present state of knowledge of heredity and variation in peas. *Proceedings of the American Philosophical Society,* 56**,** 487-588.

ORTIZ, R. 1998. Critical role of plant biotechnology for the genetic improvement of food crops: Perspectives for the next millennium. *Electronic Journal of Biotechnology; Vol 1, No 3 (1998)*.

OTSUKA, M., KENMOKU, H., OGAWA, M., OKADA, K., MITSUHASHI, W., SASSA, T., KAMIYA, Y., TOYOMASU, T. & YAMAGUCHI, S. 2004. Emission of ent-kaurene, a diterpenoid hydrocarbon precursor for gibberellins, into the headspace from plants. *Plant and Cell Physiology,* 45**,** 1129-1138.

PARK, J., KIM, Y. S., KIM, S. G., JUNG, J. H., WOO, J. C. & PARK, C. M. 2011. Integration of auxin and salt signals by the nac transcription factor ntm2 during seed germination in arabidopsis. *Plant Physiology,* 156**,** 537-549.

PARK, S. H., BANG, S. W., JEONG, J. S., JUNG, H., CHRISTIAN, M., REDILLAS, F. R., KIM, H. I., LEE, K. H., KIM, Y. S. & KIM, J. K. 2012. Analysis of the apx, pgd1 and r1g1b constitutive gene promoters in various organs over three homozygous generations of transgenic rice plants. *Planta,* 235**,** 1397-1408.

PARK, S. H., YI, N., KIM, Y. S., JEONG, M. H., BANG, S. W., CHOI, Y. D. & KIM, J. K. 2010. Analysis of five novel putative constitutive gene promoters in transgenic rice plants. *Journal of Experimental Botany,* 61**,** 2459-2467.

PARKER, M. L., NG, A. & WALDRON, K. W. 2005. The phenolic acid and polysaccharide composition of cell walls of bran layers of mature wheat (triticum aestivum l. Cv. Avalon) grains. *Journal of the Science of Food and Agriculture,* 85**,** 2539-2547.

PASTORI, G. M., STEELE, S. H., JONES, H. D. & SHEWRY, P. R. 2001. Improving the breadmaking quality of elite wheat varieties by genetic engineering. *Aspects of Applied Biology*.

PATE, J. S. & GUNNING, B. E. S. 1972. Transfer cells. *Machlis, Leonard, Winslow R. Briggs and Roderic B. Park (Ed.). Annual Review of Plant Physiology,*

Vol. 23. Xi+505p. Illus. Annual Reviews Inc.: Palo Alto, Calif., U.S.A, 173-196.

PATTERSON, H. D. & THOMPSON, R. 1971. Recovery of inter-block information when block sizes are unequal. *Biometrika,* 58, 545-+.

PAULS, K. P., CHAMBERS, J. A., DUMBROFF, E. B. & THOMPSON, J. E. 1982. Perturbation of phospholipid-membranes by gibberellins. *New Phytologist,* 91, 1-17.

PEARCE, S., HUTTLY, A. K., PROSSER, I. M., LI, Y. D., VAUGHAN, S. P., GALLOVA, B., PATIL, A., COGHILL, J. A., DUBCOVSKY, J., HEDDEN, P. & PHILLIPS, A. L. 2015. Heterologous expression and transcript analysis of gibberellin biosynthetic genes of grasses reveals novel functionality in the ga3ox family. *Bmc Plant Biology,* 15, 18.

PEARSON, T., WILSON, J., GWIRTZ, J., MAGHIRANG, E., DOWELL, F., MCCLUSKEY, P. & BEAN, S. 2007. Relationship between single wheat kernel particle-size distribution and perten skcs 4100 hardness index. *Cereal Chemistry,* 84, 567-575.

PENFIELD, S., GILDAY, A. D., HALLIDAY, K. J. & GRAHAM, I. A. 2006. Della-mediated cotyledon expansion breaks coat-imposed seed dormancy. *Current Biology,* 16, 2366-2370.

PENG, J. R., CAROL, P., RICHARDS, D. E., KING, K. E., COWLING, R. J., MURPHY, G. P. & HARBERD, N. P. 1997. The arabidopsis gai gene defines a signaling pathway that negatively regulates gibberellin responses. *Genes & Development,* 11, 3194-3205.

PENG, J. R., RICHARDS, D. E., HARTLEY, N. M., MURPHY, G. P., DEVOS, K. M., FLINTHAM, J. E., BEALES, J., FISH, L. J., WORLAND, A. J., PELICA, F., SUDHAKAR, D., CHRISTOU, P., SNAPE, J. W., GALE, M. D. & HARBERD, N. P. 1999. 'Green revolution' genes encode mutant gibberellin response modulators. *Nature,* 400, 256-261.

PERCIVAL, J. 1921. *The wheat plant,* London, Duckworth and Co.

PERTEN, H. 1964. Application of falling number method for evaluating alpha-amylase activity. *Cereal Chemistry,* 41, 127-&.

PETERSON, R. E. 1965. *Wheat: Botany, cultivation, and utilization*, Hill Books.

PHILLIPS, A. L. 1998. Gibberellins in arabidopsis. *Plant Physiology and Biochemistry,* 36, 115-124.

PHILLIPS, A. L., WARD, D. A., UKNES, S., APPLEFORD, N. E. J., LANGE, T., HUTTLY, A. K., GASKIN, P., GRAEBE, J. E. & HEDDEN, P. 1995. Isolation and expression of 3 gibberellin 20-oxidase cdna clones from arabidopsis. *Plant Physiology,* 108, 1049-1057.

PINO, M. T., SKINNER, J. S., PARK, E. J., JEKNIC, Z., HAYES, P. M., THORNASHOW, M. F. & CHEN, T. H. H. 2007. Use of a stress inducible promoter to drive ectopic atcbf expression improves potato freezing tolerance while

minimizing negative effects on tuber yield. *Plant Biotechnology Journal,* 5**,** 591-604.

PISKUREWICZ, U. & LOPEZ-MOLINA, L. 2009. The ga-signaling repressor rgl3 represses testa rupture in response to changes in ga and aba levels. *Plant Signaling & Behavior,* 4**,** 63-65.

PLACKETT, A. R. G., POWERS, S. J., FERNANDEZ-GARCIA, N., URBANOVA, T., TAKEBAYASHI, Y., SEO, M., JIKUMARU, Y., BENLLOCH, R., NILSSON, O., RUIZ-RIVERO, O., PHILLIPS, A. L., WILSON, Z. A., THOMAS, S. G. & HEDDEN, P. 2012. Analysis of the developmental roles of the arabidopsis gibberellin 20-oxidases demonstrates that ga20ox1, -2, and -3 are the dominant paralogs. *Plant Cell,* 24**,** 941-960.

PLANT-HORMONES.INFO. 2016. Gibberellins [Online]. Available: http://www.phytohormones.info/gibberellins.htm [Accessed].

POMERANZ, Y. 1988. Chemical composition of kernel structures. St. Paul, Minnesota: American Association of Cereal Chemists.

POOLE, N. 2005. Cereal growth stage. *In:* CORPORATION, G. R. A. D. (ed.).

PORTER, J. R., XIE, L., CHALLINOR, A. J., COCHRANE, K., HOWDEN, S. M., IQBAL, M. M., LOBELL, D. B. & TRAVASSO, M. I. 2014. Food security and food production systems. *In:* FIELD, C. B., BARROS, V. R., DOKKEN, D. J., MACH, K. J., MASTRANDREA, M. D., BILIR, T. E., CHATTERJEE, M., EBI, K. L., ESTRADA, Y. O., GENOVA, R. C., GIRMA, B., KISSEL, E. S., LEVY, A. N., MACCRACKEN, S., MASTRANDREA, P. R. & WHITE, L. L. (eds.) *Climate change 2014: Impacts, adaptation, and vulnerability. Part a: Global and sectoral aspects. Contribution of working group ii to the fifth assessment report of the intergovernmental panel of climate change.* Cambridge, United Kingdom and New York, NY, USA: Cambridge University Press.

PORTO, M. S., PINHEIRO, M. P. N., BATISTA, V. G. L., DOS SANTOS, R. C., MELO, P. D. & DE LIMA, L. M. 2014. Plant promoters: An approach of structure and function. *Molecular Biotechnology,* 56**,** 38-49.

POTENZA, C., ALEMAN, L. & SENGUPTA-GOPALAN, C. 2004. Targeting transgene expression in research, agricultural, and environmental applications: Promoters used in plant transformation. *In Vitro Cellular & Developmental Biology-Plant,* 40**,** 1-22.

PROEBSTING, W. M., HEDDEN, P., LEWIS, M. J., CROKER, S. J. & PROEBSTING, L. N. 1992. Gibberellin concentration and transport in genetic lines of pea - effects of grafting. *Plant Physiology,* 100**,** 1354-1360.

QAIM, M. 2016a. Introduction. *Genetically modified crops and agricultural development.* New York: Palgrave Macmillan US.

QAIM, M. 2016b. Potentials and risks of gm crops. *Genetically modified crops and agricultural development.* New York: Palgrave Macmillan US.

QAIM, M. & KOUSER, S. 2013. Genetically modified crops and food security. *Plos One,* 8**,** 7.

QIU, C. X., SANGHA, J. S., SONG, F. S., ZHOU, Z. Y., YIN, A., GU, K. Y., TIAN, D. S., YANG, J. B. & YIN, Z. C. 2010. Production of marker-free transgenic rice expressing tissue-specific bt gene. *Plant Cell Reports,* 29**,** 1097-1107.

RADI, A., LANGE, T., NIKI, T., KOSHIOKA, M. & LANGE, M. J. P. 2006. Ectopic expression of pumpkin gibberellin oxidases alters gibberellin biosynthesis and development of transgenic arabidopsis plants. *Plant Physiology,* 140**,** 528-536.

RADLEY, M. 1956. Occurrence of substances similar to gibberellic acid in higher plants. *Nature,* 178**,** 1070-1071.

RADLEY, M. 1970. Comparison of endogenous gibberellins and response to applied gibberellin of some dwarf and tall wheat cultivars. *Planta,* 92**,** 292-&.

RAGNI, L., NIEMINEN, K., PACHECO-VILLALOBOS, D., SIBOUT, R., SCHWECHHEIMER, C. & HARDTKE, C. S. 2011. Mobile gibberellin directly stimulates arabidopsis hypocotyl xylem expansion. *Plant Cell,* 23**,** 1322-1336.

RAJEEVKUMAR, S., ANUNANTHINI, P. & SATHISHKUMAR, R. 2015. Epigenetic silencing in transgenic plants. *Frontiers in Plant Science,* 6.

RAMAKERS, C., RUIJTER, J. M., DEPREZ, R. H. L. & MOORMAN, A. F. M. 2003. Assumption-free analysis of quantitative real-time polymerase chain reaction (pcr) data. *Neuroscience Letters,* 339**,** 62-66.

RANJAN, R., PATRO, S., KUMARI, S., KUMAR, D., DEY, N. & MAITI, I. B. 2011. Efficient chimeric promoters derived from full-length and sub-genomic transcript promoters of figwort mosaic virus (fmv). *Journal of Biotechnology,* 152**,** 58-62.

REGNAULT, T., DAVIERE, J.-M. & ACHARD, P. 2016. Long-distance transport of endogenous gibberellins in arabidopsis. *Plant Signaling & Behavior,* 11.

REGNAULT, T., DAVIERE, J. M., WILD, M., SAKVARELIDZE-ACHARD, L., HEINTZ, D., BERGUA, E. C., DIAZ, I. L., GONG, F., HEDDEN, P. & ACHARD, P. 2015. The gibberellin precursor ga(12) acts as a long-distance growth signal in arabidopsis. *Nature Plants,* 1**,** 6.

REID, J. B., MURFET, I. C. & POTTS, W. C. 1983. Internode length in pisum .2. Additional information on the relationship and action of loci le, la, cry, na and lm. *Journal of Experimental Botany,* 34**,** 349-364.

REISBIG, R. R. & BRULAND, O. 1983. The protein-synthesis inhibitors from wheat, barley, and rye have identical antigenic determinants. *Biochemical and Biophysical Research Communications,* 114**,** 190-196.

RESENTINI, F., FELIPO-BENAVENT, A., COLOMBO, L., BLAZQUEZ, M. A., ALABADI, D. & MASIERO, S. 2015. Tcp14 and tcp15 mediate the promotion of seed germination by gibberellins in arabidopsis thaliana. *Molecular Plant,* 8**,** 482-485.

REYNOLDS, M., FOULKES, M. J., SLAFER, G. A., BERRY, P., PARRY, M. A. J., SNAPE, J. W. & ANGUS, W. J. 2009. Raising yield potential in wheat. *Journal of Experimental Botany,* 60**,** 1899-1918.

REYNOLDS, M. P. & BORLAUG, N. E. 2006. Impacts of breeding on international collaborative wheat improvement. *Journal of Agricultural Science,* 144**,** 3-17.

REYNOLDS, M. P., PELLEGRINESCHI, A. & SKOVMAND, B. 2005. Sink-limitation to yield and biomass: A summary of some investigations in spring wheat. *Annals of Applied Biology,* 146**,** 39-49.

RIEU, I., ERIKSSON, S., POWERS, S. J., GONG, F., GRIFFITHS, J., WOOLLEY, L., BENLLOCH, R., NILSSON, O., THOMAS, S. G., HEDDEN, P. & PHILLIPS, A. L. 2008a. Genetic analysis reveals that c-19-ga 2-oxidation is a major gibberellin inactivation pathway in arabidopsis. *Plant Cell,* 20**,** 2420-2436.

RIEU, I., RUIZ-RIVERO, O., FERNANDEZ-GARCIA, N., GRIFFITHS, J., POWERS, S. J., GONG, F., LINHARTOVA, T., ERIKSSON, S., NILSSON, O., THOMAS, S. G., PHILLIPS, A. L. & HEDDEN, P. 2008b. The gibberellin biosynthetic genes atga20ox1 and atga20ox2 act, partially redundantly, to promote growth and development throughout the arabidopsis life cycle. *Plant Journal,* 53**,** 488-504.

ROBERT, L. S., ADELL, K. & ALTOSAAR, I. 1985. Homology among 3s and 7s globulins from cereals and pea. *Plant Physiology,* 78**,** 812-816.

ROBERT, L. S., THOMPSON, R. D. & FLAVELL, R. B. 1989. Tissue-specific expression of a wheat high molecular-weight glutenin gene in transgenic tobacco. *Plant Cell,* 1**,** 569-578.

RODRIGO, M. J., GARCIAMARTINEZ, J. L., SAUTES, C. M., GASKIN, P. & HEDDEN, P. 1997. The role of gibberellins a(1) and a(3) in fruit growth of pisum sativum l and the identification of gibberellins a(4) and a(7) in young seeds. *Planta,* 201**,** 446-455.

ROGERS, S. O. & QUATRANO, R. S. 1983. Morphological staging of wheat caryopsis development. *American Journal of Botany,* 70**,** 308-311.

ROITSCH, T. 1999. Source-sink regulation by sugar and stress. *Current Opinion in Plant Biology,* 2**,** 198-206.

RONG, J., LU, B. R., SONG, Z. P., SU, J., SNOW, A. A., ZHANG, X. S., SUN, S. G., CHEN, R. & WANG, F. 2007. Dramatic reduction of crop-to-crop gene flow within a short distance from transgenic rice fields. *New Phytologist,* 173**,** 346-353.

ROSEGRANT, M. W. & CLINE, S. A. 2003. Global food security: Challenges and policies. *Science,* 302**,** 1917-1919.

ROSS, J. J., MURFET, I. C. & REID, J. B. 1997. Gibberellin mutants. *PHYSIOLOGIA PLANTARUM,* 100**,** 550-560.

RUAN, Y. L. 2014. Sucrose metabolism: Gateway to diverse carbon use and sugar signaling. *In:* MERCHANT, S. S. (ed.) *Annual review of plant biology, vol 65.* Palo Alto: Annual Reviews.

RUSSELL, P. J. 1996. *Genetics, 4th edn.,* New York, Harper Collins College.

SABELLI, P. A. & LARKINS, B. A. 2009. The development of endosperm in grasses. *Plant Physiology,* 149**,** 14-26.

SAITO, H., OIKAWA, T., HAMAMOTO, S., ISHIMARU, Y., KANAMORI-SATO, M., SASAKI-SEKIMOTO, Y., UTSUMI, T., CHEN, J., KANNO, Y., MASUDA, S., KAMIYA, Y., SEO, M., UOZUMI, N., UEDA, M. & OHTA, H. 2015. The jasmonate-responsive gtr1 transporter is required for gibberellin-mediated stamen development in arabidopsis. *Nature Communications,* 6**,** 11.

SAITO, T., ABE, H., YAMANE, H., SAKURAI, A., MUROFUSHI, N., TAKIO, K., TAKAHASHI, N. & KAMIYA, Y. 1995. Purification and properties of ent-kaurene synthase-b from immature seeds of pumpkin. *Plant Physiology,* 109**,** 1239-1245.

SAKAMOTO, T., KAMIYA, N., UEGUCHI-TANAKA, M., IWAHORI, S. & MATSUOKA, M. 2001a. Knox homeodomain protein directly suppresses the expression of a gibberellin biosynthetic gene in the tobacco shoot apical meristem. *Genes & Development,* 15**,** 581-590.

SAKAMOTO, T., KOBAYASHI, M., ITOH, H., TAGIRI, A., KAYANO, T., TANAKA, H., IWAHORI, S. & MATSUOKA, M. 2001b. Expression of a gibberellin 2-oxidase gene around the shoot apex is related to phase transition in rice. *Plant Physiology,* 125**,** 1508-1516.

SAKAMOTO, T., MIURA, K., ITOH, H., TATSUMI, T., UEGUCHI-TANAKA, M., ISHIYAMA, K., KOBAYASHI, M., AGRAWAL, G. K., TAKEDA, S., ABE, K., MIYAO, A., HIROCHIKA, H., KITANO, H., ASHIKARI, M. & MATSUOKA, M. 2004. An overview of gibberellin metabolism enzyme genes and their related mutants in rice. *Plant Physiology,* 134**,** 1642-1653.

SAMBROOK, J., FRITSCH, E. F. & MANIATIS, T. 1989. *Molecular cloning: A laboratory manual*, Cold Spring Harbor Laboratory Press.

SANDSTEDT, R. M. 1946. Photomicrographic studies of wheat starch .1. Development of the starch granules. *Cereal Chemistry,* 23**,** 337-359.

SARNOWSKA, E. A., ROLICKA, A. T., BUCIOR, E., CWIEK, P., TOHGE, T., FERNIE, A. R., JIKUMARU, Y., KAMIYA, Y., FRANZEN, R., SCHMELZER, E., PORRI, A., SACHAROWSKI, S., GRATKOWSKA, D. M., ZUGAJ, D. L., TAFF, A., ZALEWSKA, A., ARCHACKI, R., DAVIS, S. J., COUPLAND, G., KONCZ, C., JERZMANOWSKI, A. & SARNOWSKI, T. J. 2013. Della-interacting swi3c core subunit of switch/sucrose nonfermenting chromatin remodeling complex modulates gibberellin responses and hormonal cross talk in arabidopsis. *Plant Physiology,* 163**,** 305-317.

SAULNIER, L., GUILLON, F. & CHATEIGNER-BOUTIN, A. L. 2012. Cell wall deposition and metabolism in wheat grain. *Journal of Cereal Science,* 56**,** 91-108.

SAWASAKI, T., NISHIHARA, M. & ENDO, Y. 2008. Rip and ralyase cleave the sarcin/ricin domain, a critical domain for ribosome function, during senescence of wheat coleoptiles. *Biochemical and Biophysical Research Communications,* 370**,** 561-565.

SAYRE, K. D., RAJARAM, S. & FISCHER, R. A. 1997. Yield potential progress in short bread wheats in northwest mexico. *Crop Science,* 37**,** 36-42.

SCHOMBURG, F. M., BIZZELL, C. M., LEE, D. J., ZEEVAART, J. A. D. & AMASINO, R. M. 2003. Overexpression of a novel class of gibberellin 2-oxidases decreases gibberellin levels and creates dwarf plants. *Plant Cell,* 15**,** 151-163.

SCHWARTZ, D. 1979. Analysis of the size alleles of the pro gene in maize - evidence for a mutant protein processor. *Molecular & General Genetics,* 174**,** 233-240.

SEO, M., HANADA, A., KUWAHARA, A., ENDO, A., OKAMOTO, M., YAMAUCHI, Y., NORTH, H., MARION-POLL, A., SUN, T. P., KOSHIBA, T., KAMIYA, Y., YAMAGUCHI, S. & NAMBARA, E. 2006. Regulation of hormone metabolism in arabidopsis seeds: Phytochrome regulation of abscisic acid metabolism and abscisic acid regulation of gibberellin metabolism. *Plant Journal,* 48**,** 354-366.

SERRANI, J. C., SANJUAN, R., RUIZ-RIVERO, O., FOS, M. & GARCIA-MARTINEZ, J. L. 2007. Gibberellin regulation of fruit set and growth in tomato. *Plant Physiology,* 145**,** 246-257.

SERRAT, X., ESTEBAN, R., PENAS, G., CATALA, M. M., MELE, E. & MESSEGUER, J. 2013. Direct and reverse pollen-mediated gene flow between gm rice and red rice weed. *Aob Plants,* 5**,** 12.

SHEWRY, P. R. 2009. Wheat. *Journal of Experimental Botany,* 60**,** 1537-1553.

SHEWRY, P. R., MITCHELL, R. A. C., TOSI, P., WAN, Y., UNDERWOOD, C., LOVEGROVE, A., FREEMAN, J., TOOLE, G. A., MILLS, E. N. C. & WARD, J. L. 2012. An integrated study of grain development of wheat (cv. Hereward). *Journal of Cereal Science,* 56**,** 21-30.

SHEWRY, P. R., NAPIER, J. A. & TATHAM, A. S. 1995. Seed storage proteins - structures and biosynthesis. *Plant Cell,* 7**,** 945-956.

SHEWRY, P. R., PELLNY, T. K. & LOVEGROVE, A. 2016. Is modern wheat bad for health? *Nature Plants,* 2**,** 3.

SHEWRY, P. R. & TATHAM, A. S. 1990. The prolamin storage proteins of cereal seeds - structure and evolution. *Biochemical Journal,* 267**,** 1-12.

SHEWRY, P. R., TATHAM, A. S. & HALFORD, N. G. 1999. The prolamins of the triticeae. *In:* SHEWRY, P. R. & CASEY, R. (eds.) *Seed proteins.* Dordrecht: Springer Netherlands.

SHU, K., LIU, X. D., XIE, Q. & HE, Z. H. 2016. Two faces of one seed: Hormonal regulation of dormancy and germination. *Molecular Plant,* 9**,** 34-45.

SHU, K., MENG, Y. J., SHUAI, H. W., LIU, W. G., DU, J. B., LIU, J. & YANG, W. Y. 2015. Dormancy and germination: How does the crop seed decide? *Plant Biology,* 17**,** 1104-1112.

SHU, K., ZHANG, H. W., WANG, S. F., CHEN, M. L., WU, Y. R., TANG, S. Y., LIU, C. Y., FENG, Y. Q., CAO, X. F. & XIE, Q. 2013. Abi4 regulates primary seed dormancy by regulating the biogenesis of abscisic acid and gibberellins in arabidopsis. *Plos Genetics,* 9**,** 14.

SILVERSTONE, A. L., CHANG, C. W., KROL, E. & SUN, T. P. 1997. Developmental regulation of the gibberellin biosynthetic gene ga1 in arabidopsis thaliana. *Plant Journal,* 12**,** 9-19.

SILVERSTONE, A. L., JUNG, H. S., DILL, A., KAWAIDE, H., KAMIYA, Y. & SUN, T. P. 2001. Repressing a repressor: Gibberellin-induced rapid reduction of the rga protein in arabidopsis. *Plant Cell,* 13**,** 1555-1565.

SINGER, T. P. & HOFSTEE, B. H. J. 1948. Studies on wheat germ lipase .1. Methods of estimation, purification, and general properties of the enzyme. *Archives of Biochemistry,* 18**,** 229-243.

SKRIVER, K., OLSEN, F. L., ROGERS, J. C. & MUNDY, J. 1991. Cis-acting DNA elements responsive to gibberellin and its antagonist abscisic-acid. *Proceedings of the National Academy of Sciences of the United States of America,* 88**,** 7266-7270.

SNELL, C., BERNHEIM, A., BERGE, J. B., KUNTZ, M., PASCAL, G., PARIS, A. & RICROCH, A. E. 2012. Assessment of the health impact of gm plant diets in long-term and multigenerational animal feeding trials: A literature review. *Food and Chemical Toxicology,* 50**,** 1134-1148.

SONG, J. C., JIANG, L. J. & JAMESON, P. E. 2012. Co-ordinate regulation of cytokinin gene family members during flag leaf and reproductive development in wheat. *Bmc Plant Biology,* 12**,** 16.

SPARKS, C. A., DOHERTY, A. & JONES, H. D. 2014. Genetic transformation of wheat via agrobacterium-mediated DNA delivery. *In:* HENRY, R. J. & FURTADO, A. (eds.) *Cereal genomics: Methods and protocols.* Totowa: Humana Press Inc.

SPARKS, C. A. & JONES, H. D. 2014. Genetic transformation of wheat via particle bombardment. *Methods in molecular biology (Clifton, N.J.),* 1099**,** 201-18.

SPIELMEYER, W., ELLIS, M., ROBERTSON, M., ALI, S., LENTON, J. R. & CHANDLER, P. M. 2004. Isolation of gibberellin and metabolic pathway genes from barley and comparative mapping in barley, wheat and rice. *Theoretical and Applied Genetics,* 109**,** 847-855.

SPONSEL, V. M. 1983. The localization, metabolism and biological-activity of gibberellins in maturing and germinating-seeds of pisum-sativum cv progress no-9. *Planta,* 159**,** 454-468.

STANGA, J. P., SMITH, S. M., BRIGGS, W. R. & NELSON, D. C. 2013. Suppressor of more axillary growth2 1 controls seed germination and seedling development in arabidopsis. *Plant Physiology,* 163**,** 318-330.

STAPPER, M. & MURRAY, D. 1986. *Siragcrop: Field observations and crop standards for wheat*. *SIRAGCROP Technical Report No. 1.* Griffith, Australia,: CSIRO and Department of Agriculture New South

Wales.

STEVENSON, L., PHILLIPS, F., O'SULLIVAN, K. & WALTON, J. 2012. Wheat bran: Its composition and benefits to health, a european perspective. *International Journal of Food Sciences and Nutrition,* 63**,** 1001-1013.

STEWART, T. S., HRUBY, D. E., SHARMA, O. K. & ROBERTS, W. K. 1977. Atp-dependent inhibition of protein-synthesis in ascites cell-extracts by wheat-germ protein. *Biochimica Et Biophysica Acta,* 479**,** 31-38.

STOLFI, A., GANDHI, S., SALEK, F. & CHRISTIAEN, L. 2014. Tissue-specific genome editing in ciona embryos by crispr/cas9. *Development,* 141**,** 4115-4120.

STRACKE, R., WERBER, M. & WEISSHAAR, B. 2001. The r2r3-myb gene family in arabidopsis thaliana. *Current Opinion in Plant Biology,* 4**,** 447-456.

SUN, T. P. & GUBLER, F. 2004. Molecular mechanism of gibberellin signaling in plants. *Annu Rev Plant Biol,* 55**,** 197-223.

SUN, T. P. & KAMIYA, Y. 1994. The arabidopsis ga1 locus encodes the cyclase ent-kaurene synthetase-a of gibberellin biosynthesis. *Plant Cell,* 6**,** 1509-1518.

SWAIN, S. M., REID, J. B. & KAMIYA, Y. 1997. Gibberellins are required for embryo growth and seed development in pea. *Plant Journal,* 12**,** 1329-1338.

TAL, I., ZHANG, Y., JORGENSEN, M. E., PISANTY, O., BARBOSA, I. C. R., ZOURELIDOU, M., REGNAULT, T., CROCOLL, C., OLSEN, C. E., WEINSTAIN, R., SCHWECHHEIMER, C., HALKIER, B. A., NOUR-ELDIN, H. H., ESTELLE, M. & SHANI, E. 2016. The arabidopsis npf3 protein is a ga transporter. *Nature Communications,* 7**,** 11.

TEALE, W. D., PAPONOV, I. A. & PALME, K. 2006. Auxin in action: Signalling, transport and the control of plant growth and development. *Nature Reviews Molecular Cell Biology,* 7**,** 847-859.

TENG, F., ZHAI, L. H., LIU, R. X., BAI, W., WANG, L. Q., HUO, D. G., TAO, Y. S., ZHENG, Y. L. & ZHANG, Z. X. 2013. Zmga3ox2, a candidate gene for a major qtl, qph3.1, for plant height in maize. *Plant Journal,* 73**,** 405-416.

THE GOLDEN RICE PROJECT. 2016. Available: http://goldenrice.org/index.php [Accessed].

THIEL, J. 2014. Development of endosperm transfer cells in barley. *Frontiers in Plant Science,* 5.

THOMAS, M. S. & FLAVELL, R. B. 1990. Identification of an enhancer element for the endosperm-specific expression of high-molecular-weight glutenin. *Plant Cell,* 2**,** 1171-1180.

THOMAS, S. G., BLÁZQUEZ, M. A. & ALABADÍ, D. 2016. Della proteins: Master regulators of gibberellin-responsive growth and development. *Annual plant reviews, volume 49.* John Wiley & Sons, Ltd.

THOMAS, S. G., PHILLIPS, A. L. & HEDDEN, P. 1999. Molecular cloning and functional expression of gibberellin 2-oxidases, multifunctional enzymes involved in gibberellin deactivation. *Proceedings of the National Academy of Sciences of the United States of America,* 96**,** 4698-4703.

THOMAS, S. G. & SUN, T. P. 2004. Update on gibberellin signaling. A tale of the tall and the short. *Plant Physiology,* 135**,** 668-676.

THOMPSON, R. D., BARTELS, D. & HARBERD, N. P. 1985. Nucleotide-sequence of a gene from chromosome-1d of wheat encoding a hmw-glutenin subunit. *Nucleic Acids Research,* 13**,** 6833-6848.

THOMPSON, R. D., HUEROS, G., BECKER, H. A. & MAITZ, M. 2001. Development and functions of seed transfer cells. *Plant Science,* 160**,** 775-783.

TILMAN, D., BALZER, C., HILL, J. & BEFORT, B. L. 2011. Global food demand and the sustainable intensification of agriculture. *Proceedings of the National Academy of Sciences of the United States of America,* 108**,** 20260-20264.

TOH, S., KAMIYA, Y., KAWAKAMI, N., NAMBARA, E., MCCOURT, P. & TSUCHIYA, Y. 2012. Thermoinhibition uncovers a role for strigolactones in arabidopsis seed germination. *Plant and Cell Physiology,* 53**,** 107-117.

TORADA, A. & AMANO, Y. 2002. Effect of seed coat color on seed dormancy in different environments. *Euphytica,* 126**,** 99-105.

TOSI, P., PARKER, M., GRITSCH, C. S., CARZANIGA, R., MARTIN, B. & SHEWRY, P. R. 2009. Trafficking of storage proteins in developing grain of wheat. *Journal of Experimental Botany,* 60**,** 979-991.

TSUJI, H., AYA, K., UEGUCHI-TANAKA, M., SHIMADA, Y., NAKAZONO, M., WATANABE, R., NISHIZAWA, N. K., GOMI, K., SHIMADA, A., KITANO, H., ASHIKARI, M. & MATSUOKA, M. 2006. Gamyb controls different sets of genes and is differentially regulated by microrna in aleurone cells and anthers. *Plant Journal,* 47**,** 427-444.

TUDZYNSKI, B., KAWAIDE, H. & KAMIYA, Y. 1998. Gibberellin biosynthesis in gibberella fujikuroi: Cloning and characterization of the copalyl diphosphate synthase gene. *Current Genetics,* 34**,** 234-240.

UBEDA-TOMAS, S., SWARUP, R., COATES, J., SWARUP, K., LAPLAZE, L., BEEMSTER, G. T. S., HEDDEN, P., BHALERAO, R. & BENNETT, M. J. 2008. Root growth in arabidopsis requires gibberellin/della signalling in the endodermis. *Nature Cell Biology,* 10**,** 625-628.

UEGUCHI-TANAKA, M., ASHIKARI, M., NAKAJIMA, M., ITOH, H., KATOH, E., KOBAYASHI, M., CHOW, T. Y., HSING, Y. I. C., KITANO, H., YAMAGUCHI, I. & MATSUOKA, M. 2005. Gibberellin insensitive dwarf1 encodes a soluble receptor for gibberellin. *Nature,* 437**,** 693-698.

UEGUCHI-TANAKA, M., NAKAJIMA, M., KATOH, E., OHMIYA, H., ASANO, K., SAJI, S., XIANG, H. Y., ASHIKARI, M., KITANO, H., YAMAGUCHI, I. & MATSUOKAA, M. 2007. Molecular interactions of a soluble gibberellin receptor, gid1, with a rice della protein, slr1, and gibberellin. *Plant Cell,* 19**,** 2140-2155.

UNICEF & MICRONUTRIENT INITIATIVE 2004. Vitamin and mineral deficiency, a global progress report.

UNTERGASSER, A., NIJVEEN, H., RAO, X., BISSELING, T., GEURTS, R. & LEUNISSEN, J. A. M. 2007. Primer3plus, an enhanced web interface to primer3. *Nucleic Acids Research,* 35**,** W71-W74.

URBANOVA, T. & LEUBNER-METZGER, G. 2016. Gibberellins and seed germination. *Annual plant reviews, volume 49.* John Wiley & Sons, Ltd.

USDA. 2016. Usda national nutrient database for standard reference [Online]. Available: http://www.ars.usda.gov/main/site_main.htm?modecode=12-35-45-00 [Accessed].

VARBANOVA, M., YAMAGUCHI, S., YANG, Y., MCKELVEY, K., HANADA, A., BOROCHOV, R., YU, F., JIKUMARU, Y., ROSS, J., CORTES, D., MA, C. J., NOEL, J. P., MANDER, L., SHULAEV, V., KAMIYA, Y., RODERMEL, S., WEISS, D. & PICHERSKY, E. 2007. Methylation of gibberellins by arabidopsis gamt1 and gamt2. *Plant Cell,* 19**,** 32-45.

VENKATESWARLU, B. & VISPERAS, R. M. 1987. Source-sink relationships in crop plants. *IRRI Research Paper Series, International Rice Research Institute***,** 19 pp.-19 pp.

VIETEN, A., SAUER, M., BREWER, P. B. & FRIML, J. 2007. Molecular and cellular aspects of auxin-transport-mediated development. *Trends in Plant Science,* 12**,** 160-168.

WALKER-SIMMONS, M. 1987. Aba levels and sensitivity in developing wheat embryos of sprouting resistant and susceptible cultivars. *Plant Physiology,* 84**,** 61-66.

WANG, C. C. & GRANT, D. R. 1969. Proteolytic enzymes in wheat flour. *Cereal Chemistry,* 46**,** 537-&.

WANG, G. F., WANG, G., ZHANG, X. W., WANG, F. & SONG, R. T. 2012. Isolation of high quality rna from cereal seeds containing high levels of starch. *Phytochemical Analysis,* 23**,** 159-163.

WANG, H., CARUSO, L. V., DOWNIE, A. B. & PERRY, S. E. 2004. The embryo mads domain protein agamous-like 15 directly regulates expression of a gene encoding an enzyme involved in gibberellin metabolism. *Plant Cell,* 16**,** 1206-1219.

WANG, H. L., OFFLER, C. E. & PATRICK, J. W. 1994a. Nucellar projection transfer cells in the developing wheat-grain. *Protoplasma,* 182**,** 39-52.

WANG, H. L., OFFLER, C. E. & PATRICK, J. W. 1995a. The cellular pathway of photosynthate transfer in the developing wheat-grain .2. A structural-analysis and histochemical-studies of the pathway from the crease phloem to the endosperm cavity. *Plant Cell and Environment,* 18**,** 373-388.

WANG, H. L., OFFLER, C. E., PATRICK, J. W. & UGALDE, T. D. 1994b. The cellular pathway of photosynthate transfer in the developing wheat-grain .1. Delineation of a potential transfer pathway using fluorescent dyes. *Plant Cell and Environment,* 17**,** 257-266.

WANG, H. L., PATRICK, J. W., OFFLER, C. E. & WANG, X. D. 1995b. The cellular pathway of photosynthate transfer in the developing wheat-grain .3. A structural-analysis and physiological-studies of the pathway from the endosperm cavity to the starchy endosperm. *Plant Cell and Environment,* 18**,** 389-407.

WANG, H. Y., YANG, H., SHIVALILA, C. S., DAWLATY, M. M., CHENG, A. W., ZHANG, F. & JAENISCH, R. 2013a. One-step generation of mice carrying mutations in multiple genes by crispr/cas-mediated genome engineering. *Cell,* 153**,** 910-918.

WANG, X. R., WU, R., LIN, X. Y., BAI, Y., SONG, C. D., YU, X. M., XU, C. M., ZHAO, N., DONG, Y. Z. & LIU, B. 2013b. Tissue culture-induced genetic and epigenetic alterations in rice pure-lines, f1 hybrids and polyploids. *Bmc Plant Biology,* 13**,** 12.

WARRAICH, E. A., AHMAD, N., BASRA, S. M. & AFZAL, I. 2002. Effect of nitrogen on source-sink relationship in wheat. *Int. J. Agri. Biol,* 4**,** 300-02.

WEN, C. K. & CHANG, C. 2002. Arabidopsis rgl1 encodes a negative regulator of gibberellin responses. *Plant Cell,* 14**,** 87-100.

WESTON, D. E., ELLIOTT, R. C., LESTER, D. R., RAMEAU, C., REID, J. B., MURFET, I. C. & ROSS, J. J. 2008. The pea della proteins la and cry are important regulators of gibberellin synthesis and root growth. *Plant Physiology,* 147**,** 199-205.

WHEATBP. 2016. Wheat, the big picture [Online]. University of Bristol. Available: http://www.cerealsdb.uk.net/cerealgenomics/WheatBP/Documents/DOC_WheatBP.php [Accessed].

WILLIGE, B. C., GHOSH, S., NILL, C., ZOURELIDOU, M., DOHMANN, E. M. N., MAIER, A. & SCHWECHHEIMER, C. 2007. The della domain of ga insensitive mediates the interaction with the ga insensitive dwarf1a gibberellin receptor of arabidopsis. *Plant Cell,* 19**,** 1209-1220.

WILSON, C., BELLEN, H. J. & GEHRING, W. J. 1990. Position effects on eukaryotic gene-expression. *Annual Review of Cell Biology,* 6**,** 679-714.

WINTON, A. L. & WINTON, B. W. 1932. The structure and composition of foods. By andrew l. Winton, ph.D., and kate barber winton, ph.D. Volume i. Cereals, starch, oil seeds, nuts, oils, forage plants. 710 pages, with 274 illustrations by the authors. *Journal of the American Pharmaceutical Association,* 21**,** 637-638.

WOODGER, F. J., MILLAR, A., MURRAY, F., JACOBSEN, J. V. & GUBLER, F. 2003. The role of gamyb transcription factors in ga-regulated gene expression. *Journal of Plant Growth Regulation,* 22**,** 176-184.

WORLD BANK 2007. World development report 2008 : Agriculture for development. Washington, DC: © World Bank.

WORLD HEALTH ORGANISATION. 2016. Micronutrient deficiencies: Vitamin a deficiency [Online]. Available: http://www.who.int/nutrition/topics/vad/en/ [Accessed].

WRIGLEY, C. W., BÉKÉS, F. & BUSHUK, W. 2006. Chapter 1 gluten: A balance of gliadin and glutenin. *Gliadin and glutenin: The unique balance of wheat quality.* AACC International, Inc.

WU, S. P., DRUKA, A., HORVATH, H., KLEINHOFS, A., KANNANGARA, C. G. & VON WETTSTEIN, D. 2000. Functional characterization of seed coat-specific members of the barley germin gene family. *Plant Physiology and Biochemistry,* 38**,** 685-698.

XIE, Z., ZHANG, Z. L., HANZLIK, S., COOK, E. & SHEN, Q. X. J. 2007. Salicylic acid inhibits gibberellin-induced alpha-amylase expression and seed germination via a pathway involving an abscisic-acid-inducible wrky gene. *Plant Molecular Biology,* 64**,** 293-303.

XING, S. F., QIN, G. J., SHI, Y., MA, Z. Q., CHEN, Z. L., GU, H. Y. & QU, L. J. 2007. Gamt2 encodes a methyltransferase of gibberellic acid that is involved in seed maturation and germination in arabidopsis. *Journal of Integrative Plant Biology,* 49**,** 368-381.

XIONG, J. S., DING, J. & LI, Y. 2015. Genome-editing technologies and their potential application in horticultural crop breeding. *Horticulture Research,* 2.

XU, Y. L., LI, L., GAGE, D. A. & ZEEVAART, J. A. D. 1999. Feedback regulation of ga5 expression and metabolic engineering of gibberellin levels in arabidopsis. *Plant Cell,* 11**,** 927-935.

YAMAGUCHI, N., WINTER, C. M., WU, M. F., KANNO, Y., YAMAGUCHI, A., SEO, M. & WAGNER, D. 2014. Gibberellin acts positively then negatively to control onset of flower formation in arabidopsis. *Science,* 344**,** 638-641.

YAMAGUCHI, S. 2008. Gibberellin metabolism and its regulation. *Annual review of plant biology,* 59**,** 225-51.

YAMAGUCHI, S., KAMIYA, Y. & NAMBARA, E. 2007. Regulation of aba and ga levels during seed development and germination in arabidopsis. *Annual plant reviews volume 27: Seed development, dormancy and germination.* Blackwell Publishing Ltd.

YAMAGUCHI, S., KAMIYA, Y. & SUN, T. P. 2001. Distinct cell-specific expression patterns of early and late gibberellin biosynthetic genes during arabidopsis seed germination. *Plant Journal,* 28**,** 443-453.

YAMAGUCHI, S., SAITO, T., ABE, H., YAMANE, H., MUROFUSHI, N. & KAMIYA, Y. 1996. Molecular cloning and characterization of a cdna encoding the gibberellin biosynthetic enzyme ent-kaurene synthase b from pumpkin (cucurbita maxima l). *Plant Journal,* 10**,** 203-213.

YAMAMOTO, Y. Y., ICHIDA, H., MATSUI, M., OBOKATA, J., SAKURAI, T., SATOU, M., SEKI, M., SHINOZAKI, K. & ABE, T. 2007. Identification of plant promoter constituents by analysis of local distribution of short sequences. *Bmc Genomics,* 8**,** 23.

YAMAUCHI, Y., TAKEDA-KAMIYA, N., HANADA, A., OGAWA, M., KUWAHARA, A., SEO, M., KAMIYA, Y. & YAMAGUCHI, S. 2007. Contribution of gibberellin deactivation by atga2ox2 to the suppression of germination of dark-imbibed arabidopsis thaliana seeds. *Plant and Cell Physiology,* 48**,** 555-561.

YANG, G. H., ZHAO, X. Q., LI, B., LIU, J. Z., ZHENG, Q., TONG, Y. P. & LI, Z. S. 2003a. Molecular cloning and characterization of a dfr from developing seeds of blue-grained wheat in anthocyanin biosynthetic pathway. *Acta Botanica Sinica,* 45**,** 1329-1338.

YANG, J. C., ZHANG, J. H., WANG, Z. Q. & ZHU, Q. S. 2003b. Hormones in the grains in relation to sink strength and postanthesis development of spikelets in rice. *Plant Growth Regulation,* 41**,** 185-195.

YANO, K., AYA, K., HIRANO, K., ORDONIO, R. L., UEGUCHI-TANAKA, M. & MATSUOKA, M. 2015. Comprehensive gene expression analysis of rice aleurone cells: Probing the existence of an alternative gibberellin receptor. *Plant Physiology,* 167**,** 531-U421.

YE, X. D., AL-BABILI, S., KLOTI, A., ZHANG, J., LUCCA, P., BEYER, P. & POTRYKUS, I. 2000. Engineering the provitamin a (beta-carotene) biosynthetic pathway into (carotenoid-free) rice endosperm. *Science,* 287**,** 303-305.

YONGJUN, H. C. & LIN, Y. J. 2013. Promise and issues of genetically modified crops. *Current Opinion in Plant Biology,* 16**,** 255-260.

YU, S.-M., LO, S.-F. & HO, T.-H. D. 2015. Source-sink communication: Regulated by hormone, nutrient, and stress cross-signaling. *Trends in Plant Science,* 20**,** 844-857.

YUPSANIS, T., BURGESS, S. R., JACKSON, P. J. & SHEWRY, P. R. 1990. Characterization of the major protein-component from aleurone cells of barley (hordeum-vulgare l). *Journal of Experimental Botany,* 41**,** 385-392.

ZADOKS, J. C., CHANG, T. T. & KONZAK, C. F. 1974. Decimal code for growth stages of cereals. *Weed Research,* 14**,** 415-421.

ZEE, S. Y. & OBRIEN, T. P. 1970. Studies on ontogeny of pigment strand in caryopsis of wheat. *Australian Journal of Biological Sciences,* 23**,** 1153-&.

ZENTELLA, R., ZHANG, Z. L., PARK, M., THOMAS, S. G., ENDO, A., MURASE, K., FLEET, C. M., JIKUMARU, Y., NAMBARA, E., KAMIYA, Y. & SUN, T. P. 2007. Global analysis of della direct targets in early gibberellin signaling in arabidopsis. *Plant Cell,* 19**,** 3037-3057.

ZHANG, C. X., TANABE, K., TAMURA, F., ITAI, A., MATSUMOTO, K. & YOSHIDA, A. 2007. Roles of gibberellins in increasing fruit size and sink demand in japanese pear fruit during rapid fruit growth. *Hortscience,* 42**,** 880-881.

ZHANG, D., JING, Y. J., JIANG, Z. M. & LIN, R. C. 2014. The chromatin-remodeling factor pickle integrates brassinosteroid and gibberellin signaling during skotomorphogenic growth in arabidopsis. *Plant Cell,* 26**,** 2472-2485.

ZHANG, Z. L., OGAWA, M., FLEET, C. M., ZENTELLA, R., HU, J. H., HEO, J. O., LIM, J., KAMIYA, Y., YAMAGUCHI, S. & SUN, T. P. 2011. Scarecrow-like 3 promotes gibberellin signaling by antagonizing master growth repressor della in arabidopsis. *Proceedings of the National Academy of Sciences of the United States of America,* 108**,** 2160-2165.

ZHENG, C. & BAUM, B. J. 2008. Evaluation of promoters for use in tissue-specific gene delivery. *In:* LE DOUX, J. M. (ed.) *Gene therapy protocols: Design and characterization of gene transfer vectors.* Totowa, NJ: Humana Press.

ZHU, Y. Y., NOMURA, T., XU, Y. H., ZHANG, Y. Y., PENG, Y., MAO, B. Z., HANADA, A., ZHOU, H. C., WANG, R. X., LI, P. J., ZHU, X. D., MANDER, L. N., KAMIYA, Y., YAMAGUCHI, S. & HE, Z. H. 2006. Elongated uppermost internode encodes a cytochrome p450 monooxygenase that epoxidizes gibberellins in a novel deactivation reaction in rice. *Plant Cell,* 18**,** 442-456.

Appendices

Appendix 1: Primer sequences

Table A.1: Sequences of genotyping primers

Name	Sequence (5' - 3')
ACTIN-F	ATACACGCTTCCTCATGCTATCC
ACTIN-R	GCTCTATTTTGGCCTCTCTTAGC
7Sg-F	ATCCACACGCCCTTCAATAG
Gai-R	CGTTGGAAGGTGTACCGAGT
Chi26-F	TTGAGCGTCGTCACAGTTTC
DFRd-F	CGACGTGGACCGACTAAAAT
20ox-R	TTGCATTCTTCTTGTGTCCG
END1-F	AGAGCGGCATGGAAGTAAGA
GerF-F	TAATGGCCAATGGGTACGAT
Tri-F	GCAGAACCTGCTACCTTTGC
2ox-R	GATGGCACTTGGGTTTCAGT
Pc2ox-F	TCATAGTGAACGCCTGTAGG
Pc2ox-R	TGTTCTTCACTGCTGTAATG
At20ox1-F	TCAAACTCCGTTAATCTTCAACC
At20ox1-R	GGAGAGAGGCATATCAAAGAAGC

Table A.2: Sequences of TaqMan assay primers and probes

Name	Sequence (5' - 3')
HvCon2-F	TGCTAACCGTGTGGCATCAC
HvCon2-R	CAGATGCAGCAGCACTATGTACC
HvCon2-probe	CATGAGCGTGTGCGTGTCTGCG - 5' JOE, 3' BHQ1
Q_PC2ox-F	CCATCAATTCCAACACCGCATAG
Q_PC2ox-R	GAAAATGCAAAGTGATTTGGGTGAG
QPc2ox-probe	CTGCTGTAATGTAGTTCTCCACCACCGCC - 5' FAM, 3' BHQ1
Q_At20ox1-F	CCCTTTCTTTCCGGTTTTGC
Q_At20ox1-R	GTTGGGACATGGGTTTCAGC
Q_At20ox1-probe	GACGACATGAGACCGCTCAAAATCCG - 5' FAM, 3' BHQ1
Q_GAi-F	ACGAGTCAAACAACGTCGAG
Q_GAi-R	GATCGCACCAGGTCGTCCCA
Q_Gai-probe	GTAAACGGCCACAAGTTCAG - 5' FAM, 3' BHQ1

Table A.3: Sequences of qRT-PCR primers

Name	Sequence (5' - 3')
qTa2526-Fext	GATCGACCAAGAATGGGATGACAAGGAAGATG
qTa2526-Rext	CTGTCCAGCAATGGGAGGATGACTGG
qGAPDH-ex3F	ACCCCTTCATCACCACCGACTACATGACC
qGAPDH-ex4R	GGCTGCAGGAACCCTGAGGAGATCC
qSDH-01F	GAGACGCTCCATTTGCTCTCCGTG
qSDH-01R	CCCTTAGGAGCTCTGCGACAGAAGAT
gai_qPCR-F	TGGTTGACTCGCAGGAGAA
gai_qPCR-R	CTTGCGCTGAAGCTGTTCAG
GFP_qPCR_F	GACGACGGCAACTACAAGAC
GFP_qPCR_R	AAGGGCATCGACTTCAAGGA
TaAmy1_F2	CCGAGATATGGACGTCGCTCGCGTA
TaAmy1_R2	TCCGGCCCCGGCACCACGTTC
Amy2_F_ext	GGAGGAACGGCAACCTGTGCTG
Amy2_R_ext	TCTCGCCGGATTCGCGTCCGG
q_At20ox1_F1	GATCCATCCTCCACTTTAGA
q_At20ox1_R1	TCAGACGCTCATGAATACAC
Q_Pc2ox-F	CACCCCGATGCCAAGAATCTCATAGT
Q_Pc2ox-R	CTTCGGCTTCTTCAAGCTTGTGAACC
Ta20ox3-F	ACTTCACTTGGCGTGAATTCC
Ta20ox3-R	GCAGAAGCACTACCGCTCTG

Appendix 2: TaqMan assay results for various constructs

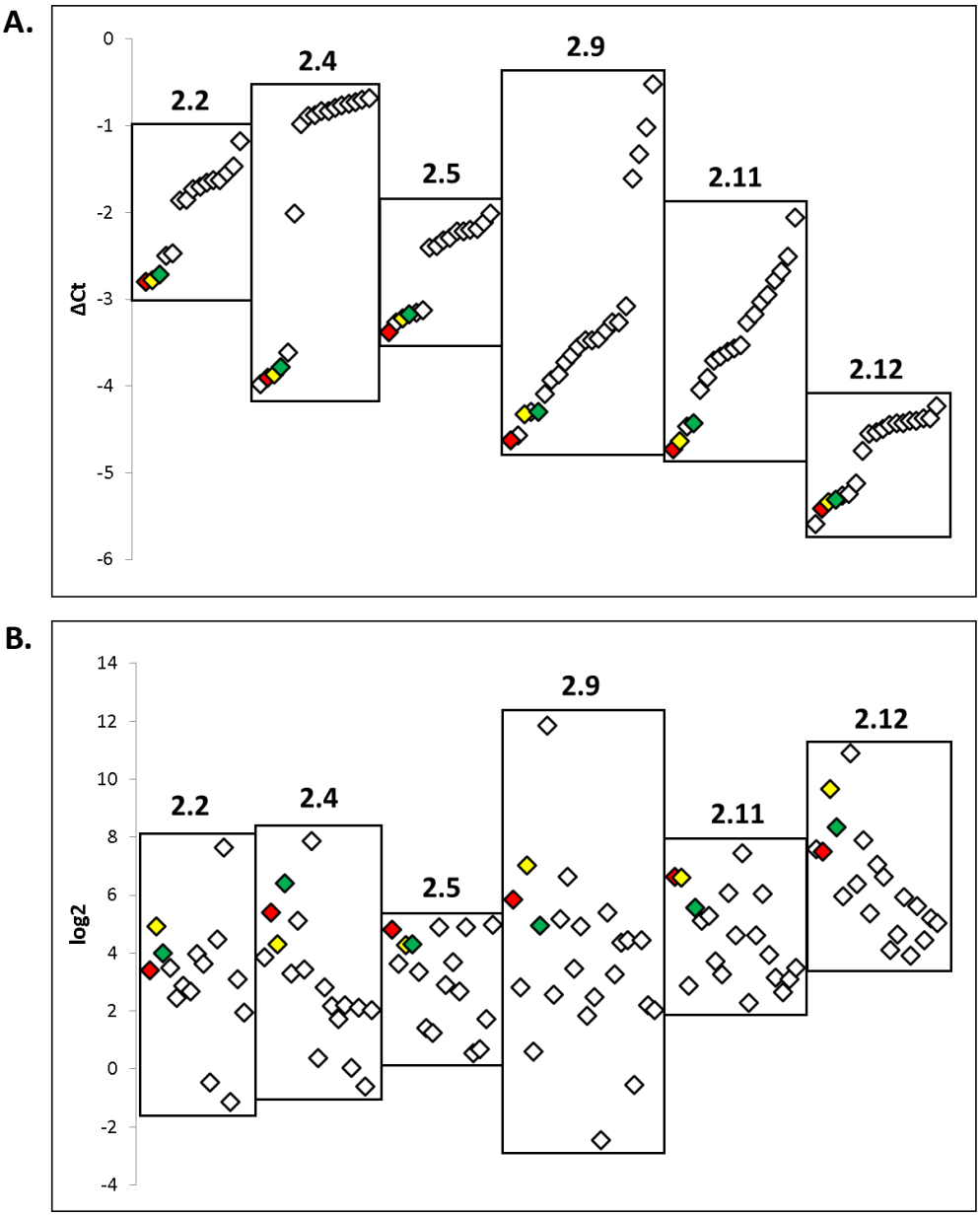


Figure A.1: TaqMan assay results for *TaEND1::AtGA20ox1*

ΔCt (A) and log2 transformed NRQ (B) values for five different lines. Each box contains values for positive progeny within an independent transgenic line. Coloured plots represent those plants selected as potential homozygotes for further analysis, with the three matching colours representing the same plants in both graphs.

Table A.4: Confirmation PCR results for T2 *TaEND1::AtGA20ox1* transgenic lines

Results of PCR on T2 generation plants of *TaEND1::AtGA20ox1* to confirm TaqMan assay results. Rows in bold show homozygous lines.

Line	No. of +ve plants	No. of -ve plants	Zygosity
2.2.21	**23**	**0**	**Homozygous**
2.2.4	**23**	**0**	**Homozygous**
2.2.14	22	2	Hemizygous
2.4.13	15	9	Hemizygous
2.4.6	14	9	Hemizygous
2.4.17	12	12	Hemizygous
2.5.2	**24**	**0**	**Homozygous**
2.5.24	**22**	**0**	**Homozygous**
2.5.17	**24**	**0**	**Homozygous**
2.9.9	**24**	**0**	**Homozygous**
2.9.5	**24**	**0**	**Homozygous**
2.9.11	**23**	**0**	**Homozygous**
2.11.21	**24**	**0**	**Homozygous**
2.11.5	22	1	Hemizygous
2.11.15	23	1	Hemizygous
2.12.3	**23**	**0**	**Homozygous**
2.12.2	21	1	Hemizygous
2.12.7	**24**	**0**	**Homozygous**

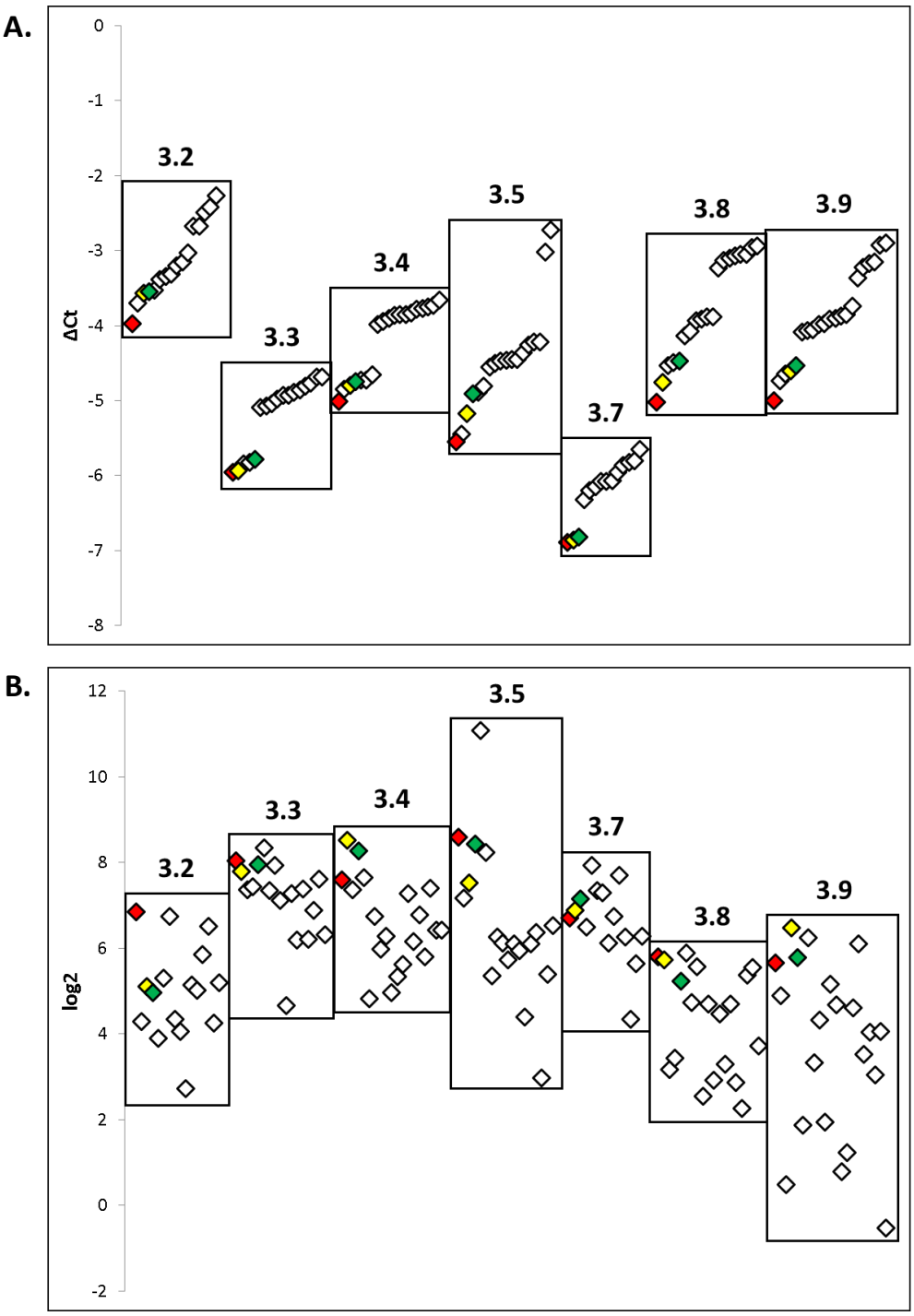


Figure A.2: TaqMan assay results for *HvGerF::AtGA20ox1*

ΔCt (A) and log2 transformed NRQ (B) values for seven different lines. Each box contains values for positive progeny within an independent transgenic line. Coloured plots represent those plants selected as potential homozygotes for further analysis, with the three matching colours representing the same plants in both graphs.

Table A.5: Confirmation PCR results for T2 *HvGerF::AtGA20ox1* transgenic lines

Results of PCR on T2 generation plants of *HvGerF::AtGA20ox1* to confirm TaqMan assay results. Rows in bold show homozygous lines.

Line	No. of +ve plants	No. of -ve plants	Zygosity
3.2.17	**24**	**0**	**Homozygous**
3.2.8	22	1	Hemizygous
3.2.22	21	3	Hemizygous
3.3.6	**23**	**0**	**Homozygous**
3.3.4	**22**	**0**	**Homozygous**
3.3.21	**24**	**0**	**Homozygous**
3.4.2	**24**	**0**	**Homozygous**
3.4.21	23	1	Hemizygous
3.4.22	**23**	**0**	**Homozygous**
3.5.21	**24**	**0**	**Homozygous**
3.5.23	**22**	**0**	**Homozygous**
3.5.4	**24**	**0**	**Homozygous**
3.7.3	**23**	**0**	**Homozygous**
3.7.5	22	1	Hemizygous
3.7.16	**22**	**0**	**Homozygous**
3.8.14	20	1	Hemizygous
3.8.24	**21**	**0**	**Homozygous**
3.8.18	**23**	**0**	**Homozygous**
3.9.6	17	7	Hemizygous
3.9.10	**22**	**0**	**Homozygous**
3.9.19	**21**	**0**	**Homozygous**

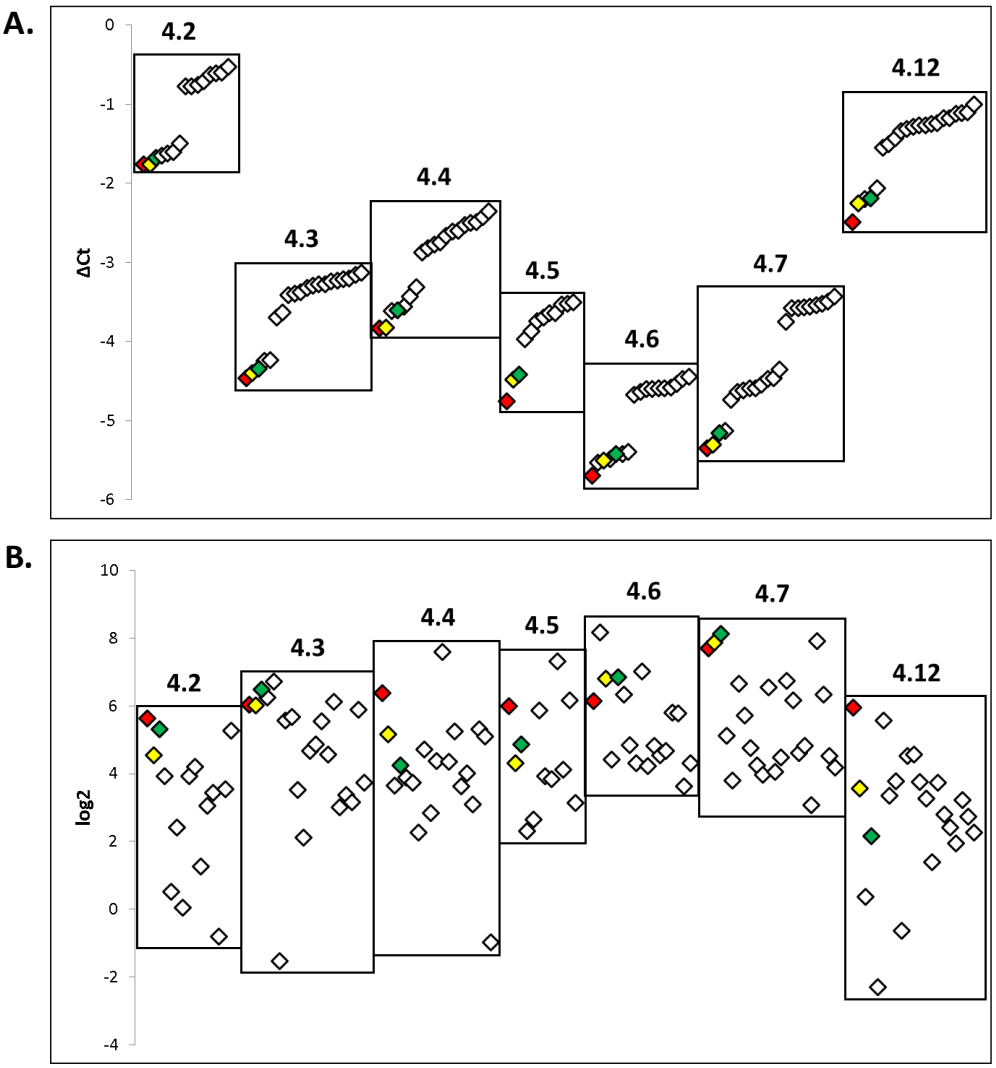


Figure A.3: TaqMan assay results for *TaDFR-D::AtGA20ox1*

ΔCt (A) and log2 transformed NRQ (B) values for seven different lines. Each box contains values for positive progeny within an independent transgenic line. Coloured plots represent those plants selected as potential homozygotes for further analysis, with the three matching colours representing the same plants in both graphs.

Table A.6: Confirmation PCR results for T2 *TaDFR-D::AtGA20ox1* transgenic lines

Results of PCR on T2 generation plants of *TaDFRd::AtGA20ox1* to confirm TaqMan assay results. Rows in bold show homozygous lines.

Line	No. of +ve plants	No. of -ve plants	Zygosity
4.2.24	**24**	**0**	**Homozygous**
4.2.11	**23**	**0**	**Homozygous**
4.2.20	23	1	Hemizygous
4.3.6	**23**	**0**	**Homozygous**
4.3.12	**24**	**0**	**Homozygous**
4.3.8	**23**	**0**	**Homozygous**
4.4.15	**23**	**0**	**Homozygous**
4.4.18	**23**	**0**	**Homozygous**
4.4.5	**24**	**0**	**Homozygous**
4.5.2	**24**	**0**	**Homozygous**
4.5.10	**23**	**0**	**Homozygous**
4.5.5	**24**	**0**	**Homozygous**
4.6.10	**23**	**0**	**Homozygous**
4.6.12	**24**	**0**	**Homozygous**
4.6.17	**24**	**0**	**Homozygous**
4.12.2	**23**	**0**	**Homozygous**
4.12.7	**22**	**0**	**Homozygous**
4.12.20	**24**	**0**	**Homozygous**

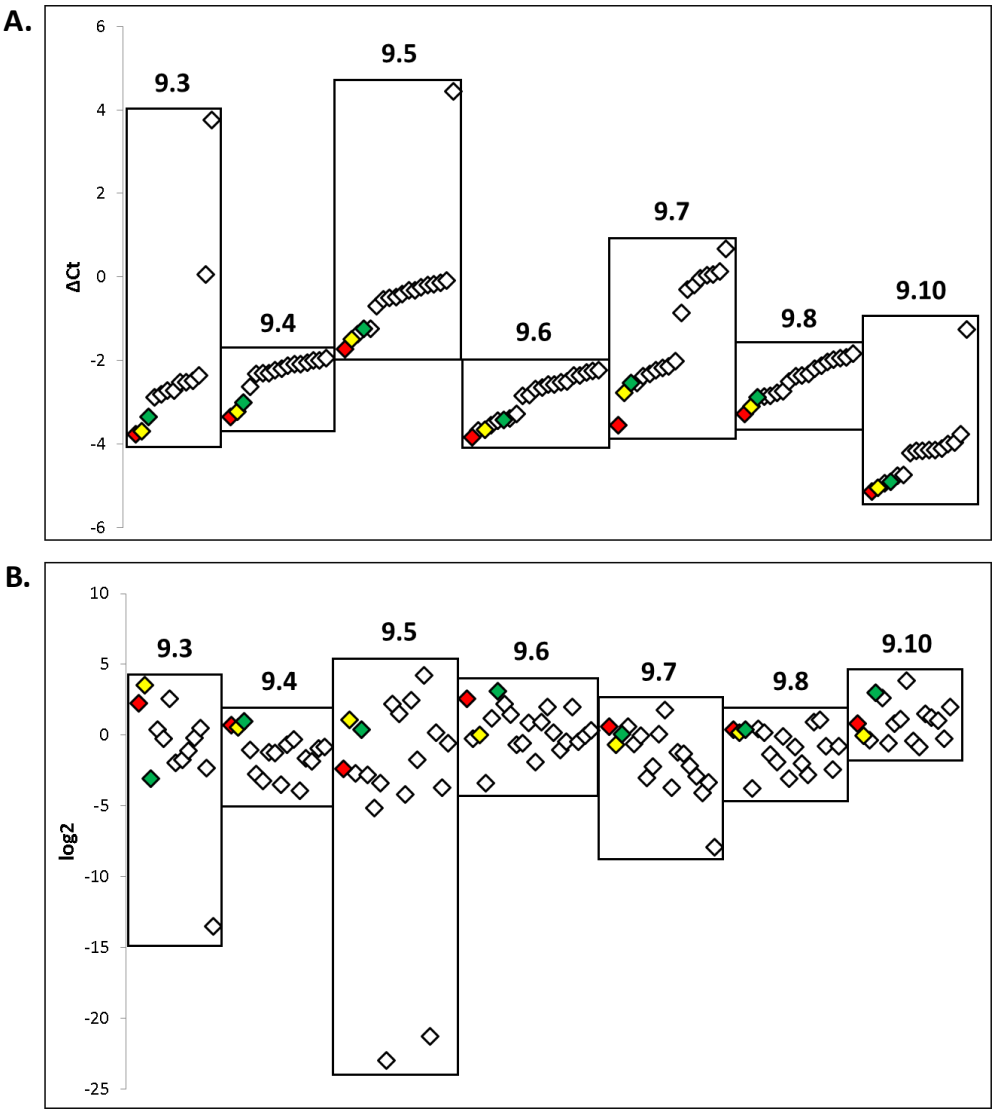


Figure A.4: TaqMan assay results for *HvChi26::Atgai*

ΔCt (A) and log2 transformed NRQ (B) values for seven different lines. Each box contains values for positive progeny within an independent transgenic line. Coloured plots represent those plants selected as potential homozygotes for further analysis, with the three matching colours representing the same plants in both graphs.

Table A.7: Confirmation PCR results for T2 *HvChi26::Atgai* transgenic lines

Results of PCR on T2 generation plants of *HvChi26::Atgai* to confirm TaqMan assay results. Rows in bold show homozygous lines.

Line	No. of +ve plants	No. of -ve plants	Zygosity
9.3.5	**24**	**0**	**Homozygous**
9.3.2	**23**	**0**	**Homozygous**
9.3.4	10	14	Hemizygous
9.4.9	**22**	**0**	**Homozygous**
9.4.6	**24**	**0**	**Homozygous**
9.4.2	**24**	**0**	**Homozygous**
9.5.22	**24**	**0**	**Homozygous**
9.5.6	**24**	**0**	**Homozygous**
9.5.12	**24**	**0**	**Homozygous**
9.6.23	23	1	Hemizygous
9.6.14	23	1	Hemizygous
9.6.4	**24**	**0**	**Homozygous**
9.7.5	20	4	Hemizygous
9.7.7	22	2	Hemizygous
9.7.8	**24**	**0**	**Homozygous**
9.8.16	20	4	Hemizygous
9.8.23	21	3	Hemizygous
9.8.2	**24**	**0**	**Homozygous**
9.10.22	**24**	**0**	**Homozygous**
9.10.6	18	6	Hemizygous
9.10.8	**23**	**0**	**Homozygous**

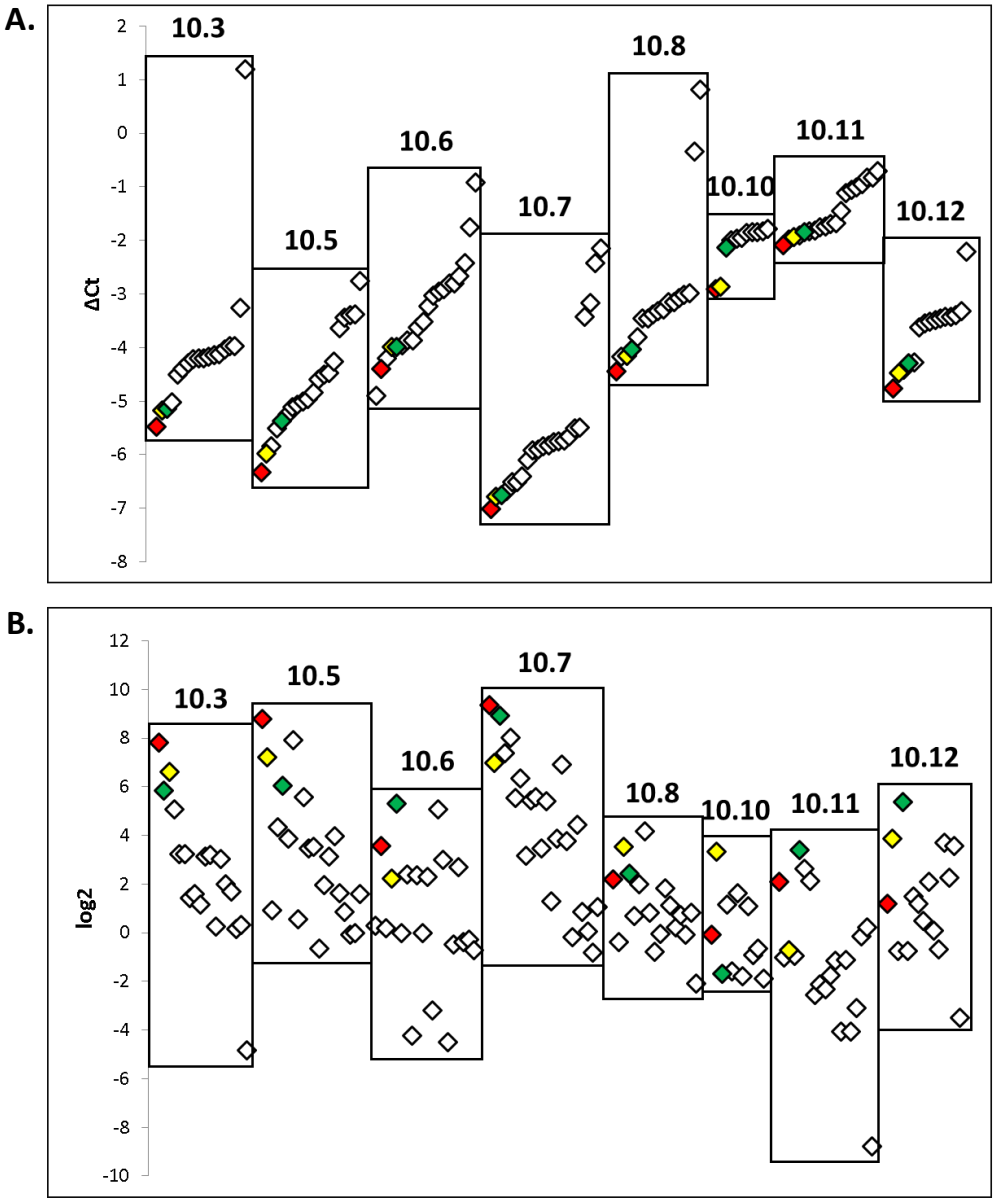


Figure A.5: TaqMan assay results for *HvBeg1::Atgai*

ΔCt (A) and log2 transformed NRQ (B) values for five different lines. Each box contains values for positive progeny within an independent transgenic line. Coloured plots represent those plants selected as potential homozygotes for further analysis, with the three matching colours representing the same plants in both graphs.

Table A.8: Confirmation PCR results for T2 *HvBeg1::Atgai* transgenic lines

Results of PCR on T2 generation plants of *HvBeg1::Atgai* to confirm TaqMan assay results. Rows in bold show homozygous lines.

Line	No. of +ve plants	No. of -ve plants	Zygosity
10.3.24	**24**	**0**	**Homozygous**
10.3.10	21	1	Hemizygous
10.3.3	23	1	Hemizygous
10.5.16	**24**	**0**	**Homozygous**
10.5.7	**24**	**0**	**Homozygous**
10.5.9	**24**	**0**	**Homozygous**
10.6.16	21	1	Hemizygous
10.6.2	20	3	Hemizygous
10.6.18	**21**	**0**	**Homozygous**
10.7.22	**24**	**0**	**Homozygous**
10.7.24	**24**	**0**	**Homozygous**
10.7.21	**23**	**0**	**Homozygous**
10.8.9	20	1	Hemizygous
10.8.14	**24**	**0**	**Homozygous**
10.8.11	**23**	**0**	**Homozygous**
10.10.24	8	16	Hemizygous
10.10.18	21	3	Hemizygous
10.10.15	9	15	Hemizygous
10.11.19	**24**	**0**	**Homozygous**
10.11.6	**24**	**0**	**Homozygous**
10.11.14	**24**	**0**	**Homozygous**
10.12.13	22	2	Hemizygous
10.12.18	**24**	**0**	**Homozygous**
10.12.4	**24**	**0**	**Homozygous**

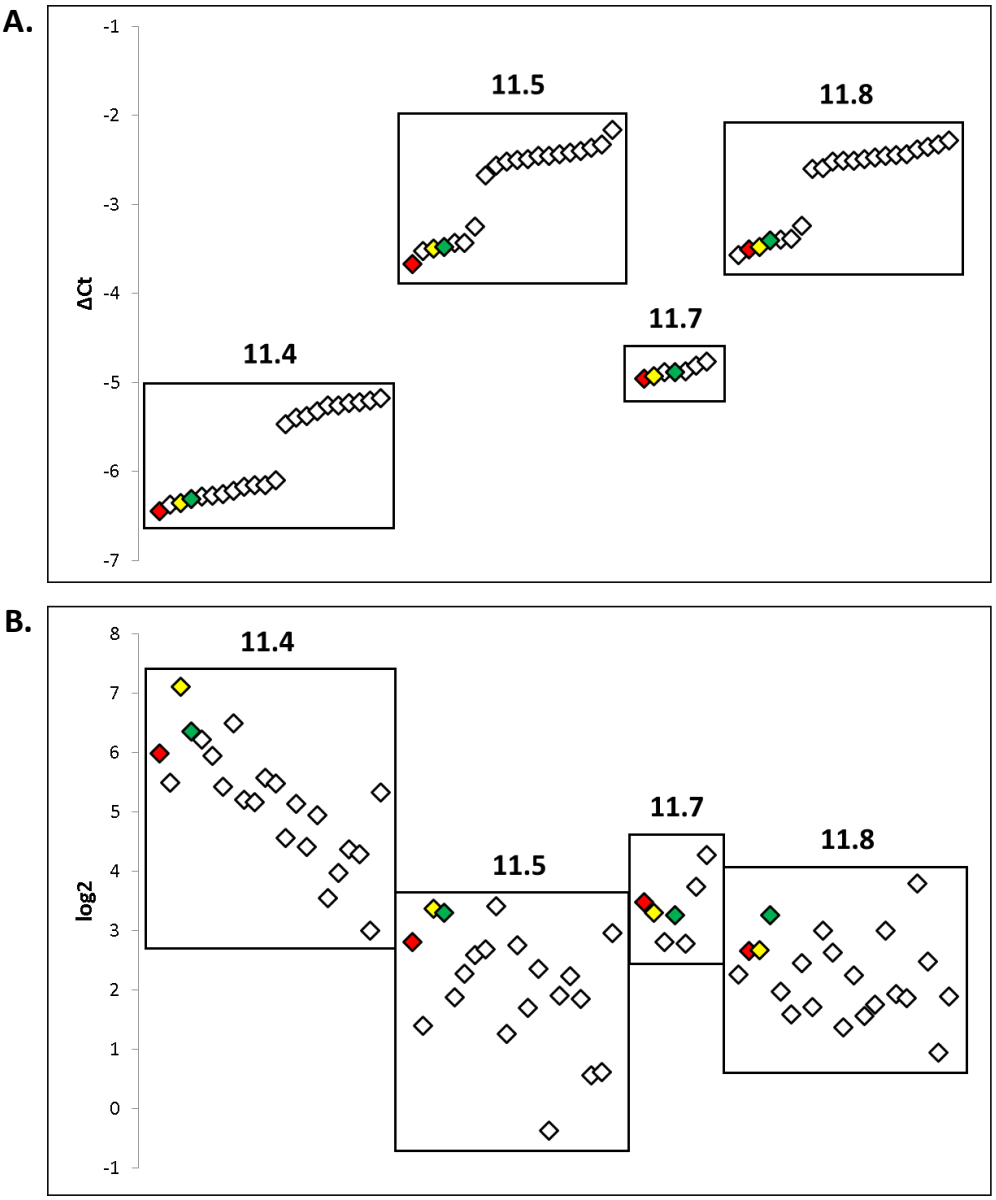


Figure A.6: TaqMan assay results for *TaEND1::Atgai*

ΔCt (A) and log2 transformed NRQ (B) values for four different lines. Each box contains values for positive progeny within an independent transgenic line. Coloured plots represent those plants selected as potential homozygotes for further analysis, with the three matching colours representing the same plants in both graphs.

Table A.9: Confirmation PCR results for T2 *TaEND1::Atgai* transgenic lines

Results of PCR on T2 generation plants of *TaEND1::gai* to confirm TaqMan assay results. Rows in bold show homozygous lines.

Line	No. of +ve plants	No. of -ve plants	Zygosity
11.4.17	**24**	**0**	**Homozygous**
11.4.9	**24**	**0**	**Homozygous**
11.4.1	**23**	**0**	**Homozygous**
11.5.12	**23**	**0**	**Homozygous**
11.5.18	**24**	**0**	**Homozygous**
11.5.11	**21**	**0**	**Homozygous**
11.7.17	17	6	Hemizygous
11.7.22	18	5	Hemizygous
11.7.11	18	5	Hemizygous
11.8.6	**24**	**0**	**Homozygous**
11.8.18	**23**	**0**	**Homozygous**
11.8.12	**24**	**0**	**Homozygous**

Appendix 3: GA internal standards

Table A.10: Amounts of $^{2}H_2$-GA standards
Amounts of $^{2}H_2$-GA internal standards added to each sample.

$^{2}H_2$-GA standards	Concentration (ng)
GA_1	2
GA_3	2
GA_4	2
GA_8	2
GA_9	2
GA_{12}	5
GA_{15}	2
GA_{19}	2
GA_{20}	2
GA_{24}	2
GA_{29}	2
GA_{34}	2
GA_{44}	2
GA_{51}	2
GA_{53}	2
GA_{54}	50